Biocatalytic Molecular Assembly Utilising Ene-Reductases and Transaminases

Alexandra Clare King

UCL

University College London

Submitted in partial fulfilment of the requirements for the degree of Doctor of Philosophy

2021

Declaration

I, Alexandra Clare King, confirm that the work presented in this thesis is my own. Where information has been derived from other sources, I confirm that this has been indicated in the thesis.

Abstract

With a growing interest in the pharmaceutical, fine chemical and agrochemical industry for environmentally benign and sustainable syntheses, biocatalysis has emerged as a forerunner in the field of green chemistry. Significant advantages over traditional chemical routes have been demonstrated, including high regio- and stereoselectivity under mild conditions.

Ene-reductases (ERs) perform the asymmetric reduction of activated alkene substrates. Operating via a stereospecific [2H] *trans*-reduction mechanism with high regio-, and stereospecificity, they are a powerful tool in the design of asymmetric synthetic pathways. Transaminases (TAms) mediate the enantioselective transfer of an amino group from an amine donor to a keto acceptor, generating an optically active amine. As enantiopure amines are valuable synthons, TAms present an efficient means for their preparation. In this PhD, the application of ERs and TAm in a biocatalytic cascade towards the molecular assembly of amino alcohols from unsaturated α-hydroxyketones was investigated. Chiral amino alcohols are an important and prevalent structural motif in value-added synthons and bioactive pharmaceuticals. Therefore, the development of an ER-TAm biocatalytic cascade for their molecular assembly represents a significant advancement in the field of green chemistry. Moreover, this work represents the first biocatalytic means of furnishing diastereomerically enriched amino alcohols.

In this PhD the potential of ERs was explored via substrate walking strategies using aromatic aldehyde, ketone and α-hydroxyketone substrates, with the systematic optimisation of assay parameters. The application of TAms with α-hydroxyketone derivatives was subsequently investigated for the molecular assembly of optically pure amino alcohols on a preparative scale via a one-pot ER-TAm cascade. Chiral amino alcohols were afforded in 30% and 32% isolated yields with further reaction providing chiral 2-aminooxazoles in 93:7 and 97:3 *dr*. Finally, to further demonstrate the use of ERs in synthesis, their use in the production of chiral fluorinated compounds was explored. With an efficient means for the production of chiral fluorinated compounds new classes of pharmaceuticals may be discovered.

Impact Statement

With an increasing call for greener and more sustainable synthetic pathways, asymmetric synthesis employing enzymes has become increasingly well established in the industrial production of pharmaceuticals, fine chemicals and agrochemical intermediates. Enzymatic biotransformations present significant advantages over traditional synthetic routes, not only due to their high yielding procedures and selective product formation, but also the sustainability of reaction conditions and reagents that can be used. As such, enzymatic syntheses can require less energy and fewer resources, whilst simultaneously generating less waste than their synthetic organic counterparts. Considering this, along with the high stereoselectivities that biocatalytic reactions can achieve, shorter synthetic syntheses are characteristically attained. Therefore, enzymatic biotransformations provide a cost-effective and efficacious strategy for the generation of chiral synthons and bioactive molecules.

The work described in this thesis employs the application of ene-reductases (ERs) and transaminases (TAms) in the biotransformation of α-hydroxyketone derivatives affording diastereomerically enriched amino alcohols, with specific emphasis on the biocatalytic design of TAAR1 agonist precursors. Chiral amino alcohols represent an important and prevalent structural motif in value-added synthons and bioactive pharmaceuticals, being found in antibiotics, alkaloids and β-blockers. As such, the development of an ER-TAm biocatalytic cascade for their molecular assembly represents a significant advancement in the field of green and sustainable technology.

On an industrial scale, hydrogenation of an alkene bond typically includes the use of a transition metal complexed to chiral ligands, with reaction conditions involving organic solvents and hydrogen at high pressure. Over-reduction is a known side-reaction, and downstream purification of the metal catalyst is often challenging. Application of ERs circumvents these challenges due to their chemo-, regio- and stereoselectivity under mild aqueous conditions. Additionally, their [2H] *trans*-reduction mechanism is stereo-complimentary to transition metal *cis*-hydrogenation.

With approximately 40% of pharmaceuticals containing a chiral amine scaffold, the enantiopure generation of amines is vital in the pharmaceutical industry. Varying chemical means are available for the production of amines, however asymmetric

reductive amination is of primary importance as it furnishes chirality from a prochiral source, with the asymmetric reductive amination of carbonyls cited as an "aspirational reaction" by the American Chemical Society Green Chemistry Institute (ACS GCI) Pharmaceutical Roundtable. Green and sustainable chemical means of asymmetric reductive amination are underdeveloped, however TAms can fulfil this need by their chemo-, regio- and stereoselective introduction of an amino group under non-hazardous conditions.

In addition to the application of ERs with α-hydroxyketone derivatives, the work described in this thesis also demonstrates the use of ERs in the production of chiral fluorinated compounds. As of 2018, 50% of blockbuster drugs approved by the Food and Drug Administration contained fluorine and of 2020, 20% of all commercial pharmaceuticals were fluoropharmaceuticals. The introduction of fluorine into drugs has been established to increase the metabolic stability of compounds by improving resistance to oxidative metabolism, thereby enhancing the pharmacokinetic profile of compounds *in vitro* and *in vivo*. Chemical means of enantioselective fluorination are limited, with advancements in the field largely credited to the design of new chiral ligands for transition metal catalysis. Additionally, limited fluorinase enzymes are readily available for biocatalytic fluorination. Therefore, ERs present as a valuable strategy for the generation of chiral fluorinated compounds.

Acknowledgements

The work presented in this thesis was made possible by a team of wonderful people, for whom I am grateful. First, I would like to thank the BBSRC for funding this work, and the management team at LIDo for their supervision over the past five years. I would like to thank Prof Helen Hailes for her guidance and relentless optimism, and Prof John Ward for his helpful conversation. Also, many thanks to Dr Abil Aliev for his generous help with NMR spectroscopy, and Dr Kersti Karu for her assistance with mass spectrometry. Additionally, thank you to Tony Field in "Stores" for keeping the show on the road and Saeed for his friendly greeting at reception in the morning. Thanks also to Martyn, Claire, Crosby, Helena, and Alan in the undergraduate teaching labs for their helpful advice and conversation over the past nine years. You make the department a brighter place.

A heartfelt thank you to the members of Lab 435, past and present. I couldn't possibly do justice to describe how you've impacted me over the years, but please know I am so grateful and you are forever in my heart. A wholehearted thank you also to Dr Helen Radovanovic, for helping me see the point in it all when I couldn't find any.

A big thank you to all the animals at Queen's Park Pets' Corner, especially my goats Baxter, Bella, Dougal, Gus and Gilly, as well as Black Sheep and White Sheep, and giant rabbit Anastasia. You've brought me such comfort.

Thank you to Sarah and Lucy, for your empathy and kindness over the years. You've assumed such an important role in my life willingly and wholeheartedly, and I am forever grateful.

Thank you to Kate, for putting up with me. I appreciate you've sacrificed for things that you think are unimportant, but you did it for me and I thank you for that.

Thank you to lovely Grandma, for being a beacon of light. I feel so lucky to have you in my life and know what sunshine embodied is.

Thank you to Dad, for giving me the world and loving me always.

Table of Contents

Abbreviations

α	alpha
ß	beta
δ	delta
ε	epsilon
γ	gamma
λ	wavelength
µg	microgram
µmol	micromole
ω	omega
aa	amino acid
ADH	alcohol dehydrogenase
Amp	ampicillin
API	active pharmaceutical ingredient
Ar	argon
Asn	asparagine
Au(I)	gold (I)
BSA	bovine serum albumin
BuLi	butyllithium
Cam	chloramphenicol
$CDCl_3$	deuterated (d) chloroform
CH_2Cl_2	dichloromethane
CI	chemical ionisation
conc.	concentrated
CPBA	chloroperoxybenzoic acid
CPME	cyclopentyl methyl ether
DMSO	dimethyl sulfoxide
DNA	deoxyribonucleic acid
dr	diastereomeric ratio
EDTA	ethylenediaminetetraacetic acid
ee	enantiomeric excess
EI	electron ionisation

Et	ethyl
EtOAc	ethyl acetate
EtOH	ethanol
eq.	equivalents
ER	ene-reductase
ESI	electrospray ionisation
ES–	negative mode electrospray ionisation
ES+	positive mode electrospray ionisation
FMN	flavin mononucleotide
g	grams
g_{CDW}	cell dry weight in grams
G6PDH	glucose-6-phosphate dehydrogenase
GC	gas chromatography
GCMS	gas chromatography mass spectrometry
h	hour
H_2	hydrogen gas
H_2O	water
H_2SO_4	sulfuric acid
HCl	hydrochloric acid
HEPES	(4-(2-hydroxyethyl)-1-piperazineethanesulfonic acid
His	histidine
HMBC	heteronuclear multiple-bond correlation spectroscopy
HPLC	high-performance liquid chromatography
i	*iso*-
IPA	isopropylamine
IPTG	isopropyl β-D-1-thiogalactopyranoside
IR	infrared spectroscopy
Kan	kanamycin
K_2CO_3	potassium carbonate
$KMnO_4$	potassium permanganate
LCMS	liquid chromatography–mass spectrometry
$LiAlH_4$	lithium aluminium hydride
LUMO	lowest unoccupied molecular orbital
m	*meta*

M	molar
MBA	Methylbenzylamine
Me	methyl
MeCN	acetonitrile
Me_3SiOTf	trimethylsilyl trifluoromethanesulfonate
MeOH	methanol
mg	milligram
$MgSO_4$	magnesium sulfate
min	minutes
mL	millilitre
mM	millimolar
mmol	millimole
MW	molecular weight
m/z	mass to charge ratio
m.p.	melting point
n	normal
nm	nanometre
$NaHCO_3$	sodium hydrogen carbonate
NEt_3	triethylamine
NAD(P)H	nicotinamide adenine dinucleotide (phosphate)
NMM	*N*-Methylmorpholine
NMR	nuclear magnetic resonance spectroscopy
o	*ortho*
OD_{600}	optical density at λ=600 nm
OYE	Old Yellow Enzyme
p	*para*
Pd/C	palladium on carbon
Pet. ether	petroleum ether, b.p. 40 – 60 °C
pH	potential of hydrogen
PLP	pyridoxal-5′-phosphate
PMP	pyridoxamine-5′-phosphate
r.t.	room temperature
s	seconds
sat.	saturated

SDS-PAGE	sodium dodecyl sulfate polyacrylamide gel electrophoresis
SPh_2	diphenylsulfide
TAAR1	trace amine-associated receptor 1
TAm	transaminase
TBME	*tert*-butyl methyl ether
tert	tertiary
THF	tetrahydrofuran
TLC	thin layer chromatography
Tris-HCl	Trizma® hydrochloride
TsOH	toluenesulfonic acid
Tyr	tyrosine
U	enzyme units
UCL	University College London
UV	ultraviolet
v/v	volume/volume
wt.	weight

List of Figures

List of Schemes

List of Tables

List of Equations

1. Introduction

1.1 Green Chemistry, Sustainability, and Biocatalysis

The emergence of the term "green chemistry" was first dated back to the U.S. Pollution Prevention Act of 1990, as a means of articulating the shift in paradigm from "end-of-pipeline" waste treatment to waste prevention at the industrial source, thus affording an overall reduction in environmental pollution. In 1998, Anastas and Warner expanded upon this model outlining the 12 principles of green chemistry.[1] These principles serve as a gold standard metric for the construction of industrial processes benign by design, and continues to guide industrial and academic researchers. In hand with these 12 principles is the concept of sustainability, defined by the United Nations as "the development of the needs of the present generation without compromising the ability of future generation to meet their own needs".[2] Thus, sustainable technology should not deplete resources at a rate faster than they can be produced nor generate waste at rates than cannot be assimilated naturally. Between green chemistry and sustainability, reduction in hazards, waste, energy, and life cycle environmental impacts are considered.

Chemical manufacturing has been identified as one of the top ten polluting industries.[3] Green chemistry, as defined above, may be used to prevent waste at the industrial source and reduce energy and life cycle impacts, thereby being essential in improving chemical manufacturing. The adoption of green chemistry into the scientific community however faces significant barriers including regulatory, financial, economic, and technical obstacles.[4–6] Those most common of these recognised in the context of the pharmaceutical industry have been documented by the International Consortium for Innovation and Quality in Pharmaceutical Development and include short development cycle, limited patent life, product quality, regulatory requirements, lack of unified metrics, high cost of development, and high project attrition.[7] The major hurdle of these is that changes to the synthetic design of an active pharmaceutical ingredient (API) becomes increasingly difficult as the drug progresses through clinical trial stages due to the increasing regulatory requirements at each phase. As the API process is regarded as the foundation of the safety and efficacy of clinical trial medication, any fundamental changes to the manufacturing process (which include

alterations to the API synthesis that may affect its impurity profile) performed after New Drug Application approval requires resubmission and approval by the FDA prior to distribution of the drug.[8] Therefore, with the incentive to avoid time-consuming revalidation and maximise the effective patent life of a drug (~12 years)[9] to recuperate research and development costs, any improvements to the API's production process must be made early in clinical trial evaluations. Unfortunately these mounting costly pressures under time restraints mean that API processes developed by pharmaceutical companies do not always reflect the most green and sustainable molecular assembly strategy.[7]

The American Chemical Society Green Chemistry Institute (ACS GCI) has identified nine key research areas for the advancement of green chemistry which they have defined as analytical chemistry, biobased chemicals, catalysis, "endangered" elements, green chemistry and engineering metrics, process engineering, rational molecular design for reduced toxicity, solvents, and waste to chemicals.[10] Improvements in analytical chemistry would involve the assessment of the "greenness" of a reaction and the development of more efficient analytical techniques such as HPLC-EAT and Eco-Scale to evaluate reaction sustainability. Use of biobased chemicals is aimed at obviating the current dependence on fossil carbon by developing new and existing chemicals from renewable resources. Catalysis precludes the need for stoichiometric equivalents, whilst the research area of "endangered" elements is focused on managing alternatives for elements used commercially that are facing critical supply risks. Green chemistry and engineering metrics is dedicated towards the implementation of metrics to better define and evaluate the "greenness" of chemical processes. Additionally, process engineering is aimed at designing processes that minimise the sustainability impacts of chemicals throughout their life cycle. Rational molecular design for reduced toxicity has the goal of designing chemicals that are less toxic, whilst the research area of "solvents" looks at techniques and applications for solvent replacement and/or removal. Finally, waste to chemicals has the goal of transforming waste into fuel, energy, and other useful chemical products.

For the work presented in this PhD thesis the research area of catalysis was explored. Catalysis allows for the reduction of resource and energy consumption, which affords a more sustainable process generating less waste. Green catalytic reactions may use either chemical (organic, organometallic, inorganic) or biological catalysts.

Organic catalysts are organic compounds that operate through the transient formation of covalent bonds (eg. enamine and iminium catalysts) as well as through non-covalent interactions (eg. hydrogen bonding catalysts). Organometallic catalysts, whilst similar to organic catalysts, differ in that they contain a metal-carbon bond. The reactivity of the metal may change significantly depending on the ligands coordinated, and so organometallic catalysts are very easily modified.[11–15] Inorganic catalysts are supported metal catalysts, with their use well established in hydrogenation[16] and cross-coupling reactions[17,18]. As these catalysts are heterogeneous (they occupy a different phase to that of the starting material and product) they are easily removed after a reaction, however they do present the disadvantage of not being easily modified, unlike organometallic catalysts.

With the goal of attaining enantiopure material in a green and sustainable manner, various chemical strategies are available including chemical catalysis and "aspirational" asymmetric reactions, as defined by the ACS GCI Pharmaceutical Roundtable.[19] First considering chemical catalysis, in the context of asymmetric hydrogenation (explored in this thesis) organometallic catalysts are classically used. Typical reaction conditions involve the application of hydrogen and organic solvents at high pressure, with over-reduction a known side-reaction.[11,13,20] Therefore, whilst the chemical catalyst may lower the activation energy barrier of the reaction, it is not an entirely green chemical process. Similar conclusions may be drawn from the use of "aspirational" asymmetric reactions, one being asymmetric reductive amination which furnishes chirality from a prochiral source. Unfortunately, green and sustainable chemical means of asymmetric reductive amination are underdeveloped, with side-reactivity of the transition metal hydride catalysts with ketones (alcohol by-product formation) a known issue,[21] and any alternative approaches only offering multi-step procedures under harsh conditions with heavy metal catalysts.[21] Biological catalysts, however, operating with catalytic ability, chemo-, regio- and stereoselectivity under mild and non-hazardous conditions, present as both a green and sustainable biotechnology that may circumvent challenges faced by chemical catalysis and chemical asymmetric reactions. Further information comparing their use to chemical methods in the context of asymmetric hydrogenation and asymmetric reductive amination may be found in sections 1.2.1.4 and 1.2.2.2 respectively.

Biocatalysis is defined as the use of enzymes or other biological molecules to catalyse a chemical reaction. Adherence to 10 of the 12 principles of green chemistry is observed, making their application amongst the forerunners in the field[22] (**Table 1**). Biocatalysis can suffer from some major drawbacks however, including its limited operational window, limited substrate scope, disfavoured equilibrium, susceptibility to inhibition by both substrate and product, as well as low organic solvent tolerance.[23–25] Additionally, access to only one enantiomeric form of a target compound can be challenging in the development of synthetic routes. Means to address these challenges by the application metagenomics and protein engineering are described in this thesis.

Table 1: Adherence of biocatalysis to the 12 principles of green chemistry.

Green Chemistry Principle	Biocatalysis
1. Waste prevention	Sustainable and shorter synthetic route
2. Atom economy	Specificity enables more efficient synthetic routes
3. Less hazardous syntheses	Low toxicity levels
4. Design for safer chemicals	--
5. Safer solvents and auxiliaries	Often performed in water with solvents required typically class I or II
6. Energy efficiency	Ambient conditions
7. Renewable feedstocks	Biocatalysts are renewable
8. Reduce derivatisation	Chemo-, regio- and enantioselectivity of enzymes obviates the need for derivatisation
9. Catalysis	Enzymes are catalysts
10. Design for degradation	Enzymes are biodegradable
11. Real-time analysis for pollution prevention	--
12. Inherently safer process	Mild conditions with minimal hazards

1.1.1 Use of Biocatalysts

Whilst the use of biocatalysis is not a novel technique, with its applications dating back thousands of years to the production of cheese, bread and wine, recent key scientific advances have enabled the use of biocatalysts for molecular synthesis. This can be attributed to the introduction of recombinant DNA technology in the 1970s, allowing

for the more efficient production of recombinant microorganisms thereby affording higher purity enzymes at a fraction of the cost.[26] As such, the industrial application of biocatalysis, specifically in the pharmaceutical and fine chemical industry, is dominated by recombinant enzymes.[27,28]

1.1.1.1 Form of the Biocatalyst

With preparative scale considerations towards enzymatic synthesis, expenses in terms of the time and materials required for enzyme purification are typically avoided by the use of whole cells or clarified lysates.[28,29]

Whole cell biocatalysis presents the advantage of requiring less purification than clarified cell lysates, as the enzyme is not isolated from the cell debris. Additionally, its application obviates the need for additional co-enzyme and cofactor, as well as ensures an ideal environment for enzymatic stability and activity.[30,31] Whole-cell biocatalysis does present significant disadvantages however, including substrate diffusion limitation, cross reactivity with cellular metabolites, sub-optimal employment of cofactors, as well as substrate and product decomposition through competing cellular processes.[32,33] Given the wide scope of variables unaccounted for, clarified lysates are employed in this work.

Following cell culture and disruption, removal of cell debris affords clarified cell lysates, soluble unpurified enzymes produced by the cell. Biocatalytic applications using clarified cell lysates avoid the further purification required for the generation of purified enzymes. Also, provided that proteases are not present, the additional protein has been known to confer enzymatic stability.[34]

1.1.1.2 Enzyme Improvements

The application of enzymes on a preparative scale can suffer from challenges typically described by the enzyme's "fitness" for a given biocatalytic process. That is, its suitability for the substrate and reaction conditions under consideration. Consequently, the synthetic route may have to be redesigned, or else the enzyme subjected to rounds of evolution/random mutations to accommodate conditions. Either option is a major hurdle and potentially sub-optimal or unviable for a given chemical process. Thus, limited fitness often challenges or restrains enzymatic applications. As a means of addressing fitness challenges, variable tactics are employed including metagenomics,

directed evolution, rational design, and semi-rational design. A notable early example includes the evolution of transaminase *Arthrobacter sp* (ATA-117) wherein 27 mutations (~8% of the sequence) were required to tolerate the concentration of isopropylamine (IPA), bulky substrate, and substrate loading required for the (*R*)-selective amination in the production of Sitagliptin.[35]

1.1.1.3 Organic Solvent Tolerance

One of the major hurdles for the industrial application of biocatalysis are enzymes insufficient stability under processing conditions, specifically their ineffective use in organic solvent systems. The employment of organic solvents presents the significant advantage of increased solubility of hydrophobic substrates, with stronger intermolecular interactions achieved between substrates and the enzyme.[36] However, this is at the expense of water present, which promotes the conformational mobility for optimal biocatalysis.[36] Additionally, increased organic solvent concentration has been established to denature enzymes. As such, varying strategies for achieving biocatalysis that are stable with organic co-solvent conditions include: i) The isolation of novel enzymes that can function under harsh conditions via metagenomic strategies (section 1.1.2), ii) The modification of enzymes to increase their tolerance towards organic solvents by enzyme immobilisation,[37,38] chemical modification with poly(ethylene glycol),[39,40] and genetic modification (section 1.1.3), iii) The modification of solvent environments to decrease their denaturing effects on enzymes including the use of additives[41,42] and surfactants[43,44].

1.1.2 Metagenomics

With the total number of microbial cells on Earth estimated to be 10^{30} and prokaryotes comprised of 10^{6} – 10^{8} separate genospecies, prokaryotes represent the largest proportion of individual organisms on the planet.[45,46] However, as only 0.1 – 1% of microorganisms in a given niche environment are readily cultured, there is a distinct lack of microbial enzymes readily available for biocatalytic applications.[47,48] Therefore, the enormous potential encoded by genetic diversity remains largely untapped; Enzymes adapted to the physical-chemical parameters of their environments – pH, temperature, pressure, chemical concentrations, etc. – and potentially suitable for biocatalytic processes remain unidentified and unexploited.

The difficulties in culturing sampled microorganisms in a laboratory settings is primarily attributed to the lack of knowledge of suitable growth conditions.[49] Therefore, an approach independent of environmental microbial cell culture was adopted in 1998 by Handelsman and coined "metagenomics". Metagenomics entails the extraction and processing of DNA from an environment without first culturing the microorganisms, instead treating the metagenome as a genomic unit.[47]

Traditional metagenomic analysis entails genomic DNA extraction from an environment, cloning the heterologous DNA into an appropriate vector and subsequent transformation into a host (**Figure 1**). Analysis of the metagenomic library produced may then proceed via two approaches: functional or sequence-based metagenomics.

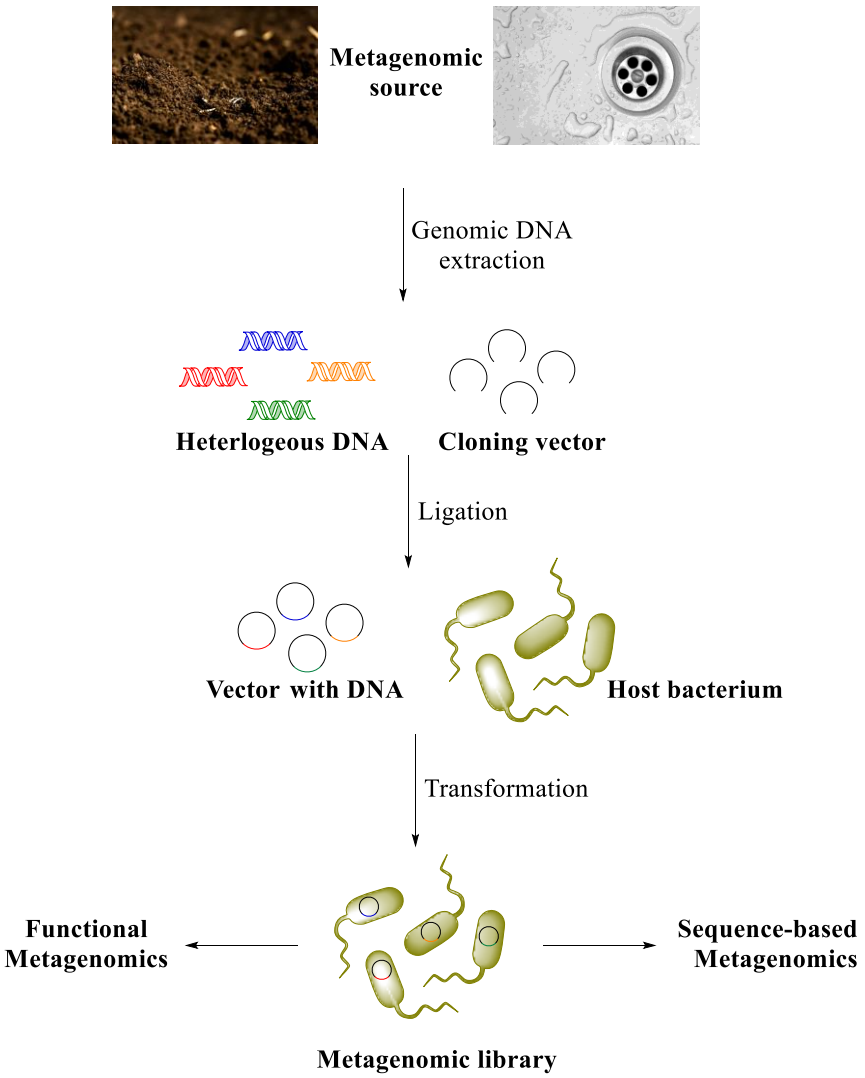

Figure 1: Traditional metagenomics. Genomic DNA is extracted from an environment, cloned into a vector and transformed into a host. The metagenomic library produced is then analysed by functional or sequence-based metagenomics.

1.1.2.1 Functional Metagenomics

Functional metagenomics is based upon the screening of metagenomic DNA libraries for metabolic activity such as enzyme activity or production.[50] As sequence information is not required for functional metagenomics, it is not hindered by the dependence on previous knowledge. Therefore, unlike sequence-based metagenomics, it bears the potential to identify novel genes encoding novel functions.[51] Functional metagenomics does possess the noteworthy disadvantage of being non-trivial to perform, requiring transcription, translation and secretion of the gene product with subsequent assays.[49] Additionally, there is the challenge of predicting novel enzymes without precedent.[48] Being taxing in both time and expense, sequence-based metagenomics is preferred by comparison

1.1.2.2 Sequence-based Metagenomics

For sequence-based metagenomics, conserved regions of known genes and protein families are identified, and DNA probes or primers are designed.[51] Therefore, only novel enzymes of known functional classes can be identified from this approach. In addition, sequence-based metagenomics is challenging as inferring protein function from the sequence is non-trivial,[52] and a large proportion of sequenced genes have little homology with known enzymes.[53] Therefore, the potential activity of these genes is hidden. In fact, newly sequenced genomes with genes of unknown function has remained fairly constant over the past decade at ~30 – 40%,[48] suggesting the need for functional metagenomics in addition to sequence-based metagenomics. Nevertheless, sequence-based metagenomics has identified genes encoding novel enzymes, including chitinases[54], nitrite reductases[55], [Fe-Fe]-hydrogenases[56], and dioxygenases[57].

1.1.2.3 UCL Metagenomics

As previously described, traditional metagenomic approaches for the identification of functional enzymes requires the construction of a physical metagenomic library. To by-pass this, the metagenomic approach developed at University College London (UCL) by the Hailes and Ward groups involves the generation of an *in silico* metagenomic library as opposed to a physical library, thus redirecting efforts from *in vitro* work to *in silico* tactics (**Figure 2**).

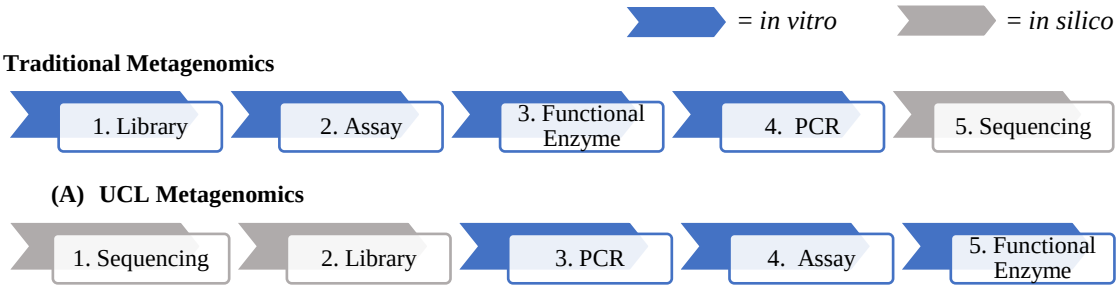

Figure 2: Comparison of the steps undertaken in **(A)** Traditional Metagenomics and **(B)** UCL Metagenomics.

In addition to the reduction of *in vitro* work, an *in silico* library bears the advantage of being continuously mined for different classes of enzyme for biocatalysis. This does necessitate the library to be very large, and so notable computational memory and power is required. Specifically, sequencing of the metagenome generates individual reads on the scale of tens of millions, with assembly into a contig library containing hundreds of thousands. It is this assembly process that necessitates the computational memory and power.

Previous work applying UCL Metagenomics has employed a sequence-based approach.[58–60] In this work, ERs from soil isolates[59] and TAms from a dometic drain metagenome[60] have been used.[i] DNA was extracted and sequenced using the Illumina MiSeq platform producing individual sequence reads on the scale of millions, which are then put through a set of quality control measures before being assembled into contiguous reads (contigs) large enough to afford full length open reading frames (ORFs). The formatted database is then annotated by PFAM ID or queried as a BLAST searchable database. Identified genes were then retrieved *via* designed primers and cloned into a host, with the enzyme expressed subject to a function-based assay to test for activity.

In all, the UCL Metagenomics approach affords the possibility of building a large enough toolbox to address enzymatic fitness requirements for biocatalysis. Previously inaccessible and undiscovered enzymes are attained from the analysis of Nature's diverse natural environments.

[i] Metagenomic ERs identified by Dr Dragana Dobrjevic and Dr Laure Benhamou, former members of the Ward and Hailes groups respectively. Metagenomic TAms identified by Dr Leona Leipold, former member of the Hailes group.

1.1.2.4 Metagenomic Source Environments

A wide variety of environments have been sampled for metagenomic analysis including soil[61,62], groundwater[63], marine picoplankton[64], glacier ice[65], and hot spring[66] microbiomes, amongst others. Here enzymes from a domestic drain and soil metagenomes have been investigated. For the drain metagenome, it was envisioned that the changes in temperature, pH, and chemical concentrations would afford enzymes with significant tolerance to environmental conditions and good activities. Indeed, a number of novel robust transaminases were identified[67], three of which were screened in this work.

It has been established that soil has the greatest source of prokaryotic diversity, orders of magnitude greater than that of aquatic environments.[47,68] This is due the structural and chemical complexity of soil, affording the partitioning of resources and well as significant chemical and pH gradients. Naturally, this promotes environmental adaptation and prokaryote specialisation. This, combined with the high population density of prokaryotes in soil, provides increased rates of lateral DNA transfer and recombination, furnishing the evolution of new traits.[68]

A combination of metagenomic Ene-Reductases (ERs) and Transaminases (TAms) from soil metagenomes have been used in this work. Further information regarding these enzymes is described in Chapter 3, Chapter 4, and Chapter 5.

1.1.3 Protein Engineering

Protein engineering methods described include rational design (section 1.1.3.1), directed evolution (section 1.1.3.2), and semi-rational design (section 1.1.3.3). Protein engineering is typically performed to improve enzymatic "fitness", as described in section 1.1.1.2.

1.1.3.1 Rational Design

First cited in the 1970s, rational design using site-directed mutagenesis was typically employed for mechanistic studies.[69] The technique entailed the replacement of a specific amino acid in a protein with another, using structural and mechanistic information available (**Figure 3A**). Naturally, the amino acid replaced was of suspected mechanistic relevance, with its substitute used to investigate any potential changes to activity. Whilst sensible, this method heavily relied upon the availability of

the structural and mechanistic information of the protein, which is not always present. Nevertheless, site-directed mutagenesis continues to be explored, yielding fascinating results. Svedendahl *et al.* reported the reversed enantiopreference of an (*S*)-selective ω-TAm CNB05-01 (*Arthrobacter citreus*) from a single point mutation (V328A) in the active site loop.[70] (*R*)-selectivity for 4-fluorophenylacetone observed, with results further confirmed by molecular docking simulations. Alternative applications using site-directed mutagenesis have also been explored in recent years, including mutagenesis on the protein surface for oriented immobilisation to a support via a covalent linkage (e.g. disulphide bond).[71]

1.1.3.2 Directed Evolution

Performed *in vitro*, directed evolution using random mutagenesis does not require any structural information about the protein as the replaced amino acid is not predetermined (**Figure 3B**). Two of the most established random mutagenesis tactics are error prone polymerase chain reaction (epPCR) and DNA shuffling.[72]

First described by Goeddel in 1989,[73] epPCR exploits the low fidelity of DNA polymerase to produce point mutations during PCR amplification. The number of PCR cycles applied and increased concentration of magnesium salts significantly increases mutation rates, thus tailoring the extent of modification of the mutant library produced.[72,74] An exemplary use of epPCR was described by Chen and Arnold to evolve industrially relevant protease, subtilisin E, to be 256 times more efficacious than the wild-type enzyme in 60% aqueous dimethylformamide.[75] In 2018, Wang *et al.* employed epPCR to engineer the carbonyl reductase RtSCR9 (*Rhodosporidium toruloides*) to afford a key intermediate in the synthesis of the pharmaceutical (*S*)-Duloxetine.[76] The mutant furnished the intermediate in 91% yield and 99.9% *ee* at 2 M substrate loading, the highest reported to date.

DNA shuffling differs from epPCR in that it emulates the natural process of homologous recombination by a re-arrangement of mutations, thus affording advantageous combinations. First reported by Stemmer,[77] DNase fragments a set of parent genes which subsequently randomly recombine in a PCR reaction without added primers. The cycling of denaturing, annealing, and extending fragments affords rearranged full-length genes comprised of recombined segments. The notable

disadvantage of DNA shuffling is that it generates very large libraries of mutants that require high-throughput screening for evaluation.

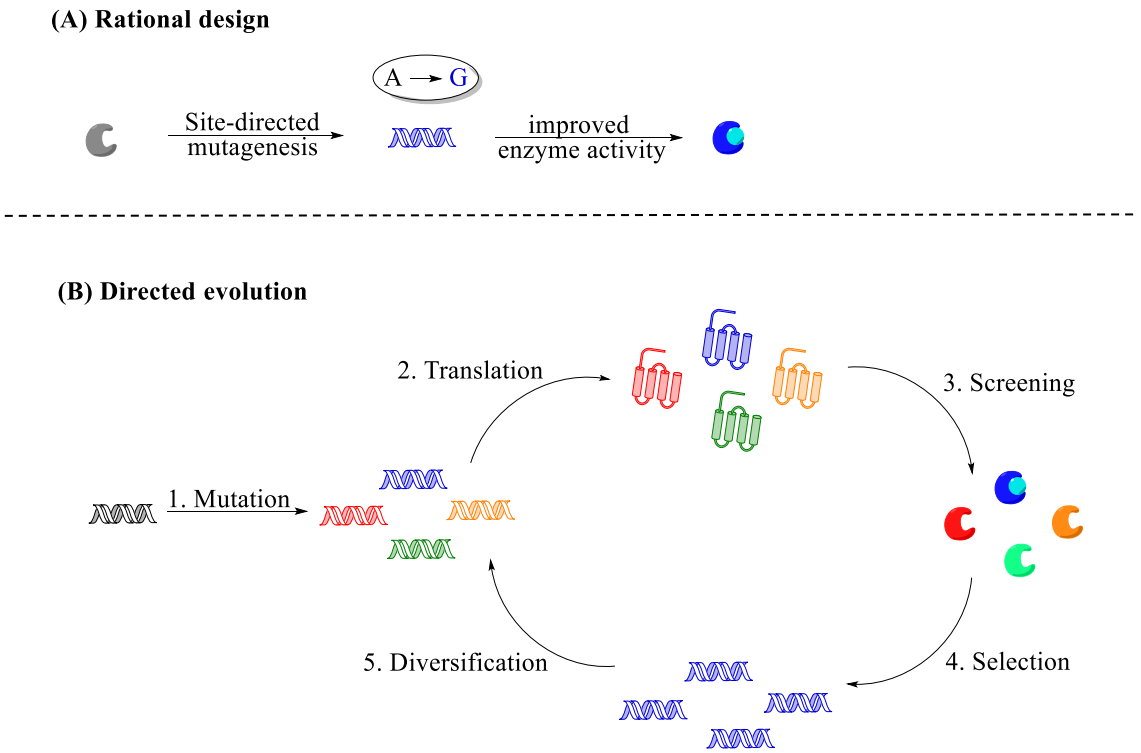

Figure 3: Protein engineering by rational design vs. directed evolution. **(A)** Rational design by site-directed mutagenesis to give improved enzyme activity. **(B)** Directed evolution. Wild type gene is mutated to generate diversity with a mutant gene library. Translation of mutant gene library into a library of gene products and activity screening proceed. The mutant gene product with desired capabilities is selected and gene diversified. The cycle repeats.

1.1.3.3 Semi-Rational Design

In recent years efforts have been focused on the development of a semi-rational methodology for the generation of small high quality mutant libraries. Techniques such as protein structure modelling, *in silico* docking, molecular dynamic simulations and predictive algorithms have formed the start points for protein engineering to afford a curated mutant library.[33,78]

1.1.4 Biocatalysis in the Pharmaceutical Industry

Of small molecule drugs (<550 molecular weight) produced by large pharmaceutical companies, >90% possess a nitrogen atom, >90% possess an aromatic group and approximately 54% are chiral.[79] In addition, pharmaceutical products are typically densely functionalised with reactive labile groups which challenge the development of a high yielding synthetic route. These groups may be protected and subsequently

deprotected, however this adds non-constructive steps in what is usually an already lengthy synthesis.

For those chiral small molecules the additional challenge of attaining enantiomeric purity (>99.5% enantiomeric excess, *ee*) also presents itself. To achieve this, the predominant tactic is to purchase chiral starting material or intermediates from the fine chemical industry.[79,80] Asymmetric synthesis is also employed, but its application is underdeveloped only producing approximately 20% of chiral centres.[79]

Besides these challenges pertaining to synthetic efficacy, reaction conditions also contribute to the efficiency, safety and cost-effectiveness of a process. As described earlier, enzymatic biotransformations meet the above challenges pertaining to both synthetic efficacy and sustainability of reaction conditions by providing high yielding and selective product formation under mild conditions. In addition, they circumvent the need for rare metal catalysts, the prices of which have significantly fluctuated over the past decade.[81] Indeed, the industrial application of enzymatic biotransformations has grown significantly in recent years.[29,82–84]

For multi-enzymatic biotransformations in an industrial setting, a biocatalytic linear cascade wherein a substrate is converted into a sole product via sequential one-pot biotransformations presents an advantageous strategy. Namely, it prevents the accumulation of hazardous or unstable intermediates, thereby 1) Making the industrial process safer and greener; 2) Circumventing the need for downstream purification steps; 3) Driving reversible biocatalytic reactions to completion.

1.1.4.1 Biocatalytic Applications

Lyrica® is a drug marketed by Pfizer for the treatment of central nervous system disorders including epilepsy and neuropathic pain. The first generation manufacturing process of its active pharmaceutical ingredient, Pregabalin, entailed formation of the regulatory starting material cyano diester **4** via Knoevenagel condensation of **1** and **2** to give **3** followed by cyanation. Basic hydrolysis, Ni-catalysed hydrogenation and decarboxylation converted cyano diester **4** into racemic γ-amino acid **5** which was subsequently resolved in a two-step crystallization process using (*S*)-(+)-mandelic acid. Further recrystallization with THF/H_2O furnished enantiopure Pregabalin (*S*)-**5** in low yield (**Scheme 1**).[85] It was proposed that the process could be improved in terms of

green chemistry, yield and chemical purity by 1) Early stage enzymatic resolution and chemical recycling of the undesired enantiomer (*R*)-**4** by racemization. As such, the application of hydrolases for stereoselective hydrolysis were investigated along with the development of a recycling system.

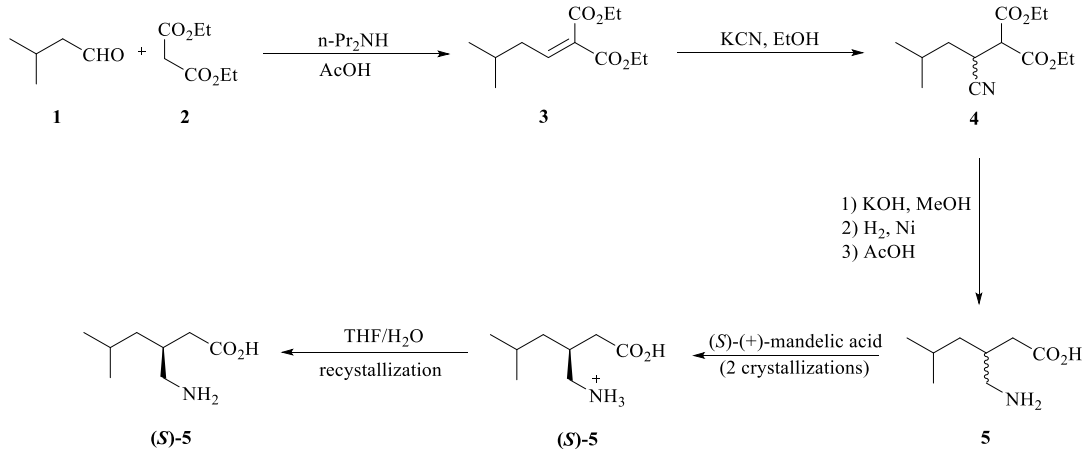

Scheme 1: First generation manufacturing process of Pregabalin (*S*)-**5**.

An optimised chemoenzymatic manufacturing route was developed with commercially available low cost Lipolase for the kinetic resolution of **4** (**Scheme 2**). After one recycling of (*R*)-**4**, Pregabalin (*S*)-**5** was obtained in 40 – 45% overall yield, >99% chemical purity and >99% *ee*, a significant improvement from the first generation route only providing 20% yield.[85,86] In addition, the optimised chemoenzymatic process was also significantly greener with five and eight times less input (kg) of chemical and solvents respectively. As a result the Environmental factor (*E* factor) of the manufacturing process reduced from 86 to 17.[85] The *E* factor is a simple metric of how "green" a reaction is, and is defined as the ratio of the mass of waste to mass of product. A lower *E* factor means less waste relative to product was formed, and so less of a negative environmental impact. The ideal *E* factor is zero.

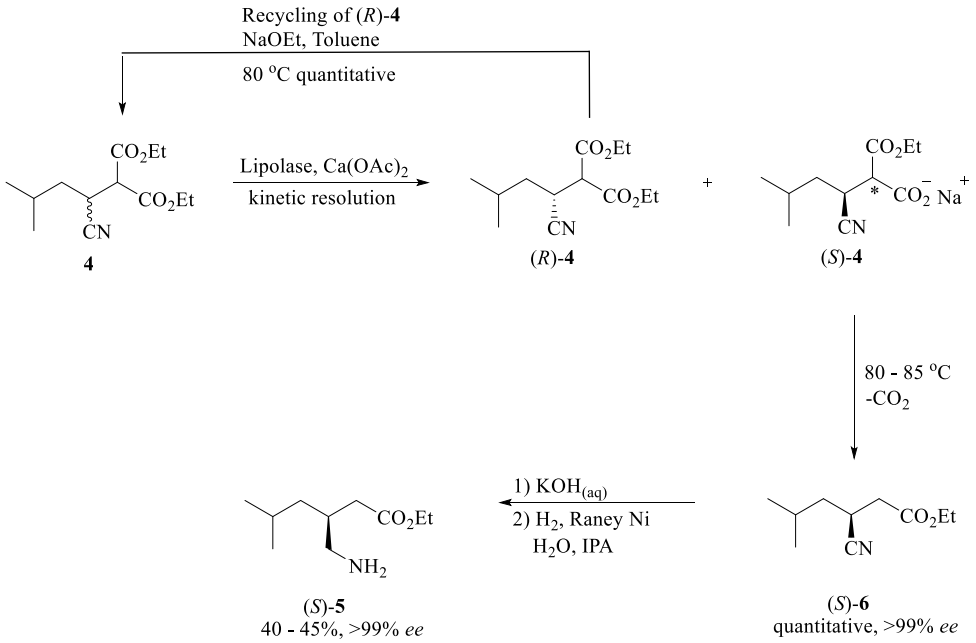

Scheme 2: Optimised chemoenzymatic Pregabalin (*S*)-**5** synthesis.

1.2 Enzymatic Biotransformations in Asymmetric Synthesis

With a growing interest in the pharmaceutical, fine chemical and agrochemical industry for environmentally benign and sustainable syntheses, biocatalysis has emerged as a forerunner in the field of green chemistry.[25,84,86–88] Significant advantages over traditional chemical routes have been demonstrated, including high regio- and stereoselectivity under mild, non-hazardous conditions, as well as high efficacy and cost-effectiveness.

1.2.1 Ene-Reductases (ERs)

The asymmetric reduction of activated alkenes is a widely employed synthetic step in the generation of up to two stereogenic centres. Whereas transition metal catalysed *cis*-hydrogenation has been thoroughly exploited for this purpose, stereo-complimentary *trans*-hydrogenation by chemical means is less well developed.[89–91] Ene-Reductases (ERs) however, operating by a stereospecific [2H] *trans*-reduction mechanism may fulfil this application and be a complementary tool in the design of asymmetric synthetic pathways for bioactive compounds.

1.2.1.1 Classification of Ene-Reductases

ERs are classified as NAD(P)H dependent oxidoreductases, with the most prevalent family being that of the Old Yellow Enzymes (OYEs).[92,93] Christian and Warburg discovered the first enzyme from the OYE family,[94] with ER "old yellow enzyme" (OYE1) characterised in subsequent years[95]. Since this pioneering discovery, the family of OYEs have been recognised to catalyse the stereoselective reduction of activated alkenes (ie. those conjugated to an electron withdrawing group, EWG) with activating groups including aldehydes, ketones, carboxylic acids, esters, nitriles and nitro moieties.[93,96–98] Currently five families of ERs have been discovered, four in addition to the OYE family (**Figure 4**).[99–101]

Flavine adenine dinucleotide (FAD)- and [4Fe-4S]- containing clostridial enoate reductases (EnoR) are another ER family, known to catalyse the bioreduction of poorly activated substrates (ie. those activated by carboxylic acid and ester moieties).[102] Their application, however, is limited due to their oxygen sensitivity. Flavin independent ER families include the salutaridine/menthone reductase-like subfamily of short chain

dehydrogenases/reductases (SDR) as well as leukotriene B4 dehydrogenase subfamily of medium chain dehydrogenases/reductases (MDR). Their application covers a wide substrate scope, but is best known for the bioreduction of aromatic and monocyclic alkenes with aldehyde or ketone activating groups.[103–106] Most recently, the quinine reductase-like family was discovered. Despite their lack of sequence homology and structural features with OYEs they demonstrate ER activity, with inverted stereopreference observed.[107]

In recent years, the OYE family has been divided into 5 enzyme subclasses on the premise of sequence homology and structural features (**Figure 4**).[101] As of 2010, there were two subclasses, "classical OYEs" and "thermophilic-like OYEs", the latter of which introduced by Scrutton *et al.* on the basis of structural differences.[93,108] Specifically, in solution "thermophilic-like OYEs" adopt functional higher order oligomeric states (e.g. a dimer of dimer), whilst classical OYEs are found as monomers or dimers. Thus, OYE homologues such as NCR (*Zymomonas mobilis*), YqjM (*Bacillus subtillis*) and XenA (*Pseudomonas putida*) were divided into Classes I, II and II respectively based upon this classification.[109] A further subclass was reported by Verma *et al.* in 2014 from the phylogenetic analysis of a range of fungal strains (Class V)[110] and in 2019, Buller *et. al.* proposed two new classes (Class III and IV) from the phylogenetic and biochemical analysis of 40 genes encoding putative novel ERs.[109]

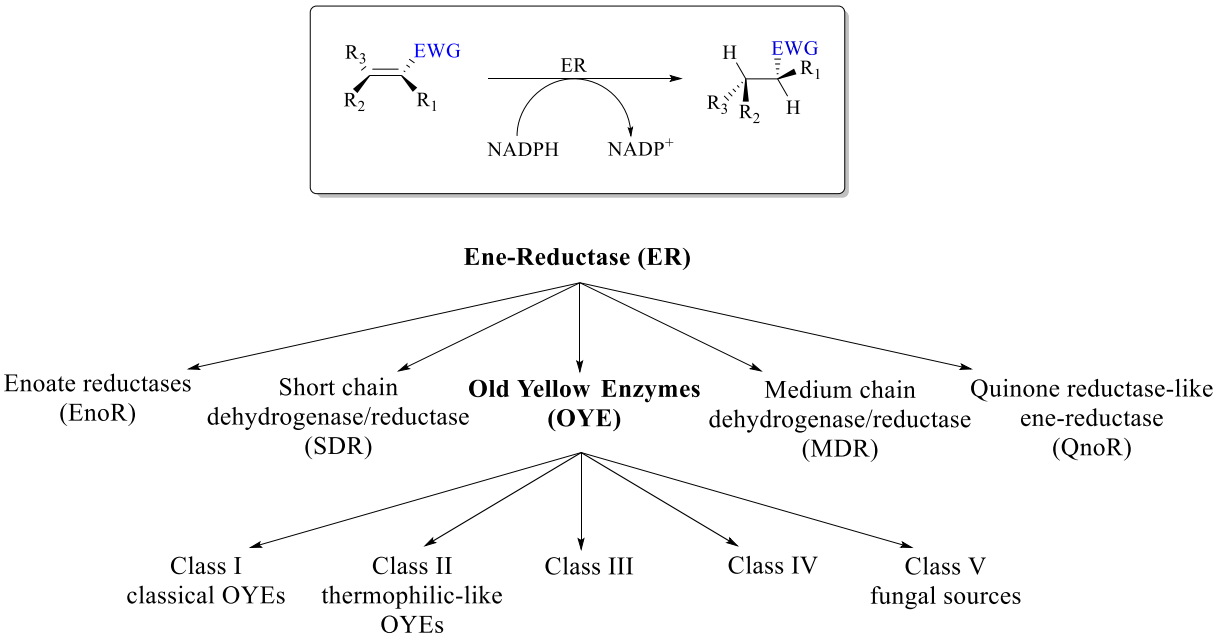

Figure 4: Schematic overview of the five Ene-reductaste families and five Old Yellow Enzyme subclasses.

1.2.1.2 Stereochemistry and Stereocontrol

The OYE family, belonging to the class of NAD(P)H dependent oxidoreductases, derive their name from the yellow colour imparted from the flavin mononucleotide (FMN) prosthetic cofactor.[111] Catalytic reduction of the α,ß-unsaturated compounds proceeds via reductive and oxidative half reactions in a bi-bi ping pong mechanism, entailing the sequential binding of reductive and oxidative substrates within the active site.[112–114] The mechanism can be described in two steps: 1) The reductive substrate NAD(P)H binds reducing the OYE-FMN cofactor via hydride transfer and is released; 2) The oxidative substrate, an α,ß-unsaturated alkene, then binds within the active site and is reduced via a *trans*-hydrogenation, thereby oxidizing the OYE-FMN cofactor (**Figure 5**).

Early studies into the ER biocatalytic mechanism were carried out by Nakamura *et al.*[115] and Kohli *et al.*[114] Specifically, the reductive half reaction (**Step 1**, **Figure 5**) elucidated by Nakamura *et. al.* was proposed based on results obtained from spectrophotometric titration experiments, stopped flow methods and electron spin resonance techniques.[115] The oxidative half reaction (**Step 2**, **Figure 5**, and **Figure 6**) mechanism characterised by Kohli *et al.* confirmed the mechanistic relevance of tyrosine 196 from mutation of this residue to phenylalanine. It was concluded that mutation of this residue had a negligible effect on ligand binding and the reductive half reaction, but significantly slowed the oxidative half reaction by six orders of magnitude when using the natural substrate cyclohex-2-en-1-one.[114] Additionally, a crystal structure of OYE1 with *p*-hydroxybenzaldehyde confirmed that the relative orientation of the hydride donor (within FMN_{red}) and the tyrosine 196 proton donor (being on opposite faces of the substrate) was in agreement with the *trans* addition stereochemistry observed in the product.[114]

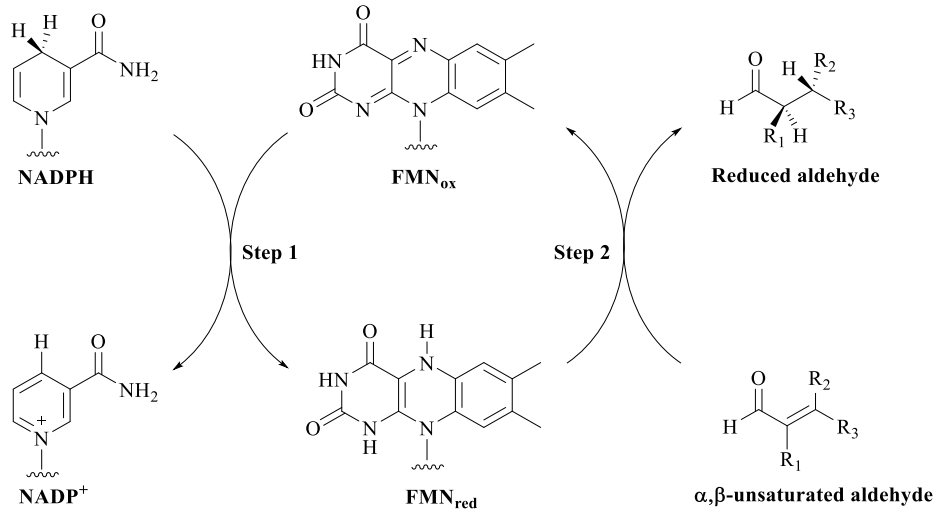

Figure 5: Overall redox reaction catalysed by OYE-FMN. An activated alkene substrate, α,ß-unsaturated aldehyde, is presented in the figure, however other activated alkene substrates may undergo hydrogenation.

The mechanism of the asymmetric bioreduction of activated alkenes has been investigated in detail, with specific attention focused on stereocontrol in the hydrogenation, and enantiopreference of product formation.[92,97,98,116–119] Alkene reduction was established to proceed via a *trans* addition of [2H] with absolute stereospecificity. The bioreduction entails hydride addition from reduced FMN cofactor to the C(ß) on one prochiral face of the alkene followed by protonation of C(α) from a tyrosine hydroxyl group on the opposite prochiral face, thereby affording the stereospecific trans-hydrogenated product (**Figure 6**). The NAD(P)H cofactor for flavin cofactor recycling is required in the ER bioreduction.

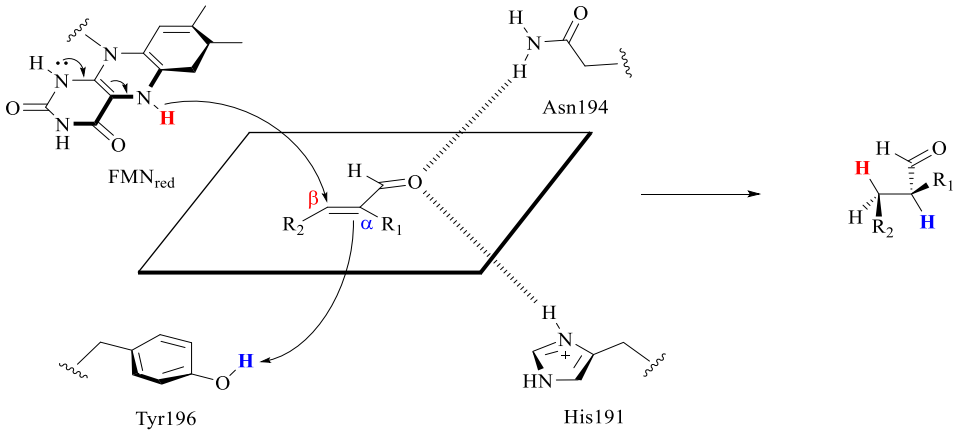

Figure 6: Stereospecific [2H] *trans* reduction of α,ß-unsaturated aldehyde by Old Yellow Enzyme.

Bearing in mind the relevance of binding modes within the active site for stereocontrol, two major modes, "classical" and "flipped", have been rationalised to predict the stereochemical outcome (**Figure 7**).[93,120–123] Determination of which binding mode is utilised has been shown to be dependent on both the ER employed and substrate undergoing bioreduction.[98,117,120] Therefore, enzyme- and substrate-based engineering tactics have provided orthogonal strategies for reaction stereocontrol.

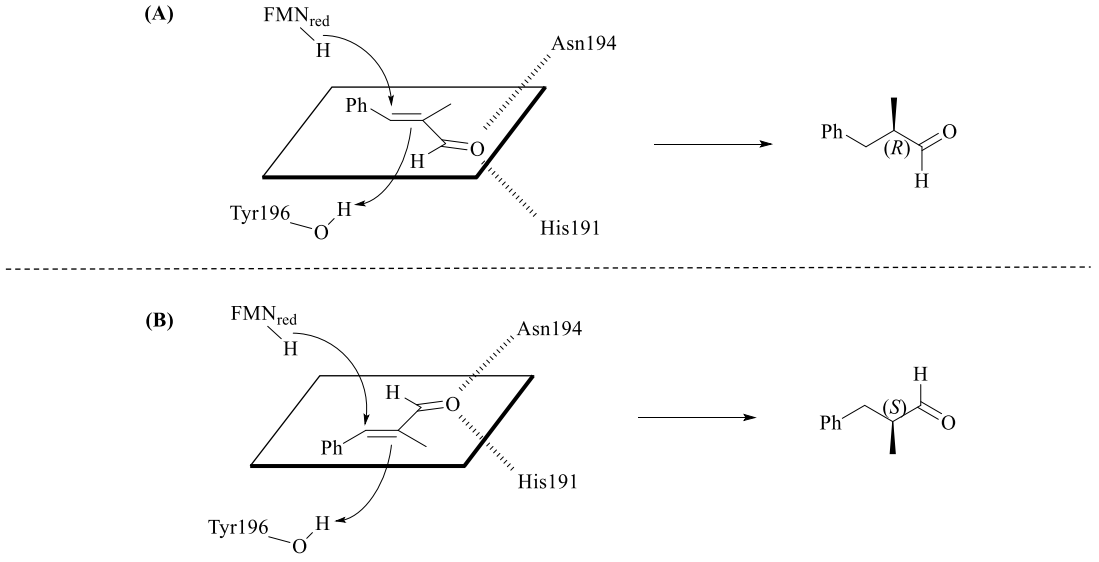

Figure 7: Representative illustration of binding modes of a substrate within the active site of Old Yellow Enzymes. Binding modes **(A)** "classical" and **(B)** "flipped" (from 180° rotation) rationalise reverse stereoselectivity of product formation from bioreduction.

Due to the high sequence homology between OYE1-3 (92% between OYE1 and OYE3, 80% between OYE1 and OYE3, 82% between OYE2 and OYE3)[120] limited examples of enzyme-based stereocontrol have been reported. One example however, has been noted entailing the bioreduction of dimethyl (*Z*)-2-butyramidofumarate with OYE3 affording the opposite enantiomer compared to OYE1-2.[118]

More commonly for OYE1-3 substrate-based tactics are employed, referred to as "substrate engineering". With this strategy the same enzyme is capable of catalysing product formation with an opposite configuration depending on the substrate undergoing the bioreduction. For example, OYE1-2 gives the (*S*)-enantiomer from methyl ketone substrate **7a** whereas the (*R*)-enantiomer is attained from the ethyl ketone substrate **7b** affording products (*S*)-**8a** and (*R*)-**8b** respectively (**Scheme 3**).[120] Product (*S*)-**8a** was afforded in excellent conversions of >99% with moderate *ee* of 56 – 61%.

Product (*R*)-**8b** was afforded in 67% conversion and 59% *ee* for OYE1, and 9% conversion and 76% *ee* for OYE2.

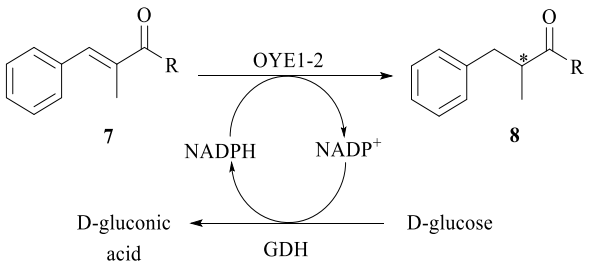

Substrate	R	Product
7a	Me	(*S*)-**8a**
7b	Et	(*R*)-**8b**

Scheme 3: Illustrative example of substrate engineering with OYE1-2 bioreduction of α-methyl-ß-phenyl enones **7a-b** producing respective products **8a-b** with opposite stereochemistries.

OYE homologue NCR possesses 31% sequence homology with OYE1 and has demonstrated a preference for cyclic substrates[124], unsurprising giving its natural substrate is cyclohex-2-en-1-one. Similar to OYE1-3, its *trans*-reduction catalytic mechanism entails a hydride (derived from the reduced FMN) transferred to Cβ of the substrate, with a proton from the catalytically active tyrosine residue (position 177) abstracted and added to Cα of the substrate.[124] In studies by Reich *et al.* Y177A mutant demonstrated catalytic activity, despite the catalytically active tyrosine residue being replaced by alanine.[124] It was presumed that when replacing the tyrosine residue the proton added to Cα of the substrate was ultimately derived from solvent in the active site. Decreased rates of bioreduction were observed, as well as decreased enantiospecificity.[124] No further information was provided on the structural positioning of substrates within the active site, or the structure-activity relationship between substrates and NCR.

Dynamic light scattering experiments have demonstrated that in solution NCR is monomeric, with the contact surface between monomers being small and non-functional, and interactions between monomers being hydrophilic with many bridging water residues.[124]

In the course of refining the structure of NCR (**Figure 8**), Reich *et al.* evaluated different electron density maps, each depicting a flat, ellipsoidal density positioned above the flavin ring of FMN.[124] As the shape suggested a substituted aromatic ring, a nicotinamide molecule was built into that density. The pyridine ring of the nicotinamide was observed to pack tightly into the flavin ring of the cofactor.[124] A substrate was not co-crystallised and so insight into the structural positioning of FMN and nicotinamide relative to each other and a substrate has yet to be provided.

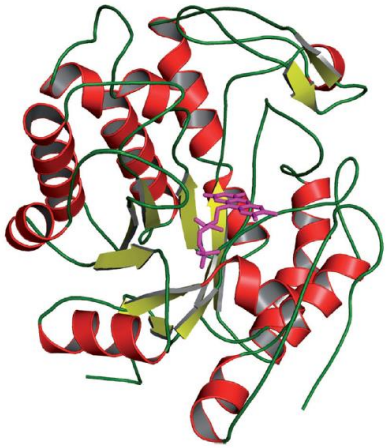

Figure 8: Crystal structure of NCR (PDB ID: 4A3U) in cartoon representation with prosthetic FMN (pink sticks), α-helices (red), β-sheets (yellow) and loop regions (green).[124]

1.2.1.3 Nicotinamide Cofactor Regeneration

With enzymes employed in the commercial synthesis of many chiral products produced on an industrial scale[125], enzymatic biotransformations are of significant industrial relevance. ERs, being a part of one of the largest classes of enzymes (oxidoreductases, ~25% of all enzymes)[126] represent notable commercial potential with their green, chemo- regio- and stereoselective generation of up to two chiral centres. As such, the industrial applications of ERs are currently being investigated.[127] One point of consideration though is their cofactor requirement. ERs utilise either NADH or NADPH as a cofactor, with greater success normally obtained with NADPH (**Figure 9**).[127] The stoichiometric supply of either, however, is not economically viable with a bulk price per mol of 3 000 USD and 215 000 USD respectively (2011).[128] As such, varying methods of cofactor regeneration have been investigated.

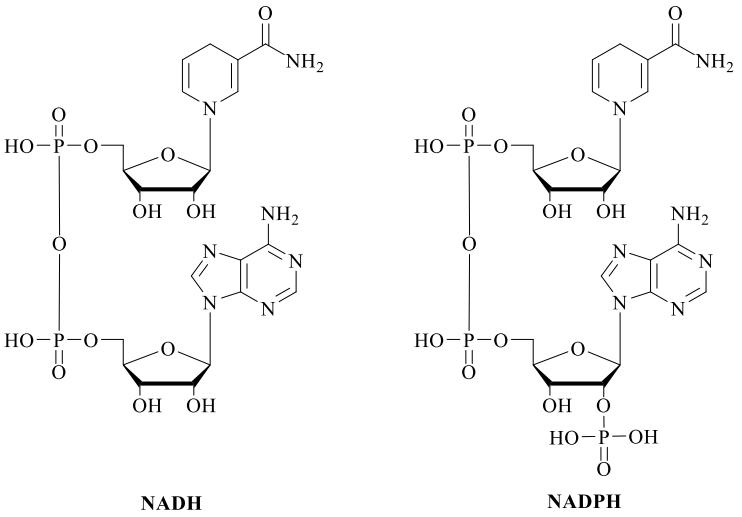

Figure 9: The structures of nicotinamide cofactors NADH and NADPH.

To date, a number of methods for nicotinamide cofactor regeneration have been described. They include: 1) Enzymatic regeneration (using enzymes and a sacrificial hydride donor)[59,129], 2) Chemical regeneration (using reducing salts/compounds such as sodium dithionite, sodium borohydride, or 1,4-dihydropyridine)[130,131], 3) Homogeneous catalytic regeneration (with Ru, Rh, or Ir complexes)[132,133], 4) Heterogeneous catalytic regeneration (using Pt/Al_2O_3)[134], 5) Electrochemical regeneration (using both direct regeneration on the electrode and indirect regeneration)[135], and 6) Photocatalytic regeneration (using copolymers and carbon nitride as a photocatalyst)[136,137]. Of these, enzymatic regeneration is the most successful and has been used at an industrial scale[126], with the others hindered primarily by their lack of efficacy, but also limited stabilities, compatibility (enzyme deactivation), low selectivity for the cofactor, high energy consumption, and downstream purification requirements.[138,139]

Enzymatic regeneration of the cofactor is performed by either a "coupled enzyme" or "coupled substrate" strategies. In a "coupled enzyme" approach, a recycling enzyme and excess of sacrificial hydride donor are employed to reduce $NAD(P)^+$ to NAD(P)H, thus recycling the cofactor (**Scheme 4A**). Common recycling enzymes include glucose dehydrogenase (GDH), formate dehydrogenase (FDH) and phosphite dehydrogenase (PDH) for NAD^+, whilst glucose-6-phosphate dehydrogenase (G6PDH) is utilised for $NADP^+$ recycling.[126,127] Among these recycling enzymes GDH and G6PDH possess the highest activity (550 U mg^{-1}, 1 U = 1 µmol min^{-1}) and stability and are the most

widely employed.[126,127] In a "coupled substrate" strategy, a single enzyme serves to both reduce the substrate for product formation and regenerate the cofactor (**Scheme 4B**). A notable example of this was described by Calvin *et al.* for the synthesis of the high-value drug precursor (*S*)-2-Bromo-2-cyclohexen-1-ol with an alcohol dehydrogenase (ADH) on a 100 g scale.[129] ADH oxidation of isopropyl alcohol served to reduce the nicotinamide cofactor (giving acetone as the by-product) whilst also reducing the substrate to afford the product in 88% yield and 99.8% *ee*. This approach afforded facile product recovery, however such systems typically require high concentrations of the sacrificial hydride donor which can lead to a loss in enzyme activity in the desired target reaction due to competition for the active site of the enzyme. As such "coupled enzyme" tactics are more widely employed.

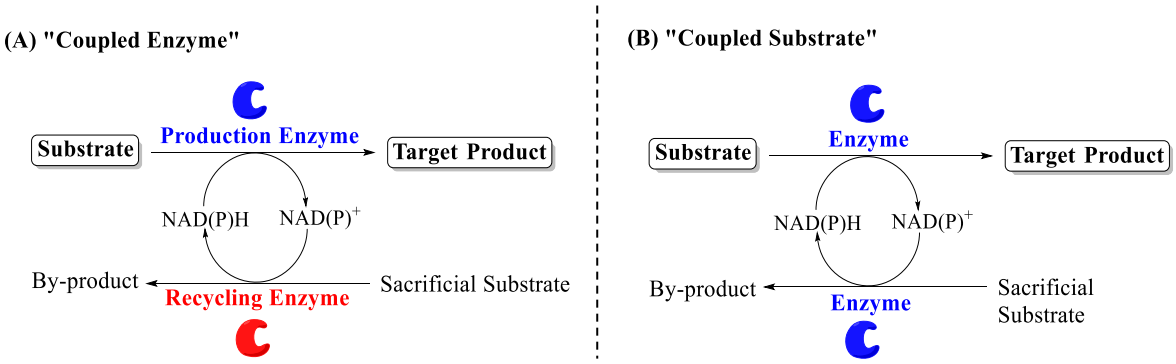

Scheme 4: Enzymatic regeneration of nicotinamide cofactor by **(A)** "Coupled enzyme" and **(B)** "Coupled substrate" tactics.

1.2.1.4 Comparison of Green Chemical and Biocatalytic Asymmetric Hydrogenation

The asymmetric reduction of unsaturated alkenes is of vital importance across the agrochemical, fine chemical and pharmaceutical industry, which rely heavily upon short, high yielding synthetic routes to enantiopure products.[125,127] Classically, chemical asymmetric hydrogenation is achieved catalytically with a soluble transition metal complex. The presence of a functional group close to the alkene is necessitated for coordination of the transition metal, akin to ERs requirement of an electron-withdrawing group for an activated alkene.[11,13,20,99] Reaction conditions typically involve the use of hydrogen and organic solvents at high pressure, with over-reduction a known side-reaction.[11,13,20]

Further challenges in chemical asymmetric hydrogenation arise from the limited applicability of a catalyst with a scope of alkene reagents. Thus, advancements in the

field are largely credited to the invention of new ligands, owing to their direct influence on the reactivity and enantioselectivity of the metal catalyst from their own electronic and steric properties.[11–15] In addition, single isomer chiral ligands for transition metal catalysts require stereoselective synthesis or can be obtained via the resolution of racemates.[140] When asymmetric chemical hydrogenation is successful though, excellent yields and *ee* can be achieved, as was observed in Knowles and Monsanto's industrially developed synthesis of L-DOPA, a drug for the treatment of Parkinson's disease (**Figure 10**).[141]

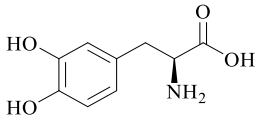

Figure 10: Structure of L-DOPA.

1.2.1.5 Commercial Outlooks

ERs belonging to the OYE family have been explored in biotransformations of α,ß-unsaturated aldehydes, ketones, carboxylic acids, esters, as well as terpenoids and nitroalkenes.[93,142] Their enantiopure products are employed commercially in fragrances, as well as intermediates in the industrial production of pharmaceuticals, fine chemicals and agrochemicals.

The olfactory properties of aldehydes make them of commercial importance in the manufacture of fragrances.[143] Bioreduction of unsaturated aldehydes **9a** and **9b** yielded (*S*)-enantiomers Lilial™ **10a** and Helional™ **10b** respectively, active olfactory principles in various perfumes.[144,145] Being marketed as "lily-of-the-valley" and "fresh marine" fragrances, a convenient means for their enantiopure preparation was developed biocatalytically with OYE1-3 (*Saccharomyces carlsbergensis*) in a bi-phasic system with *t*-butyl methyl ether/Tris buffer (20% v/v) (**Scheme 5**).[146] Products **10a** and **10b** were afforded in 84 – 99% conversion and 90 – 96% *ee*.

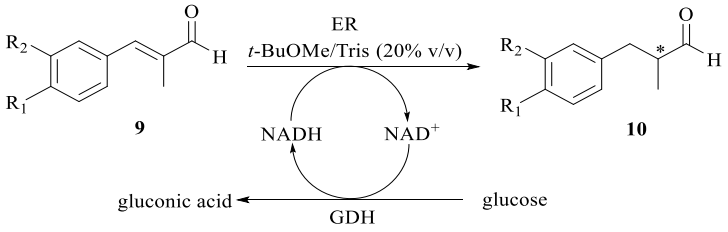

Substrate	R_1	R_2
9a	*t*-Bu	H
9b	OCH_2O	

Scheme 5: ER bioreduction of α-methylcinnamaldehyde derivatives **9a-b**.

Beyond fragrances, enantio-enriched products afford valuable chiral synthons in pharmaceutical applications. A prominent example includes the bioreduction of ketoisophorone **11** to afford (*R*)-levodione (*R*)-**12**, a precursor in the synthesis of carotenoids including zeaxanthin, cryptoxanthin and xanthoxin.[147] Carotenoids are primarily used as dietary supplements in the pharmaceutical industry.[148] A sequential one-pot enzymatic cascade was developed with OYE2 and levodione reductase (*Corynebacterium aquaticum* M-13). Hydrogenation of ketoisophorone **11** followed by carbonyl reduction of (*R*)-levodione (*R*)-**16** afforded the product actinol (4*R*,6*R*)-**13**, almost stoichiometrically in 94% *ee* (**Scheme 6**).[149]

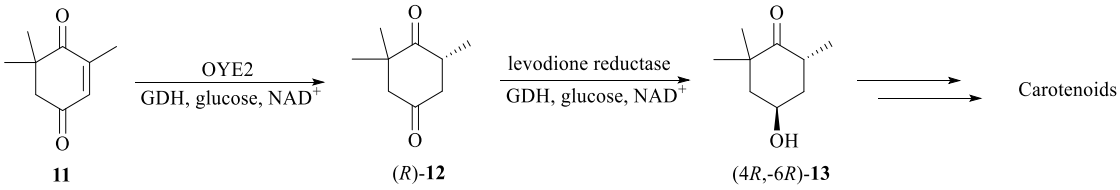

Scheme 6: Enzymatic cascade entailing ER bioreduction of ketoisophorone **11** to (*R*)-levodione (*R*)-**12** followed by levodione reduction to afford actinol (4*R*,-6*R*)-**13**.

(*R*)-3-Hydroxy-2-methylpropanoate or the "Roche ester" is a popular chiral building block with widespread applications including the synthesis of vitamin E, pharmaceuticals (eg. rapamycin) and natural products (eg. spiculoic acid A).[150–152] Recently, an efficient asymmetric bioreduction of hydroxyl protected 2-hydroxymethylacrylate derivatives **14a-c** for the preparation of the (*R*)-Roche ester **15a-c** was developed (**Scheme 7**).[153] Application of OPR1 (*Lycopersicon esculentum*) and XenA (*Pseudomonas putida*) ERs afforded products in good yields and >99% *ee*

(**Table 2**). Protection of the hydroxyl group was found to significantly enhance substrate acceptance.

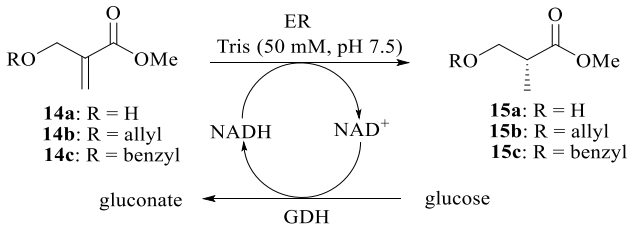

Scheme 7: Asymmetric bioreduction of methyl 2-hydroxy-methylacrylate derivatives **14a-c**.[153]

Table 2: Conversion, C (%) and enantiomeric excess, *ee* (%) of bioreduction products **15a-c**.[153]

	15a		**15b**		**15c**	
	C (%)	***ee* (%)**	**C (%)**	***ee* (%)**	**C (%)**	***ee* (%)**
OPR1	n.d.	n.d.	76	>99 (*R*)	84	>99 (*R*)
XenA	28	60 (*R*)	97	>99 (*R*)	90	>99 (*R*)

C = Conversion
n.d. = not determined

Terpenoids are a large and diverse class of natural products and provide access to many industrially relevant optically active compounds. For example, dihydrocarvone has demonstrated its applicability as a chiral synthon for natural products, antimalarial drugs and shape memory polyesters.[154–156] Whilst investigating substrate promiscuity and stereochemical outcome from a pentaerythritol tetranitrate reductase (PETNR) (*Enterobacter cloacae* st. PB2) bioreduction it was found that the asymmetric reduction of *rac*-carvone **16** furnished the same absolute (*R*)-configuration at the newly generated C-2 stereocentre yielding diastereoisomeric products (2*R*,5*S*)- and (2*R*,5*R*)-dihydrocarvone **17** respectively (**Scheme 8**).[157]

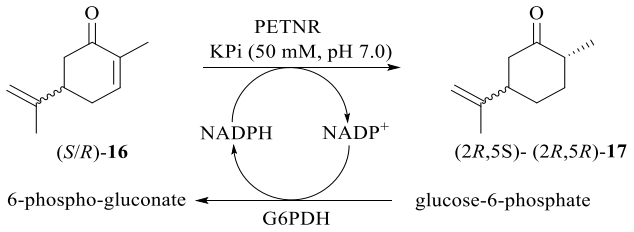

Scheme 8: Asymmetric bioreduction of terpenoid *rac*-carvone **16** yielding diastereoisomeric products (2*R*,5*S*)- and (2*R*,5*R*)-dihydrocarvone **17** respectively.

The bioreduction product of terpenoid (*E*/*Z*)-citral **18** provides access to the enantiomers of citronellal **19**, chiral intermediates in menthol synthesis. Whilst (*S*)-citronella (*S*)-**19** could be produced in excellent yields and *ee* from OPR1 and OPR3 with both (*E*/*Z*)-citral **18**, a maximum *ee* of 53% was obtained for (*R*)-**19** with EBP1 (*Candida albicans)* (**Scheme 9**).[98,116,158] The importance of using purified enzymes was exemplified as application of whole-cells or clarified lysates resulted in over-reduction of the product to corresponding saturated alcohol.[98,158]

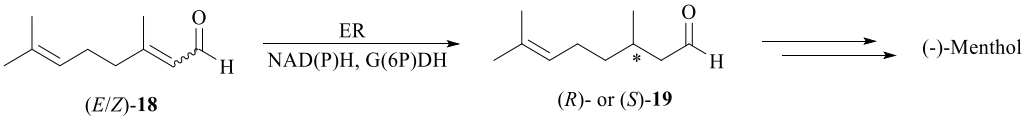

Scheme 9: Bioreduction of (*E*/*Z*)-citral **18** to afford (*R*)- or (*S*)-citronellal **19**.

Whilst the industrial employment of ERs is still in its infancy, its potential applications are increasingly being explored. Recently Almac, a drug development company, investigated the sequential one-pot biocatalytic cascade with an ER and hydrolase for the asymmetric synthesis of (*R*)-**22**, an intermediate of interest in a complex convergent synthesis (**Scheme 10**).[159] A 70 g scale reaction was successfully undertaken, with a 98% conversion of (*R*)-**21** from **20** and the desired monoacid (*R*)-**22** isolated in 89% yield.

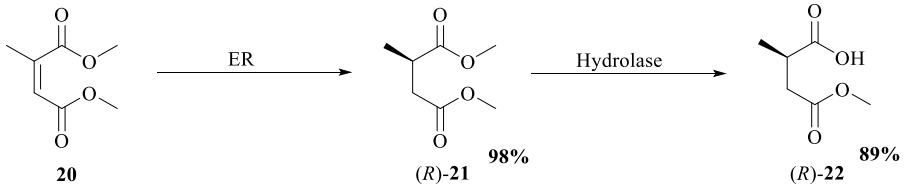

Scheme 10: Biocatalytic route to monoacid (*R*)-**22** via ER and hydrolase enzymes.

1.2.1.6 Recent Relevant Research for Ene-Reductases in Relation to this PhD

In relation to the PhD work carried out, that of Brenna *et al.* in 2013[120] and Crotti *et al.* in 2019[160] is particularly of note. The author will first describe the work of Brenna *et al.* in 2013 and then that of Crotti *et al* in 2019. Brenna *et al.* reported substrate-based stereocontrol in the biotransformation of methyl- and ethyl ketone derivatives **7a-b** with OYE1-3 (**Scheme 11**), affording the (*S*)-enantiomer with methyl ketone derivative (*S*)-**8a** and (*R*)-enantiomer with ethyl ketone derivative (*R*)-**8b** (**Table 3**). The

biotransformation of **7b** with OYE3 did not furnish the (*R*)-enantiomer, however, instead retaining (*S*)-enantioselectivity.[120]

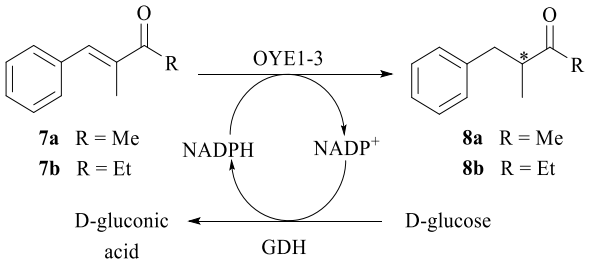

Scheme 11: OYE1-3 biotransformation of methyl and ethyl ketone derivatives **7a-b** producing respective products **8a-b**.[120]

Table 3: Conversion (%) and ee (%) from bioreduction of methyl and ethyl ketone derivatives **7a-b** with OYE1-3.[120]

		7a		**7b**	
		C (%)[a]	***ee (%)***[b]	**C (%)**[a]	***ee (%)***[b]
ER	**OYE1**	>99	56 (*S*)	67	59 (*R*)
	OYE2	>99	61 (*S*)	9	76 (*R*)
	OYE3	>99	98 (*S*)	14	89 (*S*)

[a] Conversion (%) determined by GC-MS.
[b] Enantiomeric excess determined by GC analysis with a chiral stationary phase.

Due to the high sequence homology between OYE1-3[120], it was postulated that substrate-based stereocontrol still prevailed, with an alternative binding mode achieved by OYE3. Following Brenna *et al.*'s report, molecular dynamic simulations by Powell *et al.* supported this hypothesis by differences in the conformations of loop 6 in solution.[161] Specifically, loop 6 closure over the active site of OYE1 was suspected to generate a greater number of active site residue contacts for the bound substrate of OYE1 compared to OYE3, thus influencing binding mode. This difference was used to rationalise substrate-based stereocontrol, with the nearly identical X-ray crystal structures of OYE1 and OYE3 also cited as evidence.

Later in 2019, further work by Crotti *et al.*[160] explored the bioreduction of methyl and ethyl ketone derivative substrates **7a-b** with a larger panel of wild type OYE homologues (**Table 4**). For the majority of ERs, the change from a methyl to ethyl ketone derivative furnished poor conversions and shift from (*S*)- to (*R*)-stereoselectivity. Application of OYE1 and OYE2.6 afforded good conversions but

formed (*R*)-**8b**, whilst LtB4DH afforded the (*S*)-enantiomer product (*S*)-**8b**, like OYE3, but with a very poor *ee* of 10%.[162]

Table 4: Conversion (%) and *ee* (%) from bioreduction of methyl and ethyl ketone derivatives **7a-b** with wild-type ERs.[120,160]

		7a		**7b**	
		C (%)[a]	***ee (%)***[b]	**C (%)**[a]	***ee (%)***[b]
ER	**OYE1**[c]	>99	56 (*S*)	67	59 (*R*)
	OYE2[c]	>99	61 (*S*)	9	76 (*R*)
	OYE3[c]	>99	98 (*S*)	14	89 (*S*)
	NemA[d]	53	58 (*S*)	16	66 (*R*)
	OPR1[d]	1	n.d.[e]	--	--
	OYE2.6[d]	>99	82 (*S*)	>99	99 (*R*)
	PpNemA[d]	7	66 (*S*)	--	--
	LeOPR1[d]	2	n.d.[e]	5	30 (*R*)
	KmOYE[d]	>99	18 (*S*)	8	88 (*R*)
	LtB4DH[d]	>99	14 (*S*)	68	10 (*S*)
	PpOYE[d]	1	n.d.[e]	--	--

[a] Conversion (%) determined by GC-MS.
[b] Enantiomeric excess determined by GC analysis with a chiral stationary phase.
[c] Reported by Brenna *et al.*[120]
[d] Reported by Crotti *et al.*[160]
[e] Not determined.

In efforts to furnish the (*S*)-product from bioreduction of ethyl ketone derivative **7b** in good yield, structural and docking studies by Crotti *et al.*[160] along with complementary computational studies of OYE1 by Powell *et al.*[161], Walton *et al.*[163] and Pompeu *et al.*[164] informed the semi-rational design of three OYE1 mutants by site-directed mutagenesis at positions F296 and W116. All 3 mutants from the study performed by Crotti *et al.* successfully attained the (*S*)-enantiomer product (*S*)-**8b** from a bioconversion of **7b** with up to 96% *ee*, but at the expense of conversion with a maximum of 19% (**Table 5**).[160] Due to the low yield, the effort was not entirely fruitful.

Table 5: Conversion (%) and *ee* (%) from bioreduction of methyl and ethyl ketone derivatives **7a-b** with OYE1 mutants.[160]

		7a		**7b**	
		C (%)[a]	***ee (%)***[b]	**C (%)**[a]	***ee (%)***[b]
ER	**OYE1 F296S**	99	94 (*S*)	6	44 (*S*)
	OYE1 F296S/W116A	35	90 (*S*)	18	96 (*S*)
	OYE1 F296S/W116V	57	94 (*S*)	19	94 (*S*)

[a] Conversion (%) determined by GC-MS.
[b] Enantiomeric excess determined by GC with a chiral stationary phase.

To the best of the author's knowledge, the ER bioreduction of α-hydroxy ketone derivatives (**Figure 11**) has not been reported. The work in this thesis will explore this motif as a substrate for ERs, with yields and *ee* determined. Prior to the analysis of α-hydroxy ketones, aldehyde and ketone derivatives will be explored for the step-wise increase in chemical complexity. In this PhD this is termed as "substrate walking". Whilst the selectivity of ketone products from bioreduction was not determined in this work, evidence of substrate-based stereocontrol moving from ketone to α-hydroxyketone derivatives has been suggested in preliminary reports with some ERs investigated and is described in further detail in section 4.2.2. This is akin to the change in selectivity for methyl ketone **7a** and ethyl ketone **7b** in bioreductions with OYE3.

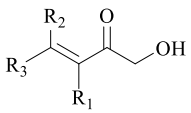

Figure 11: General structure of α-hydroxy ketone derivative.

1.2.2 Transaminases (TAms)

Belonging to the family of pyridoxal 5'-phosphate (PLP) dependent enzymes, Transaminases (TAms), also known as aminotransferases, catalyse the enantioselective transfer of an amino functional group from an amine donor to an aldehyde or keto-acceptor, thus generating a primary amine or optically active amine product, respectively. Due to the transfer of the amino group TAms are classified as transferases (EC2) by the Enzyme Commission.[165,166] PLP dependent enzymes are divided into 7 different fold types, with TAms present in fold types I and IV.[165] Enantioselectivity arises from these fold types, as described below.

1.2.2.1 Classification of Transaminases

The classification of TAms has developed over the years on the premise of both their activity and structure. In the 1980s, a general classification was established on the basis of enzymatic activity, with TAms divided into one of two groups, α and ω (**Table 6**).[167,168] TAms that were found to transfer an amino group at the α-carbon to a carboxyl moiety were deemed α-TAms, whilst ω-TAms were known to transfer a distal amino group (β- or γ- of a carboxyl moiety) or else catalyse the transamination of a substrate not bearing a carboxyl group.[165,169] Thus, α-TAms accepted amino and keto-acids whereas ω-TAms accepted amine donors with amino groups β- and γ- to a carboxyl moiety, as well as "simple" amine donors and keto-acceptors. Due to the lack of substrate restrictions for ω-TAms their application is more widespread than their α-TAms counterparts and has made them a central tool in the field of biocatalysis.

In 1993, Mehta *et al.* presented the first structural classification of TAms on the basis of sequence homology, hydropathy patters and secondary structure predictions.[170] Their work analysing 32 TAms provided four distinct sub-goups: Class I, II, III and IV. In 2005, Pfam, a widely used protein database, revised this classification dividing Class I into Class I and II, as well as adding a further group known as "sugar amino-transferases" (Class VI) (**Table 6**).[166] Both functional and structural classification systems are employed today, with an emphasis on structural classification when it is known.

Table 6: Stuctural and functional classifications of TAm members.[166,170]

Mehta Class	Pfam Class	Specificity	TAm Members
I	I & II	α	Aspartate TAm
		α	Alanine TAm
		α	Aromatic TAm
		α	Histodinal phosphate TAm
II	III	ω	Acetyl ornitihine TAm
		ω	Ornithine TAm
		ω	ω-Amino acid TAm
		β	β-Aminocarboxylic acid TAm
		γ	γ-Aminobutyrate TAm
		ω	Diaminopelargonate TAm
III	IV	α	D-Alanine TAm
		α	Branched chain TAm
IV	V	α	Serine TAm
		α	Phosphoserine TAm
--	VI	--	TDP-4-amino-4,6-dideoxy-D-glucose TAm
		--	L-Glutamine:Scyllo-inosine aminotransferase
		--	TDP-3-keto-6-D-hexose-aminotransferase

1.2.2.2 Stereochemistry and Stereocontrol

As earlier in section 1.2.2, the class of ω-Transaminases (ω-TAms) in conjunction with the co-enzyme PLP, mediate the stereoselective transfer of an amino group from an amine donor to a keto acceptor, whereby at least one of the two participants is not an α-amino acid or α-keto acid. As optically pure amines are highly valuable synthons in bioactive compounds, ω-TAms present an efficient means for their preparation.

A definitive detailed mechanism for ω-TAm has not been established, however due to similarities between ω-TAms and aspartate transaminases a similar mechanism operating via two half-transamination reactions in a bi-bi ping pong mechanism has been described in the literature (**Figure 12**).[70,171,172]

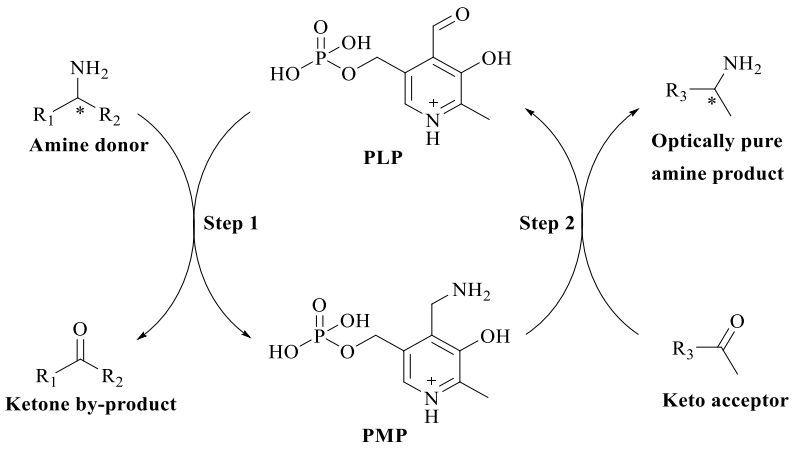

Figure 12: Overview of the transamination reaction catalysed by TAm-PLP consisting of two half-transamination reactions: 1) The oxidative deamination of the amine donor 2) The reductive amination of the keto acceptor.

In the first half-transamination, a Schiff base linkage is formed between the aldehyde of PLP and ε-amino group of a lysine specific to the ω-TAm (internal amino group) thereby giving an internal aldimine. Following this transaldimination occurs, whereby the amino group of an external amine donor displaces the ε-amino group of the internal aldimine hence producing an external aldimine. It is proposed that the lysine residue then acts as a base, abstracting a proton to give a planar quinoid intermediate and then subsequently protonating at an alternate position to produce a ketimine. Hydrolysis follows, resulting in release of the corresponding ketone of the amine donor (here acetone) and pyridoxamine-5′-phosphate (PMP) (**Scheme 12**). Completion of the catalytic cycle with the second half reaction entails reversal of the first half with a keto acceptor, hence resulting in enantioselective amino transfer and the regeneration of PLP.

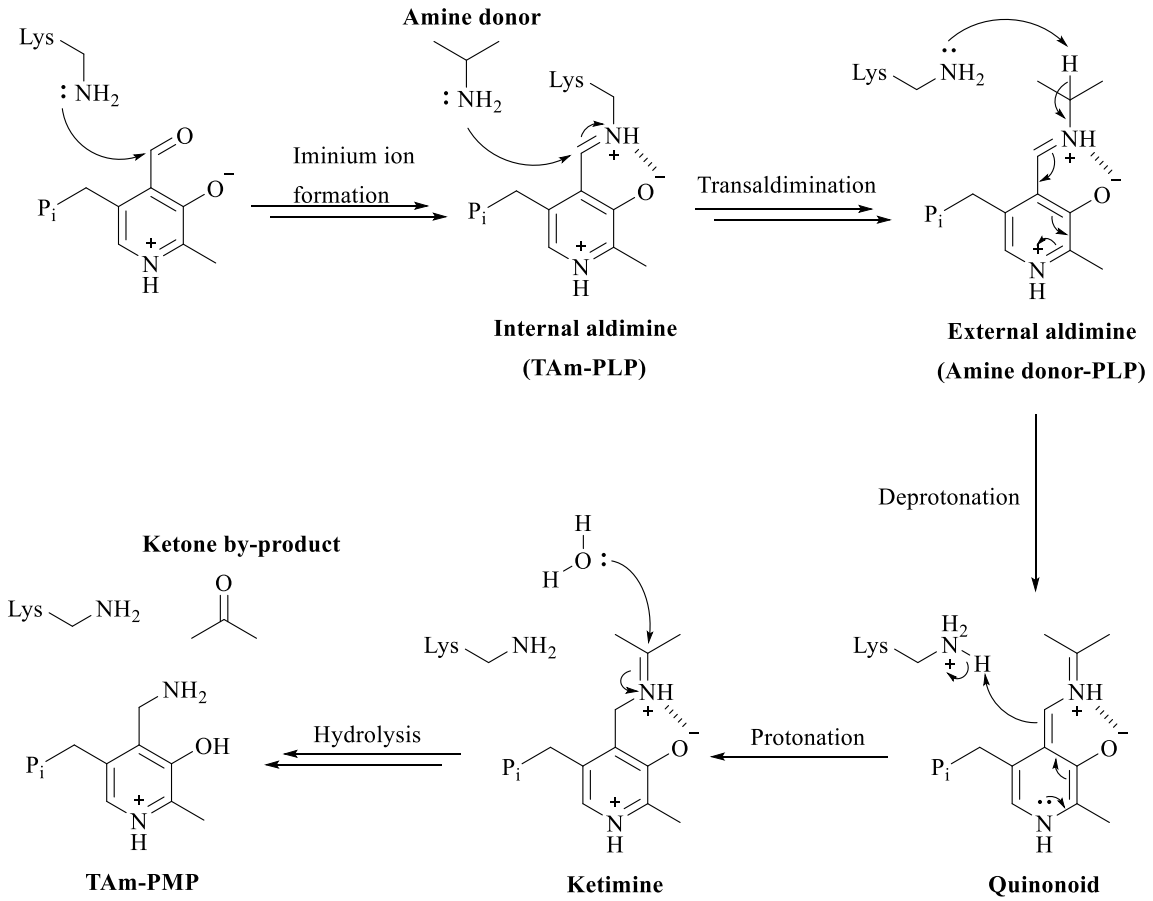

Scheme 12: Proposed mechanism for the first half-transamination, oxidative deamination of amine donor, isopropylamine (IPA). As a result IPA is converted into corresponding ketone by-product, acetone, whilst PLP is converted into PMP.

The enzyme active site plays an important role in stereocontrol for ω-TAm transamination. Specifically, enantiopreference may be attributed to the position of the catalytic lysine on either the *si*- or *re*-face of PLP during the second half-transamination reaction, reductive amination of the keto-acceptor (**Scheme 13**).[173–176] (*S*)-selective ω-TAms possess catalytic lysine on the *si*-face affording (*S*)-enantiomers (or L-amino acids) while conversely (*R*)-selective ω-TAms possess the catalytic lysine on the *re*-face affording (*R*)-enantiomers (or D-amino acids). In addition, (*S*)- and (*R*)-selective ω-TAms belong to different folding classes (I and IV respectively) thereby discouraging alternate substrate binding modes.[170,173,177]

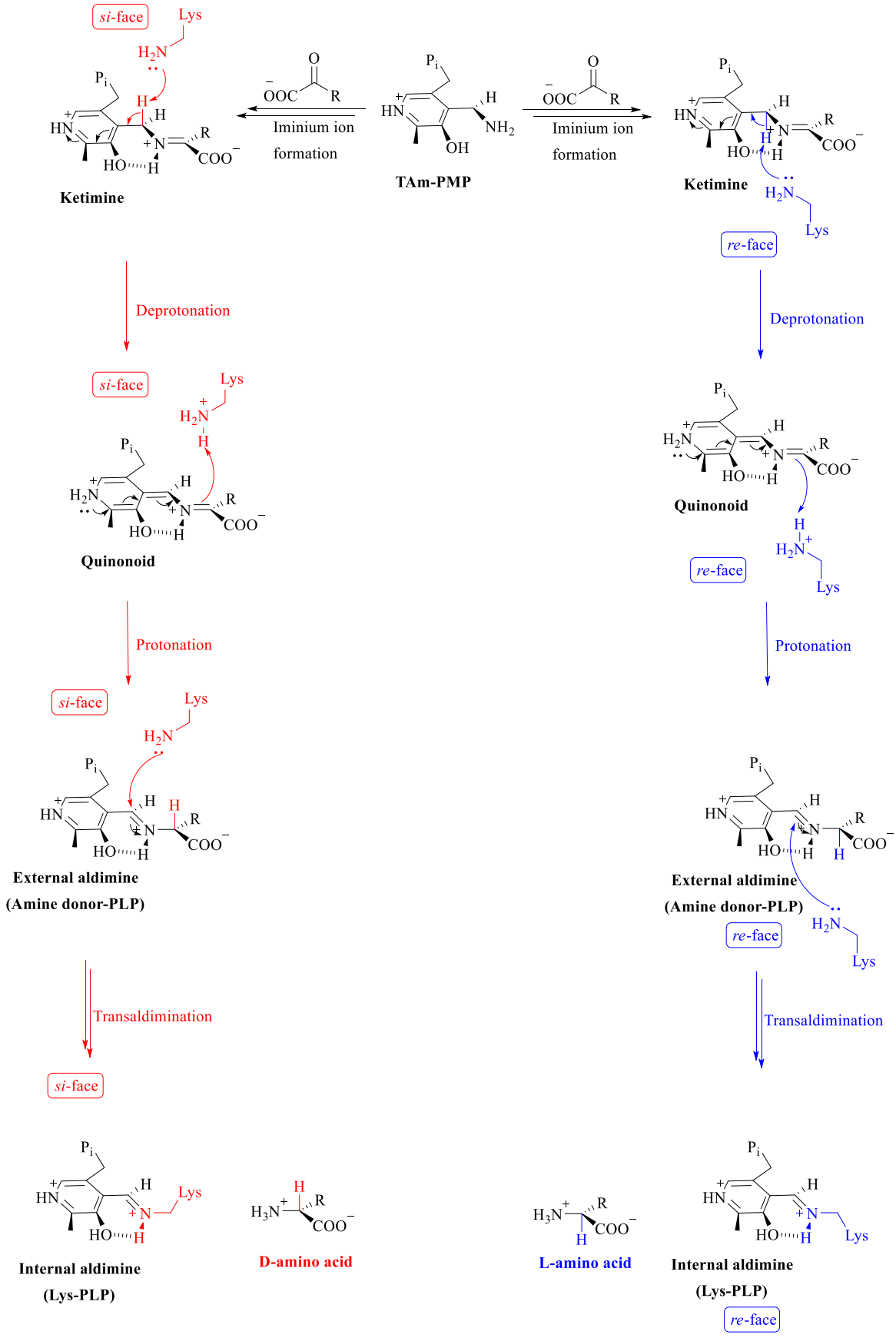

Scheme 13: Stereocontrol of (*S*)- and (*R*)-selective TAms depending on the position of catalytic lysine on *si*- or *re*-face respectively. (*S*)- and (*R*)-selective TAms afford D- and L-amino acids respectively.

One of the first ω-TAms explored in academia was (*S*)-selective Vf-TAm (*Vibrio fluvialis* JS17)[178], which has since become one of the most widely investigated.[179–181] A BLASTP search of the sequence of Vf-TAm led to the discovery of Cv-TAm (*Chromobacterium violaceum* DSM30191) possessing 38% sequence homology.[182] With respect to wild-type (*S*)-selective ω-TAms, Cv-TAm has been acknowledged as a "gold standard" due to its substrate promiscuity and high stereoselectivity.[182]

(*R*)-selective TAms are less commonplace than their (*S*)-selective counterparts, with the first identified in 2003 from *Arthrobacter sp.* KNK168[183] exhibiting activity with a range of substrates.[184] In 2010, Hohne *et al.* pursued the identification of other (*R*)-selective TAms using a rational design *in silico* sequence-based prediction strategy.[185] Their efforts furnished 17 (*R*)-selective TAms demonstrating activity with a scope of substrates with up to 99% *ee*. Research into the discovery and engineering of ω-TAms, especially those to accept bulky substrates, has continued with a growing number being identified.[186–189]

One of the TAms identified by Hohne *et al.*, Mv-TAm, (*Mycobacterium vanbaalenii*)[185] is employed in Chapter 5 and Chapter 6 of this thesis. To the best of the author's knowledge a crystal structure of Mv-TAm was not available in the literature at the time of writing, and so no further structural and mechanistic information can be described.

1.2.2.3 Equilibrium Limitations

In practise ω-TAm biotransformations in asymmetric synthesis are hindered due to challenges pertaining to reaction equilibrium and inhibition by substrates or ketone by-products formed during the first half-transamination.[172,190] Specifically, the equilibrium of the first half-transamination resides on the side of the starting material making the biotransformation unfavourable.[190] Thus, the predominant strategy for shifting the reaction equilibrium is two-fold: 1) Applying a significant excess of amine donor and 2) Removal of the ketone by-product.[191–193]

Typically aliphatic or benzylic amines such as isopropyl amine (IPA) and α-methylbenzylamine (α-MBA) are utilised as amine donors as they offer a more favourable thermodynamic equilibrium.[190,193] Whereas the equilibrium with MBA favours product formation more than that of IPA, IPA presents the additional advantages of being achiral and giving a volatile ketone by-product, acetone, following

the first half-transamination.[194] The volatility of acetone provides a facile method for removal of the ketone by-product, not only preventing ω-TAm inhibition but also shifting the reaction equilibrium to product formation. Unfortunately, IPA is not a broadly accepted amine donor, and the significant excess required for a more favourable equilibrium can result in the denaturation of the ω-TAm.[192,195,196] Therefore, the instability of ω-TAms in the presence of a significant excess of amine donor as well co-solvent requirements for substrate solubilisation present challenges in ω-TAm application.

Recently, a variety of "smart" amine donors have been explored to shift the thermodynamic equilibrium to product formation (**Scheme 14**).[197–202] Their means of shifting the equilibrium vary slightly, but all entail the spontaneous tautomerization/reaction of the ketone by-product to preclude the reverse TAm transamination. In spite of this benefit, the application of "smart" amine donors is not widely employed owing to the downstream processing and purification required for product isolation. Additionally, the cost of some of the donors is prohibitive. As such, application of IPA as the amine donor for transamination is still primarily pursued.

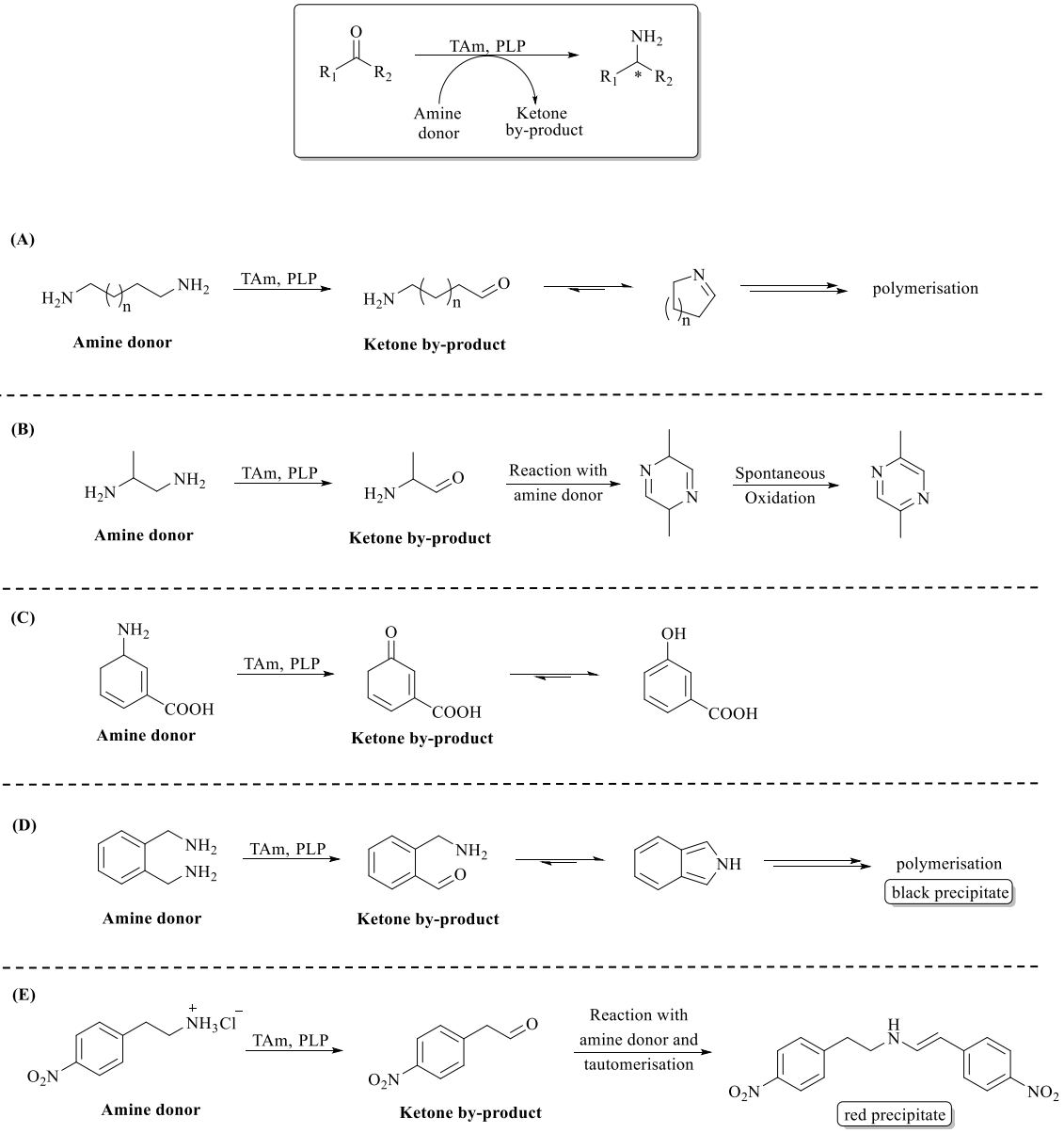

Scheme 14: Application of "smart" amine donors for transamination. **(A)** Slabu *et al.* and Gomm *et al.* presented transamination using diamines with subsequent intramolecular cyclisation and irreversible polymerisation.[197,198] **(B)** Payer *et al.* presented transamination using diamines with subsequent dimerization and spontaneous oxidation.[199] **(C)** Wang *et al.* presented the tautomerisation of the ketone by-product to its more stable form.[200] **(D)** Green *et al.* presented transamination using aromatic diamines with subsequent spontaneous cyclisation, tautomerization, and irreversible polymerisation.[201] **(E)** Baud *et al.* presented transamination using an aromatic amine donor with subsequent reaction with excess amine donor and tautomerization to afford a coloured product.[202]

Recently, twenty-nine robust TAms were sequenced and cloned by the Hailes and Ward groups. Twelve of these TAms demonstrated activity with a range of substrates and one of which was found to be especially robust: tolerance of up to 50% DMSO without a decrease in efficacy was observed, as well as stability at a range of temperatures (20 – 60 °C) and pH values (6 – 11).[67] Notably, relative activity with one equivalent of IPA

was found to be comparable with that of fifty equivalents. As such, 3 of these metagenomic enzymes cloned from pQR2189, pQR2191 and pQR2208 will be explored in this work. Further information about these enzymes is discussed in later chapters.

1.2.2.4 Comparison of Green Chemical and Biocatalytic Synthesis of Amines

Amines represent a valuable chemical moiety in the pharmaceutical industry, with >90% of small molecule drugs possessing a nitrogen atom[79] and approximately 40% of pharmaceuticals containing a chiral amine scaffold.[203,204] A variety of synthetic chemical means are available to access amines, specifically the reduction of nitrogen containing functional groups (amide, azide, cyano, nitro), reductive amination of carbonyls, nucleophilic substitution of primary alkyl halides, as well as established reactions including the Hofmann rearrangement, Curtius rearrangement and Staudinger reaction. Of these reactions, reductive amination remains of primary importance as it affords the opportunity to generate chirality from a prochiral source, with the asymmetric reductive amination of carbonyls cited as an "aspirational reaction" by the ACS GCI Pharmaceutical Roundtable.[19] The first asymmetric reductive amination was developed by Blaser is 1999[205], but offerings in the interim have been distinctly lacking owing to side-reactivity of the transition metal hydride catalysts with ketones (alcohol by-product formation) or else catalyst inhibition from either the amine reagent or product.[21] Alternative approaches have been presented, but these include multi-step procedures under harsh conditions with heavy metal catalysts.[21] Thus, the green asymmetric introduction of an amino group by chemical means is underdeveloped.

In recent years biocatalysis has been investigated to fulfil this need, due to its chemo-, regio- and stereoselectivity under mild non-hazardous conditions. A variety of enzymes have been recognized to afford chiral amines either by asymmetric synthesis or chiral resolution. They include transaminases[67,193], amine dehydrogenases[206,207], imine reductases[208,209], monoamine oxidases[210,211], and lyases[212,213] (**Figure 13**). Of these, transaminases have amassed significant interest, with recognised applications in industrial settings.[214] Compared to imine reductases and amine dehydrogenases they offer the notable advantage of not requiring an NAD(P)H cofactor.[203] Additionally, they do not have the restrictions of lyases (requiring 7-methylideneimidazole-5-one (MIO) cofactor and a substrate with carboxyl moiety) and operate by asymmetric

synthesis theoretically affording 100% yield, unlike the chiral resolution of monoamine oxidases.

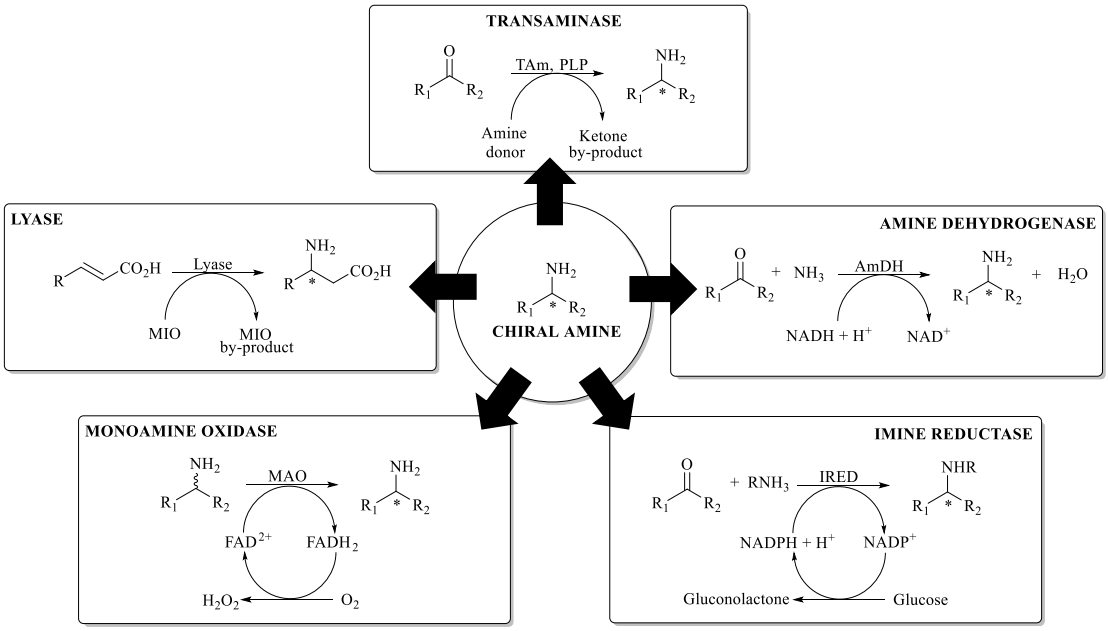

Figure 13: Biocatalytic means for the synthesis of enantiopure amines including the application of transaminases, amine dehydrogenases, imine reductases, monoamine oxidases, and lyases.

1.2.2.5 Commercial Outlooks

ω-TAms have been applied to an extensive scope of aliphatic and aromatic substrates. Due to their (*S*)- or (*R*)-selectivity, their applications include kinetic resolution of racemic amines and asymmetric synthesis with prochiral carbonyls.

Whilst kinetic resolution with TAms can only theoretically achieve up to 50% yield, development of resolution processes can provide complete deracemisation yielding a single enantiomer. This was achieved in the preparation of (*R*)-mexiletine, an antiarrhythmic agent, by employing stereocomplementary ω-TAms (**Scheme 15**).[215] For the preparation of (*R*)-mexiletine (*R*)-**23** from its racemic mixture, an (*S*)-selective TAm was first utilised for kinetic resolution. This provided the unreacted (*R*)-**23**, as well as forming the corresponding ketone **24**. Application of a (*R*)-selective TAm transformed the ketone to (*R*)-**23** affording the enantiopure product in 97% yield and >99% *ee*.

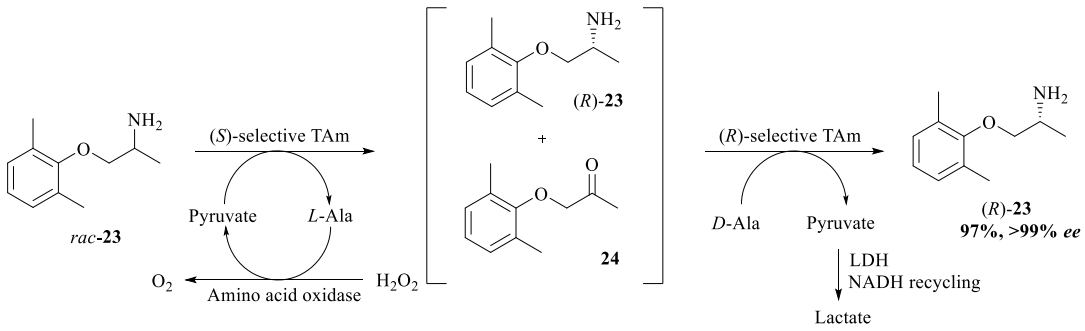

Scheme 15: Deracemization of *rac*-mexiletine *rac*-**23** by sequential one-pot TAm kinetic resolution.

In 2014 promising results from Pfizer's phase 1 clinical trials necessitated a practical scalable synthesis of a potent inhibitor of the smoothened receptor (SMO) in the hedgehog signalling pathway (a novel target for cancer therapeutics).[216] Previous synthetic routes were not viable for industrial application, being low yielding and suffering from safety concerns on large scale preparation (specific concerns were not noted). As such, enzymatic transamination was pursued due to the significant advantages it presented over traditional chemical synthesis.

With the key synthetic challenge being the establishment of *anti* stereogenic centres on the piperidine ring, it was envisaged that a stereoselective TAm biotransformation in conjunction with a dynamic kinetic resolution of **25** would concurrently establish the two stereogenic centres in a single step (**Scheme 17**). Racemisation via dynamic kinetic resolution of 2-aryl-4-piperidones had previously been reported in the literature (**Scheme 16**).[217]

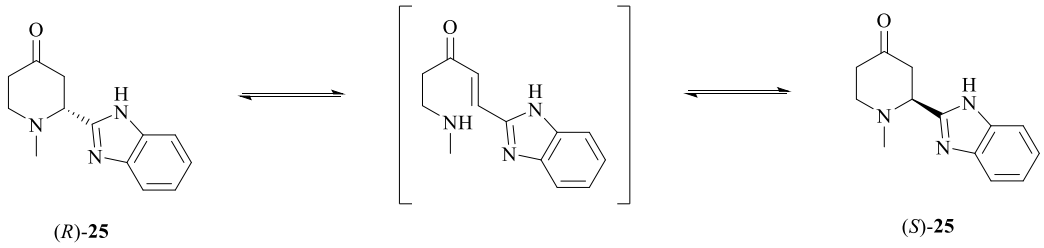

Scheme 16: Racemisation of **25** via dynamic kinetic resolution.

Success of the biocatalytic route with the commercial ω-TAm ATA-036 yielded the desired *anti* amine **26** in an *anti*:*syn* ratio of > 10:1 and >99% *ee*. SMO inhibitor **27** was afforded in 5 synthetic steps without the need for chromatographic purifications.

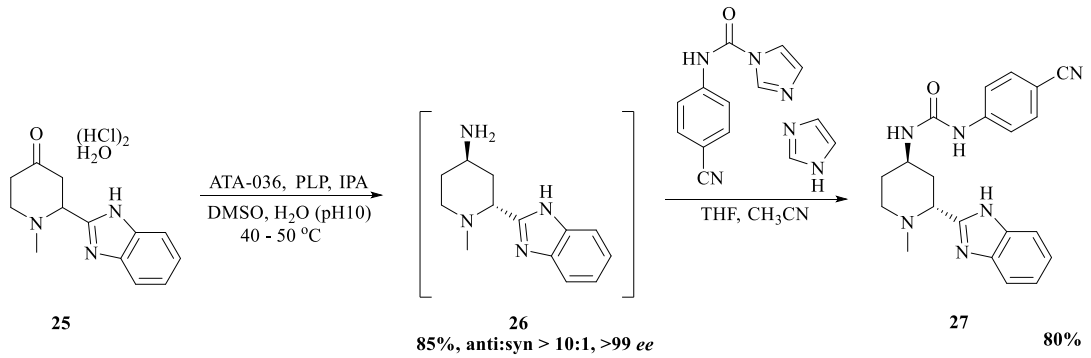

Scheme 17: Biocatalytic synthesis of the smoothened receptor inhibitor **27**.

Furfurals, attained from processing of cellulosic biomass waste, have received interest in recent years as they represent a valuable chemical platform derived from renewable feedstocks such as lignocellulosic biorefineries, food crop residues and wood wastes.[218,219] Namely, furfurylamines are a useful scaffold for the potential production of pharmaceuticals and polymers.[220,221] Due to the sensitivity of the furan ring under reductive conditions, traditional chemical synthesis of furfurlamines from furfurals is challenging. Thus, the application of ω-TAms for the enzymatic animation to afford furfurylamines in good yields under mild conditions was investigated.[193]

ω-TAm biotransformation was investigated on a preparative scale (20 mM) with Cv-TAm (from *Chromobacterium violaceum* DSM30191) and IPA. Furfurylamines **28**, **29** and **30**•HCl were afforded in 83%, 54% and 31% yields respectively (**Figure 14**).

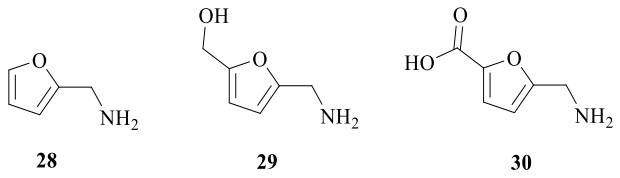

Figure 14: Furfurylamines **28-30** attained from preparative scale ω-TAm biotransformation of the corresponding furfurals.

TAms employment in pharmaceutical syntheses has become increasing commonplace. A notable example includes the asymmetric synthesis of the Merck's Sitagliptin, a drug for the treatment of Type II diabetes. The chemocatalytic manufacturing process of Sitagliptin included asymmetric hydrogenation at high pressure (250 psi) with a costly rhodium chiral catalyst, a process suffering from insufficient stereoselectivity and

rhodium contamination of the product (**Scheme 18**).[35,222] As a result additional purification was required, sacrificing yield for an improved chemical purity and enantiomeric excess (*ee*).[35] Merck's answer for a more efficient, economical, and environmentally benign process was the application of a TAm, yielding the enantiomerically pure product **31** with a yield increased by 10 – 13%.[222]

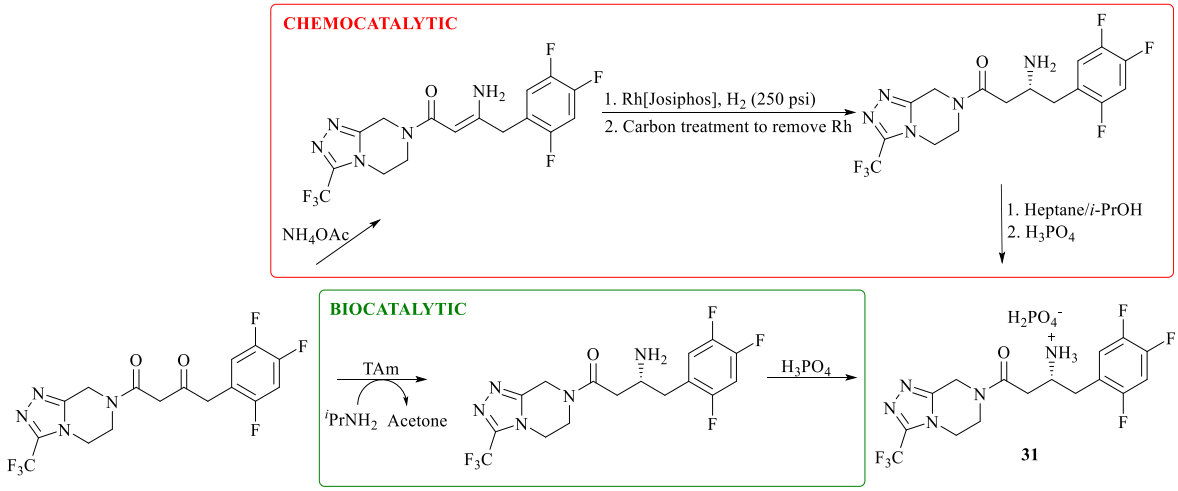

Scheme 18: Chemocatalytic and biocatalytic synthesis pathways of Sitagliptin phosphate **31**.

1.2.2.6 Recent Relevant Research for Transaminases in Relation to this PhD

To the best of the author's knowledge the TAm biotransformation of α-hydroxy ketone derivatives has not been reported. For this work it will be noted that there is currently only one recently published (2015) biocatalytic ER-TAm cascade yielding diastereomerically enriched amines (**Scheme 19**).[223] OYE3 was screened with commercially available TAms in a sequential one-pot cascade, first reducing **32** to give **33** which then underwent enzymatic amination to afford optically pure (2*R*,3*S*)-**34** in high *de* and conversion (**Table 7**).

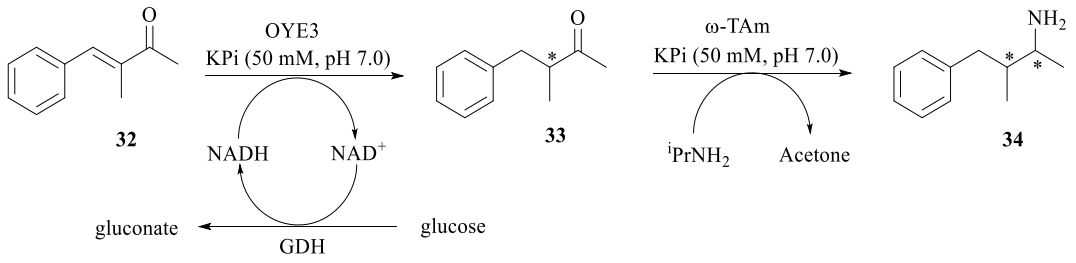

Scheme 19: Biocatalytic ER-TAm cascade for the biotransformation of **32** to **34** via **33**.

Table 7: Conversion (%) and *de* (%) provided by commercial TAms from the sequential one-pot ER-TAm cascade with **33**.

ω-TAm	**Conversion (%)**	***de* (%)**
ATA-025	>99	96 (2*R*,3*S*)-**34**
ATA-113	>99	>99 (2*S*,3*S*)-**34**
ATA-237	>99	95 (2*S*,3*S*)-**34**
ATA-251	>99	98 (2*S*,3*S*)-**34**
ATA-256	>99	96 (2*S*,3*S*)-**34**

1.3 Aims

With the advent of green chemistry and sustainability, a shift in paradigm has developed focused on the reduction of hazards, waste, and energy during production, as well as consideration of life cycle environmental impacts. Biocatalysis, operating with catalytic ability, chemo-, regio- and stereoselectivity under mild and non-hazardous conditions has emerged as a forerunner in the field of green chemistry, surpassing many traditional synthetic chemistry approaches (transition metal catalysis and reductive amination) and becoming a powerful tool in the synthetic design of chiral synthons and bioactive molecules.

The work presented in this thesis aimed to develop a biocatalytic ER-TAm cascade using α-hydroxyketone derivatives for the molecular assembly of diastereomerically enriched amino alcohols with potential applications in the synthesis of bioactive molecules. To date, the α-hydroxyketone motif has not been explored with ERs or TAms, though structurally similar and less chemically complex aldehyde and ketone motifs have. Therefore, substrate walking strategies (the step-wise increase in the chemical complexity of substrates) were adopted to evaluate the tolerance of novel and literature enzymes with new motifs, as well as afford opportunities to compare the efficacy of new ERs against those used in the literature.

To date, α,β-unsaturated aldehyde, ketone, ester and nitrile motifs have previously been explored with ERs. Therefore, evaluation of the α-hydroxyketone motif would potentially afford a new class of substrates accepted, thereby broadening substrate scope. In addition, previous work by Brenna *et. al.*[120] and Crotti *et. al.*[162] using wild-type OYE1 rationalised substrate-based stereocontrol between methyl and ethyl ketone substrates **7a – b** affording (*S*)- and (*R*)-products respectively. This work aimed to examine if substrate-based stereocontrol still prevailed with the hydroxyl group from the α-hydroxyketone present in place of the alkyl group (ie CH_2OH from the α-hydroxyketone vs CH_2CH_3 from **7b**).

Ene-reductases, operating by a stereospecific [2H] *trans*-reduction mechanism, afford the generation of up to two stereogenic centres. As such, they are a powerful tool in the design of asymmetric synthetic pathways, as well as being a greener alternative to traditional transition metal catalysis requiring organic solvents and hydrogen at high pressure. Investigations with metagenomic enzymes (sequenced by the Hailes and

Ward groups) in addition to well-studied ERs was pursued via substrate walking from aldehyde to ketone and then α-hydroxy ketone derivatives (**Scheme 20**). This work aimed to develop the means of affording the stereoselective formation of each enantiomer from bioreduction. Additionally, substrate scope was to be examined to determine potential wide-spread application, and ER biotransformations were to be optimised by varying assay parameters, with yields and enantiomeric excess determined. The application was to be developed on a preparative scale, with the aim of affording hundreds of milligrams of the target compound.

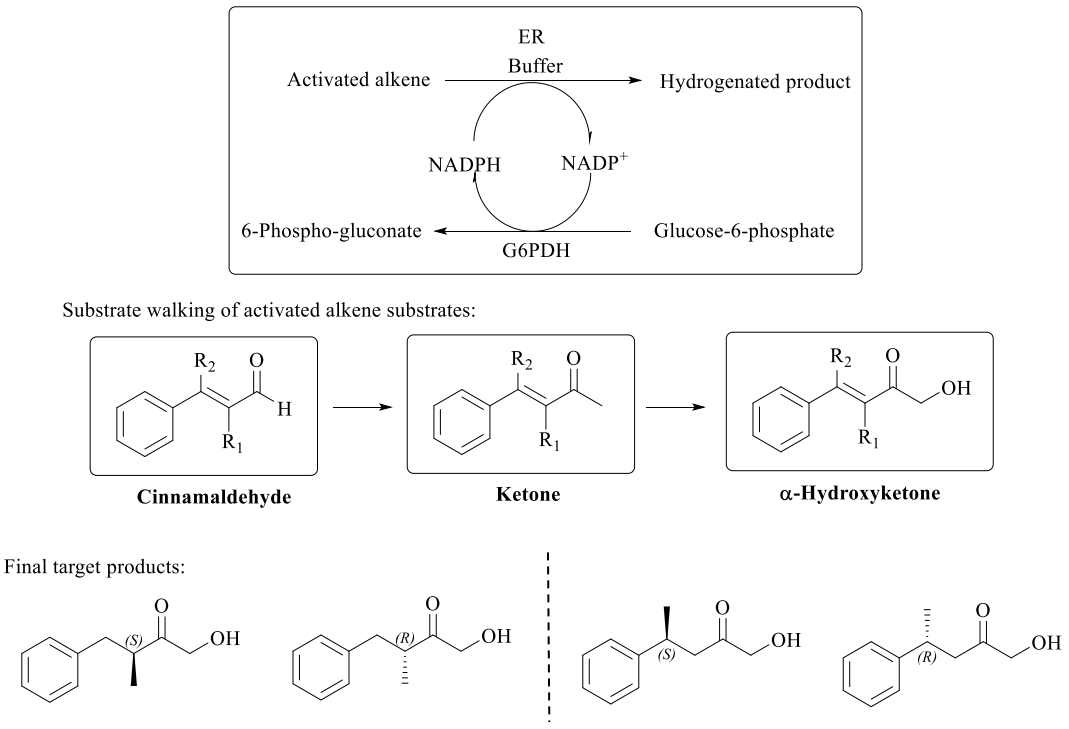

Scheme 20: General scheme depicting biotransformations with ERs using substrate walking strategies from cinnamaldehyde to ketone and α-hydroxyketone derivatives. Potential final target α-hydroyketone products aimed to be generated stereoselectively from bioreduction.

Transaminases catalyse the enantioselective transfer of an amino functional group from an amine donor to an aldehyde or keto-acceptor, thus generating a primary amine or optically active amine product, respectively. As optically pure amines are highly valuable and prevalent scaffolds in bioactive compounds, TAms present an efficient means for their preparation, as well as a greener alternative to chemical reductive amination. Amination of α-hydroxy ketone derivatives with metagenomic and well-studied TAms was to be investigated, with complimentary conditions to ER biotransformation pursued for applicability in a cascade (**Scheme 21**). This work aimed to identify an (*S*)- and (*R*)- selective TAm for the stereoselective formation of each

enantiomer from transamination. Additionally, their respective amination was to be optimised (by varying assay parameters) and substrate scope was to be examined to determine potential wide-spread application. The application was to be developed on a preparative scale to afford the chiral amino alcohol products in hundreds of milligrams.

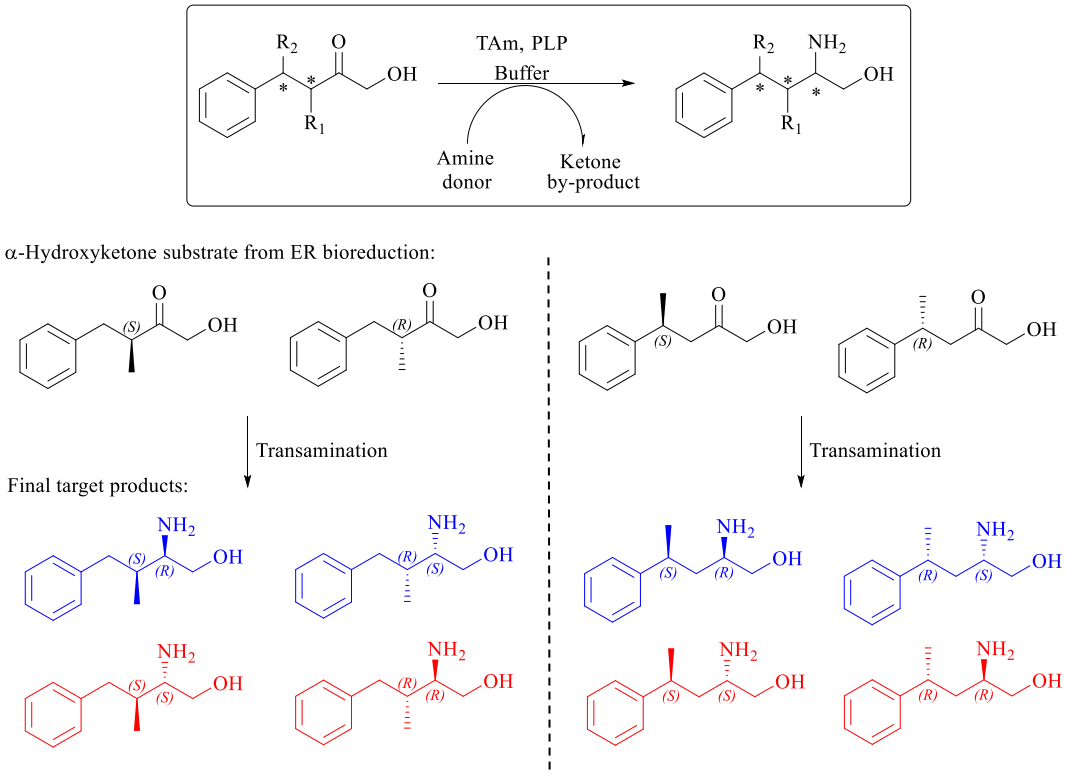

Scheme 21: General scheme depicting biotransformations with TAms using enantiopure α-hydroxyketone substrates. Potential final target amino alcohols products aimed to be generated stereoselectively with enantiomer pairs highlighted in the same colour (blue or red).

Following the successful establishment of the single-step ER and TAm biotransformations, a one-pot cascade was to be pursued (for reasons already discussed in detail in section 1.1.4, namely to avoid the isolation of intermediates and drive the reaction forward), ideally as a one-step one-pot cascade but if deemed unviable as a two-step one-pot cascade.

Using ERs and TAms in a biocatalytic cascade with α-hydroxyketone substrates would afford chiral amino alcohols as the final product. Chiral amino alcohols represent a prevalent structural motif in value-added synthons and bioactive pharmaceuticals, being found in antibiotics, alkaloids and β-blockers.[224] In recent years, a range of 2-aminooxazolines have been patented as TAAR1 agonists (eg. (4*S*)-**37** and (4*S*)-**38**) for numerous neuropsychiatric disorders including depression, schizophrenia, and

Parkinson's disease, amongst others.[225] Herein the aim was to examine the biocatalytic design of TAAR1 agonist precursor **35** with ERs and TAms in a biocatalytic cascade with further reaction providing 2-aminooxazoles **36** (**Scheme 22**). Isolating cyclic 2-aminooxazoles **36** would aim to establish the stereochemistry generated from the biocatalytic cascade.

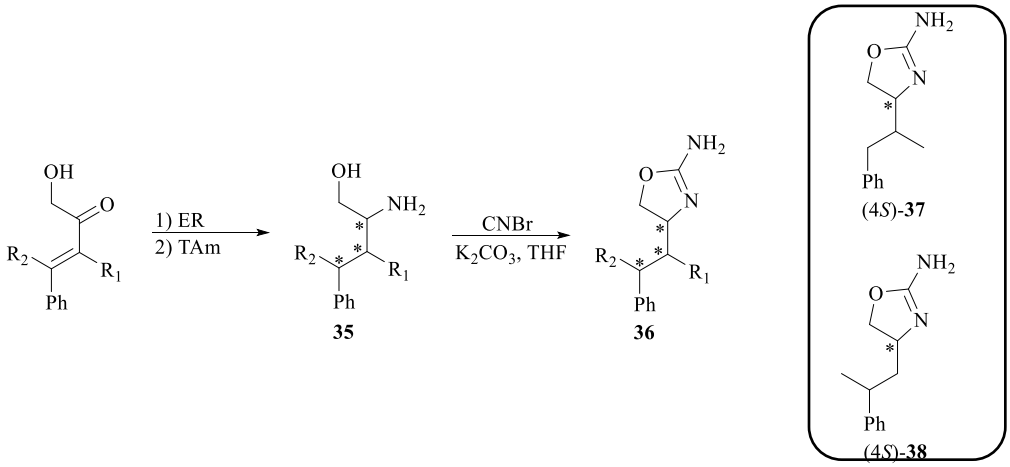

Scheme 22: Chemoenzymatic cascade for the synthesis of chiral 2-aminooxazolines **36** via chiral amino alcohols **35**. TAAR1 agonists (4*S*)-**37** and (4*S*)-**38** exhibited.

In this PhD thesis, Chapter 2 described the chemical synthesis of aldehyde, ketone and α-hydroxyketone derivatives for substrate walking strategies with ERs to afford the step-wise increase in chemical complexity. Substrate walking strategies with ERs were initially described in Chapter 3 with the bioreduction of substituted cinnamaldehyde derivatives, as cinnamaldehyde is a well reported substrate for ER bioreduction.[96,108,120,121,146,157,226,227] In Chapter 4, the aim was to increase substrate complexity with substrate walking to ketone and then to α-hydroxyketone derivatives. Derivatives to be investigated were unsubstituted, α-methyl substituted, and β-methyl substituted ketones, given the relevance of these derivatives in the formation of TAAR1 inhibitors. Additionally, the small methyl group would minimise any steric effects. Concurrently, in Chapter 5 the biotransformation of a panel of reported and metagenomic TAms with α,ß-unsaturated and saturated hydroxyketone derivatives was described to identify a suitable substrate, as well as (*R*)- and (*S*)-selective TAms viable in an one-pot ER-TAm cascade. Preparative scale bioconversions using the substrate on the scale of hundreds of milligrams, were performed and optimised as described in Chapter 6. In Chapter 7, the biocatalytic generation of chiral fluorine from prochiral

substrates was described. This is a separate project to the work described in Chapter 2 through to Chapter 6. The introduction of fluorine into drugs has been established to increase the metabolic stability of compounds by improving resistance to oxidative metabolism, thereby enhancing the pharmacokinetic profile of compounds *in vitro* and *in vivo*.[228–231] There are limited means for the enantiocontrolled introduction of fluorine, however. Chapter 7 provides further background, and offers exploratory work into the biocatalytic generation of chiral fluorine using ERs.

2. Synthetic Chemistry

2.1 Introduction

A range of substrates were explored in biotransformation with ERs via a substrate walking approach, a step-wise tactic for building substrate complexity, starting from aldehyde derivatives, and then moving onto ketone and α-hydroxyketone derivatives. This was previously communicated in section 1.2.1.6 and section 1.3. Herein we describe the synthetic approaches undertaken for the synthesis of these substrates, as well as their corresponding reduced products used as chemical standards.

Preliminary work with ERs explored commercially available and chemically synthesised aldehydes. Substrate walking via ketone derivatives investigated substitution effects in the alpha and beta positions with a methyl group. Following this, α-hydroxylation of unsaturated ketone derivatives exclusively afforded the corresponding primary α-hydroxyketone derivatives.

2.2 Synthesis of Aldehyde Derivative

As previously mentioned, commercially available aldehydes were the primary focus of initial investigations. β-Methyl cinnamaldehyde **40** was not commercially available so it was synthesised via reduction of the available ethyl ester to the alcohol **39** in good yield. No reduction of the alkene was observed. This was readily followed by oxidation using activated manganese (IV) oxide and purification by flash column chromatography (**Scheme 23**).

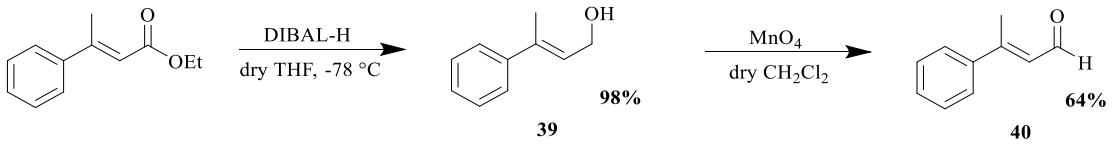

Scheme 23: Reduction of ethyl-(*E*)-3-phenylbut-2-enoate to yield **39**, followed by oxidation to afford **40**.

2.3 Synthesis of Ketone Derivatives

Substrate walking strategies initially considered **41** along with α- and ß-methyl derivatives **7a** and **42** (**Figure 15**) as it was envisioned that their corresponding α-hydroxyketone derivatives would be successfully applicable in an ER-TAm cascade, with subsequent steps affording optically active 2-aminooxazolines.

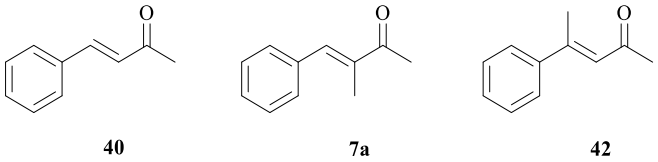

Figure 15: Structures of ketones **41**, **7a** and **42** initially considered in substrate walking strategies.

2.3.1 Bovine Albumin Serum

Previous reports have described the preparation of enones using bovine serum albumin (BSA) via a cross aldol condensation in its hydrophobic pocket.[232] If successful, the transformation may provide a facile method for the preparation of a variety of ketone derivatives. Thus, the preparation of enone **40** was initially investigated using BSA and benzaldehyde **43** in a 1:1 acetone:water reaction medium (**Scheme 24**). Pleasingly, the reaction afforded **40** in 58% yield.

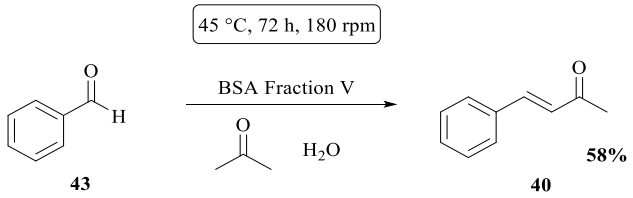

Scheme 24: Cross aldol condensation promoted by BSA affording α,ß-unsaturated ketone **40**.

To diversify molecular complexity, 2-butanone **44** was employed in place of acetone for the reaction with **43** in an attempt to afford the α-methyl ketone derivative **7a**. An excess (50 and 100 eq.) of **44** was trialed giving a translucent yellow gel that could not be characterised (**Scheme 25**). Additionally, an attempted synthesis of the β-methyl ketone derivative **42** with acetophenone **45** and acetone was also unsuccessful (**Scheme 26**).

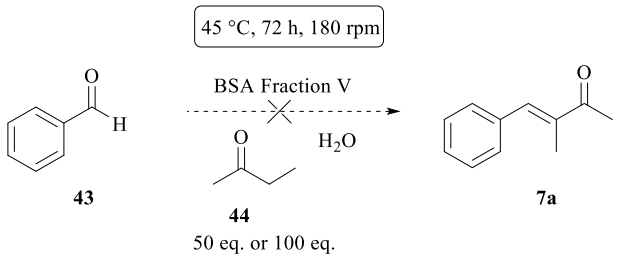

Scheme 25: Unsuccessful attempt at a cross aldol condensation promoted by BSA with **43** and **44** to afford **7a**.

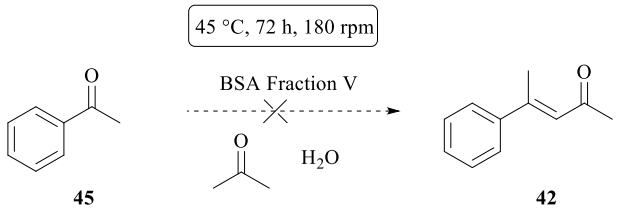

Scheme 26: Unsuccessful attempt at cross aldol condensation promoted by BSA to afford **42**.

2.3.2 Acid-Catalysed Aldol Condensation

The cross aldol condensation was therefore performed with conc. H_2SO_4 in acetic acid to yield the α-methyl ketone derivative **7a** (**Scheme 27**).[233] Acid catalysis yielded the thermodynamic enol and the (*E*)-alkene preferentially. Basic aqueous work-up followed by flash column chromatography afforded **7a** in 67% yield. The application of the acid-catalysed aldol condensation was extended to yield further α-methyl ketone derivatives in moderate yields (**Figure 16**).

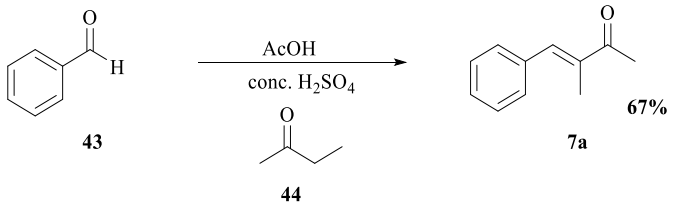

Scheme 27: Acid-catalysed aldol condensation to yield **7a**.

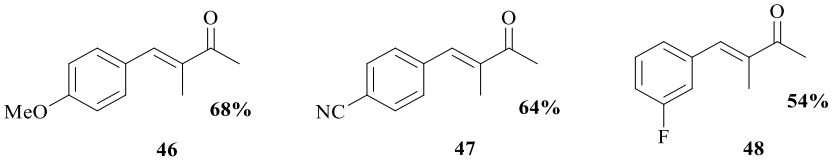

Figure 16: α-Methyl ketone derivatives **46 – 48** attained from an aldol condensation.

2.3.3 Weinreb Ketone Synthesis

The synthesis of **40** was pursued with commercially available **49** via a Weinreb amide (**Scheme 28**).[234] Purification by flash column chromatography afforded amide **50** in 92% yield. Further reaction of **50** with MeMgBr via a Grignard reaction and purification by flash column chromatography yielded the β-methyl ketone derivative **40** in 86% yield. The reaction was performed at low temperature to ensure a second Grignard reaction did not occur.

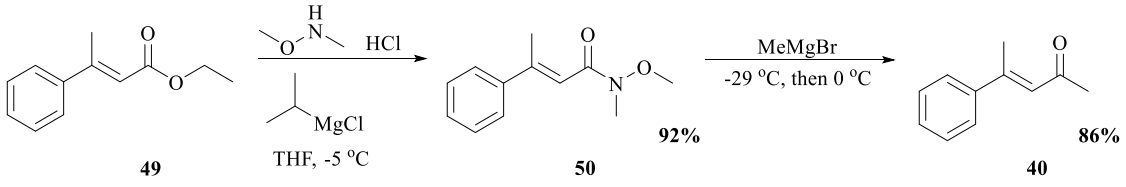

Scheme 28: Weinreb ketone synthesis of **40**.

2.4 Synthesis of α-Hydroxy Ketone Derivatives

Varying chemical approaches were explored for primary α-hydroxylation to afford the α-hydroxyketone derivatives. These included a gold (I) mediated rearrangement[235], the application of hypervalent iodine[236], the Rubottom oxidation[237], and employment of hydrogen peroxide under basic conditions[238]. Prior to these investigations the potential use of BSA for promoted cross aldol condensation was probed.

2.4.1 Bovine Albumin Serum

With the successful application of BSA to provide enone **41**, extension of its application for the preparation of α-hydroxy ketone derivatives was explored (**Scheme 29**). For this, hydroxyacetone **51** was utilised in place of acetone. In parallel, transformations at pH 6.5 and 7.4 were performed yielding interesting results – At pH 6.5, an orange crystalline solid was obtained and at pH 7.4, a translucent orange gel. The capability of BSA to form gels has previously been reported.[239–241] A clear understanding of how the gel is formed has yet to be established.

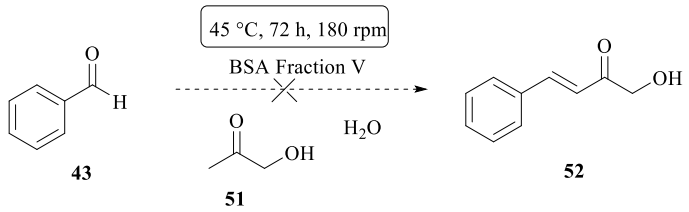

Scheme 29: Unsuccessful attempt at BSA promoted cross aldol condensation with **43** and **51** to afford **52**.

To deter gel formation, 1-methoxypropan-2-one **53** was applied in place of **51** at pH 7 (**Scheme 30**). Sadly this was unsuccessful, yielding a viscous yellow oil with uncharacterizable NMR spectroscopic data.

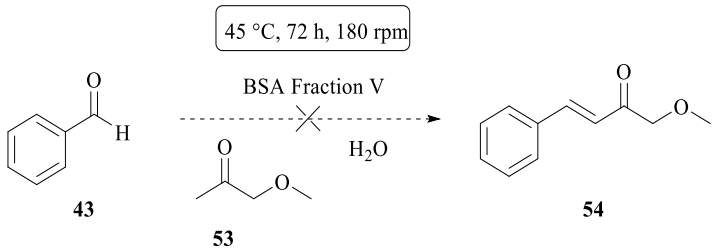

Scheme 30: Unsuccessful attempt at BSA promoted cross aldol condensation with **53** to afford **54**.

2.4.2 Gold (I) Mediated Rearrangement

The literature reports a gold (I) mediated rearrangement to afford ß-methyl hydroxyketone derivative **55** in 3 synthetic steps (**Figure 17**).[235] This involved

protection of a propargylic alcohol, alkyne deprotonation and reaction with acetophenone, followed by a catalytic Au (I) rearrangement. Preliminary work towards **55** followed the literature protocols optimising reactions where required.

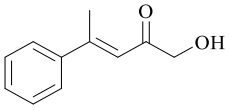

55

Figure 17: β-Methyl hydroxyketone derivative **55**.

Protection of propargyl alcohol with 3,4-dihydro-2*H*-pyran and purification by flash column chromatography yielded the purified product **56** in 75% yield (**Scheme *31***). This is broadly consistent with the literature quoted crude product yield of 98%.[242]

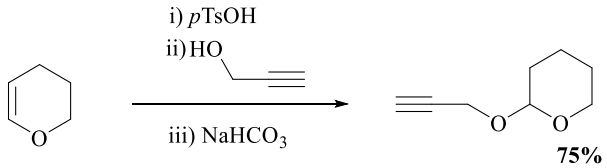

75%

56

Scheme 31: THP protection of propargyl alcohol to yield **56**.

The β-methyl group of the target compound **55** could be afforded using acetophenone. The coupling of **56** with **45** was first investigated utilising benzyl trimethylammonium hydroxide, a weak base employed in catalytic quantities, as it had previously been reported to catalyse the alkynylation of ketones and aldehydes (**Scheme 32**).[243] Unfortunately, this provided a disappointing yield of 4% so *n*-BuLi was employed instead affording **57** in 61% yield following purification by flash column chromatography (**Scheme 32**).

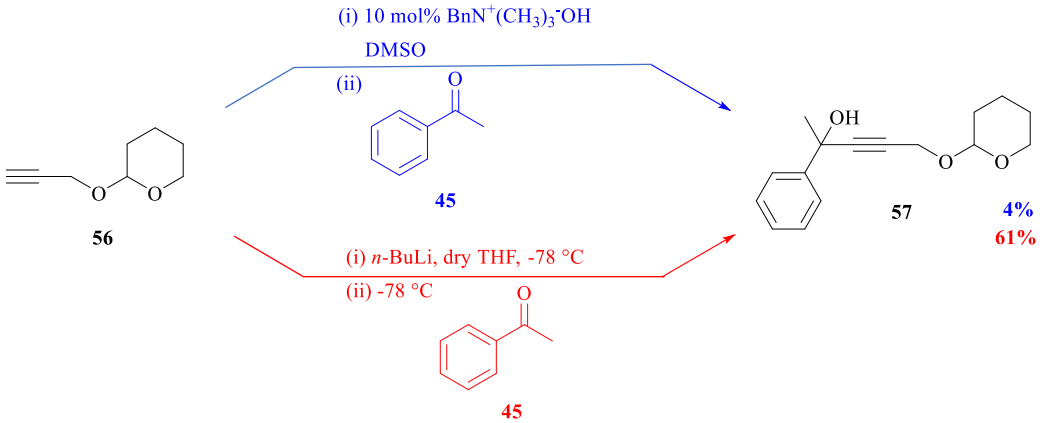

Scheme 32: In blue, coupling of **56** to **45** using catalytic benzyl trimethylammonium hydroxide yielding **57**. In red, coupling of **56** to **45** using *n*-BuLi yielding **57**.

As described by Chung *et. al.*[235], the gold (I) rearrangement was achieved utilising catalytic chloro(triphenylphosphine) gold(I) and silver triflate. A reaction time of 18 h provided the desired product **55**, which subsequently underwent intramolecular conjugate addition to yield the cyclic ether by-product **58** in 40% yield (**Scheme 33**). Conjugate addition is a well-observed reaction in organic chemistry. The β-position of the α,β-unsaturated enone possesses a slight positive charge as electron density may be conjugated up the ketone onto the oxygen.

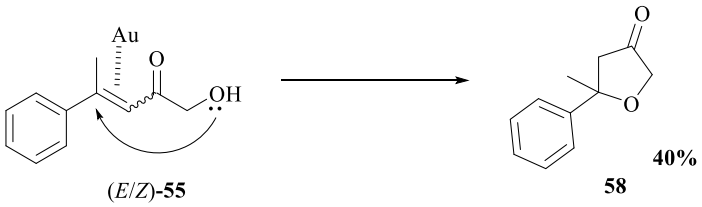

Scheme 33: Intramolecular conjugate addition of product (*E*/*Z*)-**55** yielding by-product **58**.

Due to the conversion rate of product **55** into the by-product **58** being greater than that of starting material to product, the reaction time was reduced. Whilst this precluded further by-product formation, only 10% of **55** was attained as a mixture of *cis* and *trans* isomers. Thus, alternative means for the generation of α-hydroxy ketone derivatives were pursued.

2.4.3 Oxidation with Hypervalent Iodine (III)

Oxidative functionalisation at the α-position of ketone derivative **41** was pursued with hypervalent iodine (III) utilising (diacetoxyiodo)benzene (DIB) in methanol under basic conditions (**Scheme 34**).[236] Hypervalent iodine (III) species **59** was prepared using potassium hydroxide and methanol (**Scheme 34A**). The reaction proceeds via carbon-iodine bond formation at the α-position (**Scheme 34B**). Hemiacetal formation and subsequent intramolecular attack can afford formation of the epoxide, additionally reducing iodine (III) to iodine (I). Subsequent epoxide ring opening with methanol can provide the dimethyl acetal and α-hydroxylation. Hydrolysis of the acetal under protic conditions should then yield the α-hydroxyketone derivative. Product **52** was afforded in 11% yield via this one pot reaction. NMR analysis of by-products was indeterminable but loss of the alkene bond was noted.

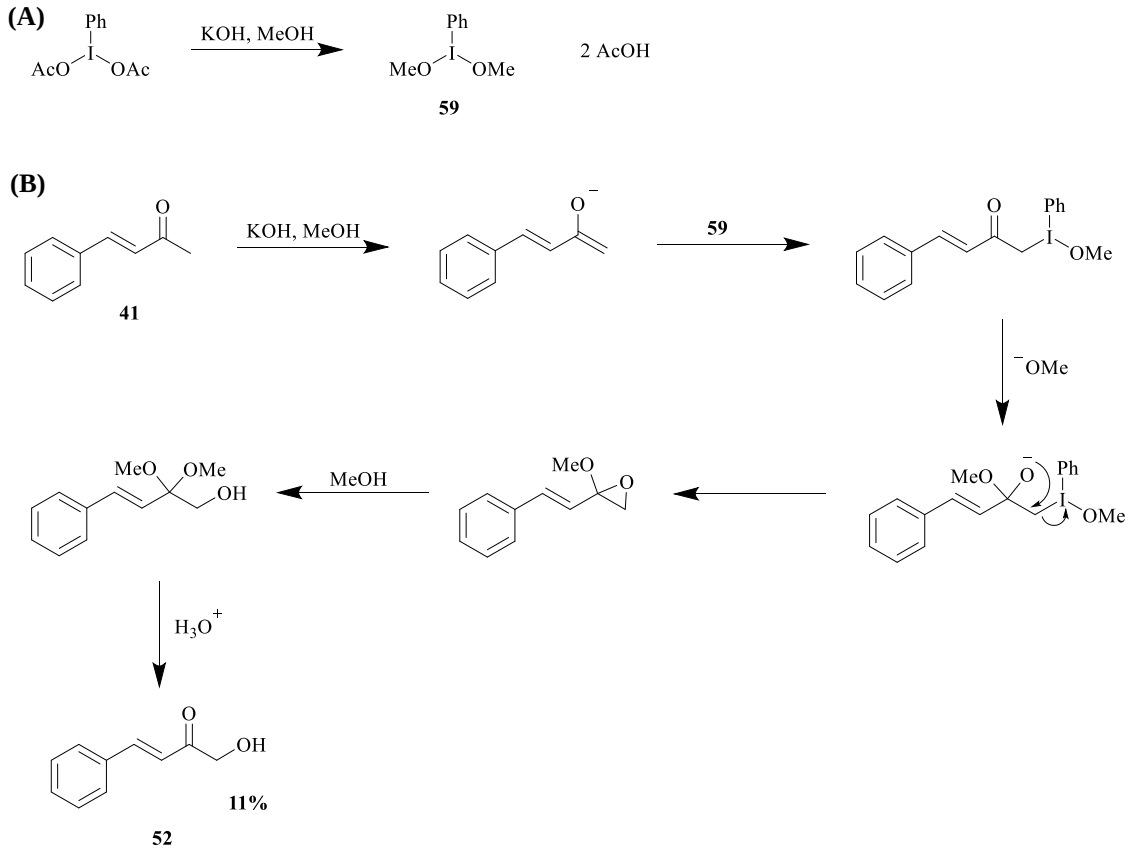

Scheme 34: Oxidative α-hydroxylation with hypervalent iodine (III) to afford **52**.

2.4.4 Rubottom Oxidation

The Rubottom oxidation was next pursued for the synthesis of α-hydroxy ketone derivatives from respective ketones.[237] The method entails reaction of a silyl enol ether with a peroxyacid to afford the α-hydroxy ketone product. Triethylamine and trimethylsilyl trifluoromethylsulfonate were employed for generation of the silyl enol ether from commercially available **41**. Oxidation was performed by *m*-chloroperbenzoic acid (*m*CPBA).

Formation of the silyl enol ether has been reported at -78 °C, however optimisation of the reaction temperature to -15 °C allowed for the quantitative formation of **60** (**Scheme 35**).

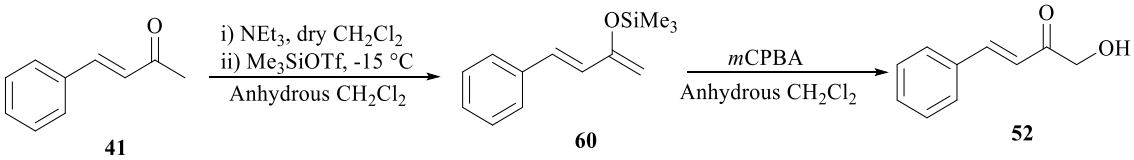

Scheme 35: The Rubottom oxidation entailing α-hydroxylation of **41** to yield **52** via silyl enol ether **60**.

The proposed mechanism for the reaction of **60** and *m*CPBA is as follows[244]: Addition of *m*CPBA generates an epoxide at the silyl enol ether alkene, with the epoxide **61** then opening to give a silyloxy carbocation **62**. Transformation into an α-silyloxy ketone is achieved via 1,4-silyl migration. Acidic work-up then affords the α-hydroxy ketone **52** (**Scheme 36**).

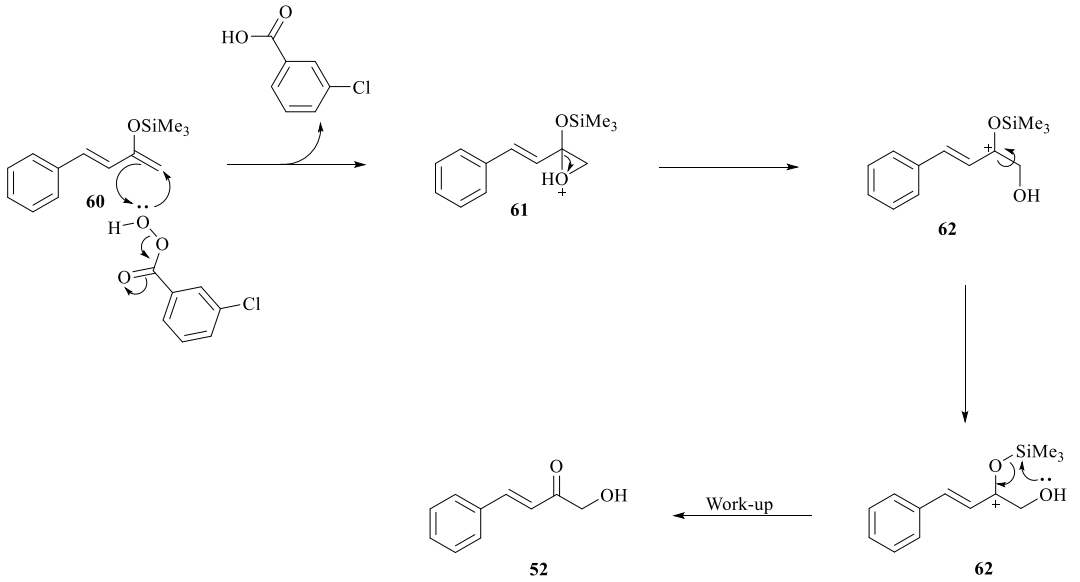

Scheme 36: Proposed mechanism for the Rubottom oxidation.

Product **52** was obtained in 30% yield after purification by flash column chromatography. Approximately 40% of starting material **41** was recovered due to the hydrolysis of **60** with water in the *m*CPBA. Due to the shock sensitive nature of *m*CPBA,[245] its purification and drying was deemed too hazardous for consideration. Provided that a minimal amount of material was required for preliminary enzymatic screening, the experimental procedure was applied to ketones **41**, **7a**, **42**, **46 – 48** to afford α-hydroxyketone derivatives **52**, **63**, **55**, **64 – 66** (**Figure 18**).

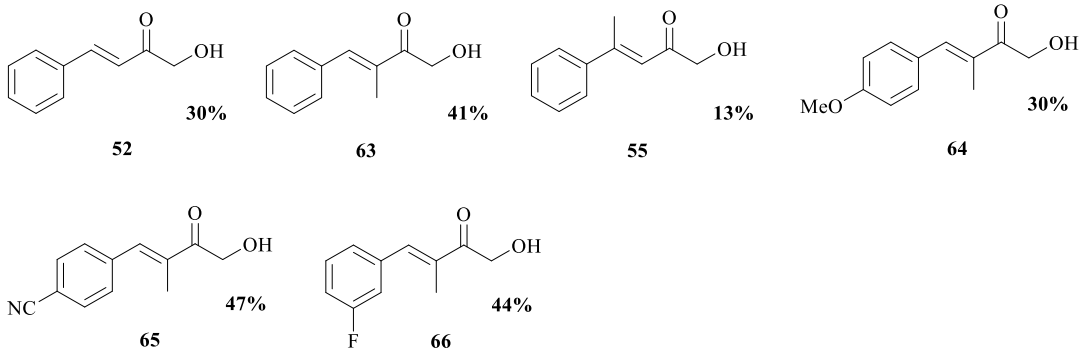

Figure 18: α-Hydroxyketone derivatives **52**, **63**, **55**, **64 – 66** produced from application of the Rubottom oxidation.

2.4.5 Oxidation under Basic Conditions

As a means of circumventing hydrolysis of the silyl enol ether, oxidation under basic conditions was explored.[238] Benzonitrile, potassium carbonate and 30% hydrogen peroxide (v/v) were applied with solvents investigated including hexane, dichloromethane, and toluene (**Scheme 37**). For each, hydrolysis of the silyl enol ether was observed. Additional equivalents of base had no effect.

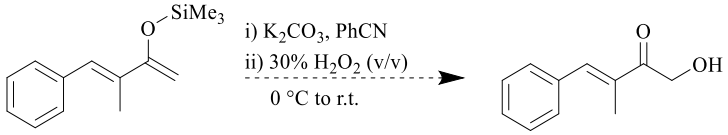

Scheme 37: Unsuccessful oxidation of the silyl enol ether under basic conditions.

2.5 Chemical Reduction

Chemical reduction using hydrogen over palladium on carbon and an iminium catalysed reduction with Hantzsh Ester were examined for the synthesis of product standards when evaluating biocatalytic reactions (Chapter 3, Chapter 4, and Chapter 5).

2.5.1 Hydrogen over Palladium on Carbon

For investigation into the enzymatic reduction of cinnamaldehyde analogues by ERs, the substrate scope with commercially available cinnamaldehydes was pursued. Bioconversion yields were determined using product standards from either commercial suppliers or chemical reduction. As such, the chemical reduction of cinnamaldehyde analogues not available was explored utilising hydrogen and palladium on activated charcoal (Pd/C) (**Scheme 38**).

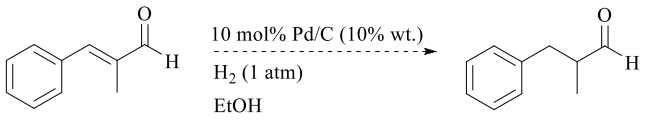

67 **68**

Scheme 38: Unsuccessful chemical reduction of α-methyl-trans-cinnamaldehyde **67** with hydrogen and palladium on activated charcoal.

Whilst reduction by this method was effective, it was not chemeoselective resulting in the reduction of both alkene and aldehyde moieties. This was circumvented by application of the catalyst "poison" diphenylsulfide, and change of solvent from ethanol to ethyl acetate (**Scheme 39**).[246] The desired product **68** was successfully attained following purification by flash column chromatography alongside by-product **69**.

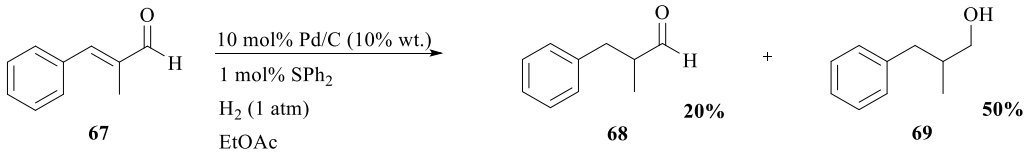

Scheme 39: Chemical reduction of **67** utilising catalyst poison, SPh_2.

Further optimisation was not pursued as material generated was solely for analytical purposes. Furthermore, alcohol by-products were isolated to inform of potential ADH activity in biocatalytic reactions (described in detail later). With the reduction procedure established, it was performed on a range of unsaturated aldehydes derivatives **40**, **67**, **70 – 73**, ketone derivatives **7a, 41, 42, 46 – 48** and α-hydroxyketone derivatives **52, 55, 63 – 66** (**Figure 19**) to furnish saturated aldehydes **68, 74 – 78** saturated ketones **8a, 79 – 83**, and saturated α-hydroxyketones **84–88**. (**Figure 20**).

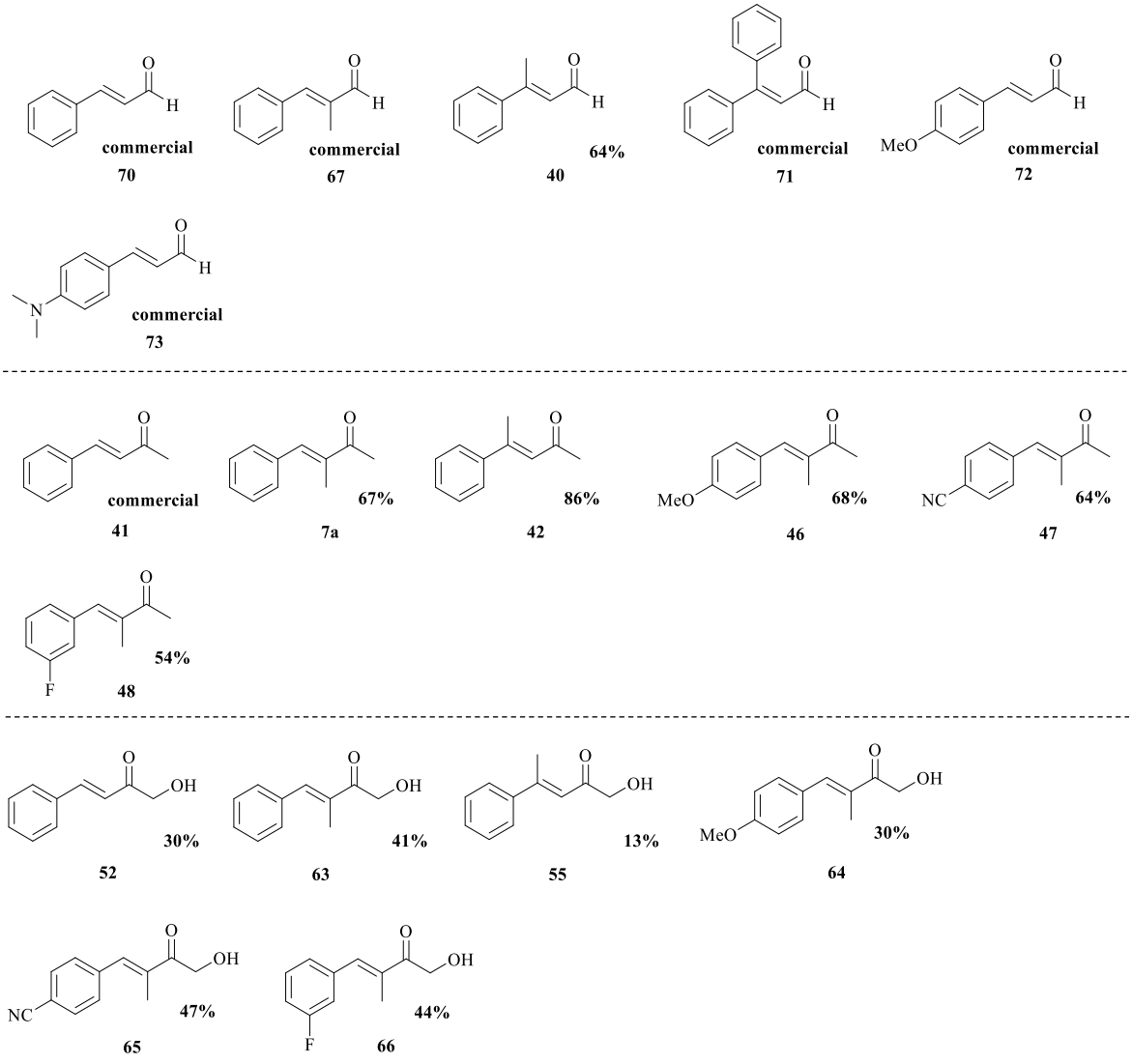

Figure 19: Unsaturated aldehyde derivatives **40**, **67**, **70 – 73**, ketone derivatives **7a**, **41**, **42**, **46 – 48** and α-hydroxyketone derivatives **52**, **55**, **63 – 66**.

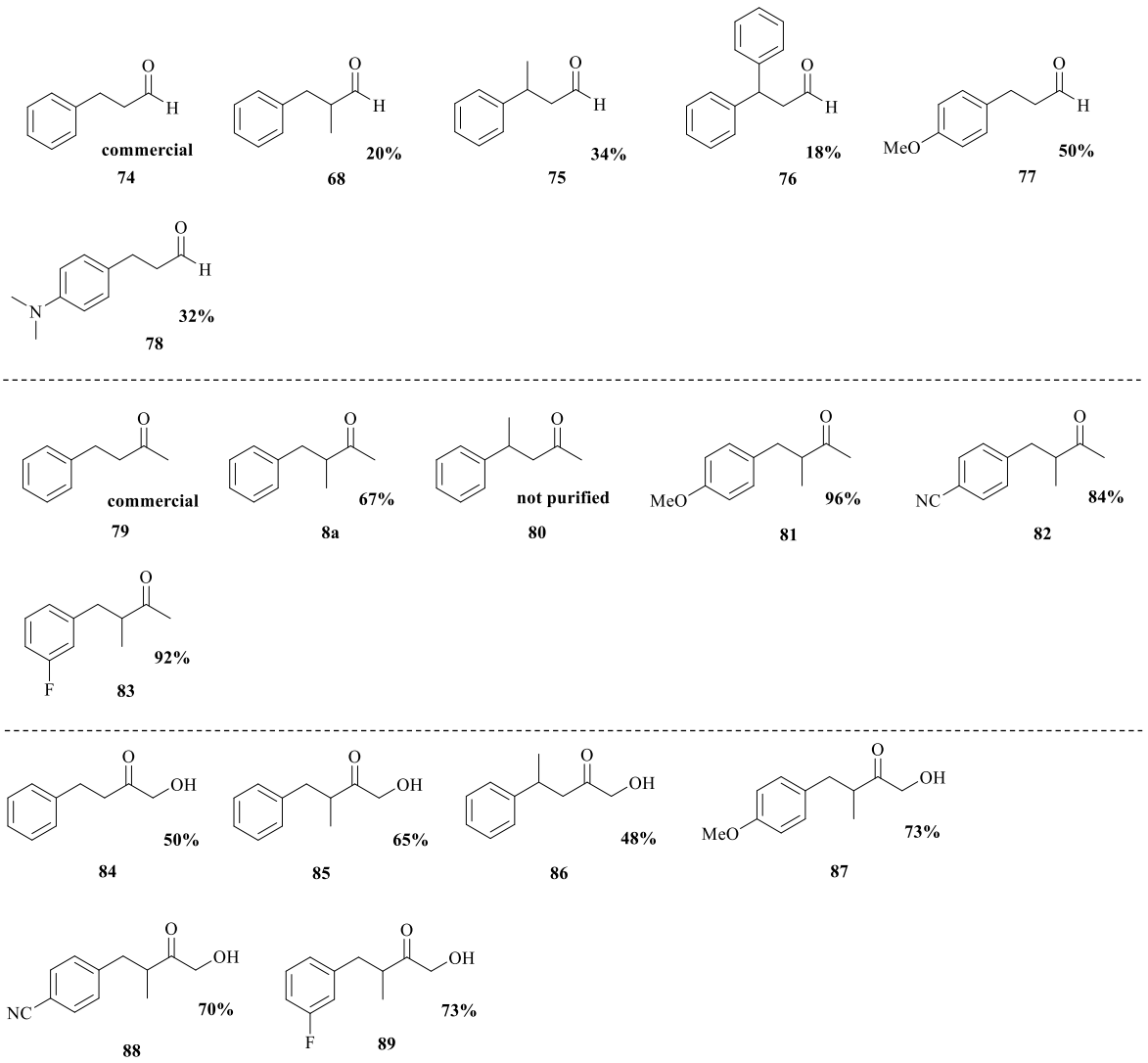

Figure 20: Saturated aldehyde derivatives **68, 74 – 78**, ketone derivatives **8a, 79 – 83** and α-hydroxyketone derivatives **84 – 89**.

2.5.2 Iminium Catalysed Reduction with Hantzsh Ester

Application of the Pd/C reduction conditions with catalyst "poison" SPh_2 to *trans*-4-nitrocinnamaldehyde resulted in reduction of the nitro group observed in as little as 30 min. Thus, an alternative means of reduction was explored. It was recently reported by Yang *et. al.* that an iminium catalysed conjugate reduction of α,ß-unsaturated aldehydes with the Hantzsh ester tolerated a wide variety of functional groups, a capability attributed to the lowering of the LUMO of iminium – substrate intermediate.[247] Unfortunately, application of this reaction with *trans*-4-nitrocinnamaldehyde proved unsuccessful, reducing the nitro group within 1 h.

2.6 Conclusions

In this chapter, the synthesis of aldehyde, ketone and α-hydroxyketone derivatives was performed for substrate walking strategies with ERs. The synthesis of β-methyl cinnamaldehyde **75** was achieved in 63% yield via reduction of the available ethyl ester followed by oxidation with MnO_4. Synthesis of ketone derivatives **7a, 41, 42, 46 – 48** was sucessfully accomplished using an acid-catalysed aldol condensation and the Weinreb ketone synthesis, with yields of 54 – 86% attained. Various approaches were explored for the formation of α-hydroxyketones including the use of BSA for promoted cross aldol condensation[232], gold (I) mediated rearrangement[235], the application of hypervalent iodine[236], the Rubottom oxidation[237], and employment of hydrogen peroxide under basic conditions[238]. Of these methods the Rubottom oxidation was found to be the most successful, and applied to afford α-hydroxyketone derivatives **52, 55, 63 – 66**.

Chemical reduction of **40**, **67**, **70 – 73**, **7a**, **41**, **42**, **46 – 48**, **52**, **55**, **63 – 66** using hydrogen over palladium on carbon was improved by use of a catalyst posion and change of solvent to minimise the reduction of the carbonyl moiety. A tolerant means of chemical reduction to preserve the chemically sensitive nitro group of *trans*-4-nitrocinnamaldehyde was explored, but was found to be unsuccessful.

Substrate walking strategies with ERs will begin in the following chapter. Substrate walking was previously communicated in section 1.2.1.6 and section 1.3 of Chapter 1, and section 2.1 of this chapter. Aldehyde substrates were first examined.

3. Ene-Reductase Bioreduction of Aldehydes

3.1 Introduction

As discussed in Chapter 1, NAD(P)H dependent ERs perform the asymmetric reduction of activated alkene substrates via a stereospecific [2H] *trans*-reduction mechanism. Operating with high chemo-, regio-, and stereospecificity, they are a powerful tool in the design of asymmetric synthetic pathways for bioactive compounds. In this chapter that potential via substrate walking with aromatic aldehyde substrates is described. Preliminary work included investigations into ER preparation, analytical methods, screening of ERs with cinnamaldehyde, and assay optimisation. The substrate scope of ER bioreductions with cinnamaldehyde derivatives was then explored, followed by aliphatic aldehydes with optimisation of aliphatic aldehyde bioreduction pursued.

3.2 Preliminary Assay Considerations

Preliminary assay considerations included finding a suitable ER and substrate in biotransformation, as well as the development of the assay and analytical methods.

3.2.1 Ene-Reductases and Substrates

Applying substrate walking strategies, aromatic aldehyde derivatives were initially investigated for ER bioreduction. Work by a predecessor[ii] reported OYE1 (*Saccharomyces pastorianus*) and OYE2-3 (*Saccharomyces cerevisiae*) to not be as efficacious in bioreduction as the OYE homologues NCR (*Zymomonas mobilis*), XenA (*Pseudomonas putida*) and YqjM (*Bacillus subtillis*) when using aromatic aldehyde substrates.[248] Therefore, cinnamaldehyde **70** was screened against NCR, XenA, and YqjM along with metagenomic ERs from a dometic drain metagenome.[60] 2-Cyclohexen-1-one **90** was employed as a positive control due to its broad acceptance as a substrate and successful bioconversion with a wide range of ERs.[249]

Metagenomic ERs were cloned with a C-terminal His6 tag with plasmid numbers termed pQR1440, pQR1445, pQR1446, and pQR1907.[iii] All were found to come from *Proteobacteria phylum*, the predominant phylum in a domestic drain metagenome, but belonged to different bacterial species.[59] In terms of classification, phylogenetic analysis concluded that the enzymes from pQR1440, pQR1445, and pQR1907 to

[ii] Dr Nadine Tappertzhofen, former member of the Hailes group.
[iii] Cloned by Dr Dragana Dobrijevic, former member of the Ward group.

belong to Group I of the OYE family whilst pQR1446 clustered with Chr-OYE1 in the newly proposed Group IV[iv].[59,109]

3.2.2 Purified Ene-Reductase Preparation and Assay Analytics

To aid experimental design, preliminary work was performed with purified ERs. Applying a "coupled enzyme" strategy, commercial G6PDH (Sigma Aldrich) was introduced for recycling of the costly cofactor NADPH. NADPH was selected over NADH due to its reported dominance in ER bioconversion[127,250], which has also been confirmed experimentally by the Hailes group[248]. ERs were expressed by recombinant *E. coli* BL21 (DE3) cultivation. Cells were cultivated in TB medium at 37 °C until an OD_{600} of 0.5 – 0.7 was attained, induced by addition of IPTG, expressed at 25 °C for 24 h and then harvested via centrifugation.

Resuspension, lyophilisation and storage of lysates at -20 °C was initially undertaken, with preparation of clarified lysates when required. This procedure was found to severly inhibit ER activity irrespective of storage time at -20 °C. With known stability of clarified lysates at -20 °C, lyophilisation was deduced to be compromising enzymatic function. Thus, cell pellets were stored instead at -80 °C for upwards of 6 months with no loss of activity. ERs were prepared as clarified cell lysates with established procedures prior to purification by immobilised Ni affinity chromatography. Purified ERs were stabilised with $(NH_4)_2SO_4$ and stored at 4 °C until a loss of activity with positive control **90** was observed.

Cinnamaldehyde **70** and the corresponding reduced product **4** were inseparable by analytical high-performance liquid chromatography (HPLC) with UV detection at 214 nm. As such, gas chromatography (GC) with a chiral column and product standards were applied for analysis using ***Method D*** or ***Method E***, as described in the experimental procedures.

3.3 Aromatic Aldehydes

A preliminary screening with cinnamaldehyde against a panel of ERs was performed, the assay was optimised, and substrate scope with cinnamaldehyde derivatives was examined.

[iv] Analysed by Dr Dragana Dobrijevic, former member of the Ward group.

3.3.1 Preliminary Screening with Cinnamaldehyde

The bioreduction of cinnamaldehyde, along with its substituted derivatives, has become a well recognised biotransformations catalysed by the OYE family, with high activity and *ee* cited for numerous ERs.[96,108,120,121,146,157,226,227] There are, however, limited reports of cinnamaldehyde bioreduction with ERs YqjM and XenA. To the best of the author's knowledge only one report has been described in the literature for each. In 2010, Stueckler *et al.* reported the bioreduction of α-methyl cinnamaldehyde with 7 wild-type ERs in a bi-phasic system; the (*R*)-enantiomer of the product was afforded by YqjM in poor *ee* and conversion while NCR exhibited (*S*)-stereoselectivity with 76% *ee* and excellent conversion.[146] Chapparo-Riggers *et al.* investigated the specific activity of XenA with cinnamaldehyde (1.56 U mg^{-1}), utilising 2-cyclohexen-1-one (2.74 U mg^{-1}) as a positive control.[96] Stereoselectivity was not reported.

Preliminary screening of **70** with ERs was performed using conditions established by a predecessor[v], similar to those described in the literature[120] (**Scheme 40**). In a 1.5 mL eppendorf at a total volume of 250 µL the reaction was performed with an alkene substrate at a concentration of 10 mM. DMSO was selected as the co-solvent to maximise substrate solubility. Purified ER enzyme concentrations were calculated from nanodrop absorption measurements at A_{280}, extinction coefficients and molecular weight as decribed in experimental procedures. Purified ERs were applied at a final concentration of 0.20 mg/mL. Bioconversions were performed in triplicate and product yield determined with product standards applying GC analysis.

[v] Dr Nadine Tappertzhofen, former member of the Hailes group.

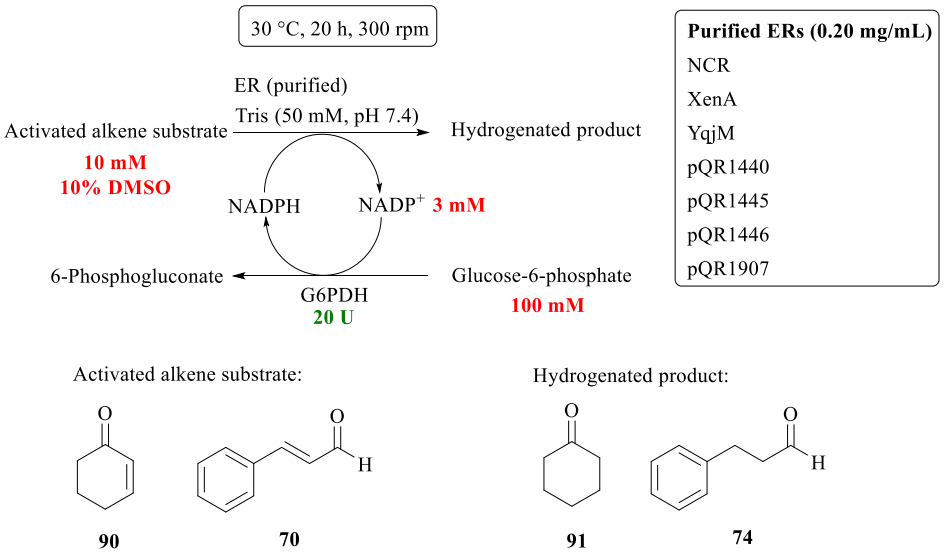

Scheme 40: Preliminary bioreduction of 2-cyclohexen-1-one **90** cinnamaldehyde **70** with purified ERs to give anticipated hydrogenated products **91** and **74** respectively. Bioconversions were performed in triplicate at 30 °C, 300 rpm for 20 h at a scale of 250 µL. Final concentration were G6PNa (100 mM), commercial G6PDH (20 U), $NADP^+$ (3 mM), and alkene substrate (10 mM) in 50 mM Tris (pH 7.4) with 10% DMSO. Purified ERs were applied at final concentrations of 0.20 mg/mL.

Product **74** was observed in good yields of 57 – 64% for 6 of the 7 ERs (all except XenA), with 2 by-products also observed (**Table 8**). Previous reports within the Hailes group (unpublished) noted the contamination of commercial G6PDH with alcohol dehydrogenases (ADH). With this theory, ADH reduction of **74** and **70** would afford by-products 3-phenyl-propan-1-ol **92** and (*E*)-3-phenylprop-2-en-1-ol **93** respectively. GC analysis of commercial **92** and **93** confirmed this hypothesis (**Figure 21**).

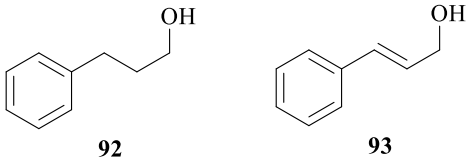

Figure 21: Alcohol by-products **92** and **93** from ADH bioconversion of **92** and **70** respectively.

Table 8: Yields (%) from bioconversions with **90** and **70** with purified ERs and commercial G6PDH, analysed by chiral GC using ***Method D***.

		NCR	XenA	YqjM	1440[a]	1445[a]	1446[a]	1907[a]
Product	**91**	61	78	77	73	80	83	82
	74	64	8	57	64	61	64	59
	92	7	--[b]	7	6	6	6	5
	93	9	18	13	14	9	7	--[b]

[a] ERs cloned from pQR numbers given.
[b] Not observed.

3.3.2 Assay Optimisation with Cinnamaldehyde

Efforts to preclude ADH activity investigated the application of co-expressed ER and G6PDH clarified lysates in biotransformations. The G6PDH enzyme employed from pQR1811 (*Saccharomyces cerevisiae*) had previously been utilised by the Hailes group demonstrating excellent activity.[59] Thus, metagenomic ERs were cloned with pQR1811[vi] and expressed by recombinant *E. coli* BL21 (DE3) cultivation. Clarified lysates were prepared by established procedures. Disappointingly, alcohol by-products **92** and **93** were still observed, likely due to innate ADHs in *E.* coli. This hypothesis was supported by Knaus *et al*. amongst others, who reported ADH formation within cells[99,227] and activity with enal substrates[251,252].

It was postulated whether the rate of ER bioreduction was greater than that of ADH reduction, thereby allowing termination of the reaction prior to ADH activity. To determine this, a reaction profile of the biotransformations of **70** with co-expressed enzymes from pQR1907+1811 over 24 h was undertaken (**Figure 22**). pQR1907 was selected as its previous application produced the minimum amount of by-product formation amongst the ERs screened (**Table 8**). Disappointingly, ADH activity was observed in as little as 3 h, with ER bioreduction maximising after 24 h.

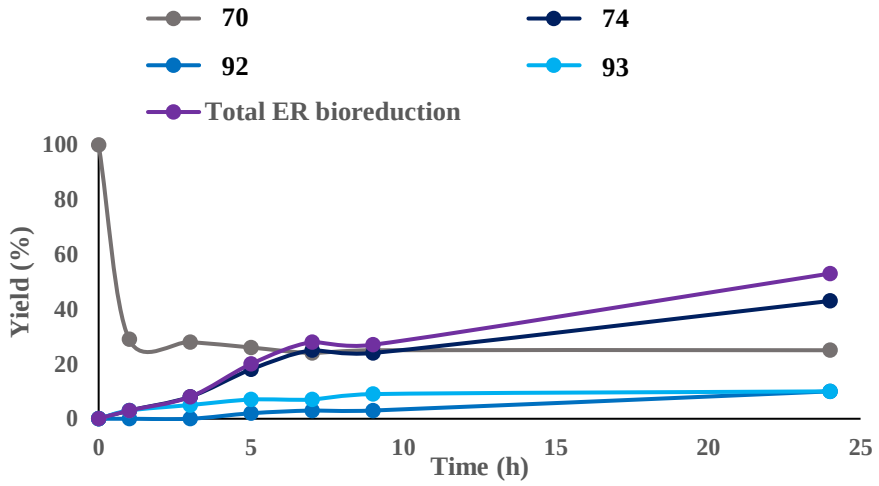

Figure 22: Bioreduction of cinnamaldehyde **70** with 1907+1811 co-expressed clarified lysate to give products **74**, **92** and **93**. Bioconversions were performed in triplicate at 30 °C, 300 rpm at a scale of 250 µL. Final concentration were G6PNa (100 mM), $NADP^+$ (3 mM), and alkene substrate (10 mM) in 50 mM Tris (pH 7.4) with 10% DMSO. Co-expressed clarified lysate was applied at final concentrations of 0.2 mg/mL. Bioconversion was analysed at 1, 3, 5, 7, 9, and 24 h timepoints and analysed by chiral GC using ***Method D***.

[vi] Cloned by Dr Dragana Dobrijevic, former member of the Ward group.

As an alternative means of circumventing ADH reduction, a panel of ERs (NCR, pQR1445, and pQR1907) were co-expressed with G6PDH recycling enzyme pQR1811 (*Saccharomyces cerevisiae*) and subsequently purified to afford the co-expressed purified ER and G6PDH. Metagenomic ERs pQR1445 and pQR1907 were selected owing to their highly successful bioreduction of sterically challenging substrates on a preparative scale, with tolerance of up to 30% co-solvent observed.[59] NCR was employed for both investigative and reference purposes, being a well-studied ER demonstrating highly successful activity with a wide range of cyclic and linear substrates.[116] The co-expressed purified lysate concentrations of ER+G6PDH were determined with a Bradford assay, as described in the experimental procedures. Bioreduction of **70** under the previous assay conditions afforded the reduced product **74** in excellent yields of 86 – 94% (**Scheme 41**, **Table 9**). Moreover, ADH reduced by-products **92** and **93** were not observed.

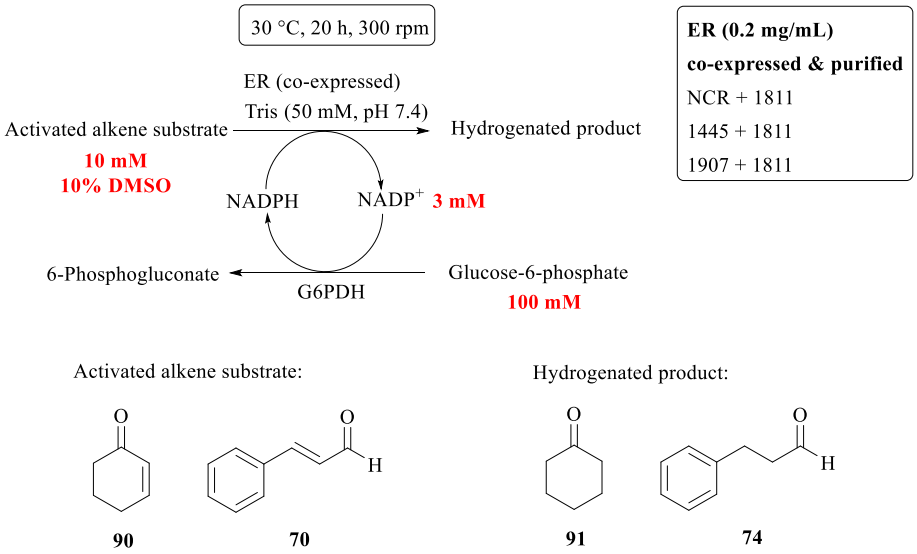

Scheme 41: Bioreduction assay with purified co-expressed ER+pQR1811 with **90** and **70**.

Table 9: Yields (%) from bioconversion of cinnamaldehyde with co-expressed purified ER+1811, analysed by chiral GC using ***Method D***.

		NCR+pQR1811	pQR1445+1811[a]	pQR1907+1811[a]
Product	**91**	quant.[b]	83	100
	74	86	89	94

[a] ERs cloned from pQR numbers given.
[b] Quantitative yield

3.3.3 Screening with Cinnamaldehyde Derivatives

With means for the successful bioreduction of **70** established, a scope of commercially available (with the exception of **40**) substituted cinnamaldehyde derivatives **67**, **40**, **71 – 73** were screened using high concentrations of purified co-expressed ER+G6PDH enzymes (0.8 – 1 mg/mL) to give anticipated products **68**, **75 – 78** (**Figure 23**). Derivatives **67** and **40** were of especial interest for substrate walking purposes owing to the relevance of their α-hydroxy ketone derivatives in the preparation of TAAR1 inhibitors (4*S*)-**37** and (4*S*)-**38**. Phenyl derivative **71** probed steric effects at the β-position whilst **72** and **73** investigated electronic effects due to their electron donating nature. As described in Chapter 2 the synthesis of product standards for derivatives with electron withdrawing (NO_2) and halogen (Cl) groups was unsuccessful and so these commercially available enals were not included in investigations. Standard deviations across the bioreduction triplicate are reported by error bars.

All cinnamaldehyde derivatives, with the exception of **71**, were accepted as substrates. This was suspected to be due to steric reasons. Fair to excellent yields of 56 – 95% were attained for each substrate with at least one ER, with NCR successful amongst all substrates. Similar activities were observed for pQR1445 and pQR1907, the only difference being the superior activity of pQR1907 with β-methyl substituted **40** compared to pQR1445. Methoxy derivative **77** was formed in excellent yields over 90% for NCR, pQR1445 and pQR1907 (**Table 10**, **Figure 24**).

α-Methyl substituted **68** was attained in a good yield of 80% with pQR1445, whilst β-methyl substituted **75** was only achieved in 18% yield (**Table 10**, **Figure 24**). This is most likely due to steric reasons, however it would be incorrect to readily discount alternate substrate binding modes achieved for substrates **67** and **40** (ie. A "classical" binding mode is attained for one substrate and "flipped" binding mode for the other; binding modes were described in detail in section 1.2.1.2). Whilst this would be unlikely as ERs typically have a perferred binding mode for substrates[93], substrate-based stereocontrol has been observed[120] and cannot be discredited with the data currently available. The (*R*)- or (*S*)-selectivity of products **68** and **75** formed would first need to be determined to conclude whether alternate substrate binding modes were achieved (if the selectivity of the products formed was the same the binding mode was the same) and thus whether sterics at the α- or β-position were directly responsible for the drop in yield. It should be noted that even with alternate substrate binding modes

sterics between the substrate and ER may still be responsible for the drop in yield, the author only wishes to highlight that it may not be possible to directly compare substrates **67** and **40** on the basis of their molecular complexity, and is certainly premature to do so with the data currently available, as all other variables have yet to be proven the same; Their interaction with the enzyme with regards to binding mode also needs to be evaluated. That being said, a substrate may have taken an alternate substrate binding mode due to sterics with the ER, however it wouldn't be wise to presume this as other factors, such as improved binding affinity between the substrate and the enzyme in the alternate binding mode need to be considered. (This is exemplified more clearly and discussed in further detail in section 4.2.2, **Scheme 42**, **Table 11**, where substrate-based stereocontrol is suspected. Moreover, β-methyl ketone substrate **42** described in section 4.2.2 was not accepted as a substrate by NCR, pQR1445 and pQR1907, which is peculiar considering the β-methyl group of aldehyde **40** was well tolerated by NCR and pQR1907 in this work.) Therefore, the author is hesitant to draw conclusions or insights on the data presented as further work is required and the author does not wish to present the reader with false or misleading insights.

Similarily, for products **77** and **78** formed from the biotransformation with pQR1445 a drop in yield from 92% to 13% respectively was observed (**Table 10**, **Figure 24**). Again this could be directly attributed to steric reasons due to the molecular complexity of substrates **72** and **73** only assuming that the binding modes of the substrates were the same. Of course no chiral centre was generated so this would be more challenging to evaluate, and would therefore rely on modelling data.

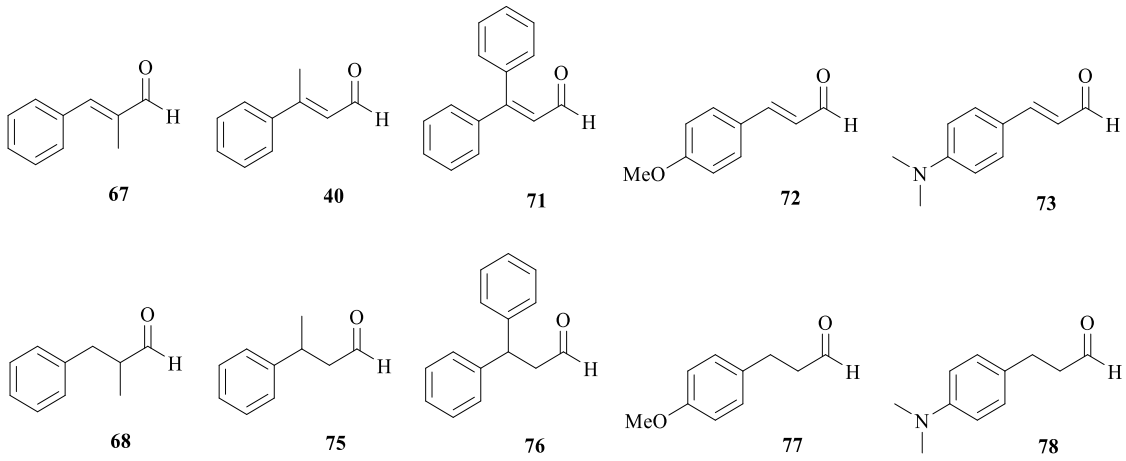

Figure 23: Cinnamaldehyde derivative **67**, **40**, **71** – **73** with hydrogenated products **68**, **75** – **78**.

Table 10: Yields (%) from bioconversion of cinnamaldehyde derivatives **7** – **11** with co-expressed purified ER+1811 clarified lysates, analysed by chiral GC using ***Method D***.

		NCR+pQR1811[a]	pQR1445+1811[a]	pQR1907+1811[a]
Product	**68**	73	80	82
	75	65	18	56
	76	--[b]	--[b]	--[b]
	77	91	92	95
	78	63	13	27

[a] Enzymes cloned from pQR numbers given.
[b] Not accepted as a substrate.

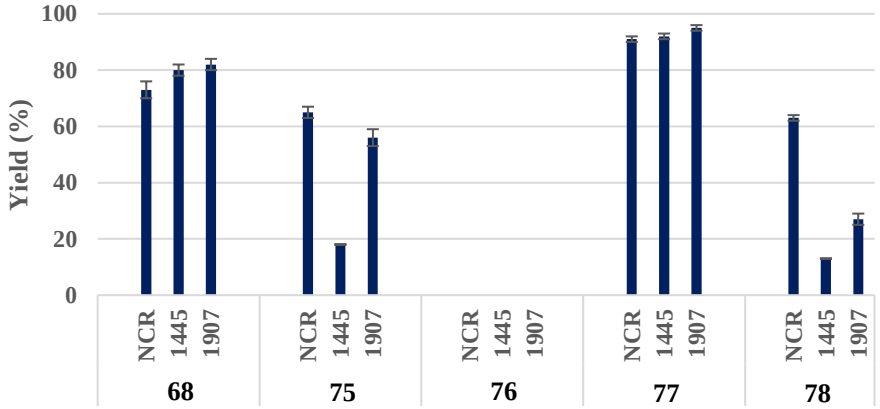

Figure 24: Bioreduction of cinnamaldehyde derivatives **67**, **40**, **71** – **73** with purified co-expressed clarified lysates NCR+pQR1811, pQR1445+1811, and pQR1907+1811 to give products **68, 75** – **78** respectively. Bioconversions were performed in triplicate at 30 °C, 300 rpm at a scale of 250 µL. Final concentration were G6PNa (100 mM), $NADP^+$ (3 mM), and alkene substrate (10 mM) in 50 mM Tris (pH 7.4) with 10% DMSO. Purified co-expressed clarified lysates were applied at final concentrations of 0.2 mg/mL.

3.4 Aliphatic Aldehydes

Aliphatic aldehydes were examined for contrast to aromatic aldehydes in the continued development of substrate scope. A preliminary screening was performed, with assay optimisation with the most successful substrates.

3.4.1 Preliminary Screening

Following the successful bioconversion of cinnamaldehyde derivatives with purified co-expressed ER+G6PDH enzyme, extension of the application was explored with several commercially available aliphatic aldehydes **94** – **99** and (*E*/*Z*)-**18** (**Figure 25**). Aldehyde **94** was selected being a simple cyclic aliphatic substrate, whilst **95** – **99** were nominated to investigate the steric effects of both chain length and substitution at the α-poisition. For reference, citral (*E*/*Z*)-**18** was chosen owing to its precedent in the literature as a precursor to (-)-Menthol.[93,98,116,122,158,251,252] A high concentration of purified clarified lysate of 1 mg/mL was applied in the assay for intial screening.

Product yields were quantified using GC analysis (***Method E***) with product standards, as described in the experimental procedures.

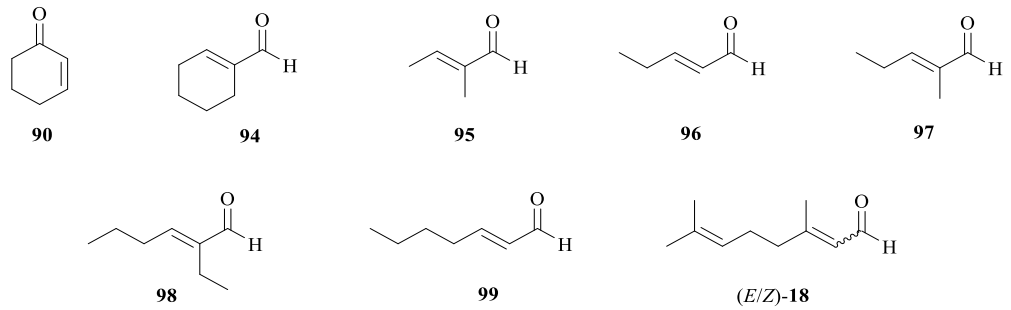

Figure 25: Aliphatic enals (*E*/*Z*)-**18**, **94** – **99**.

Bioconversions were inconsistent across the triplicate experiments for aldehydes **94** – **97**. Thus, their experimental results were deemed inconclusive and are not included. Products from longer chain aliphatic aldehydes **99** and (*E*/*Z*)-**18** were attained in low yields of up to 15% with NCR+pQR1811, pQR1445+1811, and pQR1907+1811 (**Figure 26**). No product formation was observed for **98**. Activities of the ERs+1811 was confirmed with the positive control **90**.

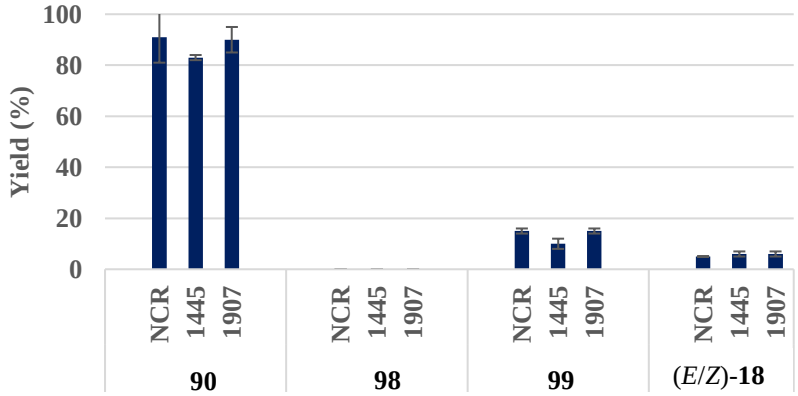

Figure 26: Bioreduction of positive control **90** and aliphatic aldehydes **94** – **99** and (*E*/*Z*)-**18** with purified co-expressed clarified lysates NCR+pQR1811, pQR1445+1811, and pQR1907+1811. Bioconversions were performed in triplicate at 30 °C, 300 rpm at a scale of 250 µL. Final concentration were G6PNa (100 mM), $NADP^+$ (3 mM), and alkene substrate (10 mM) in 50 mM Tris (pH 7.4) with 10% DMSO. Purified co-expressed clarified lysates were applied at final concentrations of 1 mg/mL. The reactions were analysed by chiral GC using ***Method E***.

3.4.2 Optimisation with Select Aliphatic Substrates

Given the lack of starting material recovered, it was hypothesized that the aliphatic enals and their hydrogenated products were sticking to the plastic eppendorf walls. Further experiments were conducted using glass syringes, glass vials, and glass inserts furnishing improved recovery rates, though still low yielding. As a high concentration of purified clarified lysate was already employed in the assay, potential cofactor limitations were investigated, and an excess of NADPH (1 – 3 eq.) was applied (**Figure 27**).

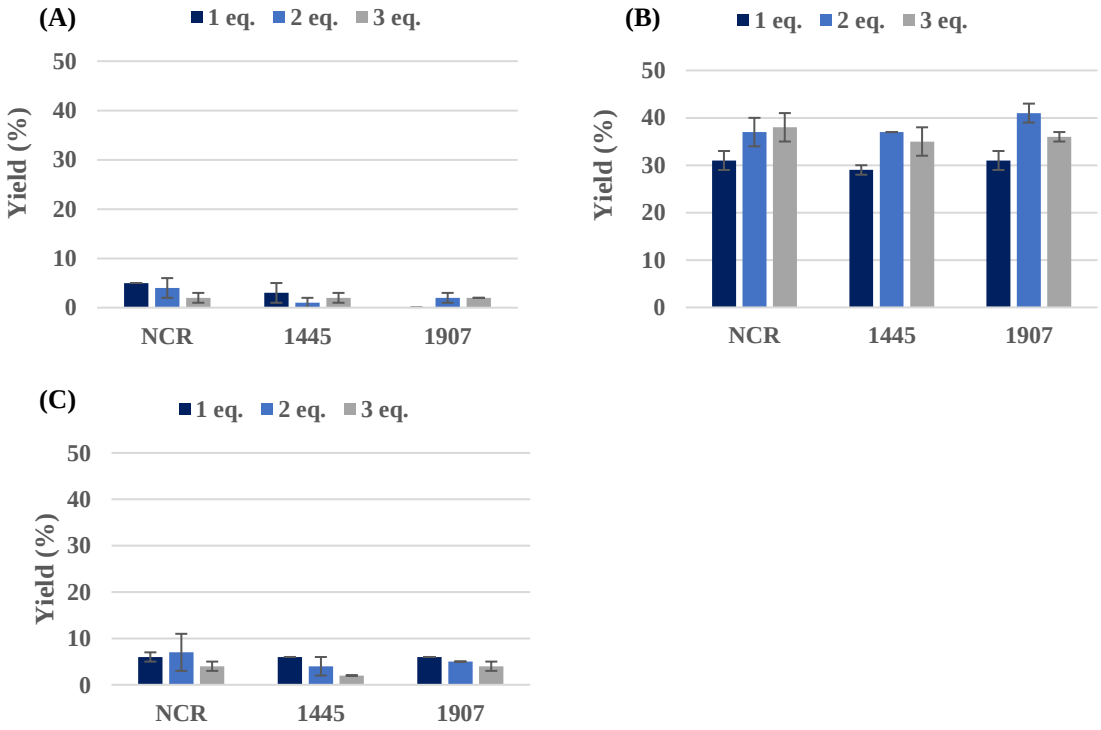

Figure 27: Bioreduction of **(A) 98**, **(B) 99**, and **(C)** (*E*/*Z*)-**18** with purified co-expressed clarified lysates NCR+pQR1811, pQR1445+1811, and pQR1907+1811 and varying $NADP^+$ equivalents. Bioconversions were performed in triplicate at 30 °C, 300 rpm at a scale of 250 µL. Final concentration were G6PNa (100 mM), and alkene substrate (10 mM) in 50 mM Tris (pH 7.4) with 10% DMSO. Purified co-expressed clarified lysates were applied at final concentrations of 1 mg/mL. Equivalents of NADPH were investigated and applied at final concentrations of 10, 20, and 30 mM. The reactions were analysed by chiral GC using ***Method E***.

In comparison to catalytic quantities of $NADP^+$, a marginal improvement was observed with **98** and no improvement with (*E*/*Z*)-**18**. Yields from the bioreduction of **99**, however, more than doubled to a maximum of 41%. For all substrates, further equivalents of NADPH were found to have a neglible effect on the biotransformation yields, and neglible difference was found across the ERs screened.

Focus was concentrated on the most successful two substrates **99** and (*E*/*Z*)-**18**. Querying whether the work-up extraction was deterring analytical results, extraction was avoided by use of an alternative GC column tolerant of water (Agilent DB-WAX UI column, 30 m × 0.320 mm, 0.50 µm). As such, enzymatic assays were only quenched with *iso*propanol and centrifuged prior to analysis. Use of *iso*propanol ensured total solubilisation of the substrate and product, as well as any by-products present. Disappointingly, no improvement was observed in the material recovered.

Finally, application of 1-octanol as an internal standard was performed, as cited by Hall *et al.* in the bioreduction of (*E*/*Z*)-**18**.[116] A 10 mM solution of 1-octanol in EtOAc was used as the extraction solvent for the biotransformation work up. Total recovery (starting material and product) of citral (*E*/*Z*)-**18** was improved to ~30% whilst no change was observed for **99**.

The author suspects the aldehydes were too volatile and were lost in gaseous form whenever the eppendorf/glass vial lid was open for the assay work-up as they had a distinct odour which was noticable during work-up.

3.5 Conclusions

In this chapter, the preparation of ER clarified lysates was established, with the lyophilisation of lysates concluded to severly inhibit ER activity. As such, cell pellets were stored at -80 °C with preparation of clarfied lysates using established procedures as required. Purification of ERs was accomplished using immobilised metal affinity chromatography. Analytical methods for the quantitative determination of product yields were established with a range of substituted cinnamaldehyde derivatives **67**, **40**, **71 – 73**, and aliphatic substrates, **94** – **99** and (*E*/*Z*)-**18**.

Application of ER clarified lysates in the biotransformation of **70** observed the formation of alcohol by-products **92** and **93** from ADH contamination. A timepoint assay concluded that ADH reduction could not be precluded by a shortened reaction time. As such, the removal of ADH enzymes was accomplished by the co-expression of ER+G6PDH and purification by immobilised metal affinity chromatography. Application of the co-expressed purified enzymes from NCR+pQR1811, pQR1445+1811 and pQR1907+1811[vii] afforded the product in excellent yields of

[vii] Enzymes cloned from pQR numbers given.

86 – 94%. Extension of this application to substituted cinnamaldehyde derivatives **67**, **40**, **71 – 73** gave fair to excellent yields of 56 – 95% with at least one ER, with the exception of the β-phenyl substituted **71** which was not accepted as a substrate.

Further work with aliphatic aldehydes **94** – **99** and (*E*/*Z*)-**18** was undertaken using co-expressed purified enzymes NCR+pQR1811, pQR1445+1811 and pQR1907+1811[viii]. Optimisation of experimental results proceeded by application of an excess of NADPH (1 – 3 eq.), use of glass materials (as opposed to plastic), modified work-up procedure (circumventing extraction), as well as modified analytical analysis (employment of an alternative GC column tolerant of water and application of an internal standard). Limited success was furnished by these efforts with a maximum of 41% yield afforded from the conversion of **99**, and recovery of starting material and product improved to a total of ~30% for (*E*/*Z*)-**18**. The author suspects the aldehydes were too volatile and were lost in gaseous form whenever the eppendorf/glass vial lid was open for the assay work-up as they had a distinct odour which was noticable during work-up.

In the following chapter substrate walking stratgies will proceed by increasing molecular complexity from aldehydes (this chapter) to ketone and α-hydroxyketone derivatives with ERs (Chapter 4). Substrate walking strategies were previously communicated in section 1.2.1.6, section 1.3, and section 2.1.

[viii] Enzymes cloned from pQR numbers given.

4. Ene-Reductase Bioreduction of Ketone Derivatives

4.1 Introduction

With the aim of building up the substrate complexity via substrate walking from substrates described in Chapter 3, the ER bioreduction of ketone and α-hydroxyketone derivatives are described in this chapter. Preliminary work screened several substrates against a panel of ERs, with further work conducted with the most successful substrate and three most successful ERs. Efforts to optimise the yield and enantiomeric purity entailed the systematic evaluation of five assay parameters. Following this, the substrate scope of analogues with varying functional groups were explored and their bioreduction optimised.

4.2 Preliminary Assay Considerations

Preliminary assay considerations included finding a suitable ER and substrate, development of assay design and analytical methods, as well as molecular docking to rationalise stereoselectivity.

4.2.1 Ene-Reductases and Substrates

The work described in Chapter 4 and Chapter 5 was investigated concurrently. Where appropriate reference is made to the work outlined in Chapter 5.

With the successful biotransformation of **70** and its α- and β-methyl substituted derivatives **67** and **40** as described in the previous chapter, substrate walking proceeded to explore the ER bioreduction of their respective ketone **41, 7a, 42** and α-hydroxyketone derivatives **52**, **63**, **55** to give hydrogenated products **79**, **8a**, **50** and **84** – **86** (**Scheme 42**). As before, compound **90** was employed as a positive control.

A combination of literature (NCR, XenA, YqjM) and metagenomic ERs (pQR1445, pQR1907, pQR1446[ix]) were explored for preliminary investigations, from sources previously described in Chapter **3**. Metagenomic ER pQR1909 was also considered as it belonged to Class II of the OYE family[59], unlike the other metagenomic ERs.

Previous work by the Hailes group did not observe the over-reduction of ketones to corresponding alcohols from the application of ER clarified lysates.[59] As such,

[ix] Enzymes cloned from pQR numbers given.

co-expressed clarified lysates of ER+G6PDH were employed in the assays with NCR and metagenomic ERs (**Scheme 42**). NCR[x], pQR1445 and pQR1907[xi] were co-expressed with the recycling enzyme from pQR1811 whilst pQR1446[xiixiii] and pQR1909[xivxv] were co-expressed with the thermophilic recycling enzyme from pQR1991. For ERs not co-expressed with cofactor recycling enzymes (XenA and YqjM)[xvi], commercial G6PDH (Sigma Aldrich) was applied. Enzymes were expressed from pQR numbers given.

4.2.2 Clarified Lysate Preparation and Assay Analytics

ERs were expressed by recombinant *E. coli* BL21 (DE3) cultivation. Cells were cultivated in TB medium at 37 °C until an OD_{600} of 0.5 – 0.7 was attained, induced by addition of IPTG, expressed at 25 °C for 24 h and then harvested via centrifugation. Cell pellets were stored up to 6 months at -80 °C with no loss of activity. Enzymes were prepared as clarified cell lysates using established procedures. The term "clarified cell lysates" refer to the total unpurified protein expressed by *E. coli*. Enzymes NCR+pQR1811, pQR1445+1811, and pQR1907+1811 in the clarified lysates had the concentrations of 1.6 mg/mL, 0.8 mg/mL and 1.6 mg/mL respectively. Clarified cell lysates were stored at -80 °C for up to 2 weeks with no loss of activity, defrosted only once, and kept at 0 °C prior to application.

As before, preliminary investigations employed a predecessor's established conditions.[248] At a total volume of 250 µL with an alkene substrate at 10 mM concentration, a high concentration of ER+G6PDH clarified lysate was applied for the initial screen (0.7 – 1.2 mg mL^{-1}). Bioconversions were performed in triplicate and product yield was measured by GC analysis (***Method D***) with product standards, as described in experimental methods section 9.2.2.2. Standard deviations in experimental results are reported by error bars.

[x] Cloned by Dr Nadine Tappertzhofen, former member of the Hailes group.
[xi] Enzymes cloned from the pQR numbers given.
[xii] Expressed by Dr Laure Benhamou, former member of the Hailes group.
[xiii] Cloned by Dr Dragana Dobrijevic, former member of the Ward group
[xiv] Expressed by Dr Laure Benhamou, former member of the Hailes group.
[xv] Cloned by Dr Dragana Dobrijevic, former member of the Ward group
[xvi] Cloned by Dr Nadine Tappertzhofen, former member of the Hailes group.

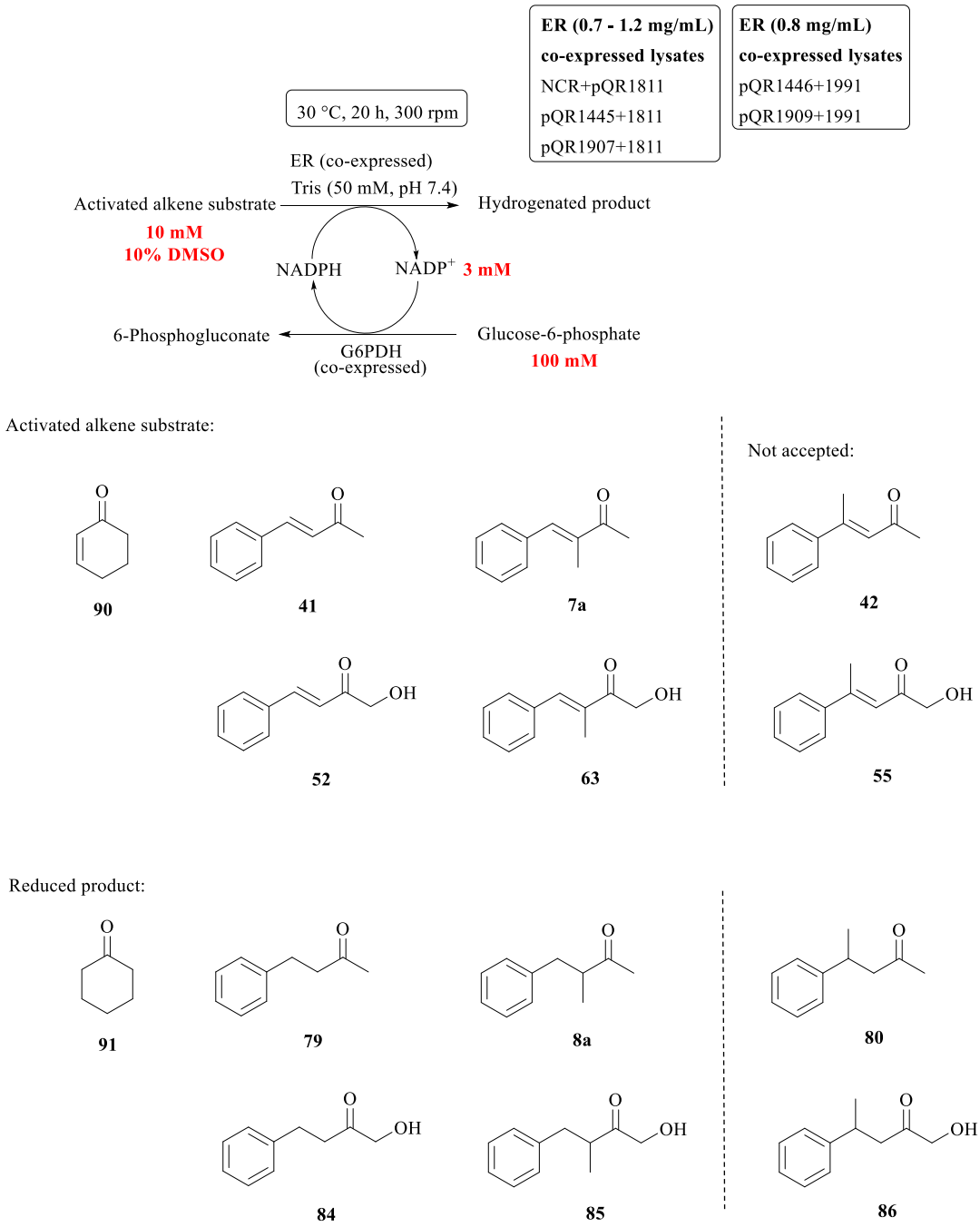

Scheme 42: Bioreduction of cyclohexenone **90**, ketone derivatives **41**, **7a**, **42** and hydroxyketone derivatives **52, 63, 55** with co-expressed clarified lysates to give potential products **91**, **79**, **8a**, **80** and **84** – **86** respectively. Bioconversions were performed in triplicate at 30 °C, 300 rpm for 20 h at a scale of 250 µL. Final concentration were G6PNa (100 mM), $NADP^+$ (3 mM), and alkene substrate (10 mM) in 50 mM Tris (pH 7.4) with 10% DMSO. Either co-expressed clarified lysates or ER lysates with commercial G6PDH were applied at final concentrations of 0.7 – 1.2 mg/mL, and 20 U respectively. Enzymes were expressed from pQR numbers listed.

The ER+G6PDH cloned from pQR1446+1991 and pQR1909+1991 gave poor results with the positive control **90**. With the knowledge that pQR1446 and commercial G6PDH successfully reduce aldehydes such as **70** (**Table 8**), it was deduced that the

recycling enzyme from pQR1991 was not optimal for the bioprocess. Fair to good yields of 48 – 79% were obtained for unsubstituted and α-methyl ketone derivatives **79** and **8a** with NCR, and enzymes from pQR1445, and pQR1907 (**Table 11**). For the unsubstituted hydroxy ketone derivative **84**, a poor yield of 9% was obtained with the ezyme from pQR1445, moderate yield of 49% obtained with the enzyme from pQR1907, and impressive yield of 93% with NCR. Excellent yields of 87 – 100% were obtained for α-methyl hydroxyketone derivative **85** with NCR, and enzymes from pQR1445 and pQR1907.

The ß-substituted derivatives **42** and **55** were not accepted as substrates by any of the ERs investigated. This finding is peculiar as the β-methyl group of aldehyde **40** was well tolerated by NCR and pQR1907 (section 3.3.3, **Figure 23**, **Table 10**) and the ketone groups of **41** and **7a** in this study (affording products **79** and **8a**) were well tolerated also. The author is hesitant to comment on these results with the data currently available but is mindful of the potential of different substrate binding modes with ERs. It is premature to conclude as much given that the selectivity of the products has yet to be determined (if the selectivity is the same the binding mode is the same when considering bioreductions with a given ER). Substrate-based stereocontrol is suspected for pQR1445 and pQR1907 between ketone and α-hydroxyketone substrates described in detail below. To the best of the author's knowledge compounds **42** and **55** have not been explored with ERs in the literature.

Table 11: Yields (%) from bioreduction of ketone derivatives **79**, **8a**, **80** and α-hydroxyketone derivatives **84 – 86** with co-expressed ER+G6PDH.

		NCR +pQR1811[a]	**pQR1445 +1811**[a]	**pQR1907 +1811**[a]	**pQR1446 +1991**[a]	**pQR1909 +1991**[a]
Control	**91**	88%	85%	87%	31%	32%
Ketone	**79**	77%	55%	79%	23%	1%
	8a	48%	56%	57%	1%	1%
	80	--[b]	--[b]	--[b]	--[b]	--[b]
α-Hydroxy Ketone	**84**	93%	9%	49%	1%	1%
	85	100%	93%	87%	2%	--[b]
	86	--[b]	--[b]	--[b]	--[b]	--[b]

[a] Enzymes cloned from pQR numbers given.
[b] Not accepted as a substrate.

For the bioreduction of α-methyl substituted hydroxyketone **63** affording product **85** (compared to unsubstituted **52** affording **84**) the addition of steric bulk (the α-methyl group) was observed to drastically improve yield in bioreductions with pQR1445 and pQR1907 (**Table 11**). However, there is no difference in the yields afforded for

unsubstituted ketone **79** with α-methyl ketone **8a** with pQR1445, suggesting that the α-methyl group was not responsible for the improved yield, and instead the addition of the hydroxyl group was responsible. As for pQR1907, the addition of the α-methyl group actually afforded a lower yield of **8a** in comparison to **79**, also suggesting that its improved yield with α-hydroxyketone derivative **85** (in comparison to **84**) was a result of the hydroxyl group. However, considering compound **84** has a lower yield than **79** for both pQR1445 and pQR1907 this argument would not be valid unless perhaps alternate substrate binding modes were achieved between ketone and α-hydroxyketone derivatives. The author tentatively suggests that this is the only way all the data would agree – that the addition of the hydroxyl group changes the substrate binding mode for ketone and α-hydroxyketone substrates in bioreductions with pQR1445 and pQR1907. Access to both (*S*)-**85** and (*R*)-**85** products is exemplified in the following section 4.2.3 (**Scheme 43**, **Figure 28**) signifying the potential acceptance of different binding modes. ERs from pQR1445 and pQR1907 have only previously been explored with sterically challenging bi- and tri-cyclic enones[59], substrates notably different from those explored in this work and so little to no insight can be provided for the substrates currently under investigation. Crystal structures of pQR1445 and pQR1907 were not available at the time of writing. Substrate-based stereocontrol has been previously described with similar substrates methyl ketone **7a** and ethyl ketone **7b** with OYE3, as described in detail in section 1.2.1.6.[120,162]

As for NCR, a drop in yield was observed comparing ketone products **79** and **8a**, with yields observed to increase for both from addition of the hydroxyl group giving products **84** and **85**. Therefore, it is possible that the substrate binding modes for ketone and α-hydroxyketone substrates with NCR may be the same, in line with modelling in section 4.2.4. Though if this were true the higher yield of **85** compared to **84** would be surprising, especially considering that the yield of ketone **8a** was lower than that of **79**.

4.2.3 Ene-Reductase Clarified Lysates

From the highly successful acceptance of **63** as a substrate for the first time, further ER optimisation was pursued solely with **63**, together with the determination of the optical purities of **85** produced. Compound **55** was not explored further as the TAm amination of **86** was unsuccessful (described in Chapter 5). A panel of metagenomic and literature OYE homologues were investigated, including NCR, pQR1445, pQR1907, and

pQR1446 with co-expressed pQR1811[xvii] as well as pQR1909[xviii], XenA, and YqjM[xix] with commercial G6PDH (Sigma Aldrich). ERs expressed from pQR1446 and pQR1909 were examined with these recycling enzymes (as opposed to pQR1991) for a more accurate evaluation of their activity (**Scheme 43**).

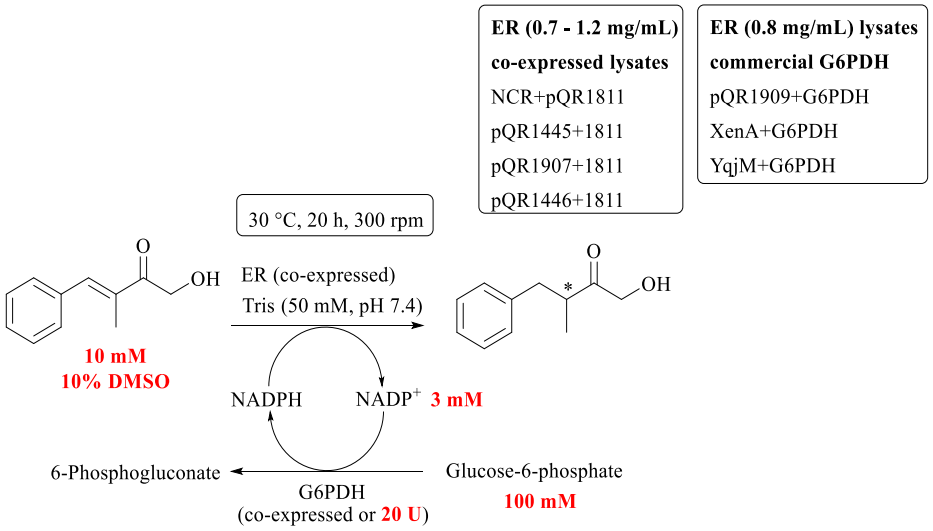

Scheme 43: Bioreduction of hydroxyketone derivative **63** with clarified lysates. Bioconversions were performed in triplicate at 30 °C, 300 rpm for 20 h at a scale of 250 µL. Final concentration were G6PNa (100 mM), $NADP^+$ (3 mM), and alkene substrate (10 mM) in 50 mM Tris (pH 7.4) with 10% DMSO. Either co-expressed clarified lysates or ER lysates with commercial G6PDH were applied at final concentrations of 0.7 – 1.2 mg/mL, and 0.8 mg/mL with 20 U G6PDH respectively. Enzymes were expressed from pQR numbers listed.

NCR, pQR1445 and pQR1907 demonstated the complete bioconversion of **63** (no starting material observed) with only one enantiomer produced from application of NCR (termed (*S*)-**85**, predicted enantioselectivity described in detail in section 4.2.4) (**Figure 28**). Both enantiomers were observed from bioconversion with pQR1445 and pQR1907, with pQR1445 producing more of (*R*)-**85** than (*S*)-**85**. Poor to fair (5 – 57%) product yields were obtained with pQR1446, XenA and YqjM with each providing both enantiomers and demonstating incomplete bioconversions as observed by starting material recovery. Activities of pQR1446, XenA and YqjM were confirmed with the positive control **90**. With their limited success in the bioreduction of **63**, they were excluded from further investigations. Thus, further work was conducted with NCR+pQR1811, pQR1445+1811 and pQR1907+1811.

[xvii] Cloned by Dr. Dragana Dobrijevic, former member of the Ward group.
[xviii] Cloned by Dr. Dragana Dobrijevic, former member of the Ward group
[xix] Cloned by Dr Nadine Tappertzhofen, former member of the Hailes group.

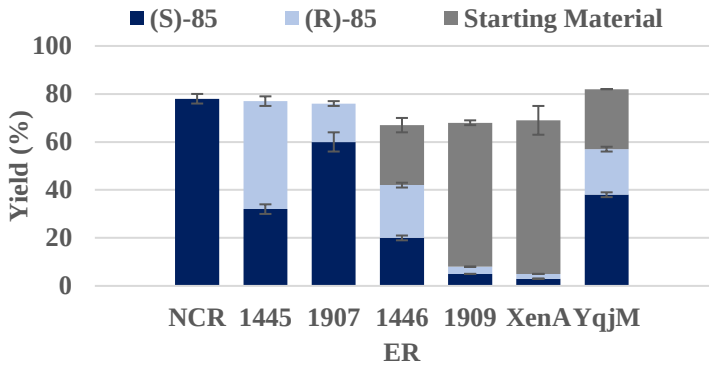

Figure 28: Enantiomeric yields obtained from bioreduction of hydroxyketone derivative **63** with ER clarified lysates. Enzymes were expressed from pQR numbers listed. Enantiomeric yields were determined by GC analysis on a chiral stationary phase with racemic product standards.

As the author has already noted, limited reports in the literature have been presented for the ERs discussed in this work with similar substrates. In 2010, Stueckler *et al.* reported the bioreduction of α-methyl cinnamaldehyde with 7 wild-type ERs in a bi-phasic system; the (*R*)-enantiomer of the product was afforded by YqjM in poor *ee* and conversion while NCR exhibited (*S*)-stereoselectivity with 76% *ee* and excellent conversion.[146] Chapparo-Riggers *et al.* investigated the specific activity of XenA with cinnamaldehyde (1.56 U mg^{-1}), utilising 2-cyclohexen-1-one (2.74 U mg^{-1}) as a positive control.[96] Stereoselectivity was not reported. The author has concluded that YqjM exhibits poor *ee* with α-hydroxyketone **63**, similar to α-methylcinnamaldehyde. NCR tentatively exhibits (*S*)-stereoselectivity and excellent conversion, and so the CH_2OH moeity of substrate **63** is well tolerated. Drawing further comparison/insights would be misleading as the assay performed by Stueckler *et al.* was different than that performed by the author (different enzyme amount, different cofactor type, different scale), and with multiple different variables direct comparison is not possible. Furthermore this is all before the substrate binding mode of **63** is considered in comparison to α-methylcinnamaldehyde. XenA does not appear to well tolerate the CH_2OH moeity of substrate **63**, however with only its specific activity with α-methylcinnamaldehyde reported in the literature it is difficult to directly attribute the low yield to the CH_2OH group of **63** studied in this work.

ERs from pQR1445 and pQR1907 have only previously been explored with sterically challenging bi- and tri-cyclic enones[59], substrates notably different from those explored in this work and so little to no insight can be provided for the substrate currently under investigation. Additionally, crystal structures of these enzymes were not available at

the time of writing. This work represents the first report of ERs from pQR1446 and pQR1909.

4.2.4 Molecular Docking

As NCR was an OYE homologue and previous reports by Brenna *et al.* determined bioreduction of **7a** with OYE1-3 to give (*S*)-**8a**,[120] similar stereochemical outcome was anticipated for the product from application of NCR with **63**. The stereochemical preference for (*S*)-enantiomers is typical of OYE mediated bioreductions of non-cyclic α,β-unsaturated substrates[121,146,227] which arises from a "flipped" binding mode of the substrate in the active site.[120] However, as discussed in Chapter 1, recent reports by Crotti *et al.* determined a switch in the enantioselectivity of OYE1-2 for the bioreduction of ethyl ketone **7b** leading to the preferential formation of the *S*-product.[162] This stereocomplementary behaviour was ascribed to the "classical" binding mode of the substrate in the active site, with later reports concluding that ethyl ketone **7b** was more influenced by the nature of amino acid in position 116 in OYE1 than methyl ketone **7a** was.[162] Provided that subtle differences between substrates had a significant impact on stereochemical outcome molecular docking studies for **7a** and **63** with NCR were performed.

Substrate binding modes for molecular docking were determined using AutoDock Vina, with results viewed in PyMol. The crystal structure of NCR was obtained from the Protein Data Bank and minimised energy conformations of substrates determined using Chem3D. Autodock Tools was applied for initial docking preparation.

Molecular docking of **7a** with NCR observed a "flipped" binding mode of the substrate (**Figure 29A**). *Trans* [2H] reduction with hydride attack at the β-position and protonation at the α-position (from the catalytically active tyrosine residue, position 177) would thus provide (*S*)-**8a** as the anticipated product. Molecular docking of **63** with NCR also observed a "flipped" binding mode with similar stereochemical outcome predicted (**Figure 29B**). As such, the enantiopure product from the application of NCR with **63** in this work was tentatively assigned as (*S*)-**85**.

The author does not put any weight on the outcome of the molecular modelling provided in this thesis. Firstly, the flavin mononucleotide and nicotinamide molecules were already docked into the crystal structure of NCR obtained from PDB[124], and so

docking of the substrate is already unreliable as in reality the relative positionings of the flavin mononucleotide and nicotinamide may be influenced by the presence of the substrate. Secondly, only using one program for molecular docking is inherently inaccurate as each modelling program has its own pitfalls. For an accurate representation of molecular modelling different programs should be used and the consistency of their results evaluated. Doing as much is non-trivial. The author presumes the binding pocket evaluated is the only one for NCR as it is the only one to be described in the literature.[124]

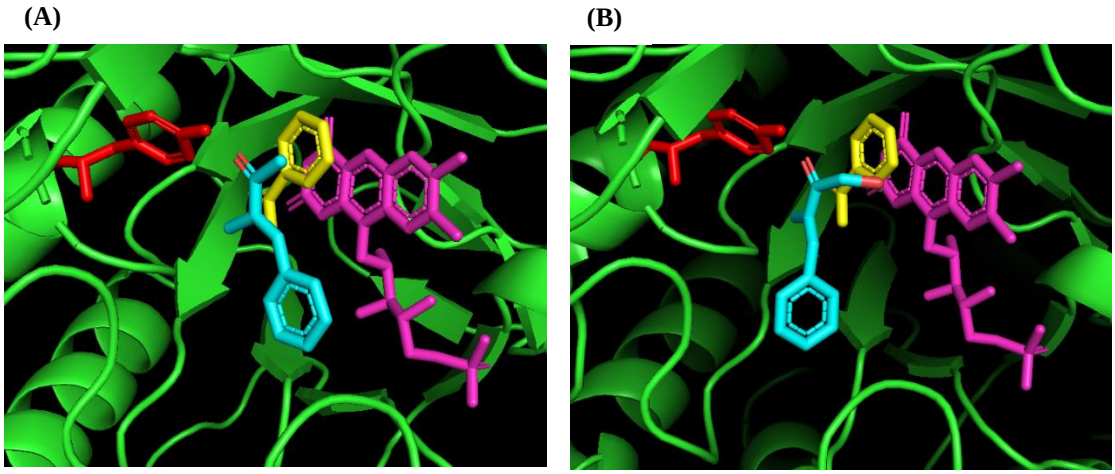

Figure 29: Molecular docking of substrates **(A) 7a** and **(B) 63** with NCR. From left to right, the catalytically active tyrosine residue at position 177 (red), the substrate (turquoise), nicotinamide (yellow), and flavin mononucleotide (magenta). Substates exhibited a "flipped" binding mode. The nictotinamide and flavin mononucleotide were already docked in the NCR crystal structure (PDB ID: 4A3U) and so the docking of substrates exhibited is not an accurate reflection of the structure-activity relationship between NCR and the substrates, as the relative positionings of the substrate, nicotinamide, and flavin mononucleotide to each other may vary in reality.[124]

4.3 Assay Optimisation

With complete bioconversion of **63** attained with NCR, pQR1445, and pQR1907 focus was concentrated on the application of these ERs in the development of alternate strategies for the enantiopure generation of both enantiomers of **85**. To this end, ER assay parameters were systematically investigated and optimised to both increase yield and tune stereoselectivity for (*R*)-**85** (as (*S*)-**85** was already successfully afforded by NCR). Herein the effects of buffer type, clarified lysate concentration, co-solvent type, temperature and substrate loading on the bioreduction of **63** with NCR+pQR1811, pQR1445+1811, and pQR1907+1811 were examined. Yields, optical purities, and starting material recovery were determined by GC analysis with racemic product and

starting material standards as descibed in experiemental methods (***Method D***). Standard deviations in experimental results are reported by error bars.

4.3.1 Optimisation of Buffer Type

From their widespread application in biocatalysis, buffers considered included KPi, HEPES and Tris-HCl. A near neutral pH of 7.4 was employed to prevent racemisation of the product. For NCR+pQR1811, pQR1445+1811 and pQR1907+1811 buffer type was found to be inconsequential for yield and stereoselectivity (**Figure 30**). Therefore, further investigations employed Tris-HCl due to its precedent in ER biocatalysis.[59,116,146] Studies by a predecessor[xx] found buffer concentration to be insignificant in bioreductions and so was not investigated.

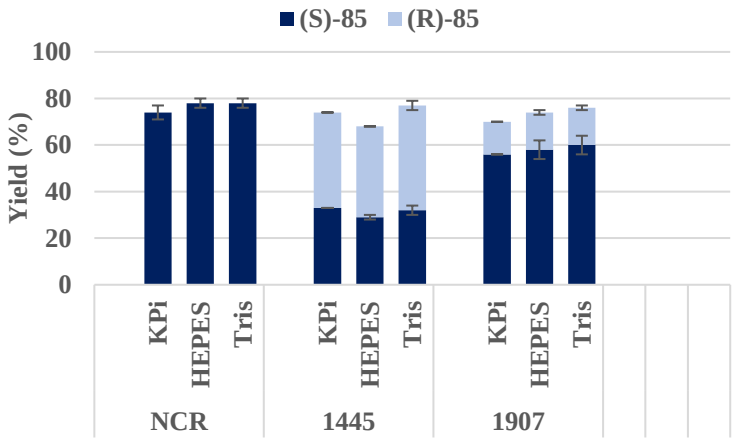

Figure 30: Buffer type investigation on the bioreduction of hydroxyketone derivative **63** with NCR+1811, pQR1445+1811 and pQR1907+1811 co-expressed clarified lysates. Bioconversions were performed in triplicate at 30 °C, 300 rpm for 20 h at a scale of 250 µL. Final concentration were G6PNa (100 mM), $NADP^+$ (3 mM), and alkene substrate (10 mM) with 10% DMSO. Co-expressed clarified lysates were applied at a final concentration of 0.8 mg/mL. Buffers KPi, HEPES and Tris HCl were investigated at 50 mM and pH 7.4. Enzymes were expressed from pQR numbers listed. Enantiomeric yields were determined by GC analysis on a chiral stationary phase with racemic product standards.

4.3.2 Optimisation of Clarified Lysate Concentration

Given the two different binding modes for ER bioreduction, "classical" and "flipped", reductions in ER lysate concentration may in theory allow for the selective uptake of the preferred binding mode, consequently affording stereocontrol on product formation. Co-expressed clarified lysate concentrations were reduced (0.2, 0.4, 0.6 and 0.8 mg/mL), with negligible effect on the stereoselectivities observed (**Figure 31**). The

[xx] Dr Laure Benhamou, former member of the Hailes group

minimum clarified lysate concentration for complete bioconversion was determined to be 0.6 mg/mL and was applied in further experiments.

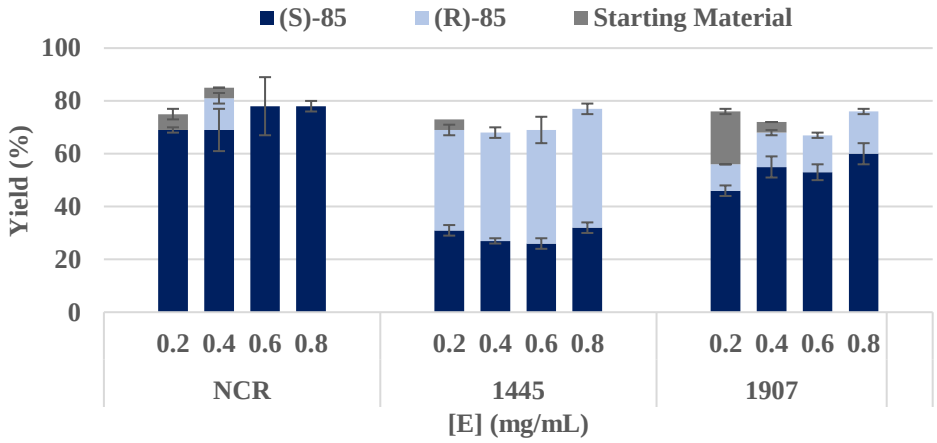

Figure 31: Investigation of the effect of clarified lysate concentration on the bioreduction of hydroxyketone derivative **63** with NCR+1811, pQR1445+1811 and pQR1907+1811 co-expressed clarified lysates. Bioconversions were performed in triplicate at 30 °C, 300 rpm for 20 h at a scale of 250 µL. Final concentration were G6PNa (100 mM), $NADP^+$ (3 mM), and alkene substrate (10 mM) in 50 mM Tris HCl (pH 7.4) with 10% DMSO. Concentration of co-expressed clarified lysates was investigated and applied at a final concentrations of 0.2, 0.4, 0.6 and 0.8 mg/mL. Enzymes were expressed from pQR numbers listed. Enantiomeric yields were determined by GC analysis on a chiral stationary phase with racemic product standards.

4.3.3 Optimisation of Co-solvent Type

Due to the high boiling point of DMSO hindering the work-up of prepative scale biotransformation, miscible lower boiling point co-solvents methanol (MeOH), acetonitrile (MeCN), cyclopentyl methyl ether (CPME) and *tert*-butyl methyl ether (TBME) were examined in the bioconversion of **63** with NCR, and enzymes from pQR1445 and pQR1907. Considering that organic solvents account for 75-80% of the waste in the synthesis of active pharmaceutical ingredients[19], a final concentration of only 10% co-solvent was applied in assays to aid substrate solublity. Across the panel of ERs MeOH was determined to be the most productive co-solvent, affording complete or near complete bioconversion and high yields (**Figure 32**). Additionally, it was the "greenest" co-solvent tested, as determined by the ACS GCI Pharmaceutical Roundtable Solvent Selection Guide.[253] Ethers CPME and TBME were also effective, however were not further investigated due to their limited success in TAm reactions, as described in Chapter 5. Notably, the application of MeCN was found to severly hinder product formation for the enzymes from pQR1445 and pQR1907. Moderate to good yields were attained with CPME and TBME.

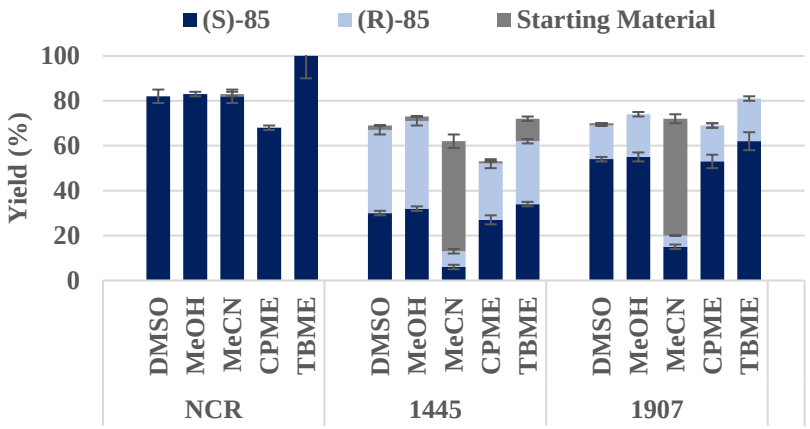

Figure 32: Co-solvent investigations on the bioreduction of hydroxyketone derivative **63** with NCR+1811, pQR1445+1811 and pQR1907+1811 co-expressed clarified lysates. Bioconversions were performed in triplicate at 30 °C, 300 rpm for 20 h at a scale of 250 µL. Final concentrations were G6PNa (100 mM), $NADP^+$ (3 mM), alkene substrate (10 mM) and co-expressed clarified lysate (0.6 mg/mL) in 50 mM Tris (pH 7.4) with 10% co-solvent. A panel of co-solvents were investigated including MeOH, MeCN, CPME and TBME. Enzymes were expressed from pQR numbers listed. Enantiomeric yields were determined by GC analysis on a chiral stationary phase with racemic product standards.

Enzyme conformational changes are the most common reason for enzyme deactivation in the presence of organic co-solvents. Specifically, hydrophilic solvents are established to penetrate the active site of enzymes and induce secondary and tertiary structural changes.[254–256] In addition, hydrophilic solvents exhibit a greater tendency to remove protein-bound water that is integral for maintaining protein structure and function.[257,258] Whilst in-depth studies of metagenomic ERs pQR1445 and pQR1907 with solvents has yet to be performed, one can only assume the affect of hydrophilic MeCN on pQR1445 and pQR1907 activity was pronounced due to its effect on structural changes within the active site. It is not clear why DMSO and MeOH did not produce similar results to MeCN, especially given the chemical similarities between MeOH and MeCN. Ethers CPME and TBME were not water miscible and so could not penetrate the active site. Excellent conversion has been observed using 20% TBME with NCR in the bioconversion of α-methylcinnamaldehyde, albeit under different assay conditions.[146]

4.3.4 Optimisation of Temperature

Temperature effects on the bioconversions were explored above and below 30 °C (25 °C, 30 °C, 37 °C and 45 °C) due to the literature precendent of this temperature in ER biocatalysis.[59,116,120,146,160] Activities for enzymes from pQR1445 and pQR1907 sharply dropped at 45 °C, likely due to their denaturation as has previously been observed with ERs at higher temperature.[127] Complete bioconversions for pQR1445

and pQR1907 were attained at 30 °C (**Figure 33**). Complete bioconversion using NCR was observed at 25 °C, 30 °C, and 37 °C. No significant change in stereoselectivity was observed.

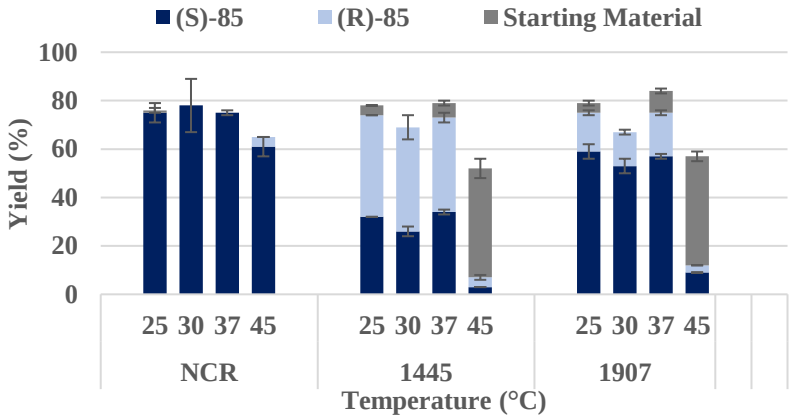

Figure 33: Temperature effects on the bioreduction of hydroxyketone derivative **63** with NCR+1811, pQR1445+1811 and pQR1907+1811 co-expressed clarified lysates. Bioconversions were performed in triplicate at 300 rpm for 20 h at a scale of 250 µL. Final concentration were G6PNa (100 mM), $NADP^+$ (3 mM), alkene substrate (10 mM) and co-expressed clarified lysate (0.6 mg/mL) in 50 mM Tris (pH 7.4) with 10% MeOH. Temperature effects were examined at 25 °C, 30 °C, 37 °C, and 45 °C. Enzymes were expressed from pQR numbers listed. Enantiomeric yields were determined by GC analysis on a chiral stationary phase with racemic product standards.

4.3.5 Optimisation of Substrate Loading

With the aim of scaling the reaction to preparative scale (hundreds of milligrams of substrate, further information provided in section 6.2.1), substrate loading was investigated to aid preparative scale development and maximise product generated. Complete and enantiopure bioconversions were attained at a maximum substrate loading of 25 mM (**Figure 34**). Over-saturation of NCR with the substrate was observed at 30 mM. As such further work was conducted at 25 mM substrate loading. A minimal amount of (*R*)-**85** was generated using 5 mM substrate loading due to there being "too much" enzyme relative to substrate resulting in the indiscriminate accpetance of substrate binding modes. A decreased overall recovery at higher substrate loadings was due to the limited solubility of both the starting material and product in aqueous solution, resulting in their removal during the centrifugation of the denatured enzymes.

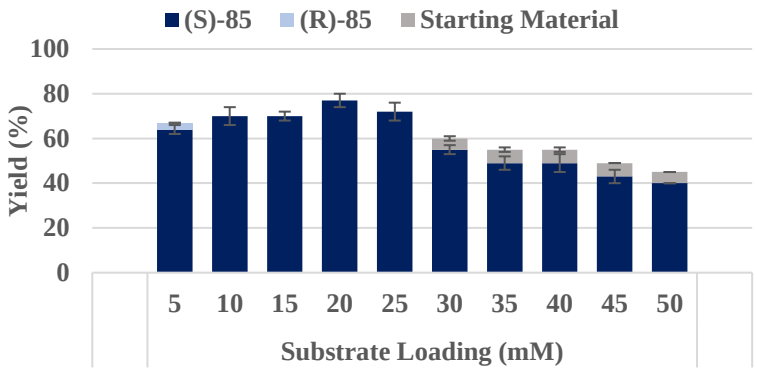

Figure 34: Substrate loading investigation on the bioreduction of hydroxyketone derivative **63** with NCR+pQR1811 co-expressed clarified lysate. Bioconversions were performed in triplicate at 30 °C, 300 rpm for 20 h at a scale of 250 µL. Final concentration were G6PNa (100 mM), $NADP^+$ (3 mM), and co-expressed clarified lysate (0.6 mg/mL) in 50 mM Tris (pH 7.4) with 10% MeOH. Substrate loading was investigated at 5, 10, 15, 20, 25, 30, 35, 40, 45, and 50 mM. Enantiomeric yields were determined by GC analysis on a chiral stationary phase with racemic product standards.

Therefore, optimised conditions for the bioreduction of **63** at a total volume of 250 µL with 10% MeOH had final concentrations of G6PNa (100 mM), $NADP^+$ (3 mM), substrate **63** (25 mM) and co-expressed NCR+pQR1811 (0.600 mg mL^{-1}). Biotranformations were performed in triplicate. Bioreductions were performed in 1.5 mL eppendorfs and incubated at 30 °C and 300 rpm for 20 h.

4.4 Substrate Scope

Substrate scope investigations included an initial screening of substrates with .NCR+pQR1811, with some assay optimisation. Analytical methods are described.

4.4.1 Initial Screening

Substrate scope was examined to determine the potential wide-spread applicability of the optimised biotransformation. An electron donating, electron withdrawing, and halogen substituent on the phenyl ring were investigated. Ketone derivatives **46** – **48** were used to give anticipated hydrogenated products **81** – **83** prior to the analysis of α-hydroxyketone derivatives **64** – **66** to afford their hydrogenated products **87** – **89** (**Figure 35**). Optimised reaction conditions developed using **28** were employed. Biotransformations were performed at a volume of 250 µL with the alkene substrate at 25 mM and co-expressed clarified lysate NCR+pQR1811 applied at a final concentrations of 0.6 mg/mL.

For **47**, a final concentration of 20% MeOH in bioconversion was applied to aid solubility. Product yields for the investigations with ketone derivatives were measured by GC-analysis (***Method D***) with product standards. Standard deviations across the triplicate experiments are given by error bars.

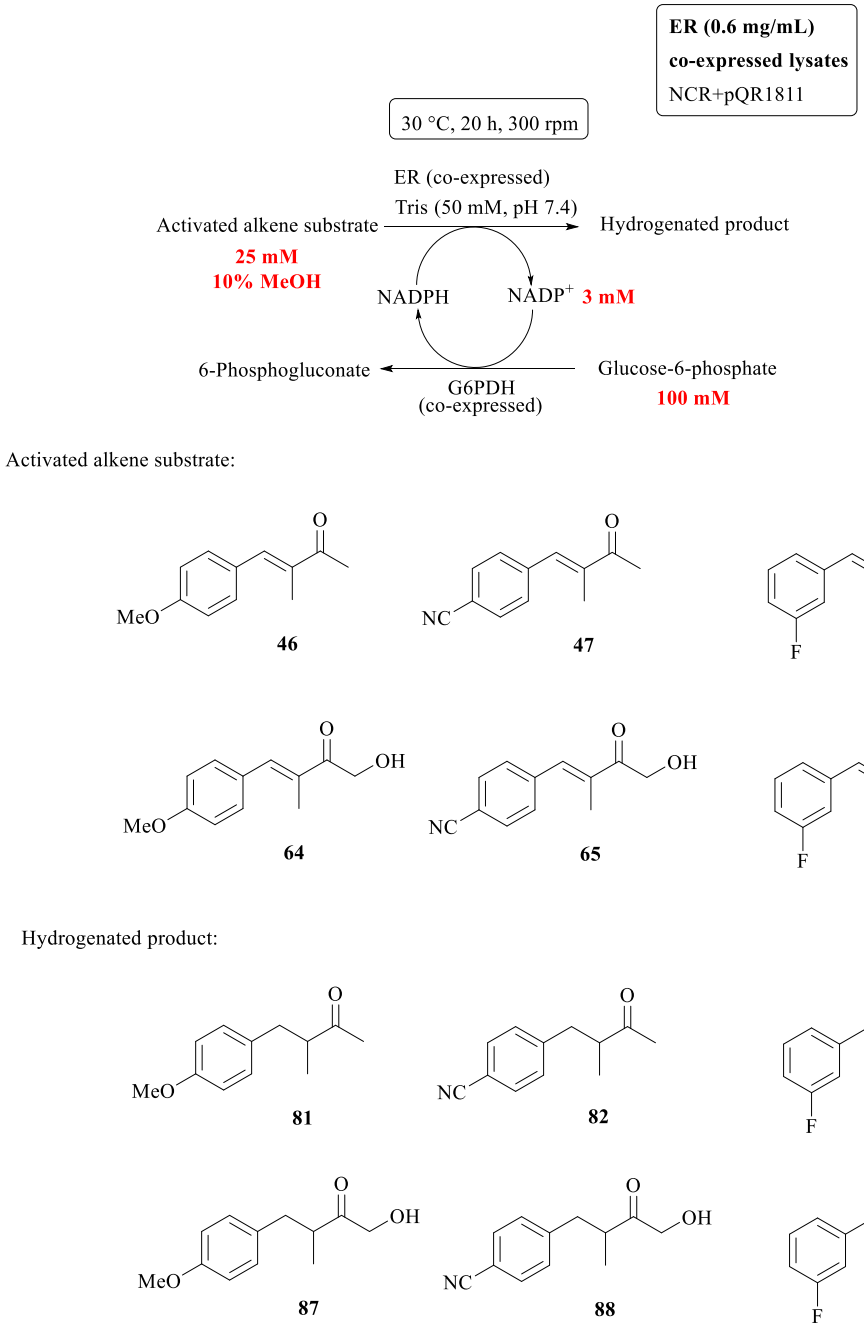

Figure 35: Bioreduction of the ketone derivatives **46** – **48** and α-hydroxyketone derivatives **64** – **66** with NCR+pQR1811 co-expressed clarified lysate to give anticipated hydrogenated products **81** – **83** and **87** – **89** respectively. Bioconversions were performed in triplicate at 30 °C, 300 rpm for 20 h at a scale of 250 µL. Final concentration were G6PNa (100 mM), $NADP^+$ (3 mM), alkene substrate (25 mM) and co-expressed clarified lysate (0.6 mg/mL) in 50 mM Tris (pH 7.4) with 10% MeOH for **46**, **48**, **64** – **66**, and 20% MeOH for **47**.

Ketones **46** – **48** were successfully accepted as substrates in ER biotranformations as evidenced by product formation, however all substrates suffered from the low overall recovery of the starting material and product. This was suspected to be due to the limited solubility of both the starting material and product in aqueous solution, resulting in their removal during the centrifugation of the denatured enzymes. Incomplete bioconversions were observed for **46** and **48** with starting material recovered whilst no starting material was detected for **47** (**Figure 36**). Direct comparison cannot be made though owing to the increased cosolvent concentration of 20% MeOH applied in the biotransformation of **47**. As all substrates were accepted reactions were not optimised and substrate walking proceeded to their respective α-hydroxy ketone derivatives **64** – **66**.

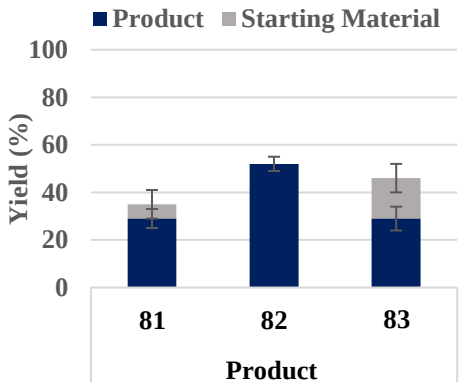

Figure 36: Yields obtained from bioreduction of **46 – 48** with NCR+pQR1811 co-expressed clarified lysates.

Investigations proceeded to α-hydroxyketone derivatives **64** – **66** with optimised bioreduction parameters employed as before for **63**. GC analysis was not viable owing to the high boiling points of to α-hydroxyketone derivatives **64** – **66** and **87** – **89**. With analytical HPLC analysis earlier deemed unfeasible in the separation of unsaturated and saturated aldehydes, success was not anticipated with α-hydroxy ketones. Thus, chiral HPLC analysis was pursued for the determination of product yield and *ee*.

Enantiomeric separations were trialled across Chiralcel OB, Chiralcel OJ, Chiralpak OD-H and Chiralpak AD-H columns at 1% ^{i}PrOH/hexane. Pleasingly, resolution was achieved for all racemic product standards **87** – **89** using a Chiralpak AD-H column with this eluent. Efforts to reduce the retention time by increasing solvent polarity suffered the loss of enantiomeric resolution for **87** and **89**, even at 2.5% ^{i}PrOH/hexane. The enantiomeric separation of **88**, however, was still afforded at 5% ^{i}PrOH/hexane.

Thus, analytical analysis of **64** and **66** biotransformations were conducted using 1% ^{i}PrOH/hexane (***Method H***) whilst 5% ^{i}PrOH/hexane was applied for the analysis of **65** (***Method I***). Excellent *ee* but low yields were observed for **87** and **88**, whereas **89** gave an excellent yield of 97% and moderate *ee* of 54% (**Figure 37**).

It is not clear why the formation of comound **87** was as low yielding as it was. The *para*-methoxy substituent has been shown to be readily accepted by NCR from work with aldehyde **72** in Chapter 3, and the α-methyl and hydroxyketone motifs has been readily accepted by NCR with compound **63**. Potentially having all three functional groups present had an affect on the substrate-enzyme binding affinity by preference for different binding modes (binding mode of α-methyl hydroxyketone **63** with NCR suspected to be "flipped", binding mode of *para*-methoxy aldehyde **72** with NCR not determined), or else the biotransformation was not performed for long enough (though biotransformations with **72** and **63** were high yielding when performed on the same timeframe). Similarily for compound **88** the biotransformation may not have been left for long enough, or else the cyano group was not readily accepted by the enzyme. As for **89** provided that it resembled compound **63** with only a small inductively electron withdrawing fluorine substituent (which would aid bioreduction whilst not hindering sterics) it is unsuprising that it was high yielding. The lower *ee* suggested that there was either "too much" enzyme for the substrate resulting in the indiscrimate acceptance of binding conformations, or else the biotransformation was performed for too long, resulting in the reverse ER reaction.

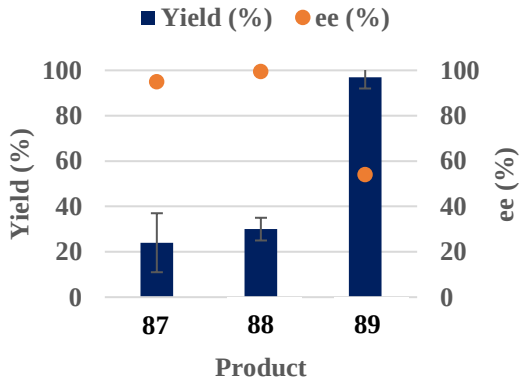

Figure 37: Yields (%) and *ee* (%) obtained from bioreduction of **64** – **66** to give products **87 – 89** with NCR+pQR1811 co-expressed clarified lysates.

Attempts to furnish improved yields of **87** and **88** examined a decreased substrate loading of 10 mM compared to 25 mM. As for **89**, reduced clarified lysate concentrations of 0.2 and 0.4 mg/mL were surveyed for the improvement of *ee* by the selective uptake of the preferred binding mode. Disappointingly, yields of **87** and **88** were not found to be significantly improved from the decreased substrate loading with only 32% and 46% attained repectively (**Figure 38**). For **89**, the *ee* was improved to 99.5% from the reduction of clarified lysate concentration to 0.4 mg/mL (as opposed to 0.6 mg/mL), however a reduction in yield to 60% was also observed (**Figure 39**). In further work, 3 extractions from the aqueous phase were undertaken in efforts to improve the yields of **87** – **89**, however no improvement was observed.

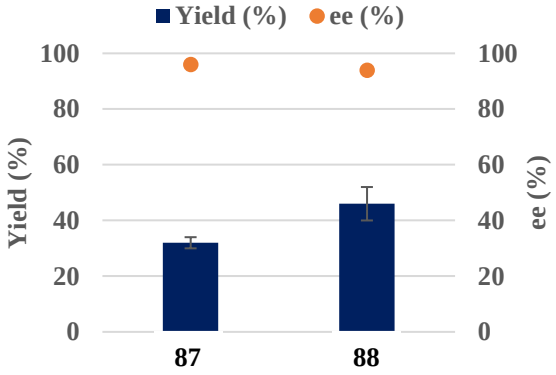

Figure 38: Bioreduction of hydroxyketone derivatives **64** and **65** with NCR+pQR1811 co-expressed clarified lysate to give products **87** and **88**. Bioconversions were performed in triplicate at 30 °C, 300 rpm for 20 h at a scale of 250 µL. Final concentration were G6PNa (100 mM), $NADP^+$ (3 mM), alkene substrate (10 mM) and co-expressed clarified lysate (0.6 mg/mL) in 50 mM Tris (pH 7.4) with 10% MeOH.

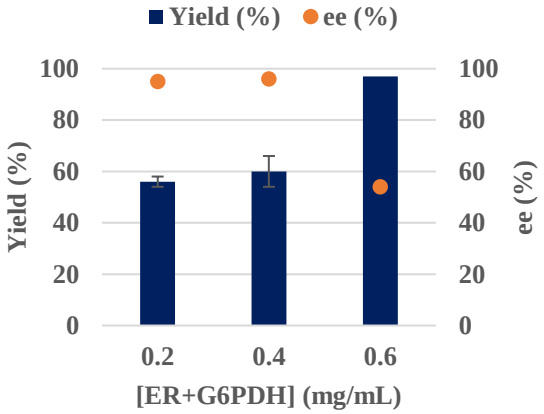

Figure 39: Bioreduction of hydroxyketone derivative **66** with NCR+pQR1811 co-expressed clarified lysate to give product **89**. Bioconversions were performed in triplicate at 30 °C, 300 rpm for 20 h at a scale of 250 µL. Final concentration were G6PNa (100 mM), $NADP^+$ (3 mM), alkene substrate (25 mM) in 50 mM Tris (pH 7.4) with 10% MeOH. Concentration of co-expressed clarified lysates was investigated and applied at a final concentrations of 0.2, 0.4, and 0.6 mg/mL.

In conclusion, products **87** and **88** were attained in excellent *ee* but low yield, even at a reduced substrate loading of 10 mM (as opposed to 25 mM). Product **89** was achieved in a high *ee* of 99.5% when the clarified lysate concentration was reduced to 0.4 mg/mL (as opposed to 0.6 mg/mL) resulting in the selective uptake of the preferred binding mode.

4.5 Conclusions

In this chapter, substrate complexity was increased via "substrate walking" from ketone to α-hydroxyketone derivatives. Derivatives investigated were unsubstituted, α-methyl substituted, and β-methyl substituted ketones, given the successful biotransformation of their respective aldehydes as well as relevance of these derivatives in the formation of TAAR1 inhibitors.

A panel of five ER+G6PDH co-expressed clarified lysates were initially screened, four from metagenomic sources and NCR, reported in the literature.[59,98,146] The β-substituted ketone and α-hydroxyketone derivatives **42** and **55** were not accepted as substrates for any of the ERs investigated. This is potentially due to steric reasons as unsubstituted derivatives **41** and **52** were well accepted and ERs typically have a preferred binding mode for substrates.[93] Yields from bioreductions of ketone and α-hydroxyketone derivatives with pQR1445 and pQR1907 tentatively suggested that alternate substrate binding modes were achieved between ketone and α-hydroxyketone substrates, however affording insights from the data produced is non-trival, especially when the stereoselectivities of the products produced had not been established. Further work should aim to identify the stereoselectivities of ketone and α-hydroxyketone products for comparison, as alternate substrate binding modes may be deduced from opposite stereoselectivities. With the current data produced it is possible that the substrate binding modes for ketone and α-hydroxyketone substrates with NCR may be the same, in line with modelling described in section 4.2.4.

Successful bioconversions were attained with unsubstituted and α-methyl substituted ketone and α-hydroxyketone derivatives. Further work was pursued solely with the α-methyl substituted analogue **63** given the inherently interesting chiral centre generated from the ER biotransformation.

Additional screening of **63** was performed for the determination of enantiomeric excesses, with NCR affording the enantiopure generation of (*S*)-**85**. Investigations proceeded with the three most successful ER+G6PDH systems (NCR+pQR1811, pQR1445+1811, pQR1907+1811) in efforts to furnish optimised yield. To this end, assay parameters (buffer type, clarified lysate concentration, co-solvent type, temperature, and substrate loading) were systematically investigated and optimised.

With assay parameters optimised to yield enantiopure (*S*)-**85** in 63% yield at 25 mM substrate loading, analogues of **63** were examined to increase the substrate scope. Quantitative analysis was established using chiral HPLC with a Chiralpak AD-H column. Optimisation of assay parameters was individually tailored to each substrate **64** – **66** to afford excellent *ee* of up to 99.5% and yields of 32 – 60% from their bioreduction with NCR+pQR1811. For reasons discussed in section 4.4.1, it was not clear why the formation of product **87** was as low yielding as it was, and similarly what was responsible for the low yield of **88**. As for product **89** a high *ee* of 99.5% was achieved when the clarified lysate concentration was reduced to 0.4 mg/mL (as opposed to 0.6 mg/mL) resulting in the selective uptake of the preferred binding mode.

With an ER and substrate identified in this chapter, and assay parameters optimised, the following chapter (Chapter 5) explored the application of TAms in the amination of α-hydroxyketone derivatives aiming to identify a substrate, as well as a (*R*)- and (*S*)-selective TAm viable in an one-step one-pot ER-TAm cascade. Assay parameters were optimised.

5. Transaminase Amination of α-Hydroxyketone Derivatives

5.1 Introduction

TAms in conjunction with the co-enzyme pyridoxal phosphate (PLP) mediate the transfer of an amino group from an amine donor to a keto acceptor, thereby generating an optically active amine product. As enantiopure amines are highly valuable synthons in bioactive compounds, TAms present an efficient means for their preparation.

In this chapter, the application of TAms with α-hydroxyketone derivatives is described for the molecular assembly of single isomer amino alcohols via a one-pot ER-TAm cascade. Screening of α,ß-unsaturated and saturated hydroxyketone derivatives against a panel of literature and metagenomic TAms aimed to identify a substrate, as well as a (*R*)- and (*S*)-selective TAm viable in an one-step one-pot ER-TAm cascade. Further work involved the systematic evaluation of seven assay parameters for the optimised amination conditions with each TAm. Examination of the analogue substrate scope was also carried out to evaluate the substrate promiscuity of the TAms with α-hydroxyketone derivatives.

5.2 Preliminary Assay Considerations

Preliminary assay considerations included finding a suitable TAm and substrate, assay design, analytical methods, and determination of the optical purity of the product.

5.2.1 Transaminases and Substrates

The work described in Chapter 4 and Chapter 5 was investigated concurrently. Where appropriate reference is made to Chapter 4.

Following the successful ER biotransformation of α-hydroxyketone derivatives, investigations proceeded to explore the TAm amination of α-hydroxyketones **52**, **63**, **55** and **84** – **86**. As discussed in Chapter 1, activated alkene substrates were required for ER bioreduction. Provided that TAm amination would inactivate these substrates by removing the electron withdrawing group, it was essential to evaluate the transamination of both α,ß-unsaturated and saturated hydroxyketone derivatives **52**, **63**, **55** and **84** – **86** respectively, to determine the potential of a one-step one-pot ER-TAm

cascade. Pyruvate was employed as a positive control, being a natural substrate for many TAms[259,260] and broadly accepted as a substrate with others[67,193].

Preliminary screening was performed with the extensively studied Cv-TAm (*Chromobacterium violaceum*)[182], Mv-TAm (*Mycobacterium vanbaalenii*)[185], Rh-TAm (*Rhodobacter sphaeroides*)[261], and As-TAm (*Arthrobacter sp.*)[35],[xxi] along with putative class III metagenomic TAms cloned from a dometic drain metagenome[xxii], with plasmid numbers termed pQR2189, pQR2192 and pQR2208[60]. Belonging to fold type IV TAms, Mv-TAm and As-TAm were (*R*)-enantioselective whilst the rest were (*S*)-enantioselective (fold type I). Previous work by the Hailes group had established Cv-TAm to sucessfully accept keto-diols thus producing chiral amino alcohols.[261] Mv-TAm and Rh-TAm have been shown to be successful in the generation of linear aminopolyols[262], whilst As-TAm had been established to successfully aminate sterically challenging 1,3-ketones[35].

Previous investigative reports by the Hailes group found that cinnamaldehyde **70** as well as linear aliphatic aldehydes to be readily accepted by the metagenomic TAms cloned from pQR2189, pQR2192 and pQR2208.[60]

5.2.2 Clarified Lysate Preparation and Assay Analytics

TAms were expressed by recombinant *E. coli* BL21 (DE3) cultivation. Cell pellets of Cv-TAm and Mv-TAm were stored up to six months at -80 °C with no loss of activity, and 13-TAm (later described) up to three months. Enzymes were prepared as clarified cell lysates with PLP additionally added at a final concentration of 1.2 mM for stability. The term "clarified cell lysates" refer to the total soluable unpurified protein expressed by *E. coli*. Enzymes Mv-TAm and 13-TAm in the clarified cell lysates were at a concentration of 2.8 mg/mL and 5 mg/mL respectively. Clarified lysates were stored at -80 °C for up to two weeks with no loss of activity, defrosted only once, and kept at 0 °C prior to application.

Varying assays for TAm amination and their subsequent analytical analysis are described in this chapter depending on the amine donor employed. For high throughput enzymatic screening of TAms with substrates, a colorimetric assay developed by the

[xxi] Cloned by Dr Nadine Tappertzhofen, former member of the Hailes group.
[xxii] Cloned by Dr Leona Leipold, former member of the Hailes group.

Hailes and Ward groups using the "smart" amine donor 2-(4-nitrophenyl)ethan-1-amine was performed.[202] As described earlier in section 1.2.2.4, TAm bioconversion is indicated by formation of a red precipitate produced from the reaction of by-product 2-(4-nitrophenyl)acetaldehyde with the excess amine donor to afford the thermodynamically stable conjugated enamine.

Quantitative analytical analysis of transamination was achieved using either α-MBA or IPA as the amine donor. For α-MBA, either (*S*)- or (*R*)-α-MBA was utilised corresponding to the selectivity of the TAm investigated. Substrate conversion was determined by HPLC analysis at 254 nm (***Method A***) of the acetophenone by-product using a product standard.[182] As such, "conversion yields" are quoted. Background acetophenone was removed in a negative control of 10% co-solvent (final concentration). Bioconversions were performed in triplicate.

Owing to the lack of chromophore of IPA and its transamination by-product acetone, substrate depletion of the α-hydroxyketone derivative was quantified. As such, "conversion" is quoted. Quantitative analysis was determined by HPLC analysis at 214 nm (***Method B***) with a starting material standard. Bioconversions were performed in triplicate.

5.2.3 Optical Purity

The analytical techniques of GC and chiral HPLC were not viable options to determine the optical purity of the chiral amino alcohol products due to their high boiling points and highly polar nature respectively. It was envisaged that following ER and TAm biotransformations the diastereomeric ratio (*dr*) of the chiral amino alcohols could be determined by analytical HPLC analysis against a product standard. As such, racemic **100** (**Figure 40**) was chemically synthesised by reductive amination, and a method pursued for its diastereomeric resolution by analytical HPLC. Unfortunately, resolution could not be obtained. Therefore, it was planned for the *dr* of the chiral amino alcohols to be determined by NMR analysis following preparative scale biotransformations and reaction with cyanogen bromide to give 2-aminooxazolines.

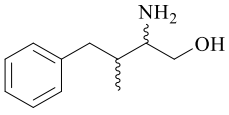

100

Figure 40: Structure of racemic amino alcohol **100**.

5.3 Initial Screening of Hydroxyketone Derivaties

Preliminary screening of α-hydroxyketone derivatives with TAms was performed using a colorimetric assay and α-MBA assay to afford initial insights regarding a suitable substrate and TAm for biotransformations.

5.3.1 Colorimetric Assay

For preliminary enzymatic screening of TAms with hydroxyketone derivatives, the colorimetric assay was performed at high lysate concentration (**Scheme 44**).[202] Two controls were used: A positive control with pyruvate **101** and a negative control of DMSO (10% final co-solvent concentration).

Colorimetric screening was performed on α,ß-unsaturated and saturated hydroxyketone derivatives **52**, **63**, **55** and **84** – **86** respectively (**Scheme 44**). TAms cloned from pQR2208, pQR2191, pQR2189, alongside Rh-TAm, As-TAm, Mv-TAm, and Cv-TAm were investigated. Initial findings (by eye, taking into account each TAms activity with the positive and negative control) depicted activity towards saturated hydroxyketone derivates **84 – 86** and interestingly, notable activity of TAms toward α,ß-unsaturated hydroxyketone derivatives **52**, **63**, **55** was also observed (**Figure 41**). Therefore, a two-step one-pot cascade was anticipated in order to retain the carbonyl functional group for ER biotransformation.

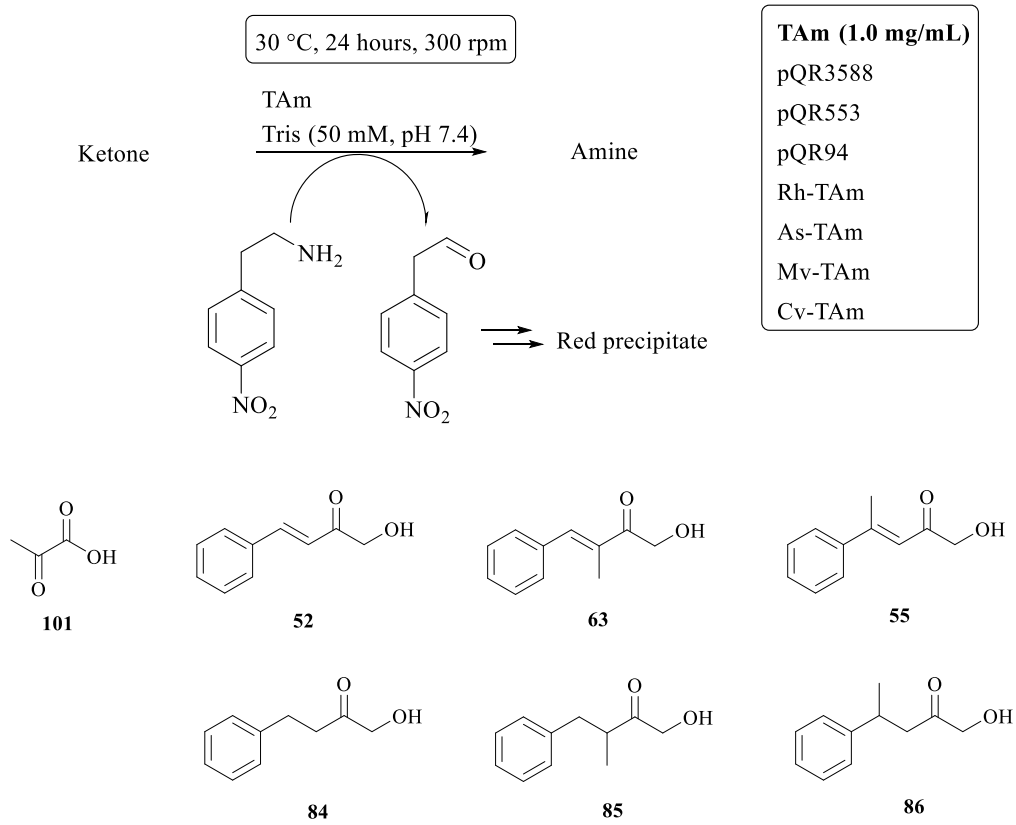

Scheme 44: TAm colorimetric assay of substrates **101**, **52**, **63**, **55** and **84 – 86** with TAm clarified lysates. Bioconversions were performed in a 96-well plate at 30 °C, 300 rpm for 24 h at a scale of 200 µL. Final concentration were PLP (1.0 mM), 2-(4-nitrophenyl)ethan-1-amine hydrochloride (25 mM), substrate (10 mM), TAm clarified lysate (1.0 mg/mL) in 50 mM Tris (pH 7.4) with 10% DMSO.

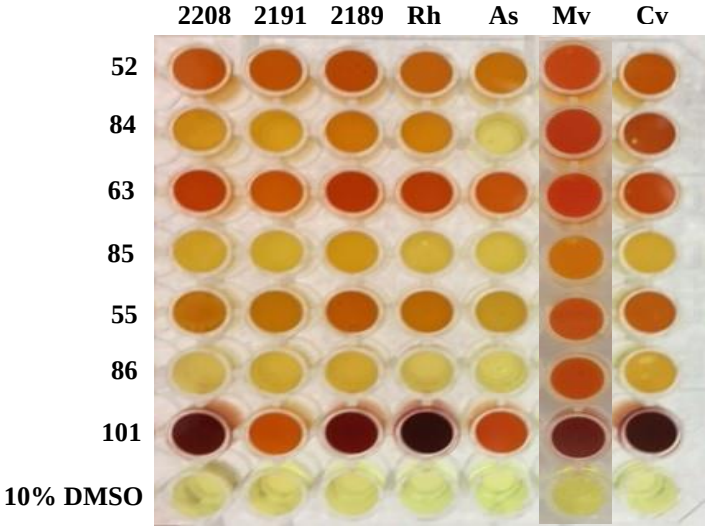

Figure 41: Colorimetric assay of substrates **52**, **63**, **55** and **84 – 86** with TAm clarified lysates. Pyruvate **101** was employed as a positive control and 10% DMSO as a negative control.

5.3.2 α-Methylbenzylamine Assay

For the quantitative evaluation of TAm amination with hydroxyketone derivatives **52**, **63**, **55** and **84** – **86** an α-MBA assay was undertaken at high lysate concentration (1.0 mg/mL) (**Scheme 45**). Conversion yields were determined as previously described. Standard deviations in experimental results are reported by error bars.

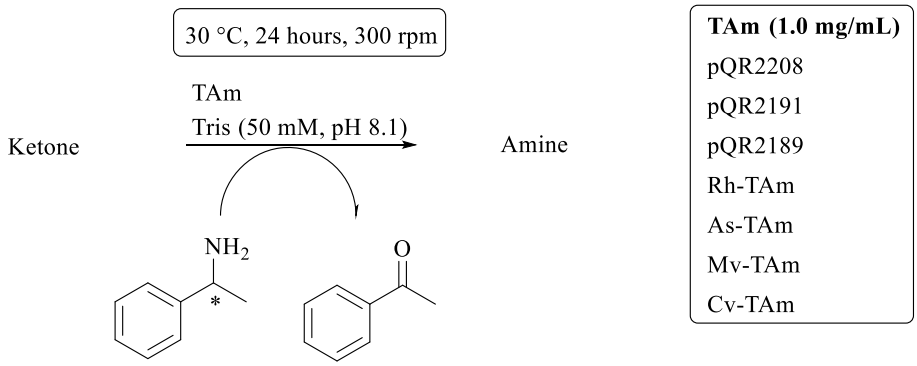

Scheme 45: α-MBA assay with hydroxyketone derivatives **52**, **63**, **55** and **84 – 86** and TAm clarified lysates. Bioconversions were performed in triplicate at 30 °C, 300 rpm for 24 h at a scale of 200 µL. Final concentrations were PLP (1.2 mM), (*R*)- or (*S*)-α-MBA (25 mM), substrate (10 mM) and TAm clarified lysate (1.0 mg/mL) in 50 mM Tris HCl (pH 8.1) with 10% DMSO.

Encouraging results were attained, with conversion yields of 67% and 56% afforded by the (*R*)-enantioselective Mv-TAm with α- and β-substituted saturated hydroxyketone derivatives **85** and **86** (**Table 12**). Interestingly, amination of unsubstituted **84** with Mv-TAm provided a poor conversion yield of only 4%, without clear reason. In addition, poor conversion yields were attained with all other TAms and substrates, with the exception of Cv-TAm with **63**. Consistent with the colorimetric assay, comparable or higher conversion yields for α,β-unsaturated hydroxyketone derivatives **52**, **63**, **55** were obtained in comparison to their corresponding saturated derivatives **84** – **86** (**Figure 42**). Thus, a two-step one-pot ER-TAm cascade with Mv-TAm was anticipated, rather than a one-step one-pot reaction with the simultaneous addition of both enzymes. Rationalising experimental results further using structural and mechanistic information specific to Mv-TAm was not possible as a crystal structure of the enzyme was not available in the literature at the time of writing.

Table 12: Conversion yields (%) of positive control **101** with α,β-unsaturated and saturated hydroxy ketone derivatives **52**, **63**, **55** and **84** – **86** respective with TAm clarified lysates.

		Cv	Mv	As	Rh	pQR2189[a]	pQR2191[a]	pQR2208[a]
Control	**101**	83	78	42	86	85	88	83
α,β-Unsatuated	**52**	2	58	6	9	9	27	3
	63	76	68	17	11	11	31	3
	55	2	48	3	7	3	9	0
Saturated	**84**	7	4	0	0	0	1	3
	85	4	67	5	1	0	18	0
	86	6	56	4	3	0	6	0

[a] TAms cloned from pQR numbers given.

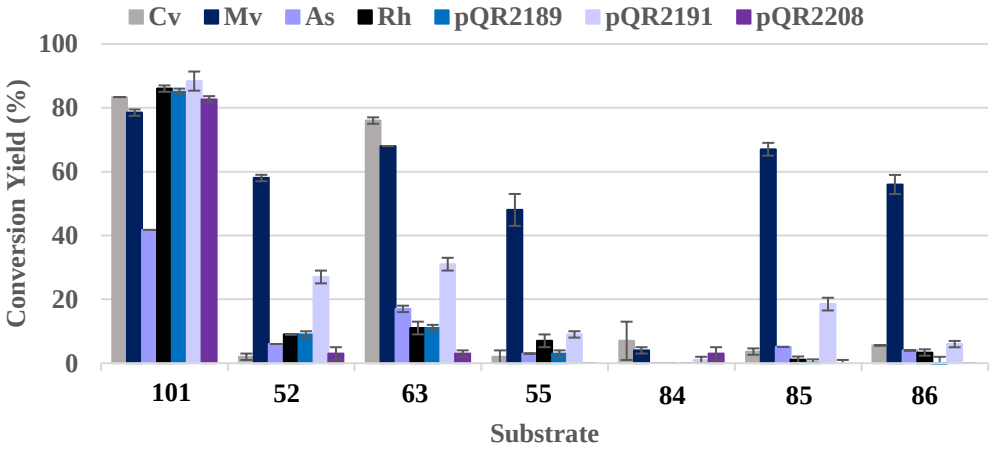

Figure 42: Conversion yields of acetophenone production from bioconversion of positive control **101**, α,β-unsaturated and saturated hydroxyketone derivatives **52**, **63**, **55** and **84 – 86** respective with TAm clarified lysates. TAms cloned from pQR numbers given.

Since a suitable (*S*)-enantioselective TAm had yet to be identified in the preliminary screen, further metagenomic TAms from a soil metagenome were explored. A panel of 4 putative class III TAms from 2 soil isolates were explored: 1-TAm, 13-TAm, 16-TAm (*Rhodococcus sp.*), and 23-TAm (*Aminobacter sp.*).[xxiii] This work represents the first application of these enzymes. With efforts in ER bioreduction concentrated on α-substituted unsaturated hydroxyketone derivative **63** (ER bioreduction of **55** unviable), attention for TAm amination was shifted to the corresponding saturated hydroxyketone **85**. The metagenomic TAms (1-TAm, 13-TAm, 16-TAm, and 23-TAm) were screened at high lysate concentration (1.0 mg/mL) with positive control **101** and saturated hydroxyketone derivative **85** in an α-MBA assay (**Figure 43**).

[xxiii] Cloned by Dr Dragana Dobrijevic.

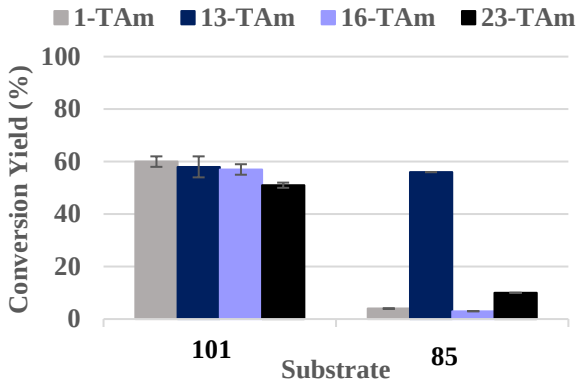

Figure 43: Conversion yields of acetophenone production from bioconversion of positive control **101** and saturated hydroxyketone derivative **85** with metagenomic TAm clarified lysates. Bioconversions were performed in triplicate at 30 °C, 300 rpm for 24 h at a scale of 200 µL. Final concentrations were PLP (1.2 mM), (*S*)-α-MBA (25 mM), substrate (10 mM) and TAm clarified lysate (1.0 mg/mL) in 50 mM Tris HCl (pH 8.1) with 10% DMSO.

Pleasingly a good conversion yield of 56% was attained with 13-TAm and **85**, comparable to that with the positive control **101**, of 58%. A further α-MBA assay was undertaken to investigate 13-TAm's applicability with α,β-unsaturated hydroxyketone derivative **63** to determine the potential of a one-step one-pot cascade. Agreeably, a low conversion yield of 11% was observed signifying the potential of an ER-TAm cascade (**Figure 44**). Rationalising experimental results further using structural and mechanistic information specific to 13-TAm was not possible as a crystal structure of the enzyme was not available in the literature at the time of writing.

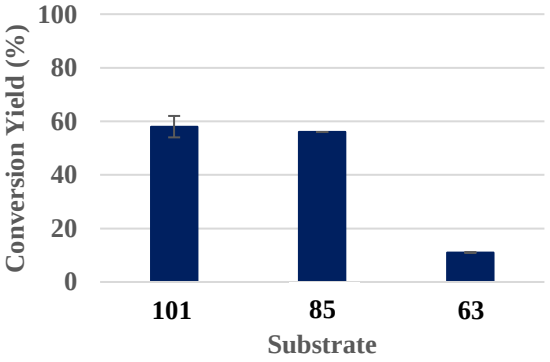

Figure 44: Conversion yields of acetophenone production from bioconversion of positive control **101** along with saturated and α,β-unsaturated hydroxyketone derivatives **85** and **63** respective with 13-TAm clarified lysates. Bioconversions were performed in triplicate at 30 °C, 300 rpm for 24 h at a scale of 200 µL. Final concentrations were PLP (1.2 mM), (*S*)-α-MBA (25 mM), substrate (10 mM) and TAm clarified lysate (1.0 mg/mL) in 50 mM Tris HCl (pH 8.1) with 10% DMSO.

5.4 Assay Optimisation

With a suitable (*S*)- and (*R*)-enantioselective TAm identified, 13-TAm and Mv-TAm respectively, assay parameters were methodically optimised to maximise the biocatalytic yields. Parameters evaluated included the clarified lysate concentration, type of co-solvent, substrate loading, type of amine donor, amine donor equivalents, temperature, and pH. As the TAm bioconversion was systematically investigated in parallel with the ER optimisation, and the two biotransformations designed for compatability in a cascade, findings from the ER optimisation experiments are referenced where appropriate.

Initial experiments employed α-MBA as the amine donor, with the application of IPA later pursued due to its inexpense and volatile ketone by-product, acetone, produced following transamination. Tris-HCl was utilised as the buffer due to its success in ER bioreductions and known compatability with TAms from previous work by the Hailes group (unpublished). For comparative purposes, investigations with the metagenomic (*S*)-enantioselective 13-TAm were performed alongside (*S*)-enantioselective Cv-TAm, acknowledged as a "gold standard" wild-type TAm due to its substrate promiscuity and high stereoselectivity.[182] Bioconversions were performed in triplicate at a 200 µL scale. Results were analysed by HPLC against the product standard acetophenone using ***Method A*** as described in section 9.3.

5.4.1 Optimisation of Clarified Lysate Concentration

Dependence of conversion yield on clarified lysate concentrations was evaluated at 0.5, 1.0, and 1.5 mg/mL. The clarified lysate concentration of 0.5 mg/mL was not found to hinder conversion yields, nor did the increase lysate concentration improve them for both Mv-TAm and 13-TAm (**Figure 45**). Therefore, future experiments were performed with 0.5 mg/mL clarified lysate. Cv-TAm provided poor conversion yields across all lysate concentrations investigated.

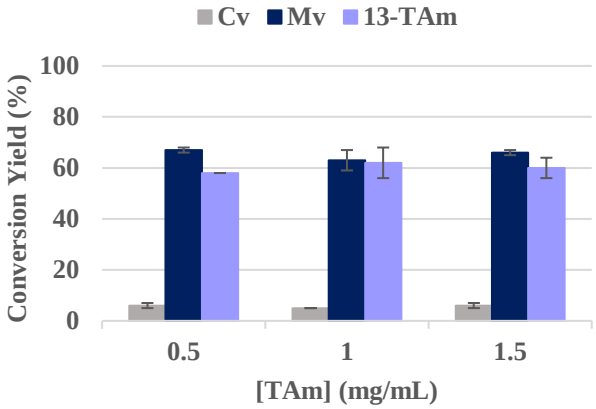

Figure 45: Investigation of TAm clarified lysate concentration on the bioconversion of α-substituted saturated hydroxyketone derivative **85** as determined by conversion yields from acetophenone production. Bioconversions were performed in triplicate at 30 °C, 300 rpm for 24 h at a scale of 200 µL. Final concentrations were PLP (1.2 mM), (*R*)- or (*S*)-α-MBA (25 mM), substrate (10 mM) in 50 mM Tris HCl (pH 7.4) with 10% DMSO. Concentration of TAm clarified lysates was investigated and applied at final concentrations of 0.5, 1.0, and 1.5 mg/mL.

5.4.2 Optimisation of Co-solvent Type

For reasons noted in the optimisation of ER bioreductions, the co-solvents methanol (MeOH), acetonitrile (MeCN), cyclopentyl methyl ether (CPME) and *tert*-butyl methyl ether (TBME) were examined at a final concentration of 10% v/v. In line with results from the ER investigations, MeOH was found to be readily tolerated by both Mv-TAm and 13-TAm (**Figure 46**). Thus, further α-MBA assays employed MeOH as a co-solvent unless otherwise specified. Acetonitrile afforded a good conversion yield of 67% with Mv-TAm but very poor conversion yield of only 3% with 13-TAm. Ethers CPME and TBME gave poor results ranging from 17 – 33% for both Mv-TAm and 13-TAm. Cv-TAm provided poor conversion yields across all co-solvents investigated.

Enzyme conformational changes are the most common reason for enzyme deactivation in the presence of organic co-solvents. Specifically, hydrophilic solvents are established to penetrate the active site of enzymes and induce secondary and tertiary structural changes.[254–256] In addition, hydrophilic solvents exhibit a greater tendency to remove protein-bound water that is integral for maintaining protein structure and function.[257,258] Whilst in-depth studies of Mv-TAm with acetonitrile have yet to be performed, and information with novel 13-TAm is lacking, one can only assume the affect of hydrophilic solvents on 13-TAm activity is pronounced due to their effect on structural changes within the active site.

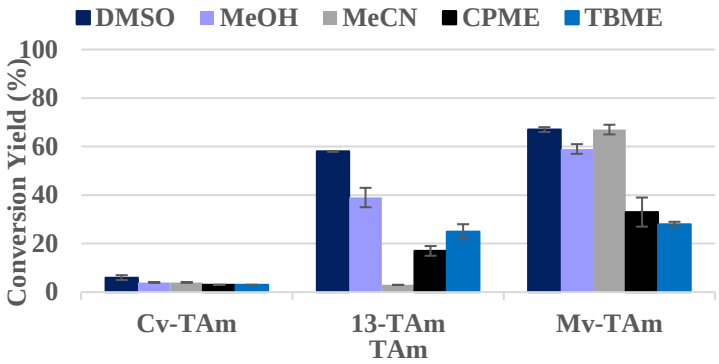

Figure 46: Investigation of type of co-solvent on the bioconversion of α-substituted saturated hydroxyketone derivative **85** with TAm clarified lysates as determined by conversion yields from acetophenone production. Bioconversions were performed in triplicate at 30 °C, 300 rpm for 24 h at a scale of 200 µL. Final concentrations were PLP (1.2 mM), (*R*)- or (*S*)-α-MBA (25 mM), substrate (10 mM) and TAm clarified lysate (0.5 mg/mL) in 50 mM Tris HCl (pH 7.4) with 10% co-solvent. A panel of co-solvents were investigated including MeOH, MeCN, CPME and TBME.

5.4.3 Optimisation of Substrate Loading

Substrate loading experiments were pursued to maximise product formation. Mv-TAm exhibited a steady decline in conversion yield with increased substrate loading, with 13-TAm also exhibiting a decrease (**Figure 47**). Provided the optimised maximum substrate loading of 25 mM for NCR, further work with TAms was conducted at a substrate loading of 25 mM unless otherwise specified.

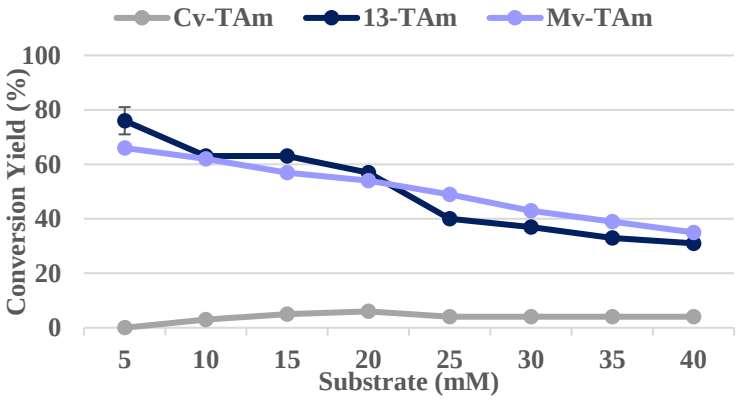

Figure 47: Investigation of substrate loading on the bioconversion of α-substituted saturated hydroxyketone derivative 34 with TAm clarified lysates as determined by conversion yields from acetophenone production. Bioconversions were performed in triplicate at 30 °C, 300 rpm for 24 h at a scale of 200 µL. Final concentrations were PLP (1.2 mM), (*R*)- or (*S*)-α-MBA (25 mM), and TAm clarified lysate (0.5 mg/mL) in 50 mM Tris HCl (pH 7.4) with 10% MeOH. Substrate loading was investigated at 5 – 40 mM.

5.4.4 Optimisation of Isopropylamine Equivalents and Co-solvent

Application of IPA as the amine donor was investigated for reasons earlier discussed. Given the change in amine donor, IPA was examined at the two best co-solvents for Mv-TAm and 13-TAm at 1 – 20 equivalents relative to substrate loading (25 mM). An increase in IPA equivalents for Mv-TAm was found to increase substrate conversion (**Figure 48A**), with little effect observed for 13-TAm (**Figure 48B**). Further work aimed to examine the effect of temperature with IPA equivalents.

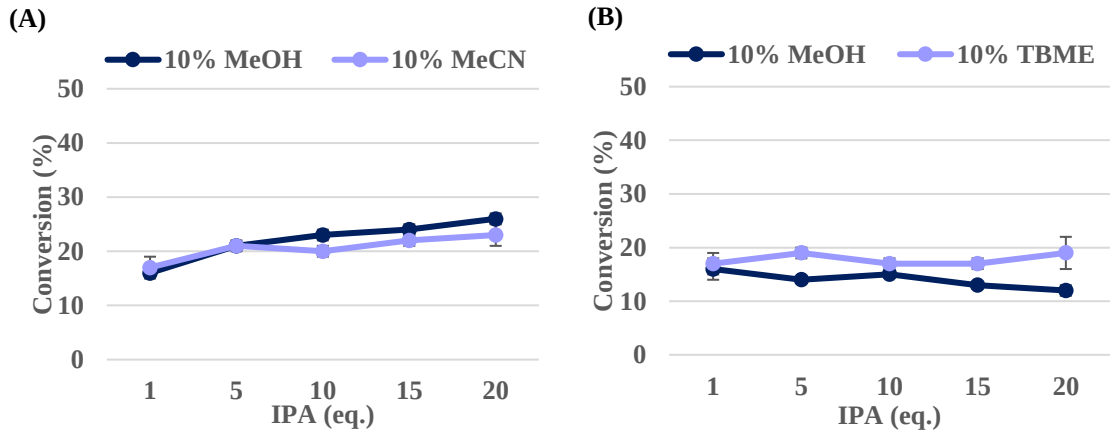

Figure 48: Investigation of IPA equivalents at two best co-solvents on the bioconversion of α-substituted saturated hydroxyketone derivative **85** with **(A)** Mv-TAm and **(B)** 13-TAm clarified lysates as determined by conversion from substrate depletion. Bioconversions were performed in triplicate at 30 °C, 300 rpm for 24 h at a scale of 200 µL. Final concentrations were PLP (1.2 mM), substrate (25 mM), and TAm clarified lysate (0.5 mg/mL) in 50 mM Tris HCl (pH 7.4) with **(A)** 10% MeOH or MeCN **(B)** 10% MeOH or TBME. IPA equivalents were investigated at 1 – 20 equivalents relative to substrate loading. Conversion was determined from HPLC detection at 214 nm for quantitative analysis of substrate depletion. Standard deviation in experimental results are given by error bars.

5.4.5 Optimisation of Isopropylamine Equivalents and Temperature

IPA as an amine donor was further examined alongside different temperatures. As before, IPA at equivalents of 1 – 20 were investigated. Temperatures of 30 °C, 37 °C and 45 °C were applied in bioconversion, in correspondence with ER temperature investigations as well as in agreement with previous TAm biotransformations performed by the Hailes group.[60,193] An optimal temperature of 37 °C was observed for Mv-TAm, with increased conversions from increased IPA equivalents (**Figure 49A**). 13-TAm was most productive at 37 °C and 45 °C, with no change in conversion observed with increased IPA equivalents (**Figure 49B**).

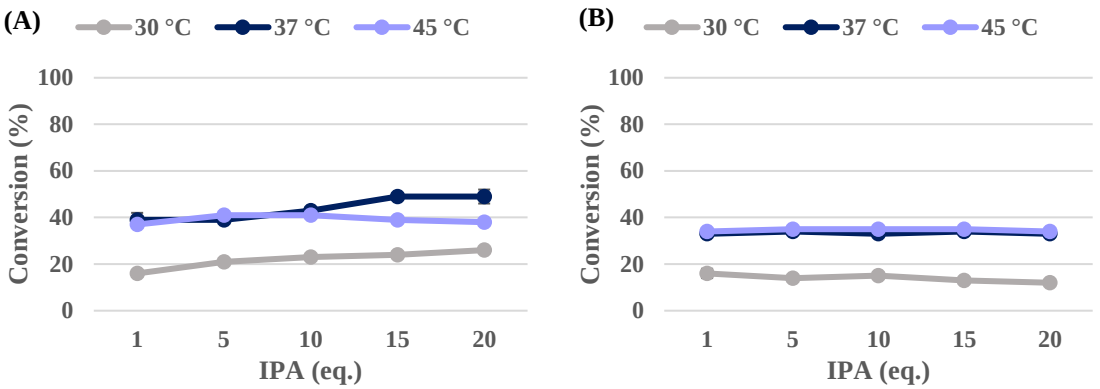

Figure 49: Investigation of IPA equivalents and temperature on the bioconversion of α-substituted saturated hydroxyketone derivative **85** with **(A)** Mv-TAm and **(B)** 13-TAm clarified lysates as determined by conversion from substrate depletion. Bioconversions were performed in triplicate at 300 rpm for 24 h at a scale of 200 µL. Final concentrations were PLP (1.2 mM), substrate (25 mM), and TAm clarified lysate (0.5 mg/mL) in 50 mM Tris HCl (pH 7.4) with 10% MeOH. IPA equivalents were investigated at 1 – 20 equivalents relative to substrate loading at temperatures of 30 °C, 37 °C, and 45 °C.

To provide further insights, additional IPA up to 40 equivalents was evaluated at the two best temperatures of 37 °C and 45 °C. As earlier projected for Mv-TAm, at 37 °C increased IPA equivalents provided and increased conversion of starting material to a maximum of 59% (**Figure 50A**). Mv-TAm had previously been established to be productive at 35 °C.[263] Increased IPA equivalents for 13-TAm was observed to have little affect at both 37 °C and 45 °C (**Figure 50B**). As such, further experiments with IPA as the amine donor were conducted at 37 °C. A maximum of 100 equivalents of IPA was evaluated for both Mv-TAm and 13-TAm at 37 °C, with 11% and 0% conversions of starting material respectively. This was most likely due to the high concentration of IPA denaturing the enzyme.

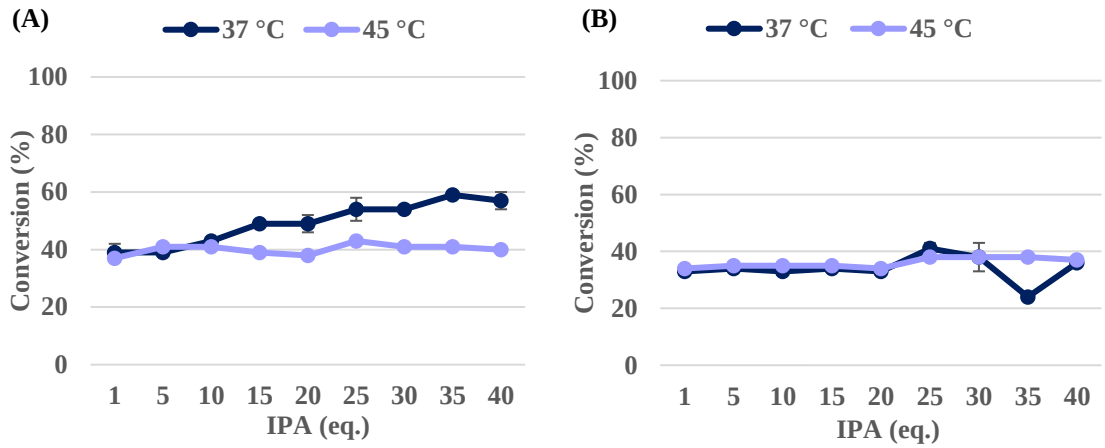

Figure 50: Further investigation of IPA equivalents and temperature on the bioconversion of α-substituted saturated hydroxyketone derivative **85** with **(A)** Mv-TAm and **(B)** 13-TAm clarified lysates as determined by conversion from substrate depletion. Bioconversions were performed in triplicate at 300 rpm for 24 h at a scale of 200 µL. Final concentrations were PLP (1.2 mM), substrate (25 mM), and TAm clarified lysate (0.5 mg/mL) in 50 mM Tris HCl (pH 7.4) with 10% MeOH. IPA equivalents were investigated at 1 – 40 equivalents relative to substrate loading at temperatures of 37 °C, and 45 °C.

5.4.6 Optimisation of Isopropylamine Equivalents and pH

Following the successful reactions of Mv-TAm and 13-TAm with increased IPA equivalents, the effect of pH on the transamination was investigated with 25 – 40 eq. IPA at pH 7.4, 8 and 9. Mv-TAm performance was found to be optimal at more basic pH 9 whilst 13-TAm activity was most successful at pH 7.4 (**Figure 51**). Mv-TAm had previously been established to be productive at a basic pH of 8 – 8.5.[263]

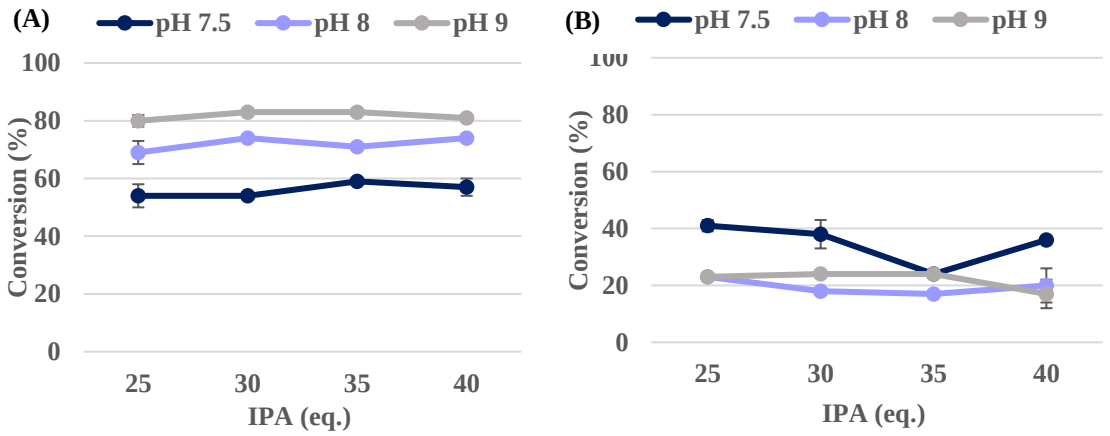

Figure 51: Investigation of IPA equivalents and pH on the bioconversion of α-substituted saturated hydroxyketone derivative **85** with **(A)** Mv-TAm and **(B)** 13-TAm clarified lysates as determined by conversion from substrate depletion. Bioconversions were performed in triplicate at 37 °C, 300 rpm for 24 h at a scale of 200 µL. Final concentrations were PLP (1.2 mM), substrate (25 mM), and TAm clarified lysate (0.5 mg/mL) in 50 mM Tris HCl with 10% MeOH. IPA equivalents were investigated at 25 – 40 equivalents relative to substrate loading at a pH of 7.4, 8, and 9.

Determination of the maximum substrate conversion with minimum IPA at pH 9 with Mv-TAm was then examined. A maximum substrate conversion of 83% was observed with 30 eq. of IPA relative to 25 mM substrate loading (**Figure 52**). Thus, transamination with the (*R*)-selective Mv-TAm at a volume of 200 µL was optimised to 37 °C, 300 rpm for 24 h in 50 mM Tris HCl (pH 9) with 10% MeOH at final concentrations of PLP (1.2 mM), IPA (750 mM, 30 eq.), substrate 34 (25 mM) and Mv-TAm (0.5 mg/mL).

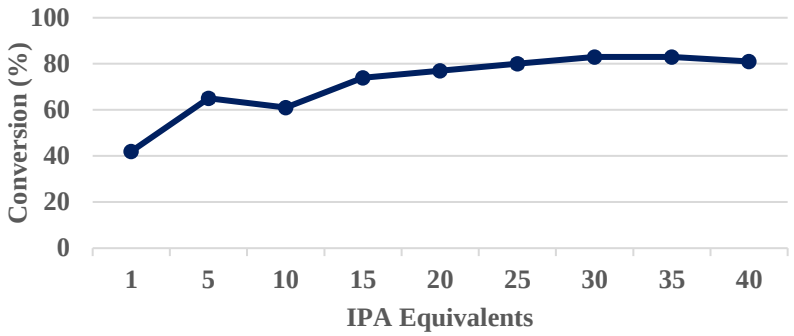

Figure 52: Investigation of IPA equivalents on the bioconversion of α-substituted saturated hydroxyketone derivative **85** with Mv-TAm clarified lysate as determined by conversion from substrate depletion. Bioconversions were performed in triplicate at 37 °C, 300 rpm for 24 h at a scale of 200 µL. Final concentrations were PLP (1.2 mM), substrate (25 mM), and TAm clarified lysate (0.5 mg/mL) in 50 mM Tris HCl (pH 9) with 10% MeOH. IPA equivalents were investigated at 1 – 40 equivalents relative to substrate loading.

5.4.7 Optimisation of α-Methylbenzylamine Equivalents, pH and Temperature

Given the lack of success of 13-TAm tolerating IPA, efforts were redirected toward utilising (*S*)-α-MBA as the amine donor. Employing a substrate loading of 25 mM, MBA equivalents, pH and temperature were investigated. An optimal pH of 7.4 and temperature of 30 °C were clearly determined, with a maximum conversion yield of 50% attained. (**Figure 53**). Unfortunately, increased pH and temperature were both found to reduce the conversion yield.

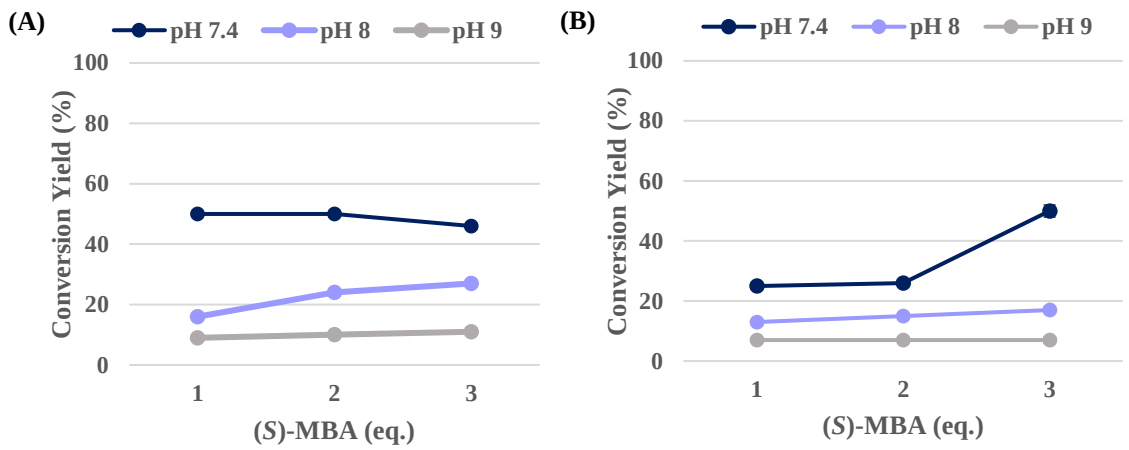

Figure 53: Investigation of (*S*)-α-MBA equivalents and pH on the bioconversion of α-substituted saturated hydroxyketone derivative **85** with 13-TAm clarified lysate at **(A)** 30 °C and **(B)** 37 °C as determined by conversion yields from acetophenone production. Bioconversions were performed in triplicate at 300 rpm for 24 h at a scale of 200 µL. Final concentrations were PLP (1.2 mM), substrate (25 mM) and 13-TAm clarified lysate (0.5 mg/mL) in 50 mM Tris HCl with 10% MeOH. (*S*)-α-MBA equivalents were investigated at 1 – 3 equivalents relative to substrate loading at a pH of 7.4, 8, and 9.

Since the optimisation of MBA, pH, and temperature parameters at 25 mM substrate loading had yet to supply a conversion yield that surpassed that observed from a 5 mM substrate loading of 34 with 13-TAm (**Figure 47**), the lower substrate loading was employed. (*S*)-α-MBA equivalents were re-examined at this lower substrate loading, at pH 7.4 and 30 °C. A maximum conversion yield of 72% was achieved at 4 equivalents of (*S*)-α-MBA (**Figure 54**). Thus, transamination with (*S*)-selective 13-TAm at a volume of 200 µL was optimised to 30 °C, 300 rpm for 24 h in 50 mM Tris-HCl (pH 7.4) with 10% MeOH at final concentrations of PLP (1.2 mM), (*S*)-α-MBA (25 mM, 5 eq.), substrate **85** (5 mM) and 13-TAm (0.5 mg/mL). Comparison to the literature is not possible as neither the substrate nor the enzyme has been reported in the literature. Additionally, to the best of the author's knowledge the α-hydroxy ketone motif has not been previously explored with TAms.

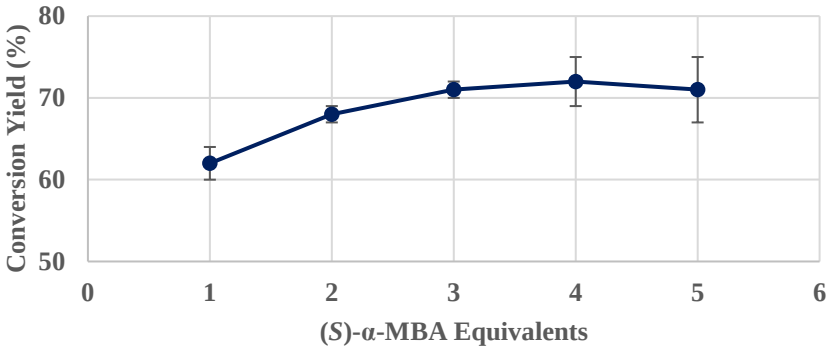

Figure 54: Investigation of (*S*)-α-MBA equivalents on the bioconversion of α-substituted saturated hydroxyketone derivative **85** with 13-TAm clarified lysate as determined by conversion yields from acetophenone production. Bioconversions were performed in triplicate at 30 °C, 300 rpm for 24 h at a scale of 200 µL. Final concentrations were PLP (1.2 mM), substrate (5 mM) and 13-TAm clarified lysate (0.5 mg/mL) in 50 mM Tris HCl (pH 7.4) with 10% MeOH. (*S*)-α-MBA equivalents were investigated at 1 – 5 equivalents relative to substrate loading.

5.5 Substrate Scope

The use of TAms for the amination of saturated α-hydroxyketone derivatives **87** – **89** was explored in parallel to the NCR bioreduction of unsaturated α-hydroxyketone derivatives **64** – **66** (described in Chapter 4). Experimental findings from the NCR bioreduction concluded that a lower substrate loading of 10 mM was required for **64** and **65**, whilst the optimised biotransformation of **66** was performed at 25 mM substrate loading. Given that compatible conditions for an ER-TAm cascade were envisaged, aminations of **87 – 89** were undertaked at their respective ER substrate loadings. Earlier determined optimised conditions for Mv-TAm and 13-TAm were applied (**Figure 55**).

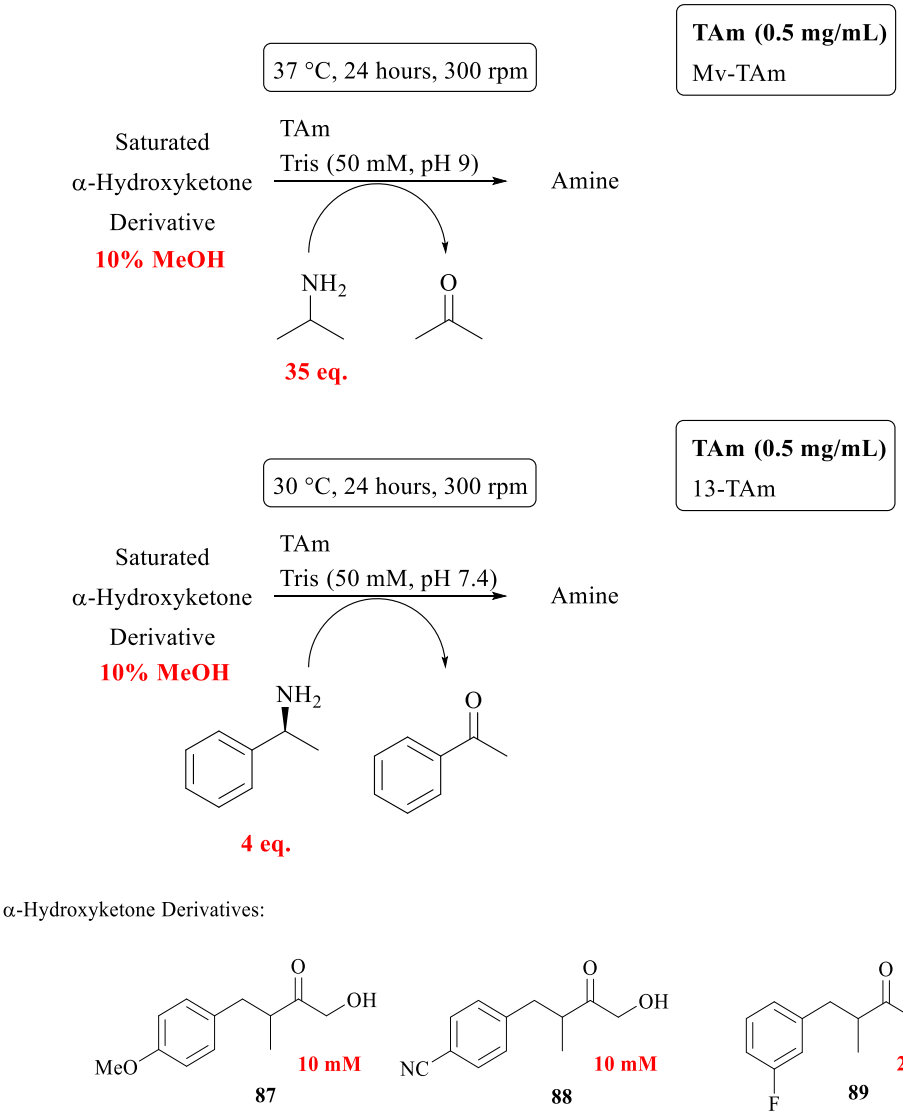

α-Hydroxyketone Derivatives:

Figure 55: Amination of α-hydroxyketone derivatives **87 – 89** with optimised transamination conditions for Mv-TAm and 13-TAm.

Quantitative conversions from Mv-TAm transaminations were determined by the HPLC detection of substrate depletion at 214 nm using starting material standards (***Method B***). A moderate conversion of 41% was observed for **87**, with fair conversions of 62% and 51% measured for **88** and **89** respectively (**Figure 56**). It was therefore determined that electron-donating and electron-withdrawing groups on the phenyl ring had little affect on transamination.

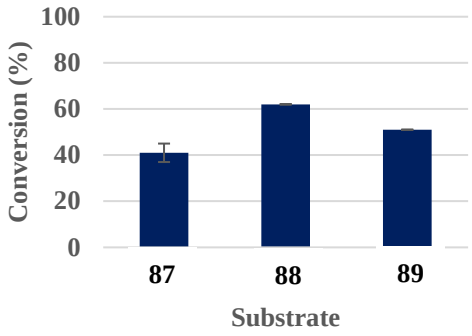

Figure 56: Initial investigation for amination of α-hydroxyketone derivatives **87 – 89** with Mv-TAm clarified lysate. Bioconversions were performed in triplicate at 37 °C, 300 rpm for 24 h at a scale of 200 µL. Final concentrations were PLP (1.2 mM), and Mv-TAm clarified lysate (0.5 mg/mL) in 50 mM Tris HCl (pH 9) with 10% MeOH. Final substrate concentrations were **87** and **88** (10 mM), and **89** (25 mM).

Quantitative analysis of the 13-TAm amination using the (*S*)-α-MBA assay was performed as before (***Method A***). Poor conversion yields of up to 23% were recorded for substrates **87** – **89** (**Figure 57**). In efforts to furnish improved conversion yields, the clarified lysate concentraion of 13-TAm was increased three-fold to 1.5 mg/mL, with a modest improvement observed for all substrates, providing conversion yields of 21 – 40% (**Figure 57**). Therefore, the substrates were not well accepted by the enzyme. Provided that substrate **85** was well accepted by 13-TAm under comparable conditions, this could be due to steric effects of the functional groups (*para*-methoxy, *para*-cyano, *meta*-fluoro) within the active site, or else the biotransformation was not performed for long enough, or 13-TAm was not stable for the entire reaction time. As the fluoro substituent of compound **89** is small, it would be reasonable to conclude that steric effects were an unlikley reason for its poor conversion. As such, further work should examine a longer reaction time. Comparison to the literature is not possible as 13-TAm is a novel enzyme and the work presented in this thesis represents its first application. Moreover to the best of the author's knowledge TAm amination of α-hydroxy ketones has yet to be reported.

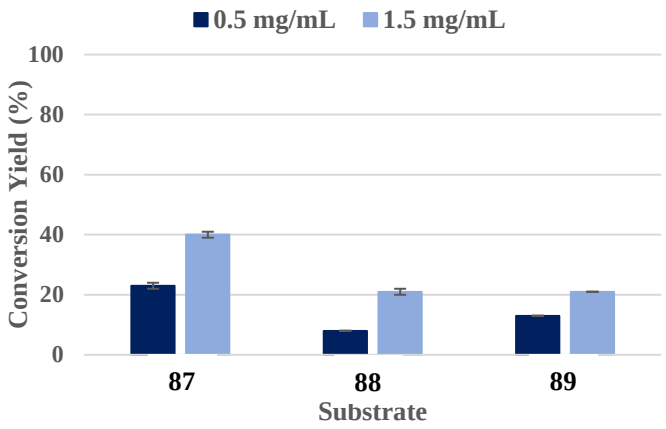

Figure 57: Amination of α-hydroxyketone derivatives **87 – 89** with 13-TAm clarified lysate at **(A)** 0.5 mg/mL and **(B)** 1.5 mg/mL. Bioconversions were performed in triplicate at 37 °C, 300 rpm for 24 h at a scale of 200 µL. Final concentrations were PLP (1.2 mM) in 50 mM Tris HCl (pH 9) with 10% MeOH. Final substrate concentrations were **87** and **88** (10 mM), and **89** (25 mM).

5.6 Conclusions

In this chapter, the biotransformation of a panel of reported and metagenomic TAms with α-hydroxyketone derivatives was investigated for the molecular assembly of chiral amino alcohols via a one-pot ER-TAm cascade. Screening of α,ß-unsaturated and saturated hydroxyketone derivatives **52**, **63**, **55** and **84** – **86** identified a suitable substrate **85**, as well as (*R*)- and (*S*)-selective TAms viable in an one-pot ER-TAm cascade, Mv-TAm and 13-TAm respectively. Assessment of the data concluded that a two-step one-pot cascade was required for the application of Mv-TAm owing to its high activity with the unsaturated compound **63**. Potential for a one-step one-pot cascade with 13-TAm was signified by its low activity with **63** and high activity with **85**.

Whilst considering complementary conditions for the ER-TAm cascade, 7 assay parameters for transamination were systematically evaluated to optimise reaction yields. They included clarified lysate concentration, type of co-solvent, substrate loading, amine donor, amine donor equivalents, temperature, and pH. The results were as follows:

Transamination with (*R*)-selective Mv-TAm at a volume of 200 µL was optimised to 37 °C, 300 rpm for 24 h in 50 mM Tris HCl (pH 9) with 10% MeOH at final concentrations of PLP (1.2 mM), IPA (750 mM, 30 eq.), substrate **85** (25 mM) and Mv-TAm (0.5 mg/mL).

Transamination with (*S*)-selective 13-TAm at a volume of 200 µL was optimised to 30 °C, 300 rpm for 24 h in 50 mM Tris HCl (pH 7.4) with 10% MeOH at final concentrations of PLP (1.2 mM), (*S*)-α-MBA (20 mM, 4 eq.), substrate **85** (5 mM) and 13-TAm (0.5 mg/mL).

Examination of analogues of **85** for substrate scope followed with transamination optimised. Amination with Mv-TAm afforded a moderate conversion of 41% for **87**, and fair conversions of 62% and 51% for **88** and **89** respectively. Applying three times the clarified lysate concentration of 13-TAm, 40% conversion yield of **87** was achieved and 21% for both **88** and **89**.

In the following chapter preparative scale ER and TAm biotransformations are explored and optimised, first applying optimised small scale assay conditions established in Chapter 4 and Chapter 5.

6. Preparative Scale ER-TAm Biotransformations

6.1 Introduction

With optimised conditions for the small scale biotransformations using NCR, Mv-TAm and 13-TAm, preparative scale conditions (hundreds of milligrams of substrate) were then trialled and optimised. The scale of the assay was considered, along with the clarified lysate concentration, type of buffer used, and amine donor equivalents. The yield and *ee* from the NCR+pQR bioreduction was also determined. Conversions from Mv-TAm and 13-TAm aminations was established, and methods for the purification of the chiral amino alcohol product were evaluated.

The potential of a one-step one-pot or two-step one-pot cascade was determined, as well as overall yield from ER – TAm biotransformations. Following this isolated products were reacted to afford chiral 2-aminooxazoles with their diastereomeric ratio (*dr*) established. Conformational analysis was performed to corroborate predicted enantioselectivities from biotransformations.

6.2 Ene-Reductases Single-Step Biotransformation

The preparative scale ER bioreduction was trialled at 25 mM and 5 mM substrate loading. Preparative scale conditions and analytical methods are described.

6.2.1 Introduction

As the goal of a one-pot ER-TAm cascade was pursued (for reasons given in section 1.1.4, primarily to avoid the isolation of intermediates and drive the cascade forward), and Mv-TAm and 13-TAm transaminations were optimised to substrate loadings of 25 mM and 5 mM respectively, the preparative scale bioconversion with NCR+1811 required optimisation at these two substrate loadings. Preparative scale enzymatic reactions conditions have not been formally defined, however they are typically reported in the literature to be on the scale of hundreds of milligrams of substrate.[59,60,193,262] To verify the *ee* chiral HPLC analysis was explored at 214 nm with a ChiralPak AD-H column, successful amongst the chiral columns trialled. Product and starting material separation, as well as enantiomeric separation was achieved at 1% *iso*propanol:hexane. Retention times varied due to temperature fluctuations. As such,

the product was confirmed by co-injection with the racemic standard **85**. Similarily, starting material **63** was confirmed by co-injection.

6.2.2 Bioreduction at 25 mM Substrate Loading

For reasons outlined later, Tris-HCl was not a viable buffer for the transamination on a preparative scale. As such, alternative buffers were investigated for NCR+pQR1811 to maintain the possibility of a one-pot cascade, including HEPES, KPi and water (**Scheme 46**). Initial investigations were performed at a 10 mL volume and 25 mM substrate loading (55 mg of substrate **63**).

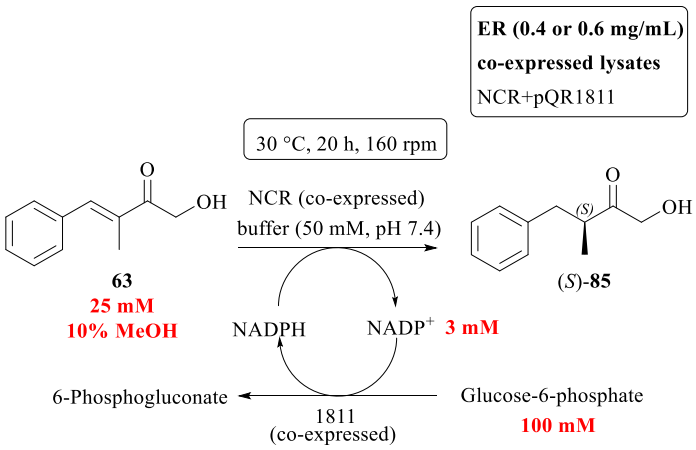

Scheme 46: Bioreduction of α-hydroxyketone derivative **63** at 25 mM substrate loading with NCR+pQR1811 co-expressed clarified lysate to afford (*S*)-**85**. Bioconversions were performed at 30 °C, 160 rpm for 20 h at a scale of 10 mL or 25 mL. Final concentration were G6PNa (100 mM), $NADP^+$ (3 mM), and alkene substrate (25 mM) in buffer (pH 7.4) with 10% MeOH. Either co-expressed clarified lysates were applied at final concentrations of 0.4 or 0.6 mg/mL. Enzymes were expressed from pQR numbers listed. Buffers investigated were 50 mM HEPES, 50 mM KPi, and H_2O all at pH 7.4.

Application of an ER bioconversion in HEPES with 0.6 mg/mL clarified lysate afforded an *ee* of 44% (**Figure 58A**). Reduction of the clarified lysate concentration to 0.4 mg/mL for selective uptake of the preferred binding mode was investigated, pleasingly providing (*S*)-**85** in 96% *ee* (**Figure 58B**). Bioconversion with buffers KPi and H_2O at 0.4 mg/mL clarified lysate was performed, each providing (*S*)-**85** in 94% *ee* (**Figure 59**). For all reactions, minimal starting material was observed.

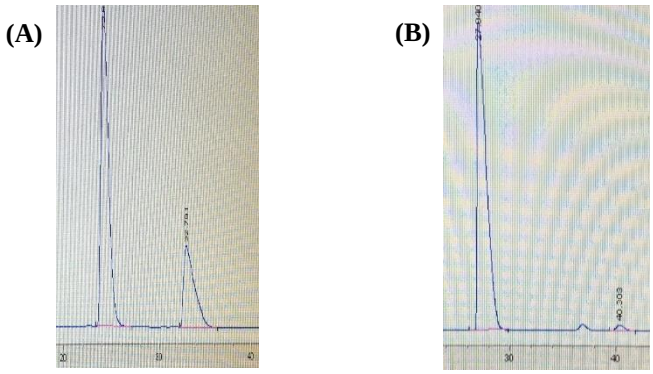

Figure 58: Preparative scale biotransformation of hydroxyketone derivative **63** with **(A)** 0.6 mg/mL and **(B)** 0.4 mg/mL NCR+pQR1811 co-expressed clarified lysate at a scale of 10 mL. Bioconversions were performed at 30 °C, 300 rpm for 20 h. Final concentration were G6PNa (100 mM), $NADP^+$ (3 mM), and alkene substrate **63** (25 mM) in 50 mM HEPES (pH 7.4) with 10% MeOH. Biotransformations were analysed by chiral HPLC using ***Method G***. **(A)** Product (*S*)-**85** Rt = 22.9 min, (*R*)-**85** Rt = 32.7 min, **B)** Product (*S*)-**85** Rt = 27.8 min, (*R*)-**85** Rt = 40.3 min, unlabelled Rt ~37 min starting material **63**. Product formation was confirmed by co-injection with the racemic product standard. Starting material **63** was confirmed by co-injection.

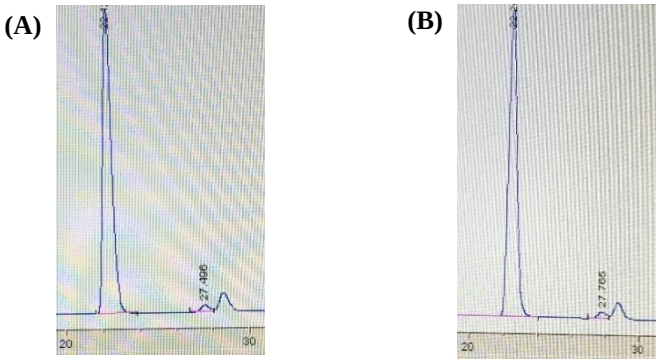

Figure 59: Preparative scale biotransformation of hydroxyketone derivative **63** in **(A)** KPi and **(B)** H_2O with 0.4 mg/mL NCR+pQR1811 co-expressed clarified lysate at a scale of 10 mL. Bioconversions were performed at 30 °C, 300 rpm for 20 h. Final concentration were G6PNa (100 mM), $NADP^+$ (3 mM), and alkene substrate **63** (25 mM) in 50 mM buffer (pH 7.4) with 10% MeOH. Biotransformations were analysed by chiral HPLC using ***Method G***. **(A)** Product (*S*)-**85** Rt = 22.4 min, (*R*)-**85** Rt = 27.5 min, unlabelled Rt ~28 min starting material **63**. **(B)** Product (*S*)-**85** Rt = 22.2 min, (*R*)-**85** Rt = 27.8 min, unlabelled Rt ~28 min starting material **63**. Product formation was confirmed by co-injection with the racemic product standard. Starting material **63** was confirmed by co-injection.

As HEPES gave the highest *ee*, its application was extended to a 25 mM substrate loading and 25 mL volume scale (110 mg of substrate **63**, thus satisfying preparative scale conditions). This too was successful, yielding (*S*)-**85** in 99.5% *ee* (**Figure 60**). An isolated yield of 96% was afforded by quenching with 10% TFA, filtration of the denatured enzyme, extraction into ethyl acetate, and drying over $MgSO_4$.

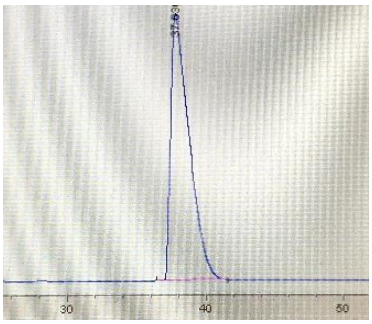

Figure 60: Preparative scale biotransformation of hydroxyketone derivative **63** with 0.4 mg/mL NCR+pQR1811 co-expressed clarified lysate at a scale of 25 mL. Bioconversions were performed at 30 °C, 160 rpm for 20 h. Final concentration were G6PNa (100 mM), $NADP^+$ (3 mM), and alkene substrate **63** (25 mM) in 50 mM HEPES (pH 7.4) with 10% MeOH. Biotransformations were analysed by chiral HPLC using ***Method G***. Product (*S*)-**85** Rt = 37.6. Product formation was confirmed by co-injection with the racemic product standard.

6.2.3 Bioreduction at 5 mM Substrate Loading

For a one-pot cascade with 13-TAm, application of NCR+pQR1811 with 5 mM substrate loading in HEPES was explored. Preliminary investigations were performed on a semi-preparative 25 mL scale (22 mg of substrate **63**) affording the product in 98% *ee* and 82% isolated yield with minimal starting material remaining (**Scheme 47**, **Figure 61**). Extension to a preparative scale of 65 mL (59 mg of substrate **63**) was less successful, yielding (*S*)-**85** in 80% *ee*. Prioritising the high *ee* attained on the semi-preparative scale, further work was conducted at a 5 mM substrate loading and 25 mL scale (22 mg of substrate **63**).

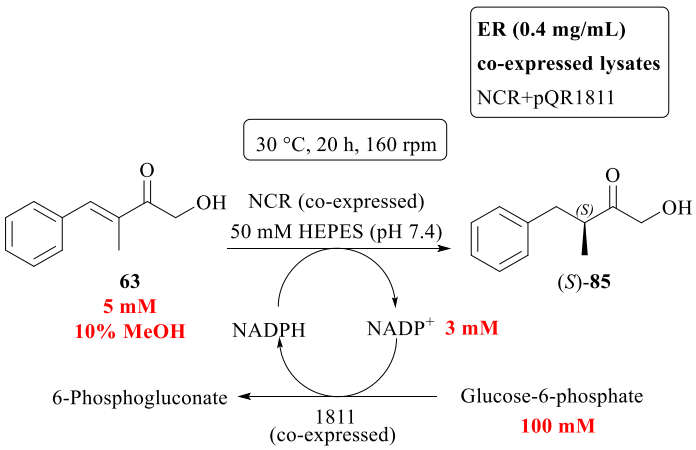

Scheme 47: Bioreduction of α-hydroxyketone derivative **63** at 5 mM substrate loading with NCR+pQR1811 co-expressed clarified lysate to afford (*S*)-**85**. Bioconversions were performed at 30 °C, 160 rpm for 20 h at a scale of 25 mL. Final concentration were G6PNa (100 mM), $NADP^+$ (3 mM), and alkene substrate (5 mM) in buffer (pH 7.4) with 10% MeOH. Co-expressed clarified lysates were applied at final concentrations of 0.4 mg/mL. Enzymes were expressed from pQR numbers listed.

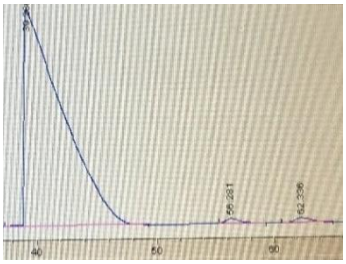

Figure 61: Preparative scale biotransformation of 5 mM hydroxyketone derivative **63** with 0.4 mg/mL NCR+1811 co-expressed clarified lysate at a scale of 25 mM in 25 mL. Bioconversions were performed at 30 °C, 160 rpm for 20 h. Final concentration were G6PNa (100 mM), $NADP^+$ (3 mM), and alkene substrate **63** (5 mM) in 50 mM HEPES (pH 7.4) with 10% MeOH. Biotransformations were analysed by chiral HPLC using ***Method G***. Product (*S*)-**85** Rt = 39.2 min, (*R*)-**85** Rt = 62.3 min, starting material **63** Rt = 56.3 min. Product formation was confirmed by co-injection with the racemic product standard. Starting material **63** was confirmed by co-injection.

6.3 Mv-TAm Single-Step Biotransformation

The preparative scale Mv-TAm amination was trialled. Buffer and IPA equivalents were re-examined.

6.3.1 Introduction

For preparative scale Mv-TAm aminations with IPA it was intended that optimised conditions would be applied and worked up using similar procedures as those reported[60,193] to afford the pure product. Following standard procedures, the biotransformation of (*S*)-**85** (**Scheme 48**) was quenched with an excess of methanol (both to denature the enzyme and ensure full solubilisation the product) prior to centrifugation for enzyme removal. Following this the supernatant was decanted, methanol removed under reduced pressure, the aqueous layer acidified to enable the extraction of the substrate (*S*)-**85**, and then basified for extraction of the amine product (2*S*,3*S*)-**100**.

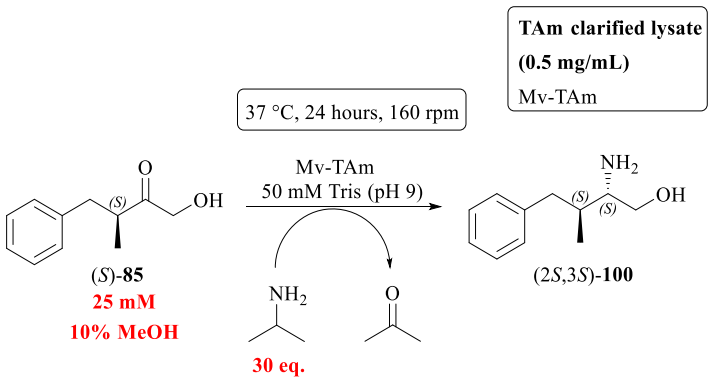

Scheme 48: Transamination of (*S*)-**85** with Mv-TAm clarified lysate to afford (2*S*,3*S*)-**100**. Bioconversion was performed at 37 °C, 160 rpm for 24 h at a scale of 25 mL. Final concentrations were PLP (1.2 mM), substrate (25 mM), IPA (750 mM, 30 eq.), and Mv-TAm clarified lysate (0.5 mg/mL) in 50 mM Tris (pH 9) with 10% MeOH.

Rather dissappointingly, basifying and extraction was only able to afford a minimal amount of product, even at highly basic pH 13. As such, alternative means were investigated for isolation of the amino alcohol product (2*S*,3*S*)-**100**. To this end, derivatisation of the product, application of a C-18 Sept-pak, ion-exchange resins, aldehyde scavenger resin, ISOLUTE® SCX-2 resin, and preparative HPLC were explored. Prior to these investigations it was required that the Tris buffer be substituted for another buffer, as its primary amine would interfere in several of the above listed purification methods (**Figure 62**). Therefore, buffers were investigated for Mv-TAm biocatalysis.

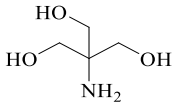

Figure 62: Structure of Tris.

6.3.2 Buffer and Isopropylamine Equivalents Investigation

Buffers KPi, HEPES, Tris and water[xxiv] at pH 9 were examined for the transamination reactions at a scale of 200 µL using HPLC analysis of substrate (*S*)-**85** depletion as previously described (**Scheme 49**, **Figure 63**). For the ER-TAm cascade, the same buffer was required. Whilst water was found to be most successful alongside Tris with 83% conversion, HEPES was selected for further investigations with water due to the high conversion of 75% as well as the high *ee* provided in the NCR bioconversion of **63**.

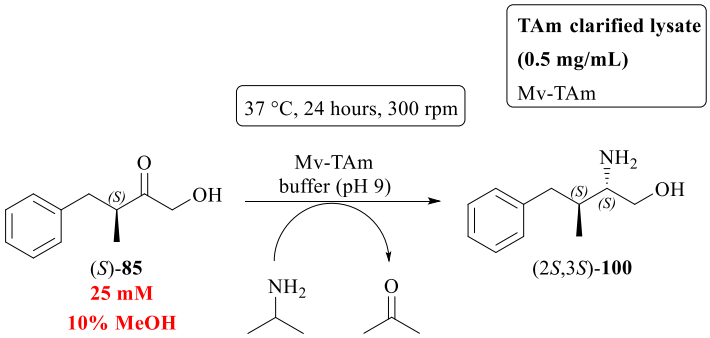

Scheme 49: Transamination of (*S*)-**85** with Mv-TAm clarified lysate investigating buffer type and number of IPA equivalents. Bioconversions were performed in triplicate at 37 °C, 300 rpm for 24 h at a scale of 200 µL. Final concentrations were PLP (1.2 mM), substrate (25 mM), IPA, and Mv-TAm clarified lysate (0.5 mg/mL) in 50 mM buffer (pH 9) with 10% MeOH. Buffers investigated were KPi, HEPES, Tris and water. IPA equivalents investigated were 5, 10, 15, 30, 45, 60, and 75 equivalents.

[xxiv] Where water is noted as the buffer it is appreciated that the amine donor (IPA) is actually the buffer, however given that IPA is present in all buffer systems investigated, water is written for clarity.

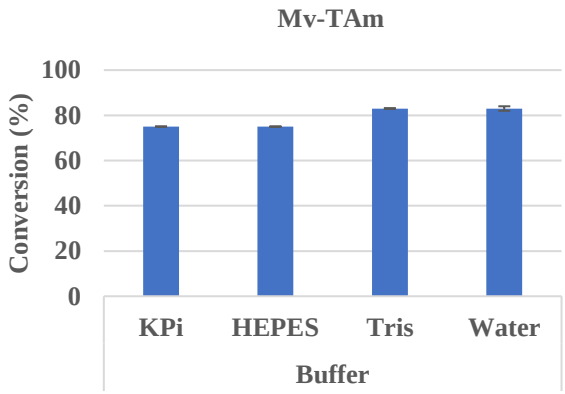

Figure 63: Investigation of buffer type on the bioconversion of α-substituted saturated hydroxyketone derivative (*S*)-**85** with Mv-TAm clarified lysates as determined by conversion from substrate depletion. Bioconversions were performed in triplicate at 37 °C, 300 rpm for 24 h at a scale of 200 µL. Final concentrations were PLP (1.2 mM), substrate (25 mM), IPA (750 mM, 30 eq.), and Mv-TAm clarified lysate (0.5 mg/mL) in 50 mM buffer (pH 9) with 10% MeOH. Buffers investigated were KPi, HEPES, Tris and water. Biotransformations were analysed by achiral HPLC using ***Method B***.

Due to the change in buffer used, the number of IPA equivalents in Mv-TAm amination of (*S*)-**85** was re-examined. For a more accurate representation of the yield from Mv-TAm amination, an HPLC method was designed to evaluate the ratio of product formed to substrate remaining with increasing IPA equivalents (in comparison to previous methods only evaluating substrate depletion). The formation of product (2*S*,3*S*)-**100** was shown to maximise at 45 eq. of IPA (**Figure 64**).

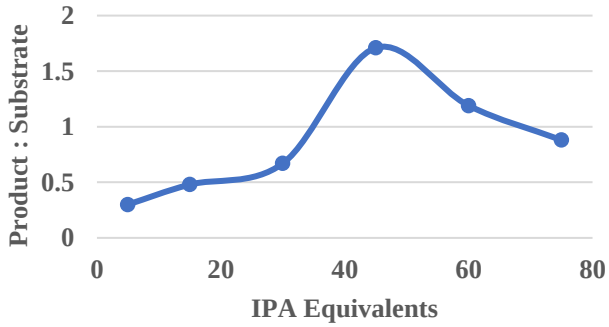

Figure 64: Investigation of IPA equivalents for bioconversion of α-substituted saturated hydroxyketone derivative (*S*)-**85** with Mv-TAm clarified lysates as determined by product formed:substrate remaining. Bioconversions were performed at 37 °C, 300 rpm for 24 h at a scale of 2 mL. Final concentrations were PLP (1.2 mM), substrate (25 mM), and Mv-TAm clarified lysate (0.5 mg/mL) in 50 mM HEPES (pH 9) with 10% MeOH. Biotransformations were analysed by chiral HPLC using ***Method C***.

6.4 13-TAm Single-Step Biotransformation

6.4.1 Reaction Scale Investigation

The extent at which 13-TAm amination could successfully be scaled up was investigated. With the goal of a semi-preparative scale as achieved in the NCR

bioreduction, volumes up to 25 mL at 5 mM substrate loading were investigated. Previously optimised conditions were applied, with HPLC analysis of the amount of acetophenone produced to determine the outcome of the reaction, as previously described. Pleasingly a good conversion yield of 66% was achieved at 25 mL to afford (2*R*,3*S*)-**100** (**Scheme 50**, **Figure 65**).

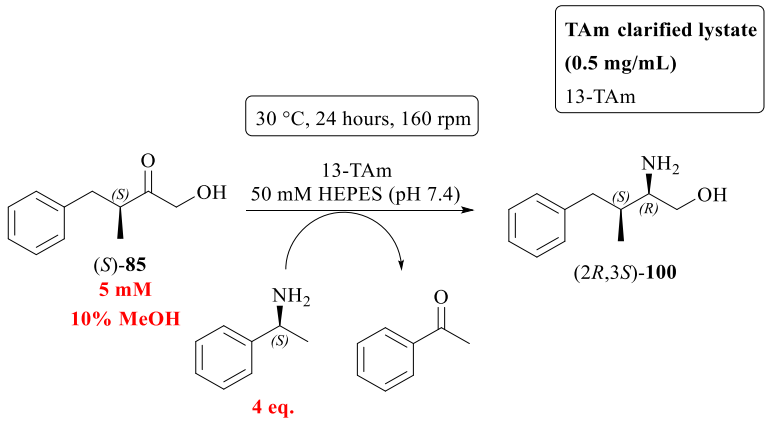

Scheme 50: Transamination of (*S*)-**85** with 13-TAm clarified lysate to afford (2*R*,3*S*)-**100**. Bioconversions were performed at 30 °C, 160 rpm for 24 h. Final concentrations were PLP (1.2 mM), (*S*)-α-MBA (20 mM), substrate (5 mM) and 13-TAm clarified lysate (0.5 mg/mL) in 50 mM HEPES (pH 7.4) with 10% MeOH. Volume scale investigated was 2, 5, 10 and 25 mL.

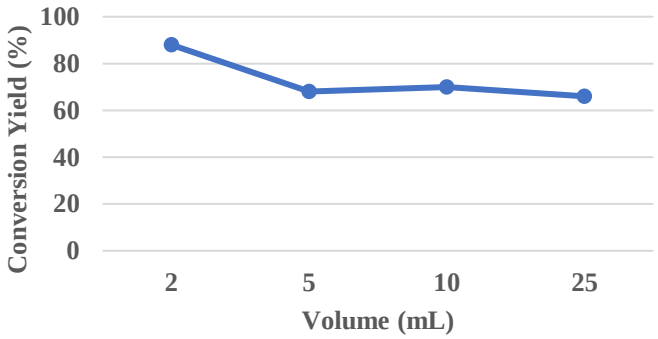

Figure 65: Investigation of volume scale on the bioconversion of α-methyl saturated hydroxyketone derivative (*S*)-**85** with 13-TAm clarified lysate as determined by conversion yields from acetophenone production. Bioconversions were performed at 30 °C, 160 rpm for 24 h. Final concentrations were PLP (1.2 mM), (*S*)-α-MBA (20 mM), and TAm clarified lysate (0.5 mg/mL) in 50 mM HEPES (pH 7.4) with 10% MeOH. Volume scale was investigated at 2, 5, 10 and 25 mL. Biotransformations were analysed by chiral HPLC using ***Method A***.

6.5 Amino Alcohol Purification

Varying methods for purification of the amino alcohol product were trialled, including derivatisation, use of C-18 Sept-pak, ion exchange chromatography, aldehyde scavenger resin, ISOLUTE® SCX-2 resin, and preparative HPLC.

6.5.1 Purification by Derivatisation

To enable extraction of the amino alcohol product, derivatisation with an acetyl goup was initially pursued (**Scheme 51**). To ensure the reaction proceeded to completion, conditions were established with commercial amino alcohol **102**. Complete conversion of starting material was observed after stirring for 2.5 h, with product formation confirmed by NMR spectroscopic analysis of the crude product.

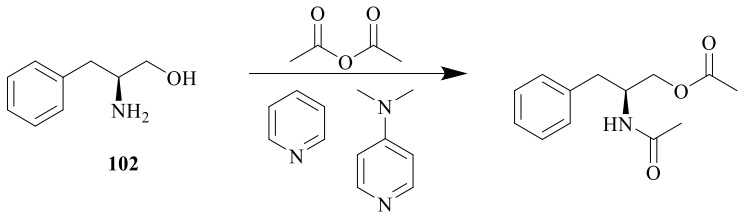

Scheme 51: Acetylation of commercial amino alcohol **102** with acetic anhydride (2 eq.), anhydrous pyridine (45 eq.) and DMAP (0.2 eq.) under anhydrous conditions.

Acetylation of the amino alcohol produced from the two-step, one-pot NCR-Mv-TAm cascade was then attempted. Prior to acetylation a work up was performed: Methanol was added to quench the TAm reaction, centrifugation removed the enzyme, the methanol was removed under reduced pressure, and the aqueous layer basified to pH 10 for the removal of IPA under reduced pressure. Half of the reaction mixture then underwent lyophilisation whilst the other half had the water removed *in vacuo*. This allowed for the acetylation of the crude reaction mixtures in parallel. Dissappointingly for both, a minimal amount of amino alcohol was acetylated despite additional acetic anhydride, anhydous pyridine and DMAP added. Efforts were re-examined by preforming the pyridine-DMAP reactive intermediate, however this was also unsuccessful. Evidently, acetylation did not tolerate the presence of the materials in the crude biocatalysis reaction mixture (HEPES buffer, glucose-6-phosphate, 6-phosphogluconate, $NADP^+$, NADPH, and PLP). As a last attempt derivitisation with Boc_2O was explored[193] though this was also unfruitful.

6.5.2 Purification by C-18 Sept-pak

As an alternate strategy, a C-18 Sept-pak was investigated for the removal of HEPES buffer and PLP. It was envisioned that the intereractions between the C-18 stationary phase and amino alcohol product would allow for the HEPES buffer and PLP to be removed with water, followed by elution of the amino alcohol with acetonitrile. Dissappointingly co-elution was observed during the water wash.

6.5.3 Purification by Ion-Exchange Chromatography

The application of ion-exchange chromatography was investigated with strongly acidic cationic exchange resin Dowex 50WX8 alongside strongly basic anionic exchange resins Amberlite IRA-410 (Type II) and Amberlite IRA-400 (Type I). The Dowex 50WX8 resin was found to retain the HEPES, PLP and the amino alcohol (**Figure 66**). Amberlite IRA-410 was found to completely retain HEPES, as well as partially retain the amino alcohol, with some of the amino alcohol eluted alongside the PLP. As such, Amberlite IRA-400 was invesitgated, with similar results produced. Thus, the use of an ion-exchange resin proved only partly successful.

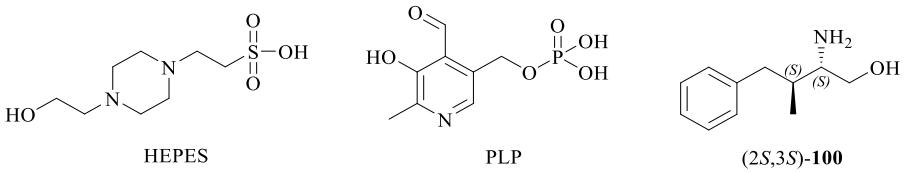

Figure 66: Structures of HEPES, PLP, and (2*S*,3*S*)-**100**.

6.5.4 Purification by Aldehyde Scavenger Resin

With the removal of HEPES established from the use of an Amberlite IRA-410 resin, efforts focued on the separation of PLP and the amino alcohol. It was envisaged that a solid-supported electrophile scavenger resin would selectively target the aldehyde moiety of the PLP, thus allowing for its removal by filtration. Given the well established reactivity of PLP and α-MBA, a chemically analagous aminomethylated polystyrene resin was selected. Preliminary investigations proceeded with commercial **102** (94 mg) and PLP (7 mg) in H_2O (25 mL), directly comparable to the planned preparative scale assay (**Scheme 52**).

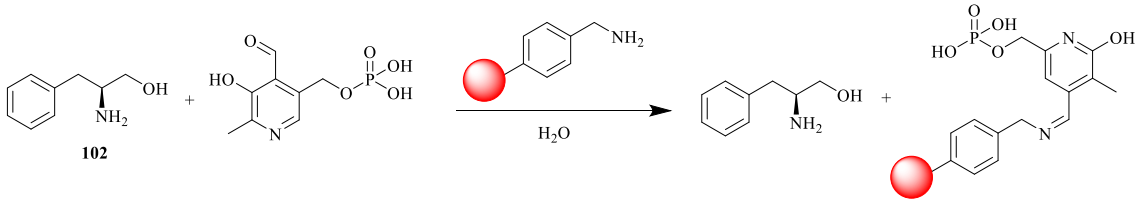

Scheme 52: Application of aminomethylated polystyrene resin for removal of PLP.

The resin (14 eq.) was added and the suspension stirred at room temperature for 18 h. With PLP still present in the water solution as observed by TLC anaylsis, an additional 70 eq. of the resin were added and suspension heated to 50 ºC for 18 h. Dissappointingly, this too was unsuccessful. It is most likely that this is due to the

polystyrene nature of the resin, that in water will shrink reducing the availability of the surface amine groups. Therefore, the application of an aldehyde scavenger resin was deemed unviable.

6.5.5 Purification by ISOLUTE® SCX-2 Resins

Efforts were then redirected to the use of ISOLUTE® SCX-2 resins. As previously described, procedures had been established for the removal of the enzyme, IPA, and HEPES from the reaction. Thus, it was envisaged that ISOLUTE® SCX-2 resins, possessing a strong cation exchange sorbent (propylsulfonic acid bonded) were capable of selectively eluting primary and secondary amines, namely the amino alcohol product and PLP by increasing the concentration of ammonia in methanol. Any unreacted α-hydroxyketone starting material would be eliminated in the preliminary methanol wash.

Efforts were investigated with commercial **102** (94 mg) and PLP (7 mg) using the same number of moles (total crude 0.654 mmol) as that planned for the preparative scale assay. A 5 g resin with loading of 0.6 meq/g was employed, with the crude sample in aqueous solution loaded. Despite ISOLUTE® SCX-2 resins boasting the extraction of basic analytes from aqueous solution, both the amino alcohol product and PLP were lost in the preliminary methanol wash. They were recovered, the organic solvent was removed *in vacuo*, were lyophilised, redissolved in MeOH and loaded onto new ISOLUTE® SCX-2 resins. Thankfully, the amino alcohol and PLP were retained for the first MeOH wash, however they were disappointingly co-eluted with 0.5 M NH_3 in methanol. Reducing the concentration of the ammonia in solution resulted in the crude mixture being retained by the resin. As such, the separation of the amino alcohol and PLP by ISOLUTE® SCX-2 resins was deemed unviable and preparative HPLC was explored.

6.5.6 Purification by Preparative HPLC

While the use of resins proved challenging, it is likely that the reaction scale and amount of material being handled (110 mg and 22 mg starting material, ~64 mg and ~15 mg product produced respectively) caused a number of issues. Further efforts using resins may look into working on a larger scale, or else finding a more selective resin the retain the HEPES buffer whilst completely eluting the amino alcohol product and PLP. To

obtain material for characterisation purposes, preparative HPLC of the crude biocatalysis mixture from the ER-TAm cascade was successfully performed using ***Method J*** as described in experimental procedures, section 9.4.

6.6 NCR – Mv-TAm Cascade

With single-step biotransformations of NCR and Mv-TAm established, as well as a method for the purification of the amino alcohol product, the ER-TAm enzymatic cascade was performed and optimised. As determined from previous investigations, a two-step, one-pot cascade was pursued owing to Mv-TAm's high activity with the ER substrate. Initial studies examined HEPES as the buffer, being the most successful buffer for NCR+pQR1811 and highly successful with Mv-TAm transformations. A scale of 2 mL for the enzymatic cascade was first probed, affording a yield of (2*S*,3*S*)-**100** in 52% (by analytical HPLC against product standards) and isolated yield of 3% following work-up with Amberlite IRA-410 resin and preparative HPLC purification (**Table 13**). In efforts to improve the isolated yield, the removal of the HEPES buffer was considered to obviate the need for the Amberlite IRA-410 resin, from which severe product loss was observed. With previous studies concluding the successful biotransformations of NCR+pQR1811 and Mv-TAm in water, water was examined instead of HEPES at 25 mL. The cascade using HEPES at a 25 mL was also investigated to ensure the increase in scale was not an issue. Pleasingly, analytical HPLC yields of 63% and 58% were attained using HEPES and H_2O respectively (**Table 13**). An isolated product yield of 32% for (2*S*,3*S*)-**100** was achieved following work-up and preparative HPLC purification for the two-step one-pot NCR – Mv-TAm cascade in water (**Scheme 53**, **Table 13**). The product was isolated as a TFA salt due to the TFA present in the preparative HPLC purification method (**Figure 67**).

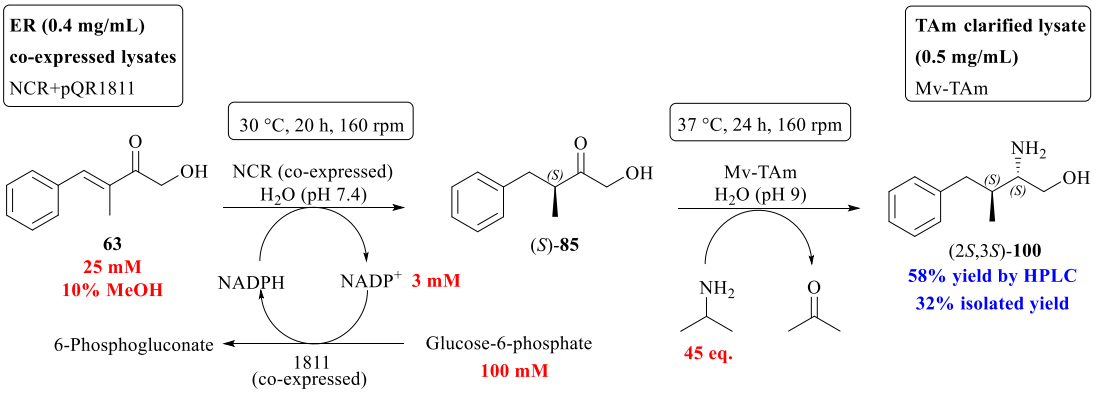

Scheme 53: Optimised two-step, one-pot NCR – Mv-TAm biocatalytic cascade with substrate **63** (25 mM) in 25 mL affording final product amino alcohol (2*S*,3*S*)-**100** via intermediate (*S*)-**85**.

Table 13: Investigations of the two-step one-pot NCR – Mv-TAm enzymatic cascade on the biotransformation of **63** examining buffer, scale and yield (isolated yield and HPLC yield using product standards). First step bioreduction with NCR+pQR1811 was performed at 30 °C, 160 rpm for 20 h in a 50 mL falcon. Final concentration were G6PNa (100 mM), $NADP^+$ (3 mM), alkene substrate **63** (25 mM), NCR+pQR1811 clarified lysate (0.4 mg/mL) in buffer (pH 7.4) with 10% MeOH. Following this PLP and IPA (4 M, pH 9) were added, the pH adjusted to 9, and Mv-TAm added for the second step performed at 37 °C, 160 rpm for 20 h. Final concentrations were PLP (1.2 mM), IPA (0.860 mM, 45 eq.), and Mv-TAm clarified lysate (0.5 mg/mL) in buffer (pH 9) with 7.7% MeOH.

Buffer	Scale (mL)	Yield by HPLC (%)[b]	Isolated Yield (%)
HEPES	2, then 2.6[a]	52	3
HEPES	25, then 32.7[a]	63	--[c]
Water	25, then 32.7[a]	58	32

[a] Increase in scale from the addition of IPA and Mv-TAm resulting in total increase in volume.
[b] HPLC analysis using ***Method C*** against product standards as described in experimental procedures.
[c] Not performed.

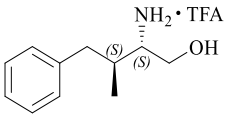

(2*S*,3*S*)-**100**

Figure 67: TFA salt of product (2*S*,3*S*)-**100** from the two-step, one-pot NCR - Mv-TAm cascade obtained following preparative HPLC purification.

6.7 NCR – 13-TAm Cascade

Following the success of the NCR – Mv-TAm cascade, the enzymatic cascade of NCR – 13-TAm was pursued and optimised. A one-step, one-pot cascade was initially considered owing to 13-TAm's low activity with the ER substrate, as shown in previous investigations. The cascade was performed on a semi-preparative scale of 5 mM substrate (22 mg) in 25 mL solvent. Preliminary studies used water at pH 7.4 as it would obviate the need for the Amberlite IRA-410 resin, from which severe product

loss had already been observed. Dissappointingly, an HPLC yield of only 29% was attained, with a crude isolated yield of 32% (**Table 14**). ^{1}H NMR analysis of the product indicated a co-elution of product (2*R*,3*S*)-**100** with by-product (2*R*)-**103** (**Figure 68**), in a ratio of 1:0.6 respectively. As the yield had significantly dropped using water alone as the solvent studies returned to using HEPES buffer. A one-step one-pot cascade was again considered to examine any changed in 13-TAm's activity with the ER substrate **63**. Whilst the HPLC yield was improved to 70%, the isolated yield following work-up and preparative HPLC purification was low at 8% (**Table 14**), with ^{1}H NMR analysis again confirming co-elution of the product (2*R*,3*S*)-**100** with by-product (2*R*)-**103** in 1:0.35 ratio respectively. As the activity of 13-TAm with **63** giving by-product (2*R*)-**103** was considerable, a two-step one-pot cascade was performed. Additionally, a work-up with resins was not performed, with the crude biocatalysis mixture directly purified by preparative HPLC to maximise the isolated yield required for the following reaction (aminooxazole formation). Pleasingly, a good yield by HPLC of 68% and isolated yield of 30% were attained for (2*R*,3*S*)-**100** (**Scheme 54**, **Table 14**). By-product (2*R*)-**103** was not observed.

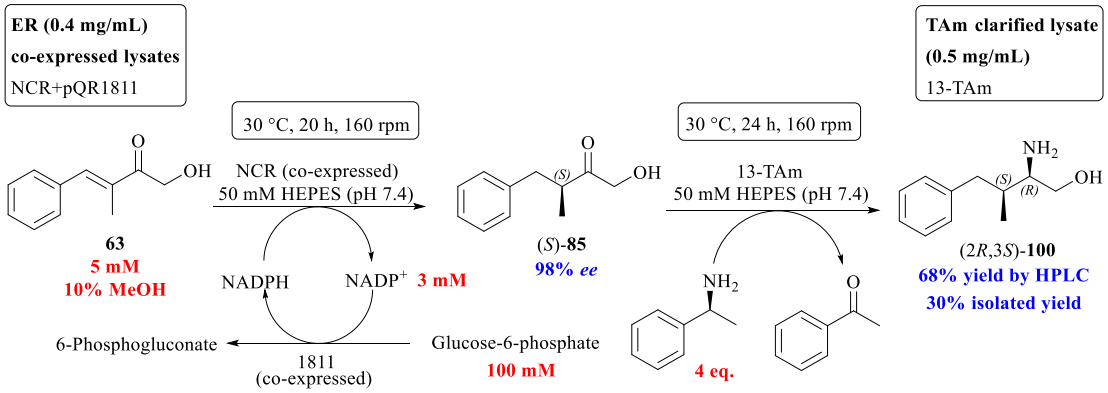

Scheme 54: Optimised two-step, one-pot NCR – 13-TAm biocatalytic cascade with substrate **63** (5 mM) in 25 mL affording final product amino alcohol (2*R*,3*S*)-**100** via intermediate (*S*)-**85**.

Table 14: Investigations of the one-pot NCR – 13-TAm enzymatic cascade on the biotransformation of **63** examining buffer, steps, and yield (isolated yield and HPLC yield using product standards). Bioreduction with NCR+pQR1811 was performed at 30 °C, 160 rpm for 20 h in a 50 mL falcon. Final concentration were G6PNa (100 mM), $NADP^+$ (3 mM), alkene substrate **63** (5 mM), NCR+pQR1811 clarified lysate (0.4 mg/mL) in buffer (pH 7.4) with 10% MeOH. 13-TAm amination was performed at 30 °C, 300 rpm for 24 h. Final concentrations were PLP (0.96 mM), (*S*)-α-MBA (20 mM), and 13-TAm clarified lysate (0.5 mg/mL) in buffer (pH 7.4) with 7.9% MeOH.

Buffer	Steps	Scale (mL)	Yield by HPLC (%)[b]	Isolated Yield (%)
H_2O	one-step	25	29	32[c]
HEPES	one-step	25	70	8[d]
HEPES	two-step	25, then 31.7[a]	68	30

[a] Increase in scale from the addition of α-(*S*)-MBA and 13-TAm resulting in total increase in volume.
[b] HPLC analysis using ***Method C*** against product standards as described in experimental procedures.
[c] Crude isolated yield, ^{1}H NMR analysis confirming 1:0.65 ratio of (2*R*,3*S*)-**100**:(2*R*)-**103**.
[d] Crude isolated yield, ^{1}H NMR analysis confirming 1:0.35 ratio of (2*R*,3*S*)-**100**:(2*R*)-**103**.

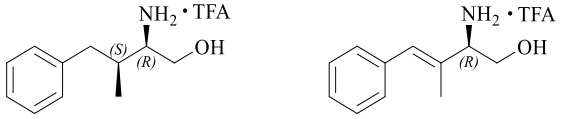

(2*R*,3*S*)-**100** (2*R*)-**103**

Figure 68: TFA salts of product (2*R*,3*S*)-**100** and by-product (2*R*)-**103** from the one-step, one-pot NCR – 13-TAm cascade obtained following preparative HPLC purification.

6.8 Aminooxazole Formation

Following the isolation of the amino alcohols in high optical purities from the preparative scale ER-TAm cascade biotransformations, reaction to give target compounds TAAR1 agonists **37** was performed. The established procedure using CNBr and K_2CO_3 in anhydrous THF was employed,[225] with purification by preparative HPLC to afford the aminooxazoles as TFA salts (**Scheme 55**). Prior to the reaction, the amino alcohols, which were isolated as TFA salts from preparative scale biotransformations, were stirred in water with K_2CO_3 for 1 h and lyophilised. Formation of the 2-aminooxazoles was successfully accomplished in yields of 18% and *dr* 93:7[xxv] for (2*S*,4*S*)-**37** (from NCR – Mv-TAm cascade) and 15% and *dr* 97:3[xxvi] for (2*S*,4*R*)-**37** (from NCR – 13-TAm cascade). As the *ee* of (*S*)-**85** generated from NCR bioreduction was very high (99.5% *ee* at 25 mM **63** substrate loading and 98% *ee* at

[xxv] Determined using ^{1}H NMR analysis of the methyl group, 93:7 *dr* ratio of (2*S*,4*S*):(2*S*,4*R*).
[xxvi] Determined using ^{1}H NMR analysis of the methyl group, 97:3 *dr* ratio of (2*S*,4*R*):(2*S*,4*S*).

5 mM **63** substrate loading) the *dr* of (2*S*,4*S*)-**37** and (2*S*,4*R*)-**37** observed arises primarily from the Mv-TAm and 13-TAm amination steps in the cascade.

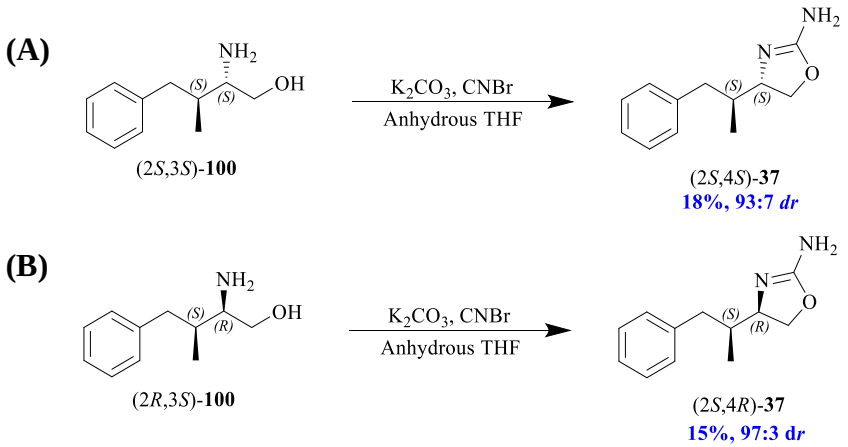

Scheme 55: Reaction of diastereomerically enriched amino alcohols with CNBr and K_2CO_3 to afford 2-aminooxazoles. **(A)** Compound (2*S*,3*S*)-**100** from the NCR – Mv-TAm cascade reacting to afford 2-aminooxazole (2*S*,4*S*)-**37**. **(B)** Compound (2*R*,3*S*)-**100** from the NCR – 13-TAm cascade reacting to afford 2-aminooxazole (2*S*,4*R*)-**37**.

6.9 Stereoselectivity of the Biotransformations

As discussed in Chapter 4, molecular docking of **63** with NCR observed a "flipped" binding mode, with the product tentatively assigned as (*S*)-**85**. The preparative scale single step NCR bioreduction of **63** affording (*S*)-**85** and analysis by optical rotation afforded a value of $[\alpha]_D^{24}$ = +51.2 (c. 1.0, $CHCl_3$). Compound (*R*)-**85** has been described in the literature, [lit.[264] $[\alpha]_D^{20}$ = –14.3 (neat)], thus indicating that the (*S*)-selectivity for the bioreduction of **63** with NCR+pQR1811 was achieved.

As discussed in Chapter 1, the enantiopreference of TAm amination may be attributed to the position of the catalytic lysine on either the *si*- or *re*-face of PLP during the second half-transamination reaction,[173–176] with (*S*)-selective TAms possessing the catalytic lysine on the *si*-face to afford (*S*)-enantiomers and (*R*)-selective TAms possessing the catalytic lysine on the *re*-face to afford (*R*)-enantiomers. Additionally, (*S*)- and (*R*)-selective TAms belong to different folding classes (I and IV respectively) thereby discouraging alternate substrate binding modes.[170,173,177] These folding classes afford a large and small binding pocket within the active site contributing to the specific binding of the substrate.

It was envisioned that the alkyl chain and phenyl group of substrate (3*S*)-**85** would fit into the large binding pocket of Mv-TAm, with the hydroxy group fitting into the small binding pocket (**Scheme 56**). For Mv-TAm, being a well established (*R*)-selective

TAm,[67,193,262] the catalytic lysine would be positioned on the *re*-face of PLP, to afford (*R*)-enantiomers, however due to Cahn-Ingold-Prelog rules an (*S*)-stereocentre is assigned.

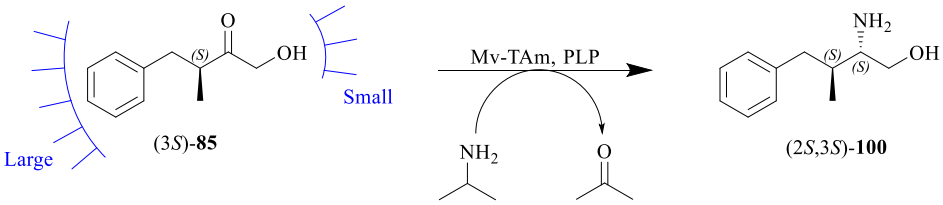

Scheme 56: Mv-TAm amination of (3*S*)-**85** bound within large and small binding pockets.

As for 13-TAm, since (*S*)-α-MBA was accepted as an amine donor, it was reasonably concluded that 13-TAm was (*S*)-selective. The phenyl group of (*S*)-α-MBA was expected to fit into the large binding pocket and methyl group into the small binding pocket (**Scheme 57**). By analogy, the alkyl chain and phenyl group of substrate (3*S*)-**85** would fit into the large pocket and hydroxy group into the small pocket, to afford a (*S*)-enantiomer, however due to Cahn-Ingold-Prelog rules an (*R*)-stereocentre is assigned.

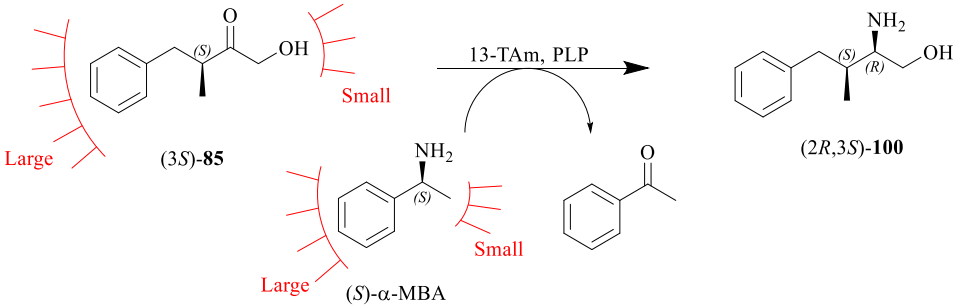

Scheme 57: 13-TAm amination of (3*S*)-**85** bound within large and small binding pockets.

6.10 Conformational Analysis

Conformational analysis was performed to corroborate the predicted enantioselectivity of ER – TAm biotransformations with the NMR spectroscopic data. Compound (2*S*,4*S*)-**37** was analysed owing to the well established stereoselectivity of Mv-TAm, giving us confidence in the 4*S*-stereocentre generated from transamination (equivalent to the 2*S*-stereocentre in (2*S*,3*S*)-**100**). Initial NMR analysis examined 2D NOEs between the alkyl CH_2 and oxazole CH_2 in order to determine whether a staggered and eclipsed conformation of (2*S*,4*S*)-**37** was prevalent (**Figure 69**). Results were deemed inconclusive, as 2D NOEs were neither sufficiently strong nor sufficiently weak to

confirm either conformation. As such, further NMR spectroscopic analysis was performed[xxvii], considering 1D NOEs, *J*-HMBC, $^{3}J_{CH}$ couplings, and $^{3}J_{CH}$ couplings (using Hecade)

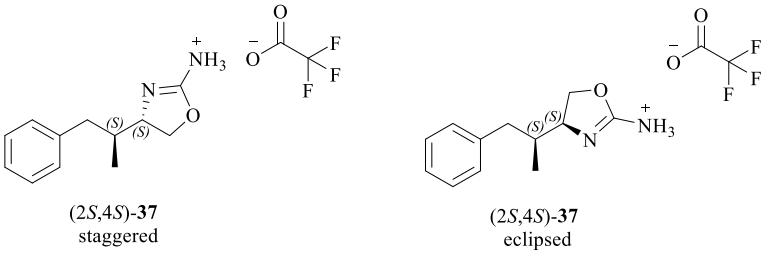

Figure 69: Staggered and eclipsed conformations of (2*S*,4*S*)-**37**.

The NOEs between the methyl group and oxazole CH_2 protons were evaluated in order to determine whether a staggered and eclipsed conformation of (2*S*,4*S*)-**37** was prevalent (**Figure 70**). The 1D NOEs of (2*S*,4*S*)-**37** exhibited a strong NOE between the methyl group and 4-*trans* proton (in red) whilst a weak NOE was observed between the methyl group and 4-*cis* proton (in blue) (**Table 15**). This result supports an eclipsed conformation wherein the 4-*trans* proton (in red) is on the same face as the methyl group, with the 4-*cis* proton (in blue) on the opposite face. Comparing this to a staggered conformation, the reverse is true with 4-*trans* proton (in red) on the opposite face as the methyl group and the 4-*cis* proton (in blue) on the same face. Therefore, the eclipsed conformation was deemed to be the most likely conformation of (2*S*,4*S*)-**37**.

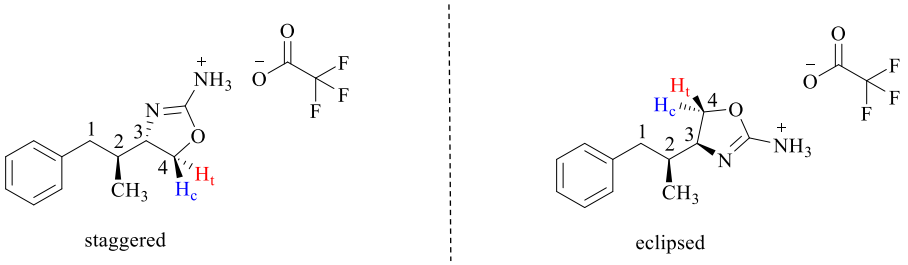

Figure 70: Staggered and eclipsed structure of (2*S*,4*S*)-**37** with NMR numbered positions. Protons 1c and 1t are relative to 2. Protons 4c and 4t are relative to 3.

[xxvii] NMR spectroscopic analysis performed by Dr Abil Aliev.

Table 15: Selective 1D NOEs (%) of (2*S*,4*S*)-**37** at +11 °C.[xxviii] Protons 1c and 1t are relative to 2. Protons 4c and 4t are relative to 3. Values in brackets are for distorted NOEs (due to *J* couplings) with positive and negative components. The values correspond to the sum of absolute values.

	o-Ph	4c	4t	3	1c	1t	2	Me
o-Ph	-	-	0.02	0.08	0.69	0.86	0.80	0.08
4c	0.03	-	4.41	1.26	0.04	-	-	**0.07**
4t	0.03	4.54	-	(0.3)	0.70	0.33	0.68	**1.09**
3	0.09	1.43	(0.5)	-	0.46	0.33	0.84	0.59
1c	0.99	-	0.69	0.59	-	6.44	0.85	0.30
1t	1.27	-	0.34	0.43	6.47	-	(0.84)	0.95
2	0.92	-	0.61	0.86	0.58	(1.3)	-	1.14
Me	0.37	**0.09**	**1.15**	0.83	0.31	1.00	1.84	-

Further confirmation was provided by analysis of the minimised energy structure of (2*S*,4*S*)-**37** using Chem3D (**Figure 71**). As anticipated, an eclipsed conformation was observed, with a dihedral angle of ~60º between H2 and H3, in accordance with the ^{1}H coupling $^{3}J(2,3)$ = 5.5 Hz and 1D NOE data.

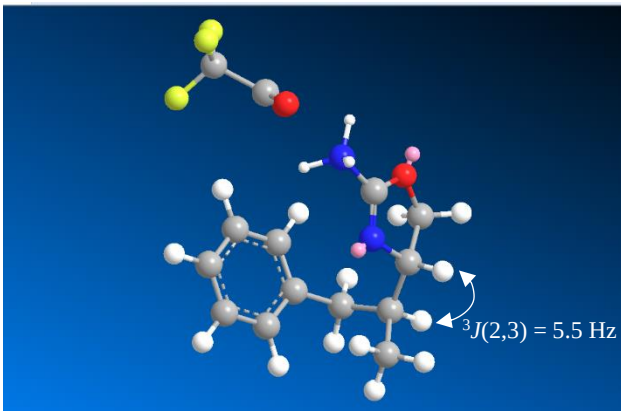

Figure 71: Minimised energy conformation of (2*S*,4*S*)-**37** exhibiting eclipsed conformation.

For completion, the possibility of an *R*-stereocentre generated from NCR bioreduction, producing compound (2*R*,4*S*)-**37** was considered. Considering the data, 1D NOEs between the methyl group and the 4 *trans* proton would point to a staggered conformation, with the proton coupling $^{3}J(2,3)$ = 5.5 Hz between 2-H and 3-H also in agreement with this structure. The minimised energy of (2*R*,4*S*)-**37** using Chem3D, however, exhibits an eclipsed conformation, not in agreement with either the 1D NOE

[xxviii] NMR spectroscopic analysis performed by Dr Abil Aliev.

data or the $^{3}J(2,3)$ proton coupling. Evaluating the evidence, from the 1D NOEs, $^{3}J(2,3)$ proton coupling, Chem3D minimised energy conformation, molecular docking of **63** with NCR, as well as NCR's *S*-selectivity with α-methylcinnamaldehyde[146] it was concluded that the bioreduction of **63** with NCR most likely generated (3*S*)-**85**, and subsequent cascade with Mv-TAm and chemical reaction afforded (2*S*,4*S*)-**37**. Future work will aim to establish the absolute stereochemistry of **85** produced from the NCR bioreduction via derivatisation and X-ray crystallography.

6.11 Conclusions

In conclusion, single step ER and TAm biotransformations were sucessfully optimised. Bioreduction using NCR+pQR1811 was high yielding and afforded a high *ee* with a range of buffers, with greatest success using 50 mM HEPES (pH 7.4) furnishing the product in 96% isolated yield and 99.5% *ee* (25 mM substrate loading, 25 mL scale) and 82% yield and 98% *ee* (5 mM substrate loading, 25 mL scale). Conversions applying Mv-TAm (25 mM substrate loading, 25 mL) were high across the range of buffers investigated, with 83% conversion in 50 mM Tris-HCl (pH 9) and H_2O (pH 9), as well as 75% conversion in 50 mM HEPES (pH 9). A conversion yield of 66% was achieved using 13-TAm in 50 mM HEPES (pH 7.4) (5 mM substrate loading, 25 mL).

Purification of the chiral amino alcohol product assessed a range of methods and techniques, including basic extraction, derivatisation of the product, application of a C-18 Sept-pak, ion-exchange resins, aldehyde scavenger resin, ISOLUTE® SCX-2 resin, and preparative HPLC. Of these, partial success was attained employing an Amberlite IRA-410 resin for removal of the HEPES buffer, following by preparative HPLC. Further optimisation when performing the ER – TAm cascade concluded that severe product loss was observed when using the Amberlite IRA-410 resin. As such, water (pH 7.4, then pH 9) was used as the buffer in the NCR – Mv-TAm cascade to obviate the need for the resin. The isolated yield of the product for the NCR – 13-TAm cascade requiring 50 mM HEPES (pH 7.4) as the buffer observed a 6% product yield[xxix] when using the resin, compared to 30% yield without using the resin, with direct purification by preparative HPLC.

[xxix] From ^{1}H NMR analysis of the crude isolate product yield of 8%, with 1:0.35 ratio product:by-product formation.

The ER – TAm cascade was successfully performed, with the NCR – Mv-TAm two-step, one-pot cascade in H_2O affording the product (2*S*,3*S*)-**100** in 58% HPLC yield, and 32% isolated yield. Further reaction gave the 2-aminooxazole (2*S*,4*S*)-**37** in 18% yield and 93:7 *dr*[xxx]. The NCR – 13-TAm cascade necessitated a two-step, one-pot reaction as exhibited from by-product (2*R*)-**103** formation. The biotransformations performed in 50 mM HEPES (pH 7.4) afforded the product (2*R*,3*S*)-**100** in 68% HPLC yield, and 30% isolated yield, with further reaction giving the 2-aminooxazole (2*S*,4*R*)-**37** in 15% yield and 97:3 *dr*[xxxi]. As the *ee* of (*S*)-**85** generated from NCR bioreduction was very high (99.5% *ee* at 25 mM **63** substrate loading and 98% *ee* at 5 mM **63** substrate loading) the *dr* of (2*S*,4*S*)-**37** and (2*S*,4*R*)-**37** observed arises primarily from the Mv-TAm and 13-TAm amination steps in the cascade.

Conformational analysis of (2*S*,4*S*)-**37** from 1D NOEs[xxxii] and ^3J(2,3) proton coupling endorsed an eclipsed conformation, with the minimised energy of (2*S*,4*S*)-**37** using Chem3D also exhibiting an eclipsed conformation. Future work will aim to establish the absolute stereochemistry of **85** produced from NCR bioreduction.

The following chapter, Chapter 7, describes the biotransformations of prochiral fluorine substrates with ERs to afford chiral fluorine. This is a separate project to that described in Chapter 2 through to Chapter 6. The work in Chapter 7 is exploratory, and so only preliminary results are described.

[xxx] Calculated using ^{1}H NMR, 93:7 *dr* ratio of (2*S*,4*S*):(2*S*,4*R*).
[xxxi] Calculated using ^{1}H NMR, 97:3 *dr* ratio of (2*S*,4*R*):(2*S*,4*S*).
[xxxii] NMR spectroscopic analysis performed by Dr Abil Aliev, Senior Research Fellow, Department of Chemistry, UCL

7. Biocatalytic Chiral Fluorine from Prochiral Substrates

7.1 Introduction

As of 2018, 50% of blockbuster drugs approved by the Food and Drug Administration contained fluorine[265] and of 2020, 20% of all commercial pharmaceuticals were fluoropharmaceuticals[266]. The introduction of fluorine into drugs has been established to increase the metabolic stability of compounds by improving resistance to oxidative metabolism, thereby enhancing the pharmacokinetic profile of compounds *in vitro* and *in vivo*.[228–231] Additionally, fluorine substitution has been shown to modulate properties such as pKa and lipophilicity, as well as exert conformational control.[230,267,268]

Often the primary purpose for incorporation of fluorine into drug molecules is to slow or prevent metabolic attack by increasing resistance to cytochrome P450 mediated oxidation, thereby prolonging the pharmacological effects of the drug.[228] Provided that the C-F bond is highly stable (the dissociation energy of the C-F bond in fluoromethane is 115 kcal/mol, greater than that of C-H in methane at 105 kcal/mol)[269] and fluorine is small in size (being only ~20% larger than hydrogen by comparison of their van der Waals radii)[231], fluorine containing drugs are well tolerated and more stable by comparison to their hydrogen counterparts.

With fluorine being the most electronegative element, its incorporation into a molecule can alter the acidity or basicity of proximal functional groups.[270,271] This modulation of pKa can perturb the binding affinity and pharmacokinetic profile of a pharmaceutical agent by impacting its bioavailability (percentage of dose reaching the circulatory system) via the absorption process (when orally administered).[272]

7.1.1 Chemical Fluorination

In recent years, research on fluorination has focused on the activation of C-H bonds as it does not necessitate the pre-functionalisation required of classical reactions such as substitutions, deoxyfluorinations, and the Balz-Schiemann reaction. Activation of C-H bonds can be largely catagorised into two approaches: Use of transition metal catalysts for insertion into C(sp^2)-H and C(sp^3)-H bonds,[273–277] and the generation of carbon centred radical intermediates for C(sp^3)-H bond activation[278–281]. Whilst enantioselective fluorination can be achieved using transition metal catalysis owing to

the use of chiral ligands, the widespread applicability of such catalysts is limited, with advancements in the field largely credited to the design of new ligands.[11–15] Additionally, it is neither a green nor sustainable technology. As for radical methods of C-H activation, the prospect of enantiocontrol is very much in its infancy.[282]

7.1.2 Biocatalytic and Chemoenzymatic Fluorination

In 2002, the first native "fluorinase" enzyme from *Streptomyces cattley* was reported.[283] It catalysed C-F bond formation by nucleophilic displacement at the innately activated carbon centre of *S*-adenosyl-L-methionine (SAM) with a fluoride ion, thereby generating 5'-fluoro-5'-deoxyfluoroadenosine (5'-FDA).[283,284] A subsequent series of enzymes (isomerase, aldolase, and aldehydye dehydrogenase, all present in *Streptomyces cattley*) converted 5'-FDA to fluoroacetate[285]. Since this discovery four additional fluorinase enzymes have been reported from genome mining, each from a different bacterial strain.[286–288]

With limited fluorinase enzymes readily available, biocatalytic fluorination has been reported by alternative chemoenzymatic strategies. For example, oxygenation using cytochrome P450 monooxygenase with subsequent deoxyfluornation from the application of a nucleophilic fluorinating reagent (DAST) has been shown to afford site selective fluorination at non-activated sites in the target molecule, positions which would have been challenging to access chemically.[289]

7.1.3 Recent Relevant Research with Prochiral Fluorine Substrates

As previously discussed in Chapter 1, enoate reductases (EnoRs) have been identified as catalysing the bioreduction of poorly activated substrates (ie. those activated by carboxylic acid and ester moieties).[102] Their application, however, is limited due to their oxygen sensitivity. In recent years the family of OYEs have been found capable of biotransforming α,β-unsaturated esters, with an additional electron withdrawing group required in the α- or β-position to sufficiently activate the alkene moeity.[290–293] Halogen activating groups have been reported in the literature, specifically chloro- and bromo-enoates (**Scheme 58**),[291,294] however to the best of the author's knowledge fluoro-enoates have yet to be investigated.

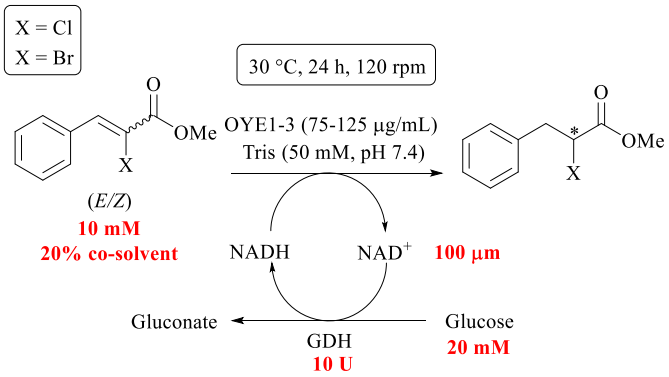

Scheme 58: Bioreduction of (*E*/*Z*)-α-haloenoates with OYE1-3 reported by Tasnádi *et al.*[291]

In this chapter, the bioreduction of (*E*/*Z*)-α-fluoro-β-phenylenoates is described. Due to the small size and high electronegativity of fluorine, it was envisaged that this group would be successfully accepted in bioreductions, thereby generating chiral C(sp^3)-F compounds stereoselectively. A range of substrates with electron withdrawing groups on the phenyl ring in α-fluorocinnamates were initially investigated to aid biocatalytic conversions.

.7.2 Preliminary Assay Considerations

Preliminary assay considerations reviewed published literature as well as the author's established assay design and analytical methods available.

7.2.1 Ene-Reductases and Substrates

Work by Utaka *et al.* in the bioreduction of 2-chloro-2-alkenoates with Baker's yeast established that the presence of the chlorine group in the α-position was vital for the bioreduction, and that only methyl esters were accepted as substrates.[295,296] Biotransformations of the investigated (*Z*)-2-chloro-2-alkenoates provided saturated (*S*)-chloro acids in >98% *ee*, whilst (*E*)-stereoisomers afforded (*R*)-chloro acids in 25 – 92% *ee*. Ester hydrolysis was observed as a side reaction in the fermentation medium, accounting for the acids formed.[296]

Brenna *et al.* further investigated these findings using some of the substrates described by Utaka *et al.*, submitting them for bioreductions with OYE1-3. They concluded that under the conditions investigated hydrolysis did not occur, and thus the methyl esters accepted as substrates in ER bioreduction.[290] Moreover, their results from the bioconversions with α-halo-β-arylacrylates demonstrated that higher conversions were

attained for more electron withdrawn substrates (those bearing a electron withdrawing group on the aryl ring) (**Figure 72**, **Table 16**).[290]

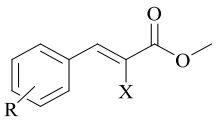

Figure 72: (*Z*)-α-Halo-β-arylenoate substrates investigated by Brenna *et al*.[290]

Table 16: Conversions (%) and *ee* (%) from OYE1-3 bioreduction of (*Z*)-α-halo-β-arylenoates reported by Brenna *et al*.[290]

Substrate	**OYE1**		**OYE2**		**OYE3**	
	C (%)	***ee* (%)**	**C (%)**	***ee* (%)**	**C (%)**	***ee* (%)**
X = Cl R = --[a]	4	82 (*S*)	5	80 (*S*)	38	99 (*S*)
X = Br R = --[a]	10	94 (*S*)	1	89 (*S*)	37	94 (*S*)
X = Cl R = *p*-OCH_3	14	60 (*S*)	6	62 (*S*)	20	88 (*S*)
X = Br R = *p*-OH	0	--	0	--	0	--
X = Cl R = *o*-NO_2	38	93	15	92	91	99
X = Cl R = *p*-CN	28	97 (*S*)	5	90 (*S*)	73	96 (*S*)

[a] No substituent present.

With this in mind, the bioreductions of (*E*/*Z*)-α-fluoro-β-arylenoates bearing an electron withdrawing group on the aromatic ring were explored. Prior to this, however, the bioreduction of α-fluoro-β-arylenones were considered, for reasons described in section 7.3.

7.2.2 Clarified Lysate Preparation and Assay Analytics

As previously described in Chapter 4, ERs were expressed by recombinant *E. coli* BL21 (DE3) cultivation. Cells were cultivated in TB medium at 37 °C until an OD_{600} of 0.5 – 0.7 was attained, induced by addition of IPTG, expressed at 25 °C for 24 h and then harvested via centrifugation. Cell pellets were stored up to 6 months at -80 °C with no loss of activity. Enzymes were prepared as clarified cell lysates using established procedures. The term "clarified cell lysates" refers to the total soluble unpurified protein expressed by *E. coli*. Enzymes NCR+pQR1811 in the clarified cell lysates had

a concentration of 1.6 mg/mL. Clarified lysates were stored at -80 °C for up to 2 weeks with no loss of activity, defrosted only once, and kept at 0 °C prior to application.

For preliminary investigations, previously optimised ER+G6PDH bioreduction conditions were employed with NCR+pQR1811, and the metagenomic enzymes cloned from pQR1440+1811, pQR1445+1811, pQR1446+1811, and pQR1907+1811. At a total volume of 250 µL and substrate loading (10 mM) a high concentration of co-expressed clarified lysate (1 mg mL^{-1}) was applied for the initial screen. Bioconversions were performed in triplicate.

Analytical analysis of the reaction mixtures was perfomed either by chiral HPLC or GC, as fluoro compounds did not tolerate the aqueous environment of achiral HPLC. By chiral HPLC, enantiomeric separation of the new products was achieved with a Chiralpak AD-H column and elution with 1% *iso*propanol:hexane (***Method F***, ***Method G***) as described in experimental procedures. For GC analysis, a chiral column was applied (***Method D***).

7.3 (*E*)-α-Fluoro-β-arylylenone

α-Fluoro-β-arylenone (*E*)-**104** was first considered prior to our investigations with (*E*/*Z*)-enoates as the ketone moiety afforded greater activation of the alkene bond, thus providing initial insight into whether NCR+pQR1811 bioreduction would be viable with ester activation.

7.3.1 Preliminary Screening

A preliminary screen was performed with (*E*)-**104**[xxxiii] (**Scheme 59**) bearing a cyano group in the *para*-position, a substituent previously established to be successfully accepted by NCR+pQR1811 from our work with **65**. A high clarified lysate concentration (1 mg/mL) was applied.

[xxxiii] Synthesised by Dr Victor Laserna Ayora as a crude product as a mixture of 93:7 *E*/*Z* isomers.

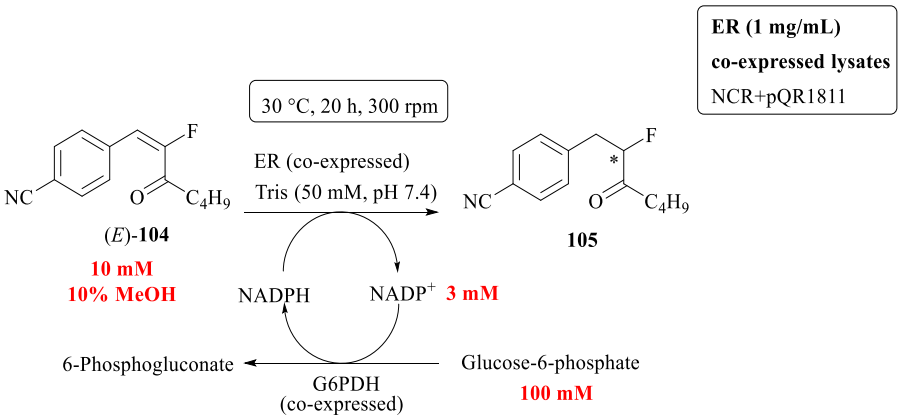

Scheme 59: Bioreduction of (E)-α-fluoro-β-arylenone (*E*)-**104** with co-expressed clarified lysate. Bioconversions were performed at 30 °C, 300 rpm for 20 h at a scale of 250 µL. Final concentrations were G6PNa (100 mM), $NADP^+$ (3 mM), and alkene substrate (10 mM) in 50 mM Tris (pH 7.4) with 10% MeOH. Co-expressed clarified lysates were applied at final concentrations of 1 mg/mL. Chiral HPLC analysis was performed using ***Method G***.

Complete conversion of the substrate was observed by chiral HPLC and ^{19}F NMR analysis. Synthesis of the racemic product standard by Pd/C hydrogenation and chiral HPLC analysis confirmed product formation in 93% *ee* (**Figure 73**), however the optical purity of the product may have been influenced by the isomeric purity of (*E*)-**104**. Additionally, ^{19}F NMR revealed by-product formation with two peaks recorded at -75.0 and -75.8 ppm (**Figure 74**), the former peak being sharp and later broad suggesting the formation of two different species as opposed to a doublet coupling. It was possible that *E.coli* ADH enzymes present in the clarified lysate were active on the substrate (*E*)-**104** affording alcohol by-products **106** and **107** (**Figure 75**), however with both peaks presenting as singlets the prospect of by-products **106** and **107** was discarded. The assay will be repeated in the future using purified enzyme.

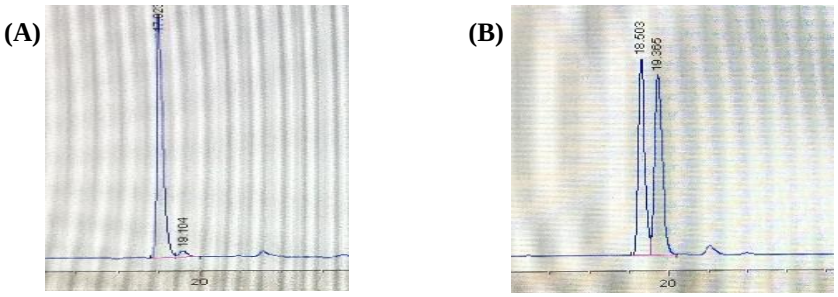

Figure 73: (A) Product, Rt = 17.8 min and Rt = 19.1 min from the bioreduction of (*E*)-**104** with NCR+pQR1811 (1 mg/mL) **(B)** Co-injection of the racemic product standard **105**, Rt = 18.5 min and Rt = 19.4 min. Product formation was confirmed by co-injection with the racemic product standard.

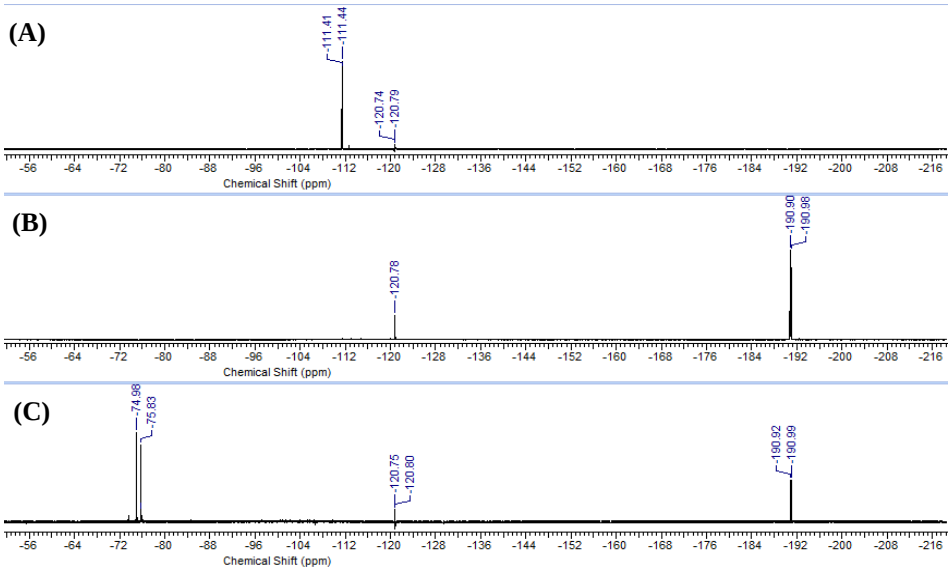

Figure 74: ^{19}F NMR of **(A)** (*E*)-**104** starting material, contaminant at -120.7 ppm **(B)** The synthesised racemic product standard **105**, contaminant at -120.7 ppm **(C)** Products produced from application of NCR+pQR1811 (1 mg/mL) clarified lysate, contaminant at -120.7 ppm.

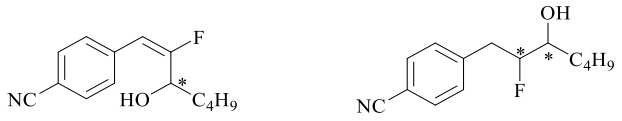

106 **107**

Figure 75: Hypothesised alcohol dehydrogenase by-products **106** and **107**.

7.4 (*Z*)-α-Fluoro-β-arylenoates

The ethyl and methyl esters of (*Z*)-α-fluoro-β-arylenoates were synthesised, a preliminary screening with ERs was performed, and substrate scope was analysed with NCR+pQR1811.

7.4.1 (Z)-Enoate Substrates

Augustine *et al*. have reported the stereoselective synthesis of (*Z*)-α-haloacrylates via a titanium-enolate mediated asymmetric aldol condensation.[297] The suggested mechanism postulated a Zimmerman-Traxler transition state for stereoselective carbon–carbon bond formation followed by E1cB elimination under basic conditions to generate the olefin. Several benzaldehydes with electron withdrawing groups were applied in the reaction with commercially available ethyl fluoroacetate **108** to afford (*Z*)-α-fluoro-β-arylenoates **109a-f** following purification by flash column chromatography (**Scheme 60**, **Table 17**). The geometry of the double bond was confirmed by the $^{3}J_{HF}$ coupling of ~30 Hz, as described in experimental procedures.

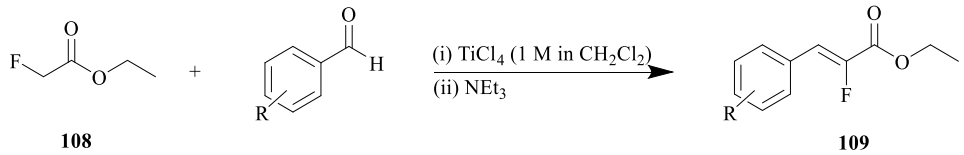

108 109

Scheme 60: Asymmetric aldol condensation of ethyl fluoroacetate **108** and substituted aldehydes to afford (*Z*)-α-fluoro-β-arylenoates **109**.

Table 17: (*Z*)-α-Fluoro-β-arylenoates **109a-f** synthesised.

Product	R	Yield (%)
(*Z*)-**109a**	*p*-CN	23
(*Z*)-**109b**	*p*-CF_3	47
(*Z*)-**109c**	*o*-CF_3	65
(*Z*)-**109d**	*p*-NO_2	16
(*Z*)-**109e**	*p*-Cl	29
(*Z*)-**109f**	*p*-Br	41

7.4.2 Transesterification

Transesterification of ethyl (*Z*)-α-fluoro-β-arylenoates to their respective methyl esters was achieved by the application of NaOMe in an excess of anhydrous MeOH (**Figure 76**).[298] Purification was attained by either flash column chromatography or removal of the solvent *in vacuo*, resolubilisation in $CHCl_3$ and filtration through Celite™ to form **110a-f** in 32 – 83% yields.

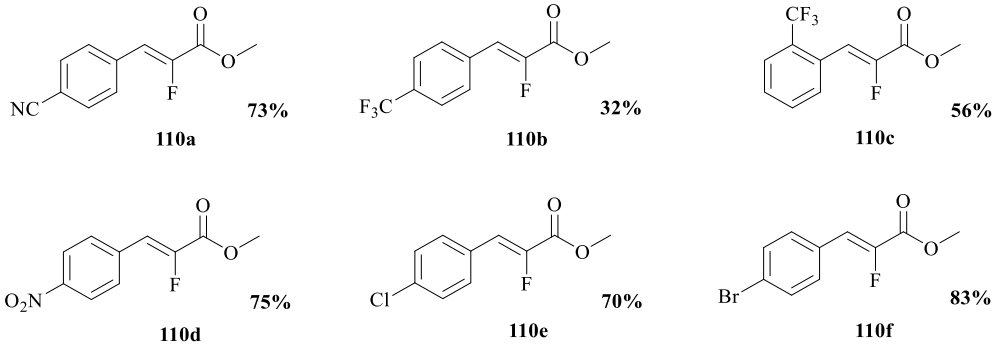

110a 110b 110c 110d 110e 110f

Figure 76: Methyl (*Z*)-a-fluoro-β-arylenoates **110a-f** afforded from transesterification of their respective ethyl esters.

7.4.3 Preliminary Screening

Continuing on from our work with (*E*)-**104**, a preliminary screen was performed with the ethyl ester (*Z*)-**109a** bearing a cyano group in the *para*-position. In addition, (*Z*)-**109a** was initially investigated to confirm if the neccessity for methyl esters also applied to NCR+pQR1811 and metagenomic enzymes cloned from pQR1440+1811, pQR1445+1811, pQR1446+1811, and pQR1907+1811 (**Scheme 61**). A high clarified

lysate concentration of 1 mg/mL was evaluated. Dissappointingly, (*Z*)-**109a** was only minimally (~1-5%) accepted by the panel of ERs following analysis by chiral HPLC. The methyl ester (*Z*)-**110a** was synthesised by transesterification as previously established and screened under analagous conditions. Again, only a minimal acceptance (~1-5%) was observed against the panel of ER+G6PDH enzymes used.

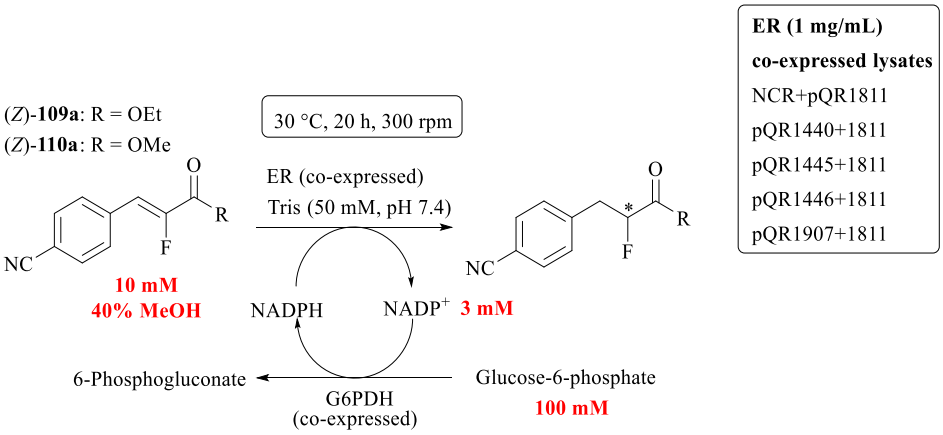

Scheme 61: Bioreduction of (*Z*)-α-fluoro-β-arylenoates **109a** and **110a** with co-expressed clarified lysates. Bioconversions were performed in duplicate at 30 °C, 300 rpm for 20 h at a scale of 250 µL. Final concentration were G6PNa (100 mM), $NADP^+$ (3 mM), and alkene substrate (10 mM) in 50 mM Tris (pH 7.4) with 40% MeOH. Co-expressed clarified lysates were applied at final concentrations of 1 mg/mL. The reactions were analysed using Chiral HPLC applying ***Method G***.

7.4.4 Substrate Scope

As a means of further investigating the potential biotransformations of (*Z*)-α-fluoro-β-arylenoates, methyl esters (*Z*)-**110a-f** bearing an electron withdrawing group on the phenyl ring were screened. Strong electron withdrawing groups NO_2 and CF_3 were selected, along with inductively electron withdrawing halogens Cl and Br. Substrates were screened against NCR+pQR1811 at a high clarified lysate concentration of 1 mg/mL and analysed by chiral HPLC (**Scheme 62**). Discouragingly, biotransformations were not observed for (*Z*)-**110a-f**. Substrate (*Z*)-**110a** was minimally accepted (~1-5%) by NCR+pQR1811, whilst (*Z*)-**110b** could not be solubilised in ^{i}PrOH for chiral HPLC analysis of substrate conversion.

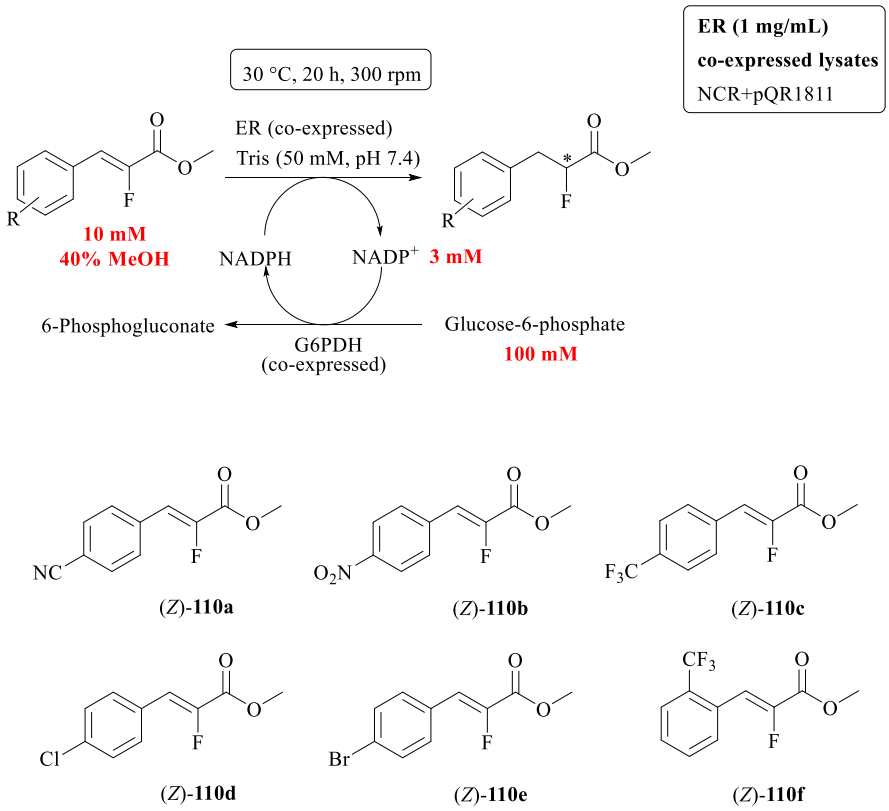

Scheme 62: Bioreduction of (*Z*)-α-fluoro-β-arylenoates **110a-f** with co-expressed clarified lysates. Bioconversions were performed in triplicate at 30 °C, 300 rpm for 20 h at a scale of 250 µL. Final concentration were G6PNa (100 mM), $NADP^+$ (3 mM), and alkene substrate (10 mM) in 50 mM Tris (pH 7.4) with 10% MeOH for (*Z*)-**110c-f** and 40% MeOH for (*Z*)-**110a-b**. Co-expressed clarified lysate was applied at final concentrations of 1 mg/mL. Chiral HPLC analysis of the product mixture was performed using ***Method F*** (*Z*)-**110c-f** and ***Method G*** for (*Z*)-**110a**.

7.5 (*E*)-α-Fluoro-β-phenylenoates

With limited success from the bioreduction of (Z)-α-fluoro-β-arylenoates, the ethyl and methyl esters of (*E*)-α-fluoro-β-arylenoates were synthesised, a preliminary screening with NCR+pQR1811 was performed, and further work was conducted with select substrates.

7.5.1 (E)-Enoate Substrates

Provided the lack of success in the biotransformations of (*Z*)-α-fluoro-β-arylenoates, their (*E*)-stereoisomers were explored and synthesised. The stereoselective formation of (*E*)-α-fluoro-β-arylenoates was achieved by the application of the Horner-Wadsworth-Emmons reaction[299] with commercially available diethoxylphosphoryl-2-fluoroacetate **111** to afford (*E*)-α-fluoro-β-arylenoates (*E*)-**109** following purification by flash column chromatography, with the $^3J_{HF}$ coupling of ~20 Hz (**Scheme 63**, **Table 18**). Reactions were not optimised due to the use of products in preliminary test assays.

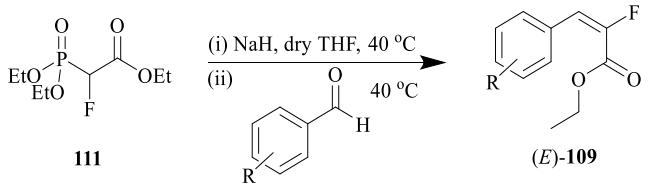

Scheme 63: Horner-Wadsworth-Emmons reaction with **111** and substituted aldehydes to afford (*E*)-α-fluoro-β-arylenoates (*E*)-**109**.

Table 18: (*E*)-α-Fluoro-β-arylenoates (*E*)-**109a-f** synthesised.

Product	R	Yield (%)
(*E*)-**109a**	*p*-CN	23
(*E*)-**109b**	*p*-CF_3	21
(*E*)-**109c**	*o*-CF_3	48
(*E*)-**109d**	*p*-NO_2	47
(*E*)-**109e**	*p*-Cl	43
(*E*)-**109f**	*p*-Br	41

7.5.2 Transesterification

Transesterification of ethyl (*E*)-α-fluoro-β-arylenoates to their respective methyl esters was achieved by the application of NaOMe in an excess of anhydrous MeOH (**Figure 77**).[298] Purification was attained by either flash column chromatography or removal of the solvent *in vacuo*, resolubilisation in $CHCl_3$ and filtration through Celite™ to form (*E*)-**110c** and (*E*)-**110e** in 33% and 36% yields respectively.

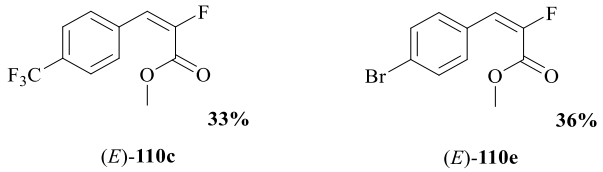

Figure 77: Methyl (*E*)-α-fluoro-β-arylenoates (*E*)-**110c** and (*E*)-**110e** afforded from transesterification of their respective ethyl esters.

7.5.3 Preliminary Screening

Ethyl esters (*E*)-**109a-f** were first investigated in biotransformations, with a high concentration of NCR+pQR1811 clarified lysate (1 mg/mL) applied (**Scheme 64**). Encouragingly, preliminary results by chiral HPLC suggested modest product formation (~20-30% substrate conversion for all) and *ee*s from 49 – 71%.

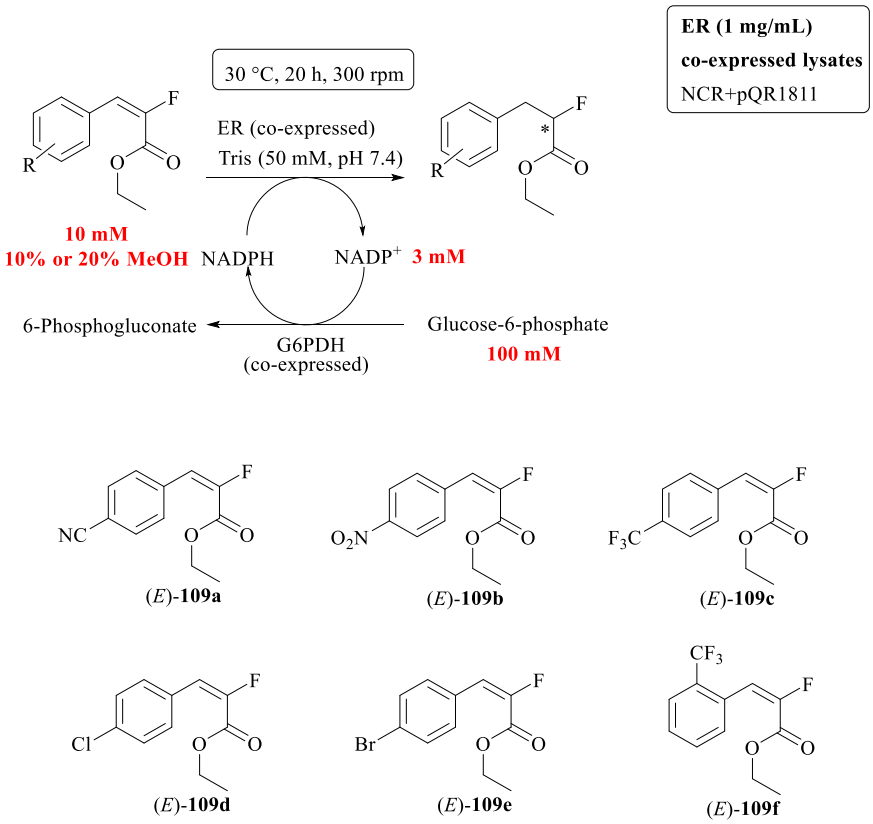

Scheme 64: Bioreduction of (*E*)-α-fluoro-β-arylenoates (*E*)-**109a-f** with co-expressed clarified lysates. Bioconversions were performed in triplicate at 30 °C, 300 rpm for 20 h at a scale of 250 µL. Final concentration were G6PNa (100 mM), NADP+ (3 mM), and alkene substrate (10 mM) in 50 mM Tris (pH 7.4) with 10% MeOH for (*E*)-**109a,c-f** and 20% MeOH for (*E*)-**109b**. Co-expressed clarified lysate was applied at final concentrations of 1 mg/mL. Chiral HPLC analysis was performed using ***Method F*** for (*E*)-**109c-f** and ***Method G*** for (*E*)-**109a-b**.

Further work was conducted with (*E*)-**109c** and (*E*)-**109e**. Compound (*E*)-**110c** was selected owing to its interesting and strongly electron withdrawing CF_3 substituent, whilst (*E*)-**109e** bearing a Br substituent was interesting for cross coupling reactions. In addition, good provisional *ee*s of 71% and 61% were respectively attained from their biotransformation with NCR+pQR1811 (**Figure 78**).

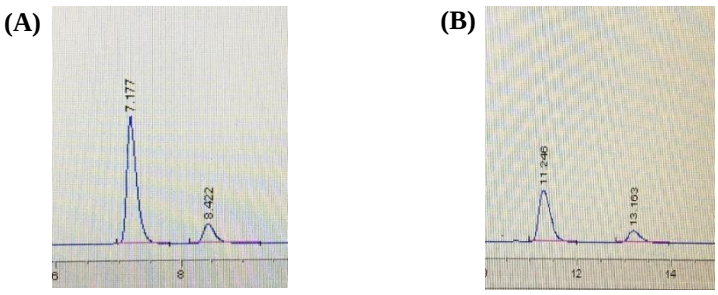

Figure 78: (A) Product, Rt = 7.2 min and Rt = 8.4 min, from the bioreduction of (*E*)-**109c** with NCR+pQR1811 (1 mg/mL), with a provisional *ee* of 71%. **(B)** Product, Rt = 11.2 min and Rt = 13.2 min, from bioconversion of (*E*)-**109e** with NCR+pQR1811 (1 mg/mL), with a provisional *ee* of 61%.

Compounds (*E*)-**109c** and (*E*)-**109e** were converted into their respective methyl esters (*E*)-**110c** and (*E*)-**110e** by transesterification and screened at NCR+pQR1811 clarified lysate concentrations of 1 – 3 mg/mL (**Scheme 65**). Chiral HPLC analysis exhibted increasing conversions with increasing lysate concentration, with 100% conversion at 3 mg/mL clarified lysate. By-product formation was also observed. By analogy of the products' retention times from bioreduction of ethyl esters (*E*)-**109c** and (*E*)-**109e**, the products' retention times from the bioreduction of methyl esters (*E*)-**110c** and (*E*)-**110e** were as anticipated, with the by-products' retention times earlier than that of products (**Figure 79**). Further work will involve the synthesis of the racemic product standards to confirm product formation as well as repeat the assay with purified enzyme.

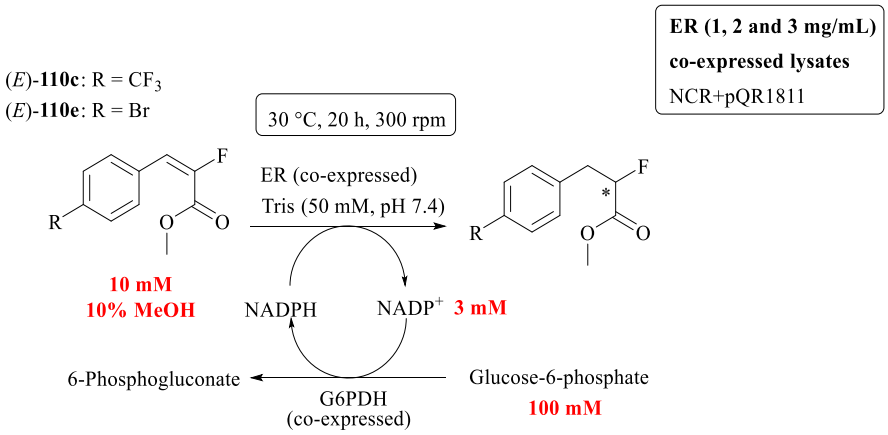

Scheme 65: Bioreduction of (*E*)-α-fluoro-β-arylenoates (*E*)-**110c** and (*E*)-**110e** with co-expressed clarified lysates. Bioconversions were performed in duplicate at 30 °C, 300 rpm for 20 h at a scale of 250 µL. Final concentration were G6PNa (100 mM), NADP+ (3 mM), and alkene substrate (10 mM) in 50 mM Tris (pH 7.4) with 40% MeOH. Co-expressed clarified lysates were applied at final concentrations of 1 – 3 mg/mL. Chiral HPLC analysis was performed using ***Method F***.

(A) 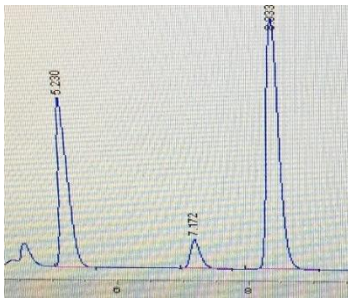

(B) 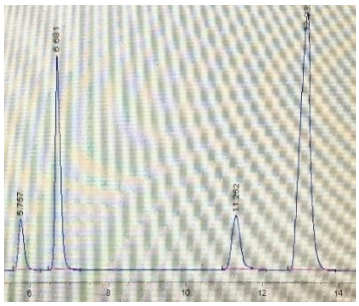

Figure 79: (A) Products, Rt = 5.2 min, Rt = 7.2 min, Rt = 8.3 min from the bioreduction of (*E*)-**110c** with NCR+pQR1811 (3 mg/mL), with a provisional *ee* of 81% for Rt = 7.2 min and Rt = 8.3 min. **(B)** Products Rt = 5.6 min, Rt = 6.7 min, Rt = 11.3 min, Rt = 12.9 min from bioconversion of (*E*)-**110e** with NCR+pQR1811 (3 mg/mL), with a provisional *ee* of 70% for Rt = 11.3 min and Rt = 12.9 min.

The established reduction using Pd/C was applied to ethyl (*Z*)-α-fluoroacrylates (*Z*)-**109c** and (*Z*)-**109e**, with the starting material of each recovered after 18 h reaction time. Performing the reaction again without SPh_2 and in EtOH showed no reaction by TLC analysis after 18 h. An additional 10 mol% Pd/C was added and the reaction monitored over a further 48 h, with still no reaction observed for (*Z*)-**109c** and defluorination observed for (*Z*)-**109e** (by NMR analysis).

Martinet et al. have previously reported solvent dependence in the catalytic Pd/C hydrogenation of α,β-difluoro α,β-unsaturated ketones and esters,[300] with other reports in the literature successfully employing MeOH as the solvent in the reduction of α-fluoro α,β-unsaturated ketones and esters.[300–302] Therefore, MeOH was employed as a solvent with 50 mol% Pd/C in the hydrogenation of (*Z*)-**109e** over 18 h. As before defluorination was observed. Reducing the reaction time to 2 h provided what was anticipated to be the product by TLC analysis, however purification by preparative HPLC was unsuccessful providing an indeterminable NMR spectrum. Further work will involve the synthesis of the racemic product standards to confirm product formation as well as repeat the assay with purified enzyme.

7.6 Conclusions

In conclusion, success was attained in the bioreduction of α-fluoro-β-arylenone (*E*)-**104** by NCR+pQR1811, with a 100% conversion and preliminary 93% *ee* observed. Further work will aim establish the absolute stereochemistry of the major isomer, identify the two by-products formed, and explore the use of purified enzymes in biotransformations.

Moderate success was attained in the biotransformations of α-fluoro-β-arylenoates. Stereoselective olefination strategies for ethyl (*E*/*Z*)-α-fluoroenoates were performed, with a titanium-enolate mediated asymmetric aldol condensation furnishing (*Z*)-α-fluoroacrylates (*Z*)-**109a-f** in 16 – 65% yield, and the Horner-Wadsworth-Emmons reaction providing (*E*)-α-fluoroacrylates (*E*)-**109a-f** in 21 – 48% yield. Transesterification of ethyl (*E*/*Z*)-α-fluoroacrylates to their respective methyl esters was accomplished by using NaOMe in anhydrous MeOH yielding (*E*)-**110a-f** and (*Z*)-**110a-f**.

Whilst (*Z*)-α-fluoro-β-arylenoates (*Z*)-**110a-f** were not readily accepted as substrates with NCR+pQR1811, (*E*)-stereoisomers (*E*)-**109a-f** were accepted with modest substrate conversions (~30% for all substrates) and preliminary *ee*s of 49 – 69%. Further work with methyl esters (*E*)-**110c** and (*E*)-**110e** at 1 – 3 mg/mL NCR+pQR1811 clarified lysate exhibited increased conversions with increased clarified lysate concentration, with 100% conversion observed using 3 mg/mL NCR+pQR1811. Future work will synthesise racemic product standards to confirm product formation, identify the by-product formed, as well as repeat the assay using purified enzymes.

It is premature for the author to comment on the success of biotransformations of α-fluoro-β-arylenoates with ERs as product standards had yet to be synthesised to confirm product formation. All that has been observed is the consumption of substrates, with preliminary product *ee*s suggested. (*E*)-α-Fluoro-β-arylenoates were more readily accepted than (*Z*)-α-fluoro-β-arylenoates, and the bioreduction of enone (*E*)-**104** was more successful than enoates.

8. Conclusions and Future Work

In conclusion, the work presented in this thesis describes the successful develoment of a biocatalytic ER-TAm cascade with α-hydroxyketone derivatives for the molecular assembly of chiral amino alcohols, a prevalent structural motif in value-added synthons and bioactive pharmaceuticals.[224] Preparative scale biotransformations and further chemical reactions successfully afforded diastereomerically enriched 2-aminooxazoles (2*S*,4*S*)-**37** and (2*S*,4*R*)-**37** in 93:7 *dr*[xxxiv] and 97:3 *dr*[xxxv] respectively.

In Chapter 2, aldehyde, ketone and α-hydroxyketone derivatives were chemically synthesised for substrate walking strategies with ERs. Synthesis of ketone derivatives **7a, 41, 42, 46 – 48** was sucessfully accomplished using an acid-catalysed aldol condensation and the Weinreb ketone synthesis, with yields of 54 – 86% attained. Various approaches were explored for the formation of α-hydroxyketones, with the Rubottom oxidation found to be the most successful and applied to afford α-hydroxyketone derivatives **52, 55, 63 – 66**. Chemical reduction of **40**, **67**, **70 – 73**, **7a**, **41**, **42**, **46 – 48**, **52**, **55**, **63 – 66** using hydrogen over palladium on carbon with a catalyst posion afforded **68**, **8a**, **74 – 89**.

Substrate walking strategies with ERs were initially explored in Chapter 3 with the bioreduction of substituted cinnamaldehyde derivatives. Application of ER clarified lysates observed alcohol by-product formation, most likely from *E.coli* ADH contamination. As such, the removal of ADH enzymes was accomplished by the co-expression of ER+G6PDH and purification by immobilised metal affinity chromatography. Application of the co-expressed purified enzymes from NCR+pQR1811, pQR1445+1811 and pQR1907+1811 with cinnamaldehyde **70** and substituted cinnamaldehyde derivatives **67**, **40**, **71** – **73** gave fair to excellent yields of 56 – 95% with at least one ER, with the exception of the β-phenyl substituted **71** which was not accepted as a substrate. Further work and optimisation with aliphatic aldehydes **94** – **99** and (*E*/*Z*)-**18** afforded limited success, with a maximum of 41% yield from the conversion of **99**, and the recovery of starting material and product for (*E*/*Z*)-**18** improved to ~30%. Bioreduction of aliphatic aldehydes **94** – **97** gave inconsistent

[xxxiv] Calculated using ^{1}H NMR as 93:7 *dr* ratio of (2*S*,4*S*):(2*S*,4*R*).
[xxxv] Calculated using ^{1}H NMR as 97:3 *dr* ratio of (2*S*,4*R*):(2*S*,4*S*).

results across the triplicate experiments, and as such their results were deemed inconclusive.

In Chapter 4, the increase of substrate complexity was described via substrate walking from ketone to α-hydroxyketone derivatives. Derivatives investigated were unsubstituted, α-methyl substituted, and β-methyl substituted ketones, given the successful biotransformation of their respective aldehydes as well as relevance of these derivatives in the formation of TAAR1 inhibitors. The β-substituted ketone and α-hydroxyketone derivatives **42** and **55** were not accepted as substrates for any of the ERs investigated. Successful bioconversions were attained with unsubstituted and α-methyl substituted ketone and α-hydroxyketone derivatives with enzymes from NCR+pQR1811, pQR1445+1811 and pQR1907+1811. Further work was pursued solely with the α-methyl substituted analogue **63** with NCR+pQR1811 given its enantiopure generation of (*S*)-**85**, tentatively assigned as a *S*-stereocentre from molecular docking studies. The systematic evaluation and optimisation of five assay parameters (buffer type, clarified lysate concentration, co-solvent type, temperature, and substrate loading) afforded the generation of (*S*)-**85** in 63% yield at 25 mM substrate loading. Substrate scope using **64** – **66** afforded an excellent *ee* of up to 99.5% and yields of 32 – 60% from their bioreduction with NCR+pQR1811.

Concurrently, in Chapter 5 the biotransformation of a panel of reported and metagenomic TAms with α,ß-unsaturated and saturated hydroxyketone derivatives **52**, **63**, **55** and **84** – **86** was described to identify a suitable substrate, as well as (*R*)- and (*S*)-selective TAms viable in an one-pot ER-TAm cascade. Substrate **85** was identified, along with Mv-TAm and 13-TAm. Assessment of the data concluded that a two-step one-pot cascade was required for the application of Mv-TAm owing to its high activity with the unsaturated compound **63**. Potential for a one-step one-pot cascade with 13-TAm was signified by its low activity with **63** and high activity with **85**. Whilst considering complementary conditions for the ER-TAm cascade, 7 assay parameters for transamination (clarified lysate concentration, type of co-solvent, substrate loading, amine donor, amine donor equivalents, temperature, and pH) were systematically evaluated and optimised. Transamination with (*R*)-selective Mv-TAm was optimised at a 25 mM substrate loading with 83% substrate conversion. Transamination with the (*S*)-selective 13-TAm was optimised at 5 mM substrate loading with 72% conversion yield. Substrate scope with Mv-TAm afforded a moderate conversion of 41% for **87**,

and fair conversions of 62% and 51% for **88** and **89** respectively. Applying the optimised reaction conditions with 13-TAm afforded a 40% conversion yield from the amination of **87** and 21% conversion yield for both **88** and **89**.

Preparative scale bioconversions performed and optimised are described in Chapter 6. Bioreduction using NCR+pQR1811 was high yielding and afforded a high *ee*, with greatest success using 50 mM HEPES (pH 7.4) furnishing the product in 96% isolated yield and 99.5% *ee* (25 mM substrate loading, 25 mL scale) and 82% yield and 98% *ee* (5 mM substrate loading, 25 mL scale). Conversions applying Mv-TAm (25 mM substrate loading, 25 mL) were high with a 83% conversion in 50 mM Tris-HCl (pH 9) and H_2O (pH 9), as well as a 75% conversion in 50 mM HEPES (pH 9). A conversion yield of 66% was achieved using 13-TAm in 50 mM HEPES (pH 7.4) (5 mM substrate loading, 25 mL).

Purification of the chiral amino alcohol product assessed a range of methods and techniques, with experimental results from the ER – TAm cascade concluding that severe product loss was observed when using the Amberlite IRA-410 resin. As such, water (pH 7.4, then pH 9) was used as the buffer in the two-step, one-pot NCR – Mv-TAm cascade to obviate the need for the resin, attaining the product (2*S*,3*S*)-**100** in in a 58% yield by HPLC, and 32% isolated yield following work-up and purification by preparative HPLC. Further reaction gave the 2-aminooxazole (2*S*,4*S*)-**37** in 18% yield and 93:7 *dr*[xxxvi] (**Scheme 66**). The NCR – 13-TAm cascade necessitated a two-step, one-pot reaction as exhibited from by-product (2*R*)-**103** formation. The biotransformations performed in 50 mM HEPES (pH 7.4) afforded the product (2*R*,3*S*)-**100** in 68% yield by HPLC, and 30% isolated yield, with further reaction giving the 2-aminooxazole (2*S*,4*R*)-**37** in 15% yield and 97:3 *dr*[xxxvii] (**Scheme 67**). As the *ee* of (*S*)-**85** generated from NCR bioreduction was very high (99.5% *ee* at 25 mM **63** substrate loading and 98% *ee* at 5 mM **63** substrate loading) the slightly lower *dr* of (2*S*,4*S*)-**37** and (2*S*,4*R*)-**37** observed arises primarily from the Mv-TAm and 13-TAm amination steps in the cascade.

[xxxvi] Calculated using ^{1}H NMR, 93:7 *dr* ratio of (2*S*,4*S*):(2*S*,4*R*).
[xxxvii] Calculated using ^{1}H NMR, 97:3 *dr* ratio of (2*S*,4*R*):(2*S*,4*S*).

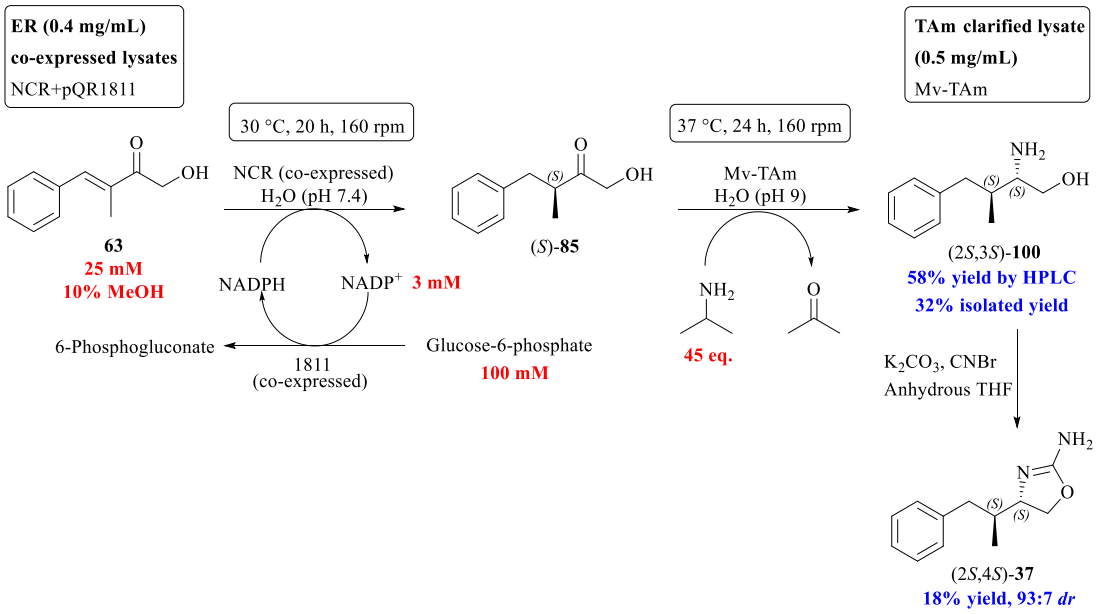

Scheme 66: Optimised two-step, one-pot NCR – Mv-TAm biocatalytic cascade with substrate **63** (25 mM) in 25 mL affording final product amino alcohol (2*S*,3*S*)-**100** via intermediate (*S*)-**85**. Further reaction of (2*S*,3*S*)-**100** with CNBr and K_2CO_3 afforded 2-aminooxazole (2*S*,4*S*)-**37**.

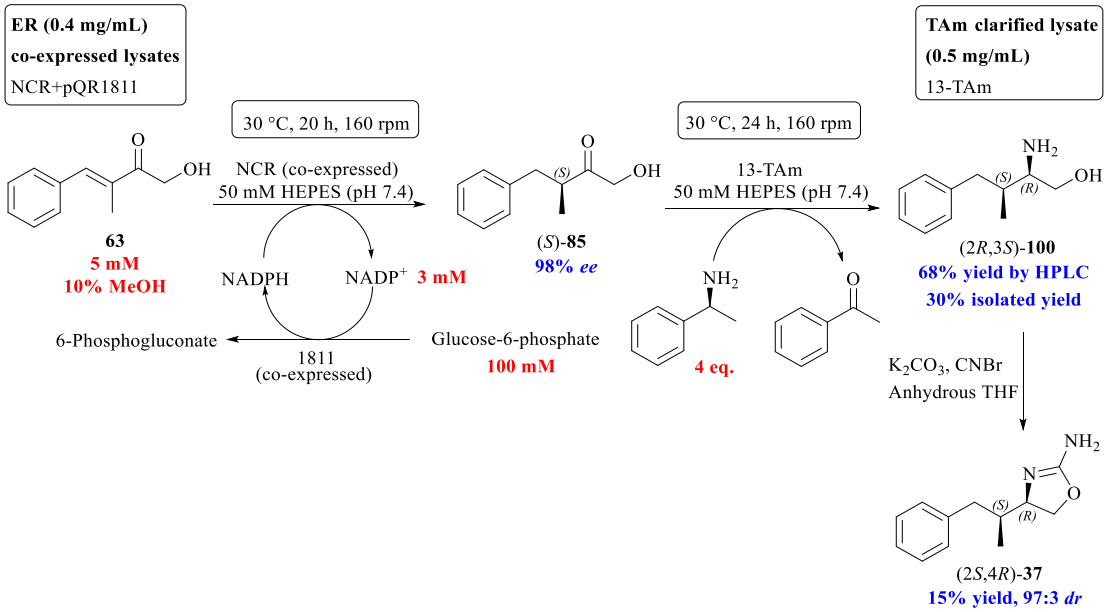

Scheme 67: Optimised two-step, one-pot NCR – 13-TAm biocatalytic cascade with substrate **63** (5 mM) in 25 mL affording final product amino alcohol (2*R*,3*S*)-**100** via intermediate (*S*)-**85**. Further reaction of (2*R*,3*S*)-**100** with CNBr and K_2CO_3 afforded 2-aminooxazole (2*S*,4*R*)-**37**.

Conformational analysis of (2*S*,4*S*)-**37** from 1D NOEs[xxxviii] and ^{3}J(2,3) proton coupling endorsed an eclipsed conformation, with the minimised energy of (2*S*,4*S*)-**37** using Chem3D also exhibiting an eclipsed conformation. Future work will aim to establish the absolute stereochemistry of **85** produced from the NCR bioreduction via derivatisation and X-ray crystallography.

In Chapter 7, the biocatalytic generation of chiral fluorine from prochiral substrates was described. Initial work considered α-fluoro-β-arylenone (*E*)-**104** prior to investigations with (*E*/*Z*)-enoates as the ketone moiety afforded greater activation of the alkene bond, thus providing initial insight into whether the NCR+pQR1811 bioreduction would be viable with ester activation. Bioreduction of (*E*)-**104** by NCR+pQR1811 was successful, with a 100% conversion and preliminary 93% *ee* observed. Further work will aim establish the absolute stereochemistry of the major isomer, identify the two by-products formed, and explore the use of purified enzymes in biotransformations. Additionally, a range of α-fluoro-β-arylenones will be synthesised for substrate scope in ER bioreduction, along with their racemic product standards, and a method developed to determine the absolute stereochemistry of the major isomer.

Stereoselective olefination strategies for ethyl (*E*/*Z*)-α-fluoroacrylates were performed, furnishing (*Z*)-α-fluoroacrylates (*Z*)-**109a-f** in 16 – 65% yield and (*E*)-α-fluoroacrylates (*E*)-**109a-f** in 21 – 48% yield. Transesterification to their respective methyl esters was accomplished by using NaOMe in anhydrous MeOH yielding (*E*)-**110a-f** and (*Z*)-**110a-f**. Whilst (*Z*)-α-fluoro-β-arylenoates (*Z*)-**110a-f** were not readily accepted as substrates with NCR+pQR1811, (*E*)-stereoisomers (*E*)-**109a-f** were accepted with modest substrate conversions (~30% for all substrates) and preliminary *ee*s of 49 – 69%. Further work with methyl esters (*E*)-**110c** and (*E*)-**110e** observed a 100% conversion using 3 mg/mL NCR+pQR1811 clarified lysate. Future work will synthesise racemic product standards to confirm product formation, identify the by-product formed, as well as repeat the assay using purified enzymes.

[xxxviii] NMR spectroscopic analysis performed by Dr Abil Aliev.

9. Experimental

9.1 General Methods

All commercially available chemicals and solvents were used as received without any further purification. Reactions were performed at room temperature and atmospheric pressure in natural lighting unless otherwise stated. Room temperature is defined as between 18-22 ºC. Anhydrous conditions refers to the use of oven dried glassware and reactions performed under Ar. Where specified flame-dried glassware may supplement oven dried glassware. The term *in vacuo* refers to solvent removal by Büchi rotary evaporation between 30 – 90 °C, at approximately 10 mm Hg.

Reactions were monitored by thin layer chromatography (TLC) on aluminium plates coated with silica gel 60 F_{254} (Merck KGaA). Detection was provided by short and long range UV lamp (254 and 365 nm respectively), as well as $KMnO_4$ and ninhydrin staining. Flash column chromatography was performed using Geduran® silicagel 60 (40 – 63 µm).

Melting points were noted with Stuart® SMP11 apperatus and are uncorrected. Infrared spectra were obtained on a Perkin Elmer Spectrum 100 FTIR Spectrometer operating in ATR mode. Specific rotation was obtained using Bellingham Stanley ADP430 Polarimeter and the equation (**Equation 1**) with α being the measured rotation in degrees, l being the cell length (0.5 dm), and c being the concentration of the sample (1 = 10 mg/mL).

$$[\alpha]_D^{20} = \frac{100\alpha}{lc}$$

Equation 1: Specific rotation monochromatic plane polarised light of 589 nm (sodium D line) at 20 ºC.

High and low resolution mass spectrometry were obtained using a VG70 SE operating in either ES+, ES–, EI, CI or GCMS mode depending on the compound. Relative intensities of molecular ion peaks and adducts are given unless peaks were not normalised. UV-Vis spectrometry measurements were obtained either from a Thermo Scientific NanoDrop 2000 using Biochrom Libra S11.

All NMR spectra were recorded at room temperature. ^{1}H NMR spectra were recorded on Bruker AMX700 (700 MHz) and AMX600 (600 MHz). ^{13}C NMR spectra were recorded on Bruker AMX700 (700 MHz) and AMX600 (600 MHz) at 176 and 151 Hz respectively. ^{19}F NMR spectra were recorded on Bruker AMX700 (700 MHz) and AMX400 (400 MHz) at 659 and 376 Hz respectively. The chemical shifts for both ^{1}H and ^{13}C spectra are expressed in parts per million (ppm) with known residual solvent peaks employed as reference: $CDCl_3$ ($\delta = 7.27$). Coupling constants (*J*) are reported in Hertz (Hz). The multiplicity of each signal is indicated as s-singlet, br. s.-broad singlet, d-doublet, dd-doublet of doublet, dt-doublet of triplet, dq-doublet of quartet, ddq-doublet of doublet of quartet, dqd-doublet of quartet of doublet, t-triplet, td-triplet of doublet, tq-triplet of quartet, q-quartet, qdd-quartet of doublet of doublet or m-multiplet.

Sterilisation of media was performed in a Priorclave autoclave at 121 °C for 30 min. Cell culture and expression was performed in Stuart® orbital incubator S1600. Cell lysis was performed by sonication using Branson Sonifier 150 with microprobe tip (Ergosonic, UK) at a power of 20 W. Bioconversions were performed in Bioer Mixing Block MB-102 and New Brunswick Scientific Excella E24 Incubator Shaker Series. The following centrifuges were used: Eppendorf Centrifuge 5415 R (for eppendorfs), Eppendorf Centrifuge 5810 R (for 15 mL falcon tubes) and Beckman Coulter Avanti Centrifuge® J-26 XP (for 50 mL falcon tubes).

Analytical reverse phase high performance liquid chromatography (HPLC) analysis was performed using Agilent 1260 Infinity equipped with G1329B autosampler, G1311C quaternary pump, G1316A column oven, G1314F variable wavelength detector, corresponding software, and Ace 5 C18 column (150 × 4.6 mm).

Preparative HPLC was performed using Agilent 1260 Infinity equipped with G2260A autosampler, G1361A prep pump, G1364B fraction collector, G7165A multiple wavelength detector, corresponding software, and Supelco Discovery®BIO Wide Pore C18-10 column (25 cm × 21.2 mm, 10 µm).

Chiral HPLC analysis was performed using HP Series 1100 HPLC equipped with G1313A autosampler, G1322A degasser, G1311A quaternary pump, G1314A variable wavelength detector, corresponding software, and a Chiralpak AD-H column (5 µm particle size, 4.5 mm × 250 mm).

Gas chromatography (GC) analysis was performed using Agilent Technologies 7820A (G4350) GC System with corresponding software, Supleco Beta Dex 225 capillary GC column (30 m × 250 µm, 0.25 µm) and flame ionization detector at 300 °C. The samples (5 µL) were injected with the autosampler tower G4567A at an injection temperature of 250 °C and applied by split injection (ratio 20:1) and a split flow of 36 mL/min.

9.2 Chemical Biology

9.2.1 General Procedure

9.2.1.1 Buffers

NaPi, Tris HCl and HEPES buffers were prepared as follows: Sodium phosphate dibasic (3.549 g) was dissolved in distilled water (25 mL) for a 1 M solution. Sodium phosphate monobasic (3.000 g) was dissolved in distilled water (25 mL) for a 1 M solution. For 50 mM NaPi buffer at pH 7.4, 1 M Na_2HPO_4 (4.01 mL) and 1 M NaH_2PO_4 (0.99 mL) were combined, and the resulting solution sampled (2 mL) and diluted with distilled water (38 mL). For 50 mM NaPi buffer at pH 8, 1 M Na_2HPO_4 (4.70 mL) and 1 M NaH_2PO_4 (0.30 mL) were combined, and the resulting solution sampled (2 mL) and diluted with distilled water (38 mL). For 50 mM NaPi buffer at pH 9, the required amount of base was added to NaPi buffer (50 mM, pH 8). Trizma® hydrochloride (6.304 g) was dissolved in distilled water (40 mL) for a 1 M stock solution. The stock solution was sampled and diluted with distilled water when required to give 50 mM buffer solution. HEPES (4.766 g) was dissolved in distilled water (400 mL) and pH adjusted to give 50 mM HEPES at pH 7.4 and 9. The pH of all buffers were checked and adjusted as required.

The 10, 50, 100 and 500 mM imidazole buffers were prepared as follows: Trizma® hydrochloride (7.88 g), NaCl (29.22 g) and imidazole (0.68, 3.40, 6.81, or 34.04 g) were dissolved in distilled water (1 L) for final concentrations of 50 mM Tris HCl, 0.5 M NaCl and imidazole (10, 50, 100, or 500 mM) respectively. All imidazole buffers were pH adjusted to 7.4.

For pH adjustment the minimum volume of required acid/base (HCl/NaOH) was used to minimise changes in solute concentrations. All final buffer pH was confirmed with a pH electrode.

9.2.1.2 Media

Terrific broth (TB) was prepared as follows: 47.6 g of commercial TB powder (Merck) and glycerol (4 mL) was dissolved in distilled water and sterilised by autoclaving. Sterilised media was prepared fresh for cell culture and expression.

9.2.1.3 Antibiotics and IPTG

Antibiotic and IPTG solutions were prepared as follows: Kanamycin (Km) (50 mg/mL) in distilled water, Chloramphenicol (Cam) (34 mg/mL) in ethanol and isopropyl β-D-1-thiogalactopyranoside (IPTG) (1 M) in distilled water. Solutions were filter sterilised, aliquoted and stored at -20 °C until use.

9.2.1.4 Glycerol Stock

Glycerol stock cultures were prepared by addition of filter sterile 50% (v/v) glycerol (500 µL) to overnight cultures with the appropriate antibiotic (500 µL). (Overnight culture growth described in section ***9.2.1.5***). Glycerol stock cultures were stored in sterile cryo-vials at -80 °C.

9.2.1.5 Cell Culture and Expression

ER and TAm expression by recombinant *E. coli* BL21 (DE3) cultivation (with or without co-expresssed G6PDH) was accomplished as follows: Pre-cultivation (37 °C, 180 rpm) was performed overnight in sterilised Terrific Broth (TB) medium (10.0 mL) with respective antibiotic(s) (10.0 µL) and inoculated with cells obtained from respective glycerol stock culture. Following this, sterilised TB medium (300 mL) with respective antibiotic(s) (300 µL) in a 2 L culture flask was inoculated with 1% (3.00 mL) overnight culture. Cells were cultivated (37 °C, 180 rpm) until OD_{600} of 0.5 – 0.7 was attained, at which point expression was induced by addition of 1 M IPTG (300 µL). Enzyme were expressed (25 °C, 180 rpm) for 24 h and harvested via centrifugation (4 650 ×g, 30 min, 4 °C) in 50 mL aliquots. The supernatant was decanted and cell pellets stored at -80 °C for up to 6 months for all enzymes except 13-TAm, which was stored up to 3 months. Cell pellets were either purified or prepared as clarified cell lysates.

9.2.1.6 Preparation of Clarified Cell Lysates

Taking the cell pellet from the 50 mL aliquot described in section ***9.2.1.5***, *E. coli* BL21 (DE3) cells harbouring TAm, ER, or ER+G6PDH were resuspended in buffer (2 mL) (with 4.8 mM PLP for TAms). Buffers and pH investigated in biocatalytic experiments included 50 mM Tris HCl, HEPES, KPi and H_2O with pH from 7.4 – 9. Cells were lysed at 0 °C by sonication for 10 cycles of 15 s on/15 s off. The suspension was then centrifuged (13 000 rpm, 4 °C) in 1.5 mL eppendorfs for 20 min, with the obtained clarified cell lysate aliquoted and stored at -80 °C for a maximum of 2 weeks. Clarified lysates were defrosted only once for use in biocatalytic experiments and kept on ice prior to use. Total protein concentrations were determined by a Bradford assay, and enzyme concentration by SDS-PAGE densitometry using ImageJ software.

9.2.1.7 Sodium Dodecyl Sulfate Polyacrylamide Gel Electrophoresis (SDS-PAGE)

SDS-PAGE was performed using 4-20% Tris-Glycine gels. Clarified cell lysates (10 µL) were supplemented with 50 mM Tris HCl or HEPES buffer (90 µL) and incubated at 95 °C for 5 min for complete denaturation. The Laemmli 2× concentrate (Sigma Aldrich) (10 µL) was added to the protein sample (10 µL) and aliquoted (2 µL) into the gel wells, alongside Precision Plus Protein™ Dual Colour Standards (10 µL). SDS-PAGE was performed at 220 Hz for 35 min in Novex® Tris-Glycine SDS Running Buffer. SDS-gels were then stained with InstantBlue™ Coomassie stain (Thermo Scientific) according to manufacturer's instructions. Enzyme concentration was determined using ImageJ software.

9.2.1.8 Enzyme Purification

His_6-tagged ERs and G6PDH were purified using immobilised metal affinity chromatography as follows: *E. coli* BL21 (DE3) cells harbouring ERs and/or G6PDH were resuspended in a minimum volume of imidazole buffer (10 mM) and lysed at 0 °C by sonication for 10 cycles of 15 s on/15 s off. The suspension was then centrifuged (13 000 rpm, 4 °C) in 1.5 mL eppendorfs for 30 min, and the obtained clarified cell lysate was loaded onto the immobilised Ni column. The elution of protein by gravity was performed by applying 2 column volumes of the following imidazole elution buffer with increasing gradient: 10 mM, 50 mM, 100 mM and 500 mM. Each imidazole buffer contained 50 mM Tris HCl (pH 7.4) and 0.5 M NaCl. Protein was identified by mixing

the eluted protein sample (2 µL) with Bradford reagent (150 µL), which resulted in a colour change from brown to blue. Fractions containing the highest protein concentration (most blue) were collected together. Purified enzymes were monitored with SDS-PAGE and ERs were stabilised with $(NH_4)_2SO_4$ at a concentration of 3.2 M. Purified enzymes were stored at 4 °C until a loss of activity was observed. The purified ER concentration was determined by nanodrop absorbance and purified co-expressed ER+G6PDH lysates were determined by a Bradford assay. Immobilised Ni columns were recharged every 3 – 5 uses or when required.

Prior to application in enzymatic assays, the suspension was mixed and the required amount transferred to a 1.5 mL Eppendorf and centrifuged (13 000 rpm, 20 min, 4 °C). The supernatant was discarded and pelleted enzyme re-dissolved in the equivalent amount of buffer (Buffer type corresponding to the assay). The purified enzyme solution was kept on ice until use.

9.2.1.9 Immobilised Nickel Column Recharge

After 3 – 5 uses or when required, immobilised Ni columns were recharged by applying the following solutions: distilled H_2O (2 column volumes), 0.5 M EDTA (pH 7.4) (1 column volume), distilled H_2O (2 column volumes), 1 M NaOH (1 column volume), distilled H_2O (2 column volumes), 100 mM $NiCl_2$ (2 column volumes), distilled H_2O (1 column volume), 20% EtOH (2 column volumes). Immobilised Ni columns were stored in 20% EtOH at 4 °C until use. Prior to application, columns were washed with distilled H_2O (2 column volumes) and 10 mM imidazole buffer (2 column volumes).

9.2.1.10 Bradford Assay

A Bradford assay to determine clarified lysate concentration was performed as follows: Commercial bovine serum albumin standard (2 mg/mL, Sigma Aldrich) was diluted with water to give solutions (200 µL) of known protein concentration (0.1, 0.2, 0.3 and 0.4 mg/mL). The solutions were sampled (100 µL), added to commercial Bradford reagent (900 µL) and incubated for 3 – 5 min. As a blank, distilled water (100 µL) was added to Bradford reagent 900 µL). Clarified lysates (10 µL) were diluted in distilled water (990 µL) for a 100× dilution. Solutions were then sampled (100 µL), added to Bradford reagent (900 µL) and incubated for 3 – 5 min. Absorbance of prepared samples was measured at 600 nm. A calibration curve was given by the protein

standard solutions, with lysate concentration determined and multiplied by 100 to correct for the dilution.

9.2.1.11 Enzyme Concentration

Enzyme concentrations were determined by SDS-PAGE densitometry. Samples were electrophoresed on 4-20% Tris-Glycine gels. The Coomassie stained gel was imaged using ImageJ software to calculate the enzyme band density relative to the total protein density. Total protein concentration was determined by a Bradford assay.

9.2.1.12 Nanodrop Absorbance

Purified protein concentration was determined by absorption measurements at A_{280} using a UV spectrophotometer (**Equation 2**). Protein extinction coefficients and molecular weight were calculated using ExPASy ProtParam online tool.

Purified protein suspensions were evenly dispersed, sampled (100 µL), centrifuged (13 000 rpm, 4 °C) in 1.5 mL eppendorfs for 20 min, had the supernatant removed, and resolubilised in Milli-Q® water (100 µL). Purified enzymes were again sampled and diluted to a total volume of 1 mL. The diluted samples were transferred to a quartz cuvette for analysis. NanoDrop 2000 (Thermo Scientific) was used in cuvette mode.

$$[Protein](mg\ mL^{-1}) = \frac{A_{280} \times dilution\ factor \times Molecular\ weight\ (Da)}{Extinction\ coefficient}$$

Equation 2: Calculation for purified protein (mg/mL) by absorption measurements at A_{280}, protein molecular weight and extinction coefficient.

9.2.2 Ene-Reductase Bioreduction

9.2.2.1 General Experimental with Commercial Recycling System

For small scale ER assays, stock cofactor solutions were made with Tris-HCl buffer (50 mM, pH 7.4) unless otherwise stated. To a 1.5 mL eppendorf, G6PDH (550 U, 35 µL), G6PNa (1 M, 25 µL), $NADP^+$ (15 mM, 50 µL) and alkene substrate (100 mM in DMSO, 25 µL) were added followed by Tris-HCl buffer (50 mM, pH 7.4) and ER to give a total volume of 250 µL with 10% DMSO at final concentrations of G6PDH (20 U), G6PNa (100 mM), $NADP^+$ (3 mM), alkene substrate (10 mM) and ER (0.200 mg mL^{-1}), unless otherwise stated.

9.2.2.2 General Experimental with Co-expressed Recycling System

For small scale ER assays, stock cofactor solutions were made with Tris-HCl buffer (50 mM, pH 7.4) unless otherwise stated. To a 1.5 mL eppendorf, G6PNa (1 M, 25 µL), $NADP^+$ (15 mM, 50 µL) and alkene substrate (100 mM in DMSO, 25 µL) were added followed by Tris•HCl buffer (50 mM, pH 7.4) and co-expressed ER with G6PDH to give a total volume of 250 µL with 10% DMSO at final concentrations of G6PNa (100 mM), $NADP^+$ (3 mM), alkene substrate (10 mM) and co-expressed enzymes (0.600 mg mL^{-1}) unless otherwise stated.

9.2.2.3 General Procedure

Biotranformations were performed in triplicate. Bioreductions were performed in 1.5 mL eppendorfs and incubated at 30 °C and 300 rpm for 20 h unless otherwise specified. Following this 10% TFA (10 µL) was added and samples centrifuged (13 000 rpm, 4 °C) for 10 min. Solutions were transferred to new eppendorfs, extracted with EtOAc (250 µL) and centrifuged (13 000 rpm, 4 °C) for 20 min. The organic phase (125 µL) was dried (Na_2SO_4) and sampled (75 µL) for analysis by chiral GC. For chiral HPLC analysis, the sampled organic phase was evaporated and redissolved in iPrOH/hexane, with the substrate fully solubilised. Samples were stored at -20 °C if they could not be immediately analysed.

Buffers investigated included: Tris-HCl, HEPES, KPi (50 mM) and H_2O. Stock cofactor solutions were made with the buffer under examination. Co-solvents investigated included: DMSO, MeOH, MeCN, CPME and TBME. The final co-solvent concentration for biocatalysis was 10%. ERs co-expressed with the recycling enzyme from pQR1811 included: NCR, pQR1445, pQR1446 and pQR1907. ERs co-expressed with the recycling enzyme pQR1991 included: pQR1446 and pQR1909.[xxxix] ERs requiring commercial G6PDH included: NCR[116], XenA[96], YqjM[146], pQR1440, pQR1445, pQR1446, pQR1907 and pQR1909[59]. Clarified lysate concentrations from 0.2 – 1.2 mg/mL were investigated. A panel of co-solvents including DMSO, MeOH, MeCN, CPME and TBME were investigated, with final concentration in assays at 10%. Temperatures 25 °C, 30 °C, 37 °C and 45 °C were investigated. Substrate loading from

[xxxix] Cloned by Dr Dragana Dobrijevic and expressed by Dr Laure Benhamou

5 – 50 mM was investigated using 250 or 500 mM stock solution with additional co-solvent supplemented to maintain a final co-solvent concentration of 10% (*v*/*v*).

9.2.2.4 Optimised Small Scale NCR+pQR1811 Bioreduction

For small scale NCR+pQR1811 assays, stock cofactor solutions were made with Tris-HCl buffer (50 mM, pH 7.4). To a 1.5 mL eppendorf, G6PNa (1 M, 25 µL), $NADP^+$ (15 mM, 50 µL) and alkene substrate (250 mM in MeOH, 25 µL) were added followed by Tris HCl buffer (50 mM, pH 7.4) and co-expressed NCR+1811 clarified lysates to give a total volume of 250 µL with 10% MeOH at final concentrations of G6PNa (100 mM), $NADP^+$ (3 mM), alkene substrate (25 mM) and co-expressed NCR+pQR1811 (0.600 mg mL^{-1}). Biotranformations were performed in triplicate. Bioreductions were performed in 1.5 mL eppendorfs and incubated at 30 °C and 300 rpm for 20 h.

9.2.2.5 Optimised Preparative Scale NCR+pQR1811 Bioreduction

Preparative scale NCR+pQR1811 biotransformations were optimised at 25 mL with substrate loadings of either 5 mM or 25 mM. Biotransformations were performed at 30 °C, 160 rpm for 20 h with 10% MeOH. Final concentration were G6PNa (100 mM), $NADP^+$ (3 mM), and the alkene substrate **63** (5 mM or 25 mM). Co-expressed clarified lysate NCR+pQR1811 was applied at final concentrations of 0.4 mg/mL.

Single step NCR+pQR1811 bioreduction, and biotransformations for an NCR – 13-TAm cascade were performed in 50 mM HEPES (pH 7.4). Bioreduction for an NCR – Mv-TAm cascade was performed in H_2O (pH 7.4). Single step NCR+pQR1811 bioreduction was followed with a work-up by quenching with 10% TFA, filtration of the denatured enzyme, extraction into ethyl acetate, and drying over $MgSO_4$, afforded the pure product (*S*)-**85** in 96% yield and 99.5% *ee*. The work-up as described was not performed for the ER-TAm cascade, with a work-up performed after transamination as described later.

9.2.3 Transaminase Amination

9.2.3.1 Colorimetric Assay

For TAm assays, stock cofactor solutions were made with Tris-HCl buffer (50 mM, pH 7.4) unless otherwise stated. The assay was performed in a 96 well plate. To each well, a solution of PLP (1.2 mM) and 2-(4-nitrophenyl)ethan-1-amine hydrochloride (31.3 mM) (160 µL) was added, along with Tris•HCl buffer (50 mM, pH 7.4, 10 µL), substrate (100 mM in DMSO, 20 µL), and overexpressed TAm (10 µL) to give a total volume of 200 µL with 10% DMSO at final concentrations of PLP (1.0 mM), 2-(4-nitrophenyl)ethan-1-amine hydrochloride (25 mM), substrate (10 mM) and TAm (1 mg/mL).

Two controls were performed: A positive control with pyruvate (100 mM in Tris•HCl) as the substrate and a negative control of DMSO without any substrate. The plate was incubated at 30 °C and 300 rpm for 24 h. A red precipitate produced from the reaction of by-product 2-(4-nitrophenyl)acetaldehyde with the excess amine donor indicated that the TAm bioconversion had occured.[202]

9.2.3.2 General Experimental Procedure for an α-MBA Assay

For α-MBA assays, stock cofactor solutions were made with Tris-HCl buffer (50 mM, pH 7.4). To a 1.5 mL eppendorf, a solution of PLP (4.8 mM) and (*R*)- or (*S*)-MBA (100 mM) (50 µL) was added, along with the substrate (100 mM in DMSO, 20 µL), and overexpressed TAm (10 µL) to give a total volume of 200 µL with 10% DMSO at final concentrations of PLP (1.2 mM) and (*R*)- or (*S*)-MBA (25 mM), substrate (10 mM) and TAm (1 mg/mL).

Two controls were performed: A positive control with pyruvate (solubilised in 50 mM Tris HCl) as the substrate and a negative control of DMSO without any substrate (10% final co-solvent concentration). Biotransformations were performed in triplicate. The eppendorfs were incubated at 30 °C and 300 rpm for 24 h. Following this 0.1% TFA (100 µL) was added and samples centrifuged (13 000 rpm, 4 °C) for 10 min. Solutions were transferred to new eppendorfs, sampled (250 µL) and diluted with either water or MeCN (250 µL) depending on substrate loading. Samples were analysed by analytical HPLC. Background acetophenone production was removed using the negative control.

Buffers investigated included: Tris-HCl, HEPES, KPi (50 mM) and H_2O. Investigated pH included: 7.5 – 9. Stock cofactor solutions were made with the buffer and pH under examination. Co-solvents investigated included: DMSO, MeOH, MeCN, CPME and TBME. Final co-solvent concentration for biocatalysis was 10%. Literature TAms investigated included: Cv-TAm[182], Mv-TAm[185]. As-TAm[35] and Rh-TAm[261]. Metagenomic TAms investigated included: pQR2189, pQR2191, pQR2208,[60] 1-TAm, 13-TAm, 16-TAm and 23-TAm. Clarified lysate concentration from 0.5 – 1.5 mg/mL was investigated. MBA concentration investigated included: 5 – 125 mM from 100 mM or 250 mM stock solution. Temperatures 30, 37 and 45 °C were investigated. Substrate loading from 5 – 40 mM was investigated using 200 or 400 mM stock solution with additional co-solvent supplemented to maintain final co-solvent concentration of 10% (v/v).

9.2.3.3 General Experimental Procedure for an IPA Assay

For IPA assays, stock cofactor solutions were made with Tris-HCl buffer (50 mM, pH 7.4) unless otherwise stated. To a 1.5 mL eppendorf, a solution of PLP (4.8 mM) (50 µL) and IPA (2 M) (75 µL) was added, along with the substrate (100 mM in DMSO, 20 µL), and overexpressed TAm (10 µL) to give a total volume of 200 µL with 10% DMSO at final concentrations of PLP (1.2 mM), IPA (300 mM), substrate (10 mM) and TAm (1.0 mg/mL).

Two controls were performed: A positive control with pyruvate (100 mM in Tris HCl) as the substrate and a negative control of DMSO without any substrate. Biotransformations were performed in triplicate. The eppendorfs were incubated at 30 °C and 300 rpm for 24 h. Following this 0.1% TFA (100 µL) was added and samples centrifuged (13 000 rpm, 4 °C) for 10 min. Solutions were transferred to new eppendorfs, sampled (250 µL) and diluted with MeCN (250 µL). Samples were analysed by analytical HPLC.

Buffers investigated included: Tris-HCl, HEPES, KPi (50 mM) and H_2O. Investigated pH included: 7.5 – 9. Stock cofactor solutions were made with the buffer and pH under examination. Co-solvents investigated included: MeOH, MeCN, and TBME. Final co-solvent concentration for biocatalysis was 10% *v*/*v*. Literature TAms investigated included: Cv-TAm[182] and Mv-TAm[185]. Metagenomic TAms investigated included: 13-TAm. IPA concentration investigated included: 25 – 1000 mM from 1 M

or 2 mM stock solution. Temperatures 30, 37 and 45 °C were investigated. Substrate loading from 5 – 40 mM was investigated using 200 or 400 mM stock solution with additional co-solvent supplemented to maintain final co-solvent concentration of 10% (v/v).

9.2.3.4 Optimised Small Scale 13-TAm Amination

Optimised small scale transamination with 13-TAm employed an α-MBA assay. Stock cofactor solutions were made with Tris-HCl buffer (50 mM, pH 7.4). To a 1.5 mL eppendorf, a solution of PLP (4.8 mM) and (*S*)-MBA (100 mM) (50 µL) was added, along with the substrate (50 mM in MeOH, 20 µL), and overexpressed 13-TAm (10 µL) to give a total volume of 200 µL with 10% MeOH at final concentrations of PLP (1.2 mM) and (*S*)-MBA (20 mM), substrate (5 mM) and 13-TAm (0.5 mg/mL). Biotransformations were performed in triplicate. The eppendorfs were incubated at 30 °C and 300 rpm for 24 h.

9.2.3.5 Optimised Small Scale Mv-TAm Amination

Optimised small scale transamination with Mv-TAm employed an IPA assay. Stock cofactor solutions were made with Tris-HCl buffer (50 mM, pH 9). To a 1.5 mL eppendorf, a solution of PLP (4.8 mM) (50 µL) and IPA (2 M) (75 µL) was added, along with the substrate (250 mM in MeOH, 20 µL), and overexpressed Mv-TAm (10 µL) to give a total volume of 200 µL with 10% MeOH at final concentrations of PLP (1.2 mM), IPA (750 mM), substrate (*S*)-**85** (25 mM) and Mv-TAm (0.5 mg/mL). Biotransformations were performed in triplicate. The eppendorfs were incubated at 37 °C and 300 rpm for 24 h.

9.2.3.6 Optimised Preparative Scale 13-TAm Amination and NCR – 13-TAm Cascade

Preparative scale transamination with (*S*)-selective 13-TAm was optimised at 5 mM substrate loading to 25 mL, 30 °C, 160 rpm for 24 h in 50 mM HEPES (pH 7.4) with 10% MeOH. Final concentrations were PLP (1.2 mM), α-(*S*)-MBA (20 mM, 4 eq.), substrate (*S*)-**85** (5 mM) and 13-TAm (0.5 mg/mL).

When performed as part of a two step, one pot NCR – 13-TAm cascade, final concentrations were PLP (0.96 mM), α-(*S*)-MBA (20 mM, 4 eq.), and 13-TAm clarified lysate (0.5 mg/mL) in 50 mM HEPES (pH 9) with 7.9% MeOH at a total volume of

31.771 mL. Work-up proceeded by quenching with MeOH (50 mL), centrifugation (4 650 ×g, 22 ºC 30 min), pooling of the supernatant and removal of MeOH *in vacuo*. The solution was further concentrated under reduced pressure and lyophilised. A solution of 1:1 H_2O:MeCN was added, and the crude product passed through a syringe filter and purified by preparative HPLC (***Method J***). The chiral amino alcohol product (2*S*,3*R*)-**100** was obtained in 30% isolated yield. The *dr* from the NCR – 13-TAm cascade was determined to be 97:3 *dr*[xl] by NMR analysis of 2-aminooxazole (2*S*,4*R*)-**37**.

9.2.3.7 Optimised Preparative Scale Mv-TAm Amination and NCR – Mv-TAm Cascade

Preparative scale transamination with (*R*)-selective Mv-TAm was optimised at 25 mM substrate loading to 25 mL, 37 °C, 160 rpm for 24 h in H_2O (pH 9) with 10% MeOH. Final concentrations were PLP (1.2 mM), IPA (1.125 M, 45 eq.), substrate (*S*)-**85** (25 mM) and Mv-TAm (0.5 mg/mL).

When performed as part of a two step, one pot NCR – Mv-TAm cascade, the IPA (4 M, pH 9) and PLP were added and the pH adjusted to 9 prior to the addition of the Mv-TAm clarified lysate. Final concentrations were PLP (1.2 mM), IPA (0.860 mM, 45 eq.), and Mv-TAm clarified lysate (0.5 mg/mL) in H_2O (pH 9) with 7.7% MeOH at a total volume of 32.677 mL. Work-up proceeded by quenching with MeOH (50 mL), centrifugation (4 650 ×g, 22 ºC 30 min), pooling of the supernatant and removal of MeOH *in vacuo*. The remaining aqueous solution was basified to pH 10 and concentrated under reduced pressure for the removal of the excess IPA. The solution was further concentrated under reduced pressure and lyophilised. Organic solvent (MeOH) was added and the suspension filtered through Celite™, with the filtrate solvent removed *in vacuo*. A solution of 1:1 H_2O:MeCN was added, and the crude product passed through a syringe filter and purified by preparative HPLC (***Method J***). The pure chiral amino alcohol product (2*S*,3*S*)-**100** was obtained in 32% isolated yield. The *dr* from the NCR – Mv-TAm cascade was determined to be 93:7 *dr*[xli] by NMR analysis of 2-aminooxazole (2*S*,4*S*)-**37**.

[xl] Determined using ^{1}H NMR, 97:3 *dr* ratio of (2*S*,4*R*):(2*S*,4*S*).
[xli] Determined using ^{1}H NMR, 93:7 *dr* ratio of (2*S*,4*S*):(2*S*,4*R*).

9.3 Analytical Methods

9.3.1 Chromatographic Achiral Methods

Quantitative analysis of TAm bioconversion was performed by analytical reverse phase HPLC using Agilent 1260 Infinity with Ace 5 C18 column (150 × 4.6 mm). Conversion yields and substrate conversions are calculated with respect to chemical standards. Elution was performed with a linear gradient of MeCN and H_2O with 0.1% TFA. The injection volume was 10 µL and the column temperature 30 °C.

9.3.1.1 Method A

UV detection of acetophenone production at 254 nm using a linear gradient of 15 – 72% MeCN over 9 min at 1 mL/min.

9.3.1.2 Method B

UV detection of substrate depletion at 214 nm using a linear gradient of 8 – 90% MeCN over 9 min at 0.8 mL/min.

9.3.1.3 Method C

UV detection of amino alcohol production at 214 nm using a linear gradient of 15 – 50% MeCN over 20 min at 0.8 mL/min.

9.3.2 Chromatographic Chiral Methods

Quantitative analysis of ER bioreduction was performed by chiral GC and chiral HPLC. GC analysis was performed by Agilent 7820A GC System with Supleco Beta Dex 225 capillary GC column 30 m × 250 µm × 0.25 µm and flame ionization detector at 300 °C. A linear temperature gradient and injection volume of 5 µL were applied. Chiral HPLC analysis was perfomed by HP Series 1100 HPLC with Chiralpak AD-H column (5 µm particle size, 4.5 mm × 250 mm).

9.3.2.1 Method D

Initial temperature 90 °C held for 1 min, ramp 5 °C/min to 150 °C, ramp 20 °C/min to 210 °C, hold 2 min.

9.3.2.2 Method E

Initial temperature 70 °C held for 1 min, ramp 5 °C/min to 150 °C, ramp 20 °C/min to 210 °C, hold 2 min.

9.3.2.3 Method F

Using Chiralpak AD-H column, UV detection at 214 nm and isocratic 1% ^{i}PrOH/hexane at 1 mL/min over 20 min.

9.3.2.4 Method G

Using Chiralpak AD-H column, UV detection at 214 nm and isocratic 1% ^{i}PrOH/hexane at 1 mL/min over 60 min.

9.3.2.5 Method H

Using Chiralpak AD-H column, UV detection at 214 nm and isocratic 1% ^{i}PrOH/hexane at 1 mL/min over 80 min.

9.3.2.6 Method I

Using Chiralpak AD-H column, UV detection at 214 nm and isocratic 5% ^{i}PrOH/hexane at 1 mL/min over 80 min.

9.4 Preparative HPLC Purification Method

9.4.1 Purification

Preparative scale purifications were performed by preparative reverse phase HPLC using an Agilent 1260 Infinity with Supelco Discovery®BIO Wide Pore C18-10 column (25 cm × 21.2 mm, 10 µm). Elution was performed with a linear gradient of MeCN and H_2O, both with 0.1% TFA. Injection volume was up to 900 µL and the column was at room temperature.

9.4.1.1 Method J

UV detection of the amino alcohol product at 214 nm using a linear gradient of 5 – 95% MeCN over 27 min at 8 mL/min.

9.5 Synthetic Chemistry

9.5.1 General Procedures

9.5.1.1 General Procedure 1: Acid Catalysed Aldol Condensation

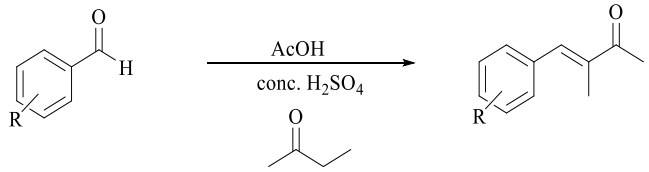

Scheme 68: General scheme for the acid catalysed aldol condensation.

With stirring, conc. H_2SO_4 (98%, 0.5 mL) was added dropwise to a solution of aldehyde (500 mg, 1 eq.) and 2-butanone (1.2 eq.) in AcOH (9.5 mL). The solution was stirred for 18 h prior to the addition of ice cold water (7.5 mL), neutralisation with aq. NaOH (12 M) and extraction with EtOAc (3 × 10 mL). The organic layer was washed subsequently with water (30 mL) and brine (30 mL), dried ($MgSO_4$) and filtered. The solvent was removed *in vacuo* and crude product subjected to flash column chromatography to afford the title compound. The general procedure was scaled when required, as described in section 9.5.2.

9.5.1.2 General Procedure 2: α-Hydroxylation

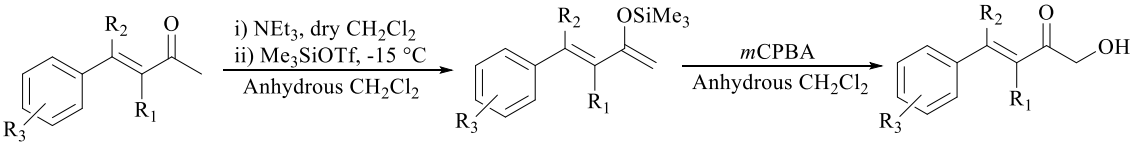

Scheme 69: General scheme for the α-hydroxylation of enones.

With stirring, triethylamine (1.5 eq.) was added to a solution of the enone (3.50 g, 1 eq.) in anhydrous CH_2Cl_2 (42 mL) under Ar. The solution was cooled to -15 °C and trimethylsilyl trifluoromethanesulfonate (1.3 eq.) was added dropwise with stirring. The solution was allowed to stir for 3 h before being quenched with sat. $NaHCO_3$, extracted with CH_2Cl_2 (3 × 40 mL), dried ($MgSO_4$) and the solvent removed *in vacuo* to afford the crude silyl enol ether. Anhydrous CH_2Cl_2 (70 mL) was added and *m*CPBA (2.5 eq.) added at -15 °C. The reaction mixture was then stirred for 18 h at room temperature. The solid was filtered off, 10% $NaHSO_3$ (w/v) (50 mL) added to the filtrate and the organic and aqueous layers separated. The organic layer was thoroughly washed with sat. $NaHCO_3$ (5 × 50 mL) and aqueous layers back extracted with CH_2Cl_2. Combined organic layers were dried ($MgSO_4$) and filtered. The solvent was removed

in vacuo and crude product subjected to flash column chromatography to afford the title compound. The general procedure was scaled when required, as described in section 9.5.2.

9.5.1.3 General Procedure 3: Chemical Reduction

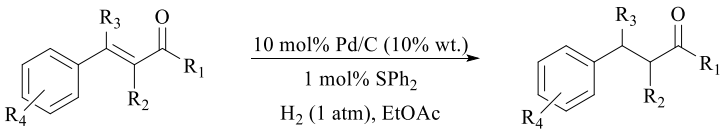

Scheme 70: General scheme for the chemical reduction of enals and enones.

Three cycles of vacuum/Ar provided the suspension of enal/enone (100 mg, 1 eq.), 10 mol% palladium on carbon (10% wt.) and diphenylsulfide (0.01 eq.) in EtOAc (5 mL) with an inert atmosphere. Vacuum was applied and hydrogen gas bubbled directly into the reaction mixture for 1 min. The reaction mixture was left to stir vigorously under a hydrogen atmosphere for 18 h and was then filtered through Celite™, had the solvent removed *in vacuo* and, when required, was subjected to flash column chromatography to yield the title compound. The general procedure was scaled when required, as described in section 9.5.2.

9.5.1.4 General Procedure 4: $TiCl_4$ Mediated Aldol Condensation

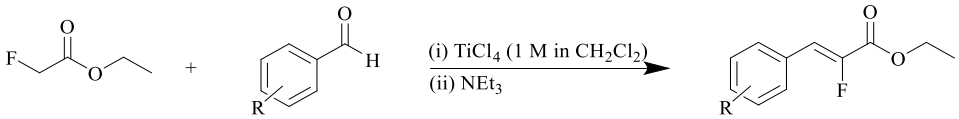

Scheme 71: General scheme for the $TiCl_4$ mediated aldol condensation with ethyl fluoroacetate and an aldehyde.

The aldehyde (500 mg, 1 eq.) and ethyl fluoroacetate (1.1 eq.) were solubilised in anhydrous CH_2Cl_2 (6 mL) under Ar. With stirring, a 1.0 M solution of $TiCl_4$ in CH_2Cl_2 (1.2 eq.) was added dropwise over 10 min. The reaction was stirred for 1 h prior to the dropwise addition on triethylamine (2 eq.) over 10 min, with the reaction temperature maintained under 30 ºC. The reaction solution was then stirred for 2 h, diluted with CH_2Cl_2 (10 mL), and washed with 1 M HCl (15 mL), water (15 mL), and brine (15 mL). The organic layer was dried ($MgSO_4$), filtered and had the solvent removed *in vacuo*. The crude product was subjected to flash column chromatography to afford the title compound.

9.5.1.5 General Procedure 5: Horner-Wadsworth-Emmons Reaction

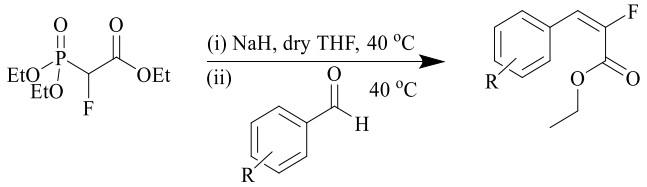

Scheme 72: General scheme for the Horner-Wadsworth-Emmons reaction with diethoxyphosphoryl-2-fluoroacetate, NaH, and an aldehyde.

Under anhydrous conditions and with stirring, diethoxyphosphoryl-2-fluoroacetate (1.1 eq.) was added dropwise to a suspension of NaH, 60% mineral dispersion (1 eq.) in dry THF (4.5 mL) at 0 ºC. The reaction mixture was stirred at 40 ºC for 1 h prior to the portion wise addition of the aldehyde (250 mg, 1 eq.) at 0 ºC. The reaction mixture was stirred for 18 h at 40 ºC and then quenched by addition of H_2O. The aqueous phase was extracted with Et_2O (3 × 10 mL), dried ($MgSO_4$), filtered and had the solvent removed *in vacuo*. The crude product subjected to flash column chromatography to yield the title compound.

9.5.1.6 General Procedure 6: Transesterification

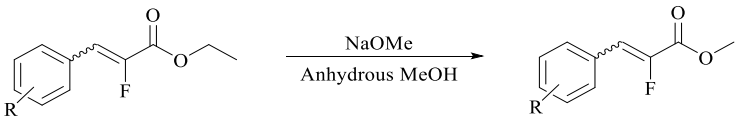

Scheme 73: General scheme for the transesterification of ethyl esters to methyl esters using sodium methoxide in anhydrous methanol.

The reaction was performed under anhydrous conditions. Sodium methoxide (1.2 eq.) was added to a solution of the ethyl ester (50 mg, 1 eq.) in anhydrous MeOH (5 mL) under an inert atmosphere. The reaction mixture was stirred until completion by TLC analysis. Celite™ was then added, and the solvent removed *in vacuo*. The crude product was subjected to flash column chromatography to yield the title compound unless otherwise stated. The reaction was scaled as required, as described in section 9.5.2.

9.5.2 Chemical Procedure

3-Methyl-4-phenylbutan-2-one (8a)

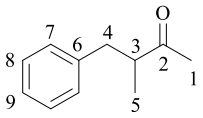

Following ***General Procedure 3***, compound **7a** (250 mg, 1 eq.) was chemically reduced.

Flash column chromatography (0 – 30% EtOAc/pet. ether) yielded title compound **8a** (139 mg, 55%) as a yellow oil:

R_f 0.41 (5% EtOAc/pet. ether);

υ_{max} (film) 2970 (CH sp^3), 1710 (C=O), 1453 (C=C aromatic) cm^{-1};

^{1}H NMR (700 MHz, $CDCl_3$) δ = 7.26 - 7.32 (2H, m, 8-H), 7.19 - 7.23 (1H, m, 9-H), 7.16 (2H, s, 7-H), 3.01 (1H, dd, *J* = 13.7 Hz, *J* = 6.8 Hz, 4-*H*H), 2.84 (1H, dqd, *J* = 7.8 Hz, *J* = 7.0 Hz, *J* = 6.8 Hz, 3-H), 2.57 (1H, dd, *J* = 13.7 Hz, *J* = 7.8 Hz, 4-H*H*), 2.10 (3H, s, 1-H), 1.10 (3H, d, *J* = 7.0 Hz, 5-H);

^{13}C NMR (176 MHz, $CDCl_3$) δ = 212.2 (C-2), 139.6 (C-6), 128.9 (C-7), 128.4 (C-8), 126.2 (C-9), 48.8 (C-3), 38.9 (C-4), 28.8 (C-1), 16.2 (C-5);

m/z [LRMS, ESI] (relative intensity, M) 162 (46, $[M+H]^+$), 147 (34, $[M-H_2O+H]^+$), 119 (21, $[M-CHOCH_3+H]^+$), 91 (100, $[M-C_5H_{10}O+H]^+$);

Data was in agreement with the literature.[303]

(*R*)-4-((*S*)-1-phenylpropan-2-yl)-4,5-dihydrooxazol-2-amine [(2*R*,4*S*)-37]

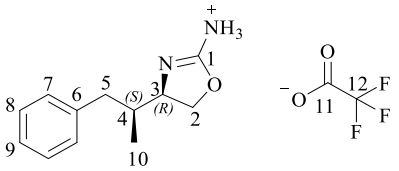

Potassium carbonate (4.5 mg, 33 µmol, 1.2 eq) was added to (2*R*,3*S*)-**100** (8 mg, 27 µmol, 1 eq.) in H_2O (1.6 mL) and stirred for 1 h prior to being lyophilised.

The reaction was performed under anhydrous conditions. A solution of cyanogen bromide (3.5 mg, 33 µmol, 1.2 eq.) in anhydrous THF (0.4 mL) was added with stirring to a solution of potassium carbonate (5.7 mg, 41 µmol, 1.5 eq.) and crude lyophilised (2*R*,3*S*)-**100** (5 mg, 27 µmol, 1 eq.) in anhydrous THF (1.6 mL) under an inert atmosphere. The reaction mixture was stirred for 18 h, diluted with EtOAc (6 mL), washed with H_2O (6 mL) and the aqueous phase back extracted with EtOAc (3 × 5 mL).

The combined organic layers were washed with brine (10 mL), dried ($MgSO_4$), filtered, and the solvent removed *in vacuo*. The crude product was resolubilised in 1:1 AcCN:H_2O (1 mL), passed through a syringe filter, and purified by preparative HPLC to yield title compound (2*R*,4*S*)-**37** (1.3 mg, 15%) as a fine white solid:

R_t 21.9 min (***Method J***);

$[\alpha]_D^{20}$ +18 (c. 0.1, H_2O);

υ_{max} (solid) 3085 (NH_2), 2977 (CH sp^3), 1721 (C=N), 1673 (C=O), 1536 (C=C aromatic) cm^{-1};

^{1}H NMR (600 MHz, D_2O) δ = 7.39 (2H, dd, *J* = 8.0 Hz, *J* = 6.9 Hz, 8-H), 7.31 (1H, d, *J* = 8.0 Hz, 9-H), 7.29 (2H, d, *J* = 6.9 Hz, 7-H), 4.78 (1H, dd, *J* = 9.2 Hz, *J* = 9.1 Hz, 2-*H*H), 4.61 (1H, dd, *J* = 9.2 Hz, *J* = 6.0 Hz, 2-H*H*), 4.22 (1H, ddd, *J* = 9.1 Hz, *J* = 6.0 Hz, *J* = 5.5 Hz, 3-H), 2.70 (1H, dd, *J* = 13.7 Hz, *J* = 6.5 Hz, 5-*H*H), 2.56 (1H, dd, *J* = 13.7 Hz, *J* = 8.5 Hz, 5-H*H*), 2.13 (1H, dqdd, *J* = 8.5 Hz, *J* = 6.8 Hz, *J* = 6.5 Hz, *J* = 5.5 Hz, 4-H), 0.91 (3H, d, *J* = 6.8 Hz, 10-H);

^{13}C NMR (151 MHz, D_2O) δ = 163.5 (C-1), 163.7 (q, *J* = 35.5 Hz, C-11), 140.4 (C-6), 129.8 (C-7), 129.3 (C-8), 127.1 (C-9), 116.0 (q, *J* = 290.0 Hz, C-12), 74.6 (C-2), 60.2 (C-3), 38.8 (C-4), 38.7 (C-5), 14.2 (C-10);

m/z [HRMS, ESI] Calcd. $(C_{12}H_{16}N_2O+H)^+$ 205.1335, found 205.1333;

(*S*)-4-((*S*)-1-phenylpropan-2-yl)-4,5-dihydrooxazol-2-amine [(2*S*,4*S*)-37]

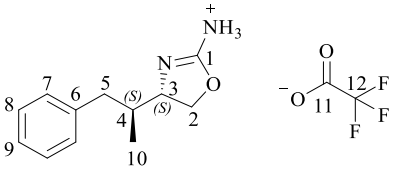

Potassium carbonate (6 mg, 41 µmol, 1.2 eq) was added to (2*S*,3*S*)-**100** (10 mg, 34 µmol, 1 eq.) in H_2O (2 mL) and stirred for 1 h prior to being lyophilised.

The reaction was performed under anhydrous conditions. A solution of cyanogen bromide (4 mg, 41 µmol, 1.2 eq.) in anhydrous THF (0.4 mL) was added with stirring to a solution of potassium carbonate (7 mg, 51 µmol, 1.5 eq.) and crude lyophilised AK8-50 (6 mg, 34 µmol, 1 eq.) in anhydrous THF (1.6 mL) under an inert atmosphere. The reaction mixture was stirred for 18 h, diluted with EtOAc (6 mL), washed with H_2O (6 mL) and the aqueous phase back extracted with EtOAc (3 × 5 mL). The combined organic layers were washed with brine (10 mL), dried ($MgSO_4$), filtered, and

the solvent removed *in vacuo*. The crude product was resolubilised in 1:1 AcCN:H_2O (1 mL), passed through a syringe filter, and purified by preparative HPLC (***Method J***) to yield title compound (2*S*,4*S*)-**37** (2 mg, 18%) as a fine white solid:

R_t 21.7 min (***Method J***);

$[\alpha]_D^{20}$ – 4 (c. 0.1, H_2O);

υ_{max} (solid) 3029 (NH_2), 2977 (CH sp^3), 1715 (C=N), 1670 (C=O), 1531 (C=C aromatic) cm^{-1};

^{1}H NMR (600 MHz, D_2O) δ = 7.29 (2H, dd, *J* = 7.5 Hz, *J* = 7.1 Hz, 8-H), 7.21 (1H, d, *J* = 7.5 Hz, 9-H), 7.19 (2H, d, *J* = 7.1 Hz, 7-H), 4.73 (1H, dd, *J* = 9.2 Hz, *J* = 9.0 Hz, 2-*H*H), 4.57 (1H, dd, *J* = 9.2 Hz, *J* = 6.2 Hz, 2-H*H*), 4.13 (1H, ddd, *J* = 9.0 Hz, *J* = 6.2 Hz, *J* = 5.9 Hz, 3-H), 2.69 (1H, dd, *J* = 13.5 Hz, *J* = 5.5 Hz, 5-*H*H), 2.36 (1H, dd, *J* = 13.5 Hz, *J* = 9.3 Hz, 5-H*H*), 2.06 (1H, dquindd, *J* = 9.3 Hz, *J* = 6.8 Hz, *J* = 5.9 Hz, *J* = 5.5 Hz, 4-H), 0.76 (3H, d, *J* = 6.8 Hz, 10-H);

^{13}C NMR (151 MHz, D_2O) δ = 163.5 (C-5), 163.7 (q, *J* = 34 Hz, C-11), 140.3 (C-6), 129.9 (C-7, 13), 129.3 (C-8), 127.1 (C-9), 117.0 (q, *J* = 290.8 Hz, C-12), 73.6 (C-2), 60.3 (C-3), 38.3 (C-4), 38.2 (C-5), 13.6 (C-10);

m/z [HRMS, ESI] Calcd. $(C_{12}H_{16}N_2O+H)^+$ 205.1335, found 205.1332;

(*E*)-3-Phenylbut-2-en-1-ol (39)

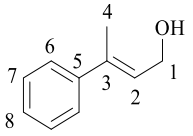

The reaction was performed under anhydrous conditions. Ethyl (*E*)-3-phenylbut-2-enoate (200 µL, 1.05 mmol) was solubilised in dry THF (2 mL) and cooled to -78 °C. With stirring DIBAL-H (1.0 M in THF, 2.63 mL, 2.63 mmol) was added dropwise over 5 min. The solution was stirred for 30 min at -78 °C followed by a further 10 min at 0 °C. At this temperature, the reaction solution was quenched by dropwise addition of 2 M HCl. The aqueous layer was separated from the organic layer and extracted with EtOAc (3 × 15 mL). Combined organic layers were dried ($MgSO_4$), filtered, and the solvent removed *in vacuo* to afford the title compound **39** (153 mg, 98%) as a colourless oil:

R_f 0.31 (20% EtOAc/pet. ether);

υ_{max} (oil) 3306 (OH), 2915 (CH sp^3), 1443 (C=C aromatic), cm^{-1};

^{1}H NMR (700 MHz, $CDCl_3$) δ = 7.42 (2H, d, *J* = 7.6 Hz, 6-H), 7.33 (2H, dd, *J* = 7.6 Hz, *J* = 7.6 Hz, 7-H), 7.28 (1H, d, *J* = 7.6 Hz, 8-H), 5.99 (1H, tq, *J* = 6.7 Hz, *J* = 1.2 Hz, 2-H), 4.36 (2H, d, *J* = 6.7 Hz, 1-H), 2.08 (3H, d, *J* = 1.2 Hz, 4-H);

^{13}C NMR (176 MHz, $CDCl_3$) δ = 142.8 (C-3), 137.6 (C-5), 128.2 (C-7), 127.2 (C-8), 126.5 (C-2), 125.7 (C-6), 59.8 (C-1), 15.9 (C-4);

[LRMS, EI] (relative intensity, M) 164 (31, $[M+NH_4]^+$), 148 (22, $[M]^+$), 131 (100, $[M-H_2O+H]^+$);

Data was in agreement with the literature.[304]

(*E*)-3-Phenylbut-2-enal (40)

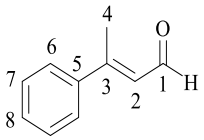

The reaction was performed under anhydrous conditions. Compound **39** (94 mg, 0.636 mmol), activated manganese (IV) oxide, 85% (325 mg, 3,18 mmol, 5 eq.), and anhydrous CH_2Cl_2 (2 mL) were added and the mixture left to stir for 6.5 h. The suspension was then filtered through Celite™, washed with CH_2Cl_2 and had the solvent removed *in vacuo*. The crude product was subjected to flash column chromatography (5 – 20%) EtOAc/pet. ether to afford the title compound **45** (59 mg, 64%) as a yellow oil:

R_f 0.29 (10% EtOAc/pet. ether);

υ_{max} (oil) 2920 (CH sp^3), 1655 (C=O), 1621 (C=C), 1444 (C=C aromatic) cm^{-1};

^{1}H NMR (700 MHz, $CDCl_3$) δ = 10.19 (1H, d, *J* = 7.7 Hz, 1-H), 7.54 - 7.57 (2H, m, 6-H), 7.43 - 7.44 (2H, m, 7-H), 7.41 - 7.43 (1H, m, 8-H), 6.41 (1H, dq, *J* = 7.7 Hz, *J* = 1.2 Hz, 2-H), 2.58 (3H, d, *J* = 1.2 Hz, 4-H);

^{13}C NMR (176 MHz, $CDCl_3$) δ = 191.2 (C-1), 157.6 (C-3), 140.5 (C-5), 130.1 (C-8), 128.7 (C-7), 127.2 (C-2), 126.2 (C-6), 16.4 (C-4);

m/z [LRMS, CI] (relative intensity, M) 164 (100, $[M+NH_4]^+$), 145 (47, $[M-H]^+$);

Data was in agreement with the literature.[305]

(*E*)-4-Phenylbut-3-en-2-one (41)

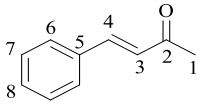

To a solution of benzaldehyde (0.500 mmol) in (1:1) acetone:water (10 mL) was added BSA Fraction V (540 mg) and the mixture incubated (45 °C, 180 rpm) for 72 h. BSA was then filtered off and washed with acetone, and the filtrates concentrated under reduced pressure leaving water. The aqueous phase was extracted with EtOAc (4 × 5 mL), the collected organic layers dried ($NaCO_3$), filtered, and the solvent removed *in vacuo*. The crude product was subjected to flash column chromatography (10% EtOAc/pet. ether) to afford title compound **41** (0.0427 g, 58%) as a white solid:

m.p. 38 – 40 °C (lit. m.p. 38 – 40 °C)[306];

υ_{max} (solid) 2919 (CH sp^3), 1664 (CO), 1356 (C=C aromatic) cm^{-1};

^{1}H NMR (700 MHz, $CDCl_3$) δ = 7.55 (2H, m, 6-H), 7.52 (1H, d, *J* = 16.2 Hz, 4-H), 7.38 - 7.43 (3H, m, 7-H and 8-H), 6.73 (1H, d, *J* = 16.2 Hz, 3-H), 2.39 (3H, s, 1-H);

^{13}C NMR (176 MHz, $CDCl_3$) δ = 198.4 (C-2), 143.4 (C-4), 134.4 (C-5), 130.5, 128.9, 128.2, 127.1, 27.5 (C-1);

m/z [LRMS, CI] (relative intensity, M) 164 (68 $[M+NH_4]^+$), 147 (100, $[M+H]^+$); [HRMS, CI] Calcd. $(C_{10}H_{10}O+H)^+$ 147.0804, found 147.0804;

(*E*)-4-Phenylpent-3-en-2-one (42)

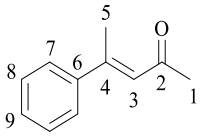

At -29 °C and with stirring, methylmagnesium bromide solution (1.0 M in THF) (35.6 mL, 35.7 mmol) was slowly added to compound **50** (5.63 g, 27.4 mmol). The solution was stirred at 0 °C for 30 min, quenched with sat. NH_4Cl (30 mL), extracted with EtOAc (3 × 60 mL), washed with brine (200 mL), dried ($MgSO_4$), and filtered. The solvent was removed *in vacuo* and the crude product subjected to flash column chromatography (0 – 30% EtOAc/pet. ether) to yield title compound **40** (3.77 g, 86%) as a yellow oil:

υ_{max} (film) 2996 (CH sp^3), 1672 (C=O), 1443 (C=C aromatic) cm^{-1};

^{1}H NMR (600 MHz, $CDCl_3$) δ = 7.47 - 7.52 (2H, m, 8-H), 7.37 - 7.41 (3H, m, 7-H and 9-H), 6.52 (1H, d, *J* = 1.2 Hz, 3-H), 2.55 (3H, d, *J* = 1.2 Hz, 5-H), 2.30 (3H, s, 1-H);

^{13}C NMR (151 MHz, $CDCl_3$) δ = 198.9 (C-2), 153.8 (C-6), 142.5 (C-4), 129.0 (C-9), 128.5 (C-7), 126.4 (C-8), 124.5 (C-3), 32.2 (C-1), 18.3 (C-5);

m/z [HRMS, ESI] Calcd. $(C_{11}H_{12}O+H)^+$ 161.0961, found 161.0960;

Data was in agreement with the literature.[234]

(*E*)-4-(4-Methoxyphenyl)-3-methylbut-3-en-2-one (46)

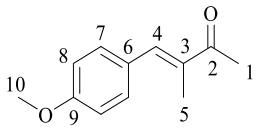

Following ***General Procedure 1***, the aldol condensation with *p*-anisaldehyde (500 mg, 3.67 mmol, 1 eq.) and 2-butanone (0.395 mL, 4.41 mmol, 1.2 eq.) was performed.

Following flash column chromatography (5 – 20% EtOAc/pet. ether) title compound **46** (473 mg, 68%) was afforded as a yellow oil:

R_f 0.34 (20% EtOAc/pet. ether);

υ_{max} (oil) 2958 (CH sp^3), 1655 (C=O), 1508 (C=C), 1314 (C=C aromatic) cm^{-1};

^{1}H NMR (700 MHz, $CDCl_3$) δ = 7.46 (1H, s, 4-H), 7.40 (2H, d, *J* = 8.7 Hz, 8-H), 6.93 (2H, d, *J* = 8.7 Hz, 7-H), 3.83 (3H, s, 10-H), 2.43 (3H, s, 1-H), 2.06 (3H, s, 5-H);

^{13}C NMR (176 MHz, $CDCl_3$) δ = 200.1 (C-2), 159.8 (C-9), 139.5 (C-1), 135.7 (C-3), 131.5 (C-8), 128.3 (C-6), 113.8 (C-7), 55.2 (C-10), 25.6 (C-1), 12.8 (C-5);

m/z [LRMS, ES+] (relative intensity, M) 191 (39, $[M+H]^+$), 173 (100, $[M-H_2O+H]^+$, 158.3 (83, $[M-CH_3OH+H]^+$; [HRMS, ESI] Calcd. $(C_{12}H_{14}O_2+H)^+$ 191.1067, found 191.1067;

Data was in agreement with the literature.[307]

(*E*)-4-(2-Methyl-3-oxobut-1-en-1-yl)benzonitrile (47)

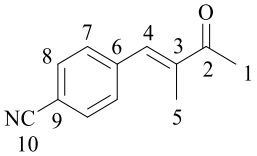

Following ***General Procedure 1***, aldol condensation with 4-formylbenzonitrile (500 mg, 3.81 mmol, 1 eq.) and 2-butanone (0.410 mL, 4.58 mmol, 1.2 eq.) was performed.

Following flash column chromatography (10 – 30% EtOAc/pet. ether), title compound **47** (449 mg, 64%) was afforded as a white solid:

R_f 0.30 (20% EtOAc/pet. ether);

m.p. 94 – 96 °C;

υ_{max} (solid) 2922 (CH sp^3), 2222 (CN), 1656 (C=O), 1389 (C=C aromatic) cm^{-1};

^{1}H NMR (700 MHz, $CDCl_3$) δ = 7.70 (2H, d, *J* = 8.3 Hz, 8-H), 7.50 (2H, d, *J* = 8.3 Hz, 7-H), 7.47 (1H, s, 4-H), 2.47 (3H, s, 1-H), 2.03 (3H, s, 5-H);

^{13}C NMR (176 MHz, $CDCl_3$) δ = 199.6 (C-2), 140.5 (C-6), 140.1 (C-3), 136.9 (C-4), 132.1 (C-8), 130.0 (C-9), 118.4 (C-10), 111.8 (C-9), 25.9 (C-1), 13.1 (C-5);

m/z [LRMS, ESI] (relative intensity, M) 250 (100, $[M+CH_3CN+Na]^+$), 228 (78, $[M+CH_3CN+H]^+$); [HRMS, ESI] Calcd. $(C_{12}H_{11}NO+H)^+$ 186.0913, found 186.0914;

Data was in agreement with the literature.[307]

(*E*)-4-(3-Fluorophenyl)-3-methylbut-3-en-2-one (48)

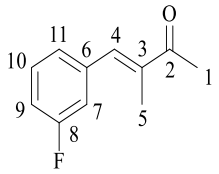

Following ***General Procedure 1***, aldol condensation with 4-fluorobenzaldehyde (500 mg, 4.03 mmol, 1 eq.) and 2-butanone (0.433 mL, 4.83 mmol, 1.2 eq.) was performed.

Following flash column chromatography (0 – 30% EtOAc/pet. ether) title compound **48** (390 mg, 54%) was afforded as a yellow oil:

R_f 0.31 (20% EtOAc/pet. ether);

υ_{max} (film) 2967 (CH sp^3), 1662 (C=O), 1578 (C=C), 1363 (C=C aromatic) cm^{-1};

^{1}H NMR (700 MHz, $CDCl_3$) δ = 7.46 (1H, d, *J* = 1.4 Hz, 4-H), 7.38 (1H, ddd, *J* = 8.2 Hz, *J* = 7.7 Hz, *J* = 6.0 Hz, 10-H), 7.19 (1H, d, *J* = 7.7 Hz, 11-H), 7.13 (1H, dt, *J* = 10.0 Hz, *J* = 2.1 Hz, 7-H), 7.05 (1H, ddd, *J* = 8.8 Hz, *J* = 8.2 Hz, *J* = 2.1 Hz, 9-H), 2.47 (3H, s, 1-H), 2.05 (3H, d, *J* = 1.4 Hz, 5-H);

^{13}C NMR (176 MHz, $CDCl_3$) δ = 200.0 (C-2), 162.6 (d, *J* = 246.81 Hz, C-8), 138.7 (d, *J* = 4.96 Hz, C-3), 138.0 (d, *J* = 2.29 Hz, C-4), 138.0 (d, *J* = 4.96 Hz, C-6), 129.9 (d, *J* = 8.01 Hz, C-10), 125.4 (d, *J* = 3.05 Hz, C-11), 116.2 (d, *J* = 21.74 Hz, C-7), 115.4 (d, *J* = 21.74 Hz, C-9), 25.9 (C-1), 12.9 (C-5);

^{19}F NMR (659 MHz, $CDCl_3$) δ = -122.69 (1F, m, 8-F);

m/z [LRMS, ES+] (relative intensity, M) 196 (41, $[M+NH_4]^+$); [HRMS, ESI] Calcd. $(C_{11}H_{11}FO+H)^+$ 179.0867, found 179.0867;

(*E*)-*N*-Methoxy-*N*-methyl-3-phenylbut-2-enamide (50)

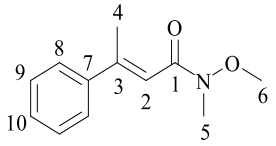

At -5 °C and with stirring, isopropylmagnesium chloride solution (2.0 M in THF) (47.3 mL, 94.6 mmol) was slowly added to a solution of ethyl trans-ß-methylcinnamate (6.00 g, 31.5 mmol) and *N*,*O*-dimethylhydroxylamine hydrochloride (6.15 g, 61.3 mmol) in anhydrous THF (118 mL). The solution was allowed to stir for 30 min at -5 °C prior to the addition of more isopropylmagnesium chloride solution (2.0 M in THF) (15.8 mL, 31.5 mmol). The reaction solution was stirred for a further 30 min, quenched with sat. NH_4Cl (60 mL), extracted with EtOAc (3 × 175 mL), washed with brine (400 mL), dried ($MgSO_4$), and filtered. The solvent was removed *in vacuo* and subjected to flash column chromatography (0 – 100% EtOAc/pet. ether) to yield title compound **50** (5.95 g, 92%) as a yellow oil:

Rf 0.32 (20% EtOAc/pet. ether);

υ_{max} (film) 2935 (CH sp^3), 1643 (C=O), 1446 (C=C aromatic) cm^{-1};

^{1}H NMR (700 MHz, $CDCl_3$) δ = 7.46 - 7.50 (2H, m, 8-H), 7.36 - 7.39 (2H, m, 9-H), 7.33 - 7.36 (1H, m, 10-H), 6.58 (1H, br s, 2-H), 3.69 - 3.73 (3H, s, 6-H), 3.25 - 3.29 (3H, s, 5-H), 2.53 (3H, s, 4-H);

^{13}C NMR (176 MHz, $CDCl_3$) δ = 167.9 (C-1), 152.2 (C-3), 142.9 (C-7), 128.4 (C-10), 128.3 (C-9), 126.2 (C-8), 115.9 (C-2), 61.5 (C-6), 32.2 (C-5), 17.9 (C-4);
m/z [HRMS, ESI] Calcd. $(C_{12}H_{15}NO_2+H)^+$ 206.1176, found 206.1179;
Data was in agreement with the literature.[234]

(*E*)-1-Hydroxy-4-phenylbut-3-en-2-one (52)

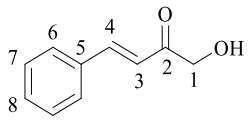

The reaction was performed under anhydrous conditions. Triethylamine (358 µL, 2.57 mmol) was added to a solution of *trans*-4-phenyl-3-buten-2-one **41** (250 mg, 1.71 mmol) in anhydrous CH_2Cl_2 (3.5 mL). The solution was cooled to -15 °C and trimethylsilyl trifluoromethanesulfonate (402 µL, 2.22 mmol) was added dropwise with stirring. The solution was allowed to stir for 1.5 h before being poured into sat. $NaHCO_3$, extracted with CH_2Cl_2 (3 × 5 mL), combined organic layers dried ($MgSO_4$) and the solvent removed *in vacuo* to afford the crude silyl enol ether. Anhydrous hexane (6 mL) was added and the solution cooled to -15 °C prior to the addition of 3-chloroperbenzoic acid (354 mg, 2.05 mmol). The reaction mixture was flushed with Ar and stirred for 18 h at room temperature. The solvent was then removed *in vacuo*, MeOH (6 mL) added and the solution stirred for a further 3 h. The solvent was removed *in vacuo* and subjected to flash column chromatography (0 – 50% Et_2O/hexane) to yiled title compound **52** (43.7 mg, 30%) as a yellow oil:

R_f 0.31 (40% Et_2O/pet. ether);
υ_{max} (film) 3397 (OH), 2917 (CH sp^3), 1752 (C=O), 1447 (C=C aromatic) cm^{-1};
^{1}H NMR (700 MHz, $CDCl_3$) δ = 7.68 (1H, d, *J* = 16.2 Hz, 4-H), 7.57 (2H, d, *J* = 7.5 Hz, 6-H), 7.40 - 7.44 (3H, m, 7-H, 8-H), 6.76 (1H, d, *J* = 16.2 Hz, 3-H), 4.55 (2H, s, 1-H);
^{13}C NMR (176 MHz, $CDCl_3$) δ = 198.1 (C-2), 144.2 (C-4), 133.8 (C-5), 131.1 (C-7 or C-8), 129.0 (C-7 or C-8), 128.5 (C-6), 121.3 (C-3), 67.0 (C-1);
m/z [LRMS, EI] (relative intensity, M) 162 (12, $[M]^+$), 131 (100, $[M-CH_3OH]^+$)
[HRMS, ESI] Calcd. $(C_{10}H_{10}O_2+H)^+$ 163.0754, found 163.0754;

(*E*)-1-Hydroxy-4-phenylpent-3-en-2-one (55)

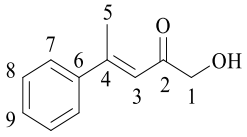

Following ***General Procedure 2***, α-hydroxylation was performed on compound **42** (2.56 g, 16.0 mmol).

Flash column chromatography (0 – 70% Et_2O/pet. ether) yielded title compound **55** (0.358 g, 13%) as a yellow oil:

R_f 0.29 (40% Et_2O/pet. ether);

υ_{max} (film) 3424 (OH), 2917 (CH sp^3), 1680 (C=O), 1600 (C=C alkene), 1445 (C=C aromatic) cm^{-1};

^1H NMR (700 MHz, $CDCl_3$) δ = 7.48 - 7.55 (2H, m, 8-H), 7.34 - 7.43 (3H, m, 7-H, 9-H), 6.41 (1H, q, *J* = 1.2 Hz, 3-H), 4.36 (2H, d, *J* = 4.0 Hz, 1-H), 3.47 (1H, t, *J* = 4.0 Hz, OH), 2.66 (3H, d, *J* = 1.2 Hz, 5-H);

^{13}C NMR (176 MHz, $CDCl_3$) δ = 198.4 (C-2), 157.4 (C-4), 141.7 (C-6), 129.7 (C-9), 128.6 (C-7), 126.5 (C-8), 118.9 (C-2), 69.2 (C-1), 19.0 (C-5);

m/z [HRMS, ESI] Calcd. $(C_{11}H_{12}O_2+H)^+$ 177.0910, found 177.0903;

Data was in agreement with the literature.[235]

2-(Prop-2-yn-1-yloxy)tetrahydro-*2H*-pyran (56)

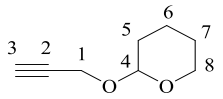

With stirring *p*-TsOH (0.95 mg, 4.99 μmol, 0.028 mol%) was added to 3,4-dihydro-*2H*-pyran (1.79 mL, 19.6 mmol) and was allowed to stir for 15 min prior to the dropwise addition of propargyl alcohol (1.04 mL, 17.8 mmol) over 30 min. Following this the resulting solution was stirred for 10 min, $NaHCO_3$ (112 mg, 1.34 mmol, 7.50 mol%) added and stirred for a further 18 h. The mixture was filtered and purified by flash column chromatography (0 – 25% EtOAc/pet. ether) to yield title compound **56** (1.87 g, 75%) as a colourless oil:

R_f 0.37 (100% pet. ether);

υ_{max} (film) 3285 (C≡C), 2939 (CH sp^3) cm^{-1};

^{1}H NMR (600 MHz, $CDCl_3$) δ = 4.84 (1H, t, *J* = 3.4 Hz, 4-H), 4.31 (1H, dd, *J* = 15.7 Hz, *J* = 2.4 Hz, 1-*H*H), 4.25 (1H, dd, *J* = 15.7 Hz, *J* = 2.4 Hz, 1-H*H*), 3.82 - 3.88 (1H, m, 8-*H*H), 3.53 - 3.58 (1H, m, 8-H*H*), 2.42 (1H, d, *J* = 2.4 Hz, *J* = 2.4 Hz, 3-H), 1.84 (1H, m, 5-*H*H), 1.73 - 1.78 (1H, m, 5-H*H*), 1.59 - 1.68 (2H, m, 6-*H*H, 6-H*H*), 1.51 - 1.57 (2H, m, 7-*H*H, 7-H*H*);

^{13}C NMR (151 MHz, $CDCl_3$) δ = 97.0 (C-4), 79.9 (C-2), 74.1 (C-3), 62.1 (C-8), 54.1 (C-1), 30.3 (C-5), 25.4 (C-6), 19.1 (C-7);

m/z [LRMS, GCMS] 85 (100, $[M\text{-}CHCCH_2O]^+$), 139 (7, $[M\text{-}H]^+$);

Data was in agreement with the literature.[308]

2-Phenyl-5-((tetrahydro-2*H*-pyran-2-yl)oxy)pent-3-yn-2-ol (57)

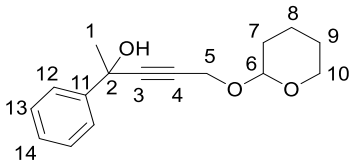

To a flame-dried round bottom flask purged with Ar was added compound **56** (2.00 g, 14.3 mmol) and dry THF (10 mL). The solution was cooled to -78 °C, *n*-BuLi (2.5 M in hexane, 6.85 mL, 17.1 mmol) added dropwise, and the solution stirred for 2 h at -78 °C. Acetophenone (1.66 mL, 14.3 mmol) was added and the reaction solution stirred for a further 6 h at -78 °C before warming to room temperature. Sat. NH_4Cl (10 mL) was added, the solution extracted with EtOAc (3 × 30 mL), and combined organic layers washed with brine (20 mL), dried ($MgSO_4$) and filtered. The solvent was removed *in vacuo* and crude product subjected to flash column chromatography (0 – 30% EtOAc/pet. ether) to yield title compound **57** (2.28 g, 61%) as a yellow oil:

R_f 0.33 (15% EtOAc/pet. ether);

υ_{max} (film) 3395 (OH), 2942 (CH sp^3), 1444 (C=C aromatic) cm^{-1};

^{1}H NMR (700 MHz, $CDCl_3$) δ = 7.65 (2H, d, *J* = 7.8 Hz, 12-H), 7.34 - 7.38 (2H, m, 13-H), 7.29 (1H, d, *J* = 7.1 Hz, 14-H), 4.82 - 4.86 (1H, m, 6-H), 4.38 (1H, d, *J* = 15.8 Hz, 5-*H*H), 4.34 (1H, d, *J* = 15.8 Hz, 5-H*H*), 3.81 - 3.88 (1H, m, 10-*H*H), 3.50 - 3.56 (1H, m, 10-H*H*), 2.83 (1H, br s, OH), 1.79 - 1.87 (1H, m, 7-*H*H), 1.78 (3H, s, 1-H), 1.70 - 1.76 (1H, m, 9-*H*H), 1.61 - 1.66 (1H, m, 9-H*H*), 1.57 - 1.61 (1H, m, 8-*H*H), 1.54 - 1.56 (1H, m, 7-H*H*), 1.50 - 1.53 (1H, m, 8-H*H*);

^{13}C NMR (176 MHz, $CDCl_3$) δ = 145.5 (C-11), 128.2 (C-13), 127.6 (C-14), 124.9 (C-12), 96.7 (C-6), 89.4 (C-3), 80.8 (C-4), 69.8 (C-2), 61.9 (C-10), 54.3 (C-5), 33.2 (C-1), 30.2 (C-9), 25.3 (C-8), 18.9 (C-7);
m/z [LRMS, CI] (relative intensity, M) 159 (100, $[M+H-C_5H_8O]^+$), 260 (3, $[M]^+$);

(*E*)-1-Hydroxy-3-methyl-4-phenylbut-3-en-2-one (63)

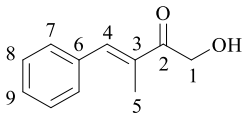

Following ***General Procedure 2***, α-hydroxylation was performed on compound **7a** (3.00 g, 18.7 mmol).

Flash column chromatography (10 – 30% EtOAc/pet. ether) yielded title compound **63** (1.36 g, 41%) as a yellow oil:
R_f 0.31 (40% Et_2O/pet. ether);
υ_{max} (film) 3445 (OH), 2960 (CH sp^3), 1663 (C=O), 1446 (C=C aromatic) cm^{-1};
^{1}H NMR (700 MHz, $CDCl_3$) δ = 7.42 - 7.46 (5H, m, 7-H, 8-H, 9-H), 7.37 - 7.40 (1H, m, 4-H), 4.72 (2H, s, 1-H), 2.16 (3H, d, *J* = 1.3 Hz, 5-H);
^{13}C NMR (176 MHz, $CDCl_3$) δ = 200.0 (C-2), 139.7 (C-aromatic), 135.0 (C-6), 133.8 (C-3), 129.9 (C-aromatic), 129.2 (C-aromatic), 128.6 (C-4), 64.7 (C-1), 12.9 (C-5);
m/z [LRMS, ES+] (relative intensity, M) 375 (32, $[2M+Na]^+$), 131 (85, $[M-C_2H_3O_2+NH_4]^+$); [HRMS, ESI] Calcd. $(C_{11}H_{12}O_2+H)^+$ 177.0910, found 177.0915;

(*E*)-1-Hydroxy-4-(4-methoxyphenyl)-3-methylbut-3-en-2-one (64)

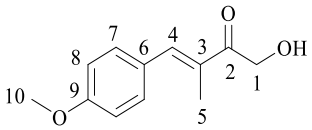

Following ***General Procedure 2***, α-hydroxylation was performed on compound **46** (400 mg, 2.10 mmol).

Flash column chromatography (5 – 50% EtOAc/pet. ether) yielded title compound **64** (129 mg, 30%) as a white solid:
m.p. 54 – 56 °C;
υ_{max} (solid) 3424 (OH), 2918 (CH sp^3), 1643 (C=O), 1507 (C=C aromatic) cm^{-1};

^{1}H NMR (700 MHz, $CDCl_3$) δ = 7.45 (2H, d, *J* = 8.9 Hz, 7-H), 7.37 (1H, d, *J* = 1.2 Hz, 4-H), 6.97 (2H, d, *J* = 8.9 Hz, 8-H), 4.69 (2H, s, 1-H), 3.86 (3H, s, 10-H), 2.16 (3H, d, *J* = 1.2 Hz, 5-H);

^{13}C NMR (176 MHz, $CDCl_3$) δ = 199.7 (C-2), 160.4 (C-9), 139.7 (C-4), 132.0 (C-7), 131.6 (C-3), 127.5 (C-6), 114.1 (C-8), 64.5 (C-1), 55.3 (C-10), 13.0 (C-5);

m/z [LRMS, ESI] (relative intensity, M) 207 (100, $[M+H]^+$), 189 (31, $[M-H_2O+H]^+$); [HRMS, ESI] Calcd. $(C_{12}H_{14}O_3+H)^+$ 207.1016, found 207.1017;

(*E*)-4-(4-Hydroxy-2-methyl-3-oxobut-1-en-1-yl)benzonitrile (65)

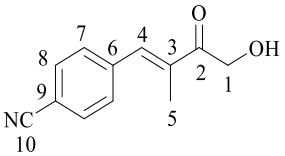

Following ***General Procedure 2***, α-hydroxylation was performed on compound **47** (225 mg, 1.21 mmol).

Flash column chromatography (5 – 60% EtOAc/pet. ether) yielded title compound **65** (116 mg, 47%) as a white solid:

m.p. 95 – 96 °C;

υ_{max} (solid) 3444 (OH), 2921 (CH sp^3), 2224 (CN), 1661 (C=O), 1446 (C=C aromatic) cm^{-1};

^{1}H NMR (700 MHz, $CDCl_3$) δ = 7.73 (2H, d, *J* = 8.2 Hz, 7-H), 7.52 (2H, d, *J* = 8.2 Hz, 8-H), 7.41 (1H, d, *J* = 1.4 Hz, 4-H), 4.71 (2H, s, 1-H), 2.13 (3H, d, *J* = 1.4 Hz, 5-H);

^{13}C NMR (176 MHz, $CDCl_3$) δ = 199.8 (C-2), 139.5 (C-6), 137.0 (C-4), 136.3 (C-3), 132.3 (C-7), 130.2 (C-8), 118.3 (C-10), 112.5 (C-9), 64.9 (C-1), 13.1 (C-5);

m/z [LRMS, ESI] (relative intensity, M) 198 (100, $[M-CN-H_2O+K]^+$); [HRMS, ESI] Calcd. $(C_{12}H_{11}NO_2+H)^+$ 202.0863, found 202.0862;

(*E*)-4-(3-Fluorophenyl)-1-hydroxy-3-methylbut-3-en-2-one (66)

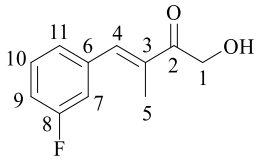

Following ***General Procedure 2***, α-hydroxylation was performed on compound **48** (0.225 mg, 1.26 mmol).

Flash column chromatography (10 – 35% EtOAc/pet. ether) yielded title compound **66** (108 mg, 44%) as a colourless oil:

υ_{max} (film) 3445 (OH), 2931 (CH sp^3), 1708 (C=O), 1580 (C=C aromatic) cm^{-1};

^{1}H NMR (700 MHz, $CDCl_3$) δ = 7.41 (1H, ddd, *J* = 8.2 Hz, *J* = 7.7 Hz, *J* = 6.2 Hz, 10-H), 7.39 (1H, d, *J* = 1.3 Hz, 4-H), 7.21 (1H, d, *J* = 7.7 Hz, 11-H), 7.15 (1H, dd, *J* = 9.8 Hz, *J* = 1.9 Hz, 7-H), 7.09 (1H, ddd, *J* = 8.9 Hz, *J* = 8.2 Hz, *J* = 1.9 Hz, 9-H), 4.71 (2H, s, 1-H), 2.15 (3H, d, *J* = 1.3 Hz, 5-H);

^{13}C NMR (176 MHz, $CDCl_3$) δ = 199.9 (C-2), 162.6 (d, *J* = 246.8 Hz, C-8), 138.2 (d, *J* = 2.3 Hz, C-4), 137.1 (d, *J* = 7.6 Hz, C-6), 134.8 (C-3), 130.2 (d, *J* = 8.4 Hz, C-10), 125.7 (d, *J* = 3.1 Hz, C-11), 116.5 (d, *J* = 22.1 Hz, C-7), 116.1 (d, *J* = 21.4 Hz, C-9), 64.8 (C-1), 13.0 (C-5);

^{19}F NMR (659 MHz, $CDCl_3$) δ = -112.3 (1F, ddd, *J* = 9.8 Hz, *J* = 8.4 Hz, *J* = 6.0 Hz, F-5);

m/z [LRMS, ESI] (relative intensity, M) 195 (100, $[M+H]^+$) 177 (10, $[M-H_2O+H]^+$; [HRMS, ESI] Calcd. $(C_{11}H_{11}FO_2+H)^+$ 195.0816, found 195.0815;

2-Methyl-3-phenylpropanal (68)

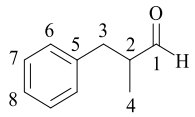

Following ***General Procedure 3***, α-methyl-*trans*-cinnamaldehyde was chemically reduced.

Flash column chromatography (0 – 25% EtOAc/pet. ether) yielded title compound **68** (51.1 mg, 20%) as a colourless oil:

R_f 0.38 (2% EtOAc/pet. ether);

υ_{max} (film) 2966 (CH sp^3), 1718 (C=O), 1452 (C=C aromatic) cm^{-1};

^{1}H NMR (600 MHz, $CDCl_3$) δ = 9.74 (1H, d, *J* = 1.5 Hz, 1-H), 7.31 (2H, m, 7-H), 7.23 (1H, d, *J* = 7.4 Hz, 8-H), 7.18 (2H, d, *J* = 7.2 Hz, 6-H), 3.11 (1H, dd, *J* = 13.7 Hz, *J* = 6.0 Hz, 3-*H*H), 2.65 - 2.73 (1H, m, 2-H), 2.62 (1H, dd, *J* = 13.7 Hz, *J* = 8.2 Hz, 3-H*H*), 1.10 (3H, d, *J* = 7.0 Hz, 4-H);

^{13}C NMR (151 MHz, $CDCl_3$) δ = 204.4 (C-1), 138.8 (C-5), 129.0 (C-6), 128.5 (C-7), 126.4 (C-8), 48.0 (C-2), 36.6 (C-3), 13.2 (C-4);

m/z [LRMS, ES+] (relative intensity, M) 131 (100, $[M-H_2O+H]^+$), 149 (18, $[M+H]^+$)

Data was in agreement with the literature.[309]

By-product: **2-Methyl-3-phenylpropanol (69)**

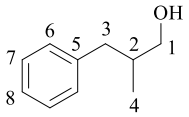

Flash column chromatography (5 – 50% EtOAc/pet. ether) yielded by-product title compound **69** (126 mg, 50%) as a colourless oil:

R_f 0.37 (37% EtOAc/pet. ether);

υ_{max} (film) 3342 (OH), 2952 (CH sp^3), 1493 (C=C aromatic) cm^{-1};

^{1}H NMR (700 MHz, $CDCl_3$) δ = 7.28 - 7.32 (2H, m, 7-H), 7.21 (1H, d, *J* = 7.3 Hz, 8-H), 7.19 (2H, d, *J* = 8.1 Hz, 6-H), 3.55 (1H, dd, *J* = 10.6 Hz, *J* = 5.8 Hz, 1-*H*H), 3.49 (1H, dd, *J* = 10.6 Hz, *J* = 6.0 Hz, 1-H*H*), 2.77 (1H, dd, *J* = 13.5 Hz, *J* = 6.4 Hz, 3-*H*H), 2.44 (1H, dd, *J*= 13.5 Hz, *J* = 8.1 Hz, 3-H*H*), 1.92 - 2.00 (1H, m, 2-H), 0.93 (3H, d, *J* = 6.7 Hz, 4-H);

^{13}C NMR (176 MHz, $CDCl_3$) δ = 140.6 (C-5), 129.1 (C-7), 128.2 (C-6), 125.8 (C-8), 67.6 (C-1), 39.7 (C-3), 37.8 (C-2), 16.4 (C-4);

m/z [LRMS, EI] 150.0 $(M)^+$;

Data was in agreement with the literature.[310]

(*E/Z*)-1-Hydroxy-4-phenylpent-3-en-2-one [(*E/Z*)-55]

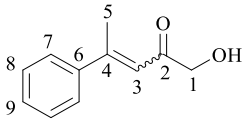

To a flame-dried round bottom flask purged with Ar was added chloro(triphenylphosphine)gold(I) (28.5 mg, 57.6 µmol, 5 mol%) and silver triflate (20.7 mg, 80.7 µmol, 7 mol%) in dry CH_2Cl_2 (10 mL). The suspension was allowed to stir for 10 min prior to the addition of compound **57** (300 mg, 1.15 mmol). The reaction mixture was stirred for 24 h, had the solvent removed *in vacuo* and subjected to flash column chromatography (30 – 45% Et_2O/hexane).

Title compound (*E/Z*)-**55** (21.8 mg, 11%) was afforded as a colourless oil in an approximate 4:5 ratio of isomers:

υ_{max} (film) 3446 (OH), 2937 (CH sp^3), 1680 (C=O), 1434 (C=C aromatic) cm^{-1};

m/z [LRMS, CI] (relative intensity, M) 194 (100, $[M+NH_4]^+$), 177 (47, $[M+H]^+$); [HRMS, CI] Calcd. $(C_{11}H_{12}O_2+H)^+$ 177.0910, found 177.0911

Major isomer

^{1}H NMR (700 MHz, $CDCl_3$) δ = 7.40 - 7.41 (2H, m, 8-H), 7.40 - 7.40 (1H, m, 9-H), 7.18 - 7.22 (2H, m, 7-H), 6.20 (1H, s, 3-H), 3.92 (2H, s, 1-H), 2.25 (3H, s, 5-H);

^{13}C NMR (176 MHz, $CDCl_3$) δ = 198.8 (C-2), 157.2 (C-4), 140.5 (C-6), 129.7 (C-9), 128.6 (C-7), 126.6 (C-8), 123.1 (C-3), 68.1 (C-1), 28.1 (C-5);

Minor isomer

^{1}H NMR (700 MHz, $CDCl_3$) δ = 7.51 (2H, dd, *J* = 7.2 Hz, *J* = 3.6 Hz, 8-H), 7.40 - 7.42 (2H, m, 7-H), 7.38 - 7.39 (1H, m, 9-H), 6.41 (1H, s, 3-H), 4.36 (2H, s, 1-H), 2.66 (3H, s, 5-H);

^{13}C NMR (176 MHz, $CDCl_3$) δ = 198.4 (C-2), 157.5 (C-4), 141.8 (C-6), 129.7 (C-9), 128.7 (C-7), 126.5 (C-8), 119.0 (C-3), 68.1 (C-1), 19.1 (C-5);

Data was in agreement with the literature.[235]

By-product: **5-Methyl-5-phenyldihydrofuran-3(*2H*)-one (58)**

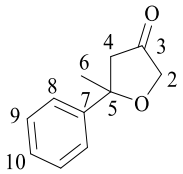

By-product title compound **58** (81.5 mg, 40%) was afforded as a colourless oil:

υ_{max} (film) 2971 (CH sp^3), 1758 (C=O), 1444 (C=C aromatic) cm^{-1};

^{1}H NMR (700 MHz, $CDCl_3$) δ = 7.39 - 7.42 (2H, m, 8-H), 7.36 - 7.39 (2H, m, 9-H), 7.28 - 7.31 (1H, m, 10-H), 4.16 (1H, d, *J* = 17.2 Hz, 4-*H*H), 3.98 (1H, d, *J* = 17.2 Hz, 4-H*H*), 2.94 (1H, d, *J* = 17.7 Hz, 2-*H*H), 2.71 (1H, d, *J* = 17.7 Hz, 2-H*H*), 1.69 (3H, s, 6-H);

^{13}C NMR (176 MHz, $CDCl_3$) δ = 215.0 (C-3), 144.6 (C-7), 128.8 (C-9), 127.6 (C-10), 124.9 (C-8), 83.9 (C-5), 70.5 (C-4), 50.1 (C-2), 30.3 (C-6);

m/z [LRMS, EI] (relative intensity, M) 176 (9, $[M]^+$), 161 (100, $[M\text{-}CH_3]^+$);

Data was in agreement with the literature.[311]

3-Phenylbutanal (75)

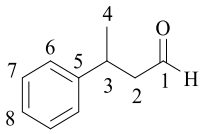

With stirring, a solution of compound **111** (200 mg, 1.33 mmol) in CH_2Cl_2 (3 mL) was added to a solution of Dess-Martin periodinane (250 mg, 1.59 mmol) in CH_2Cl_2 (8 mL) and stirred for 1.5 h. The reaction was diluted with Et_2O (10 mL) before being poured into sodium thiosulfate (1.47 g, 9.32 mmol) in sat. aq. $NaHCO_3$ (35 mL) and stirred for 10 min. The organic and aqueous layers were separated, and the organic layer washed sequentially with sat. $NaHCO_3$ and deionised water. The organic layers were combined, dried ($MgSO_4$) and filtered. The solvent was removed *in vacuo* and the crude product subjected to flash column chromatography (0 – 30% EtOAc/pet. ether) to yield the title compound **75** (67 mg, 34%) as a yellow oil:

υ_{max} (oil) 2962 (CH sp^3), 1722 (C=O), 1452 (C=C aromatic) cm^{-1};

^{1}H NMR (600 MHz, $CDCl_3$) δ = 9.72 (1H, t, *J* = 2.0 Hz, 1-H), 7.31 - 7.35 (2H, m, 7-H), 7.22 - 7.25 (3H, m, 6-H, 8-H), 3.38 (1H, dqd, *J* = 7.7 Hz, *J* = 7.2 Hz, *J* = 6.9 Hz, 3-H),

2.77 (1H, ddd, *J* = 16.7 Hz, *J* = 6.9 Hz, *J* = 2.0 Hz, 2-*H*H), 2.68 (1H, ddd, *J* = 16.7 Hz, *J* = 7.7 Hz, *J* = 2.0 Hz, 2-H*H*), 1.34 (3H, d, *J* = 7.2 Hz, 4-H);

^{13}C NMR (151 MHz, $CDCl_3$) δ = 201.9 (C-1), 145.4 (C-5), 128.6 (C-7), 126.7 (C-6 or C-8), 126.5 (C-6, or C-8), 51.7 (C-2), 34.2 (C-3), 22.1 (C-4);

m/z [LRMS, EI] (relative intensity, M) 148 (47, $[M]^+$), 133 (48, $[M\text{-}H_2O+H]^+$);

Data was in agreement with the literature.[312]

3,3-Diphenylpropanal (76)

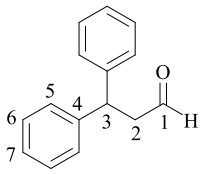

Following ***General Procedure 3***, β-phenylcinnamaldehyde was chemically reduced.

Flash column chromatography (0 – 25% EtOAc/pet. ether) yielded title compound **76** (46.3 mg, 18%) as a white solid:

R_f 0.30 (8% EtOAc/pet. ether);

m.p. 54 – 55 °C (lit. m.p. 50 – 51 °C)[313];

υ_{max} (solid) 3024 (CH sp^3), 1708 (C=O), 1491 (C=C aromatic) cm^{-1};

^{1}H NMR (600 MHz, $CDCl_3$) δ = 9.75 (1H, t, *J* = 1.9 Hz, 1-H), 7.29 - 7.32 (4H, m, 6-H), 7.25 (4H, d, *J* = 7.2 Hz, 5-H), 7.22 (2H, d, *J* = 7.3 Hz, 7-H), 4.64 (1H, d, *J* = 7.8 Hz, 3-H), 3.19 (2H, dd, *J* = 7.8 Hz, *J* = 1.9 Hz, 2-H);

^{13}C NMR (151 MHz, $CDCl_3$) δ = 201.2 (C-1), 143.3 (C-4), 128.9 (C-6), 127.8 (C-5), 126.8 (C-7), 49.5 (C-2), 45.1 (C-3);

m/z [LRMS, EI] (relative intensity, M) 210 (60, $[M]^+$), 167 (100, $[M\text{-}CHOCH_3]^+$),

Data was in agreement with the literature.[314]

By-product: **3,3-Diphenylpropan-1-ol (112)**

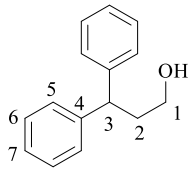

Flash column chromatography (0 – 25% EtOAc/pet. ether) yielded by-product title compound **112** (160 mg, 63%) as colourless oil:

R_f 0.30 (20% EtOAc/pet. ether);

υ_{max} (film) 3311 (OH), 2933 (CH sp^3), 1491 (C=C aromatic) cm^{-1};

^{1}H NMR (600 MHz, $CDCl_3$-d) δ = 7.28 - 7.31 (4H, m, 6-H), 7.25 - 7.28 (4H, m, 5-H), 7.16 - 7.21 (2H, m, 7-H), 4.14 (1H, t, *J* = 8.0 Hz, 3-H), 3.61 (2H, t, *J* = 6.5 Hz, 1-H), 2.33 (2H, dt, *J* = 8.0 Hz, *J* = 6.5 Hz, 2-H), 1.42 (1H, br s, OH);

^{13}C NMR (151 MHz, $CDCl_3$) δ = 144.4 (C-4), 128.5 (C-6), 127.8 (C-5), 126.3 (C-7), 61.0 (C-1), 47.3 (C-3), 38.1 (C-2);

m/z [LRMS, ESI] 235 $(M+Na)^+$, 135 $(M+H-C_6H_5)^+$; [HRMS, ESI] Calcd. $(C_{15}H_{16}O+Na)^+$ 235.1093, found 235.1093

Data was in agreement with the literature.[315]

3-(4-Methoxyphenyl)propanal (77)

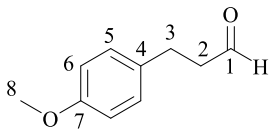

Following ***General Procedure 3***, *trans-p*-methoxycinnamaldehyde was chemically reduced.

Flash column chromatography (5 – 40% EtOAc/pet. ether) yielded title compound **77** (127 mg, 50%) as a colourless oil:

R_f 0.32 (10% EtOAc/pet. ether);

υ_{max} (film) 2931 (CH sp^3), 1719 (CO), 1610 (C=C aromatic) cm^{-1};

^{1}H NMR (700 MHz, $CDCl_3$) δ = 9.82 (1H, t, *J* = 1.0 Hz, 1-H), 7.12 (2H, d, *J* = 8.5 Hz, 5-H), 6.85 (2H, d, *J* = 8.5 Hz, 6-H), 3.80 (3H, s, 8-H), 2.92 (2H, t, *J* = 7.6 Hz, 3-H), 2.76 (1H, td, *J* = 7.6 Hz, *J* = 1.0 Hz, 2-H);

^{13}C NMR (176 MHz, $CDCl_3$) δ = 201.9 (C-1), 158.2 (C-7), 132.5 (C-4), 129.4 (C-6), 114.2 (C-5), 55.4 (C-8), 45.7 (C-2), 27.4 (C-3);

m/z [LRMS, EI] (relative intensity, M) 165 (88, $[M+H]^+$), 164 (12, $[M]^+$), 108 (84, $[M-COCH_2-CH_3]^+$);

Data was in agreement with the literature.[316]

By-product: **3-(4-Methoxyphenyl)propan-1-ol (113)**

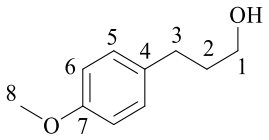

Flash column chromatography (5 – 40% EtOAc/pet. ether) yielded by-product title compound **113** (81 mg, 31%) as a colourless oil:

R_f 0.27 (30% EtOAc/pet. ether);

υ_{max} (film) 3351 (OH), 2932 (CH sp^3), 1610 (C=C aromatic) cm^{-1};

^1H NMR (700 MHz, $CDCl_3$) δ = 7.13 (2H, d, *J* = 8.5 Hz, 5-H), 6.85 (2H, d, *J* = 8.5 Hz, 6-H), 3.80 (3H, s, 8-H), 3.68 (2H, t, *J* = 6.4 Hz, 1-H), 2.66 (2H, t, *J* = 7.5 Hz, 3-H), 1.88 (2H, tt, *J* = 7.5 Hz, *J* = 6.4 Hz, 2-H);

^{13}C NMR (176 MHz, $CDCl_3$) δ = 157.8 (C-7), 133.8 (C-4), 129.3 (C-5), 113.8 (C-6), 62.2 (C-1), 55.2 (C-8), 34.4 (C-2), 31.1 (C-3);

m/z [LRMS, CI] (relative intensity, M) 184 (100, $[M+NH_4]^+$), 166 (34, $[M]^+$); [HRMS, CI] Calcd. $(C_{10}H_{14}O_2+NH_4)^+$ 184.1332, found 184.1332;

Data was in agreement with the literature.[317]

3-(4-(Dimethylamino)phenyl)propanal (78)

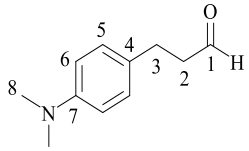

Following ***General Procedure 3***, (*E*)-3-(4-(diethylamino)phenyl)acrylaldehyde was chemically reduced.

Flash column chromatography (5 – 40% EtOAc/pet. ether) yielded title compound **78** (79 mg, 32%) as a yellow oil:

R_f 0.42 (15% EtOAc/pet. ether);

υ_{max} (film) 2886 (CH sp^3), 1720 (CO), 1614 (C=C aromatic) cm^{-1};

^{1}H NMR (700 MHz, $CDCl_3$) δ = 9.83 (1H, t, *J* = 1.6 Hz, 1-H), 7.09 (2H, d, *J* = 8.6 Hz, 5-H), 6.71 (2H, d, *J* = 8.6 Hz, 6-H), 2.93 (6H, s, 8-H), 2.89 (2H, t, *J* = 7.6 Hz, 3-H), 2.74 (2H, td, *J* = 7.6 Hz, *J* = 1.6 Hz, 2-H);

^{13}C NMR (176 MHz, $CDCl_3$) δ = 202.2 (C-1), 149.3 (C-4), 128.9 (C-5), 128.1 (C-7), 113.0 (C-6), 45.6 (C-2), 40.8 (C-8), 27.2 (C-3);

m/z [LRMS, ESI] 218 $(M+H+CH_3CN)^+$, 196 $(M+NH_4)^+$, 178 $(M+H)^+$;

Data was in agreement with the literature.[318]

By-product: **3-(4-(Dimethylamino)phenyl)propan-1-ol (114)**

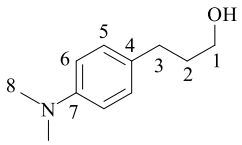

Flash column chromatography (5 – 50% EtOAc/pet. ether) yielded by-product title compound **114** (150 mg, 68%) as a yellow oil:

R_f 0.33 (35% EtOAc/pet. ether);

υ_{max} (oil) 3325 (OH), 2933 (CH sp^3), 1718 (C=O), 1613 (C=C aromatic) cm^{-1};

^{1}H NMR (700 MHz, $CDCl_3$) δ = 7.10 (2H, d, *J* = 7.6 Hz, 5-H), 6.73 (2H, d, *J* = 7.6 Hz, 6-H), 3.68 (2H, t, *J* = 6.4 Hz, 1-H), 2.93 (6H, s, 8-H), 2.63 (2H, t, *J* = 7.7 Hz, 3-H), 1.83 - 1.92 (2H, m, 2-H), 1.56 (1H, br s, OH);

^{13}C NMR (176 MHz, $CDCl_3$) δ = 149.1 (C-7), 129.9 (C-4), 128.9 (C-5), 113.1 (C-6), 62.4 (C-1), 40.9 (C-8), 34.5 (C-2), 31.0 (C-3);

m/z [LRMS, ESI] 196 $(M+NH_4)^+$, 180 $(M+H)^+$;

Data was in agreement with the literature.[317]

4-(4-Methoxyphenyl)-3-methylbutan-2-one (81)

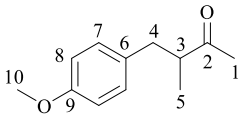

Following ***General Procedure 3***, compound **46** (100 mg, 0.526 mmol, 1 eq.) was chemically reduced.

Title compound **81** (97 mg, 96%) was afforded as a colourless oil:

υ_{max} (film) 2930 (CH sp^3), 1706 (C=O), 1509 (C=C aromatic) cm^{-1};

^{1}H NMR (700 MHz, $CDCl_3$) δ = 7.07 (2H, d, *J* = 8.6 Hz, 7-H), 6.83 (2H, d, *J* = 8.6 Hz, 8-H), 3.79 (3H, s, 10-H), 2.94 (1H, dd, *J* = 13.8 Hz, *J* = 7.0 Hz, 4-*H*H), 2.80 (1H, ddq, *J* = 7.6 Hz, *J* = 7.0 Hz, *J* = 7.0 Hz, 3-H), 2.53 (1H, dd, *J* = 13.8 Hz, *J* = 7.6 Hz, 4-H*H*), 2.09 (3H, s, 1-H), 1.09 (3H, d, *J* = 7.0 Hz, 5-H);

^{13}C NMR (176 MHz, $CDCl_3$) δ = 212.4 (C-2), 158.0 (C-9), 131.7 (C-6), 129.8 (C-7), 113.8 (C-8), 55.2 (C-10), 49.0 (C-3), 38.1 (C-4), 28.9 (C-1), 16.2 (C-5);

m/z [LRMS, ES+] (relative intensity, M) 145.2 (90, $[M\text{-}C_4H_6O+Na]^+$); [HRMS, ESI] Calcd. $(C_{12}H_{16}O_2+H)^+$ 193.1223, found 193.1225;

4-(3-Fluorophenyl)-3-methylbutan-2-one (83)

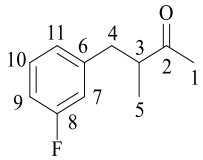

Following ***General Procedure 3***, compound **48** (100 mg, 0.561 mmol, 1 eq.) was chemically reduced.

Title compound **83** (93 mg, 92%) was afforded as a colourless oil:

υ_{max} (film) 2968 (CH sp^3), 1709 (C=O), 1587 (C=C aromatic) cm^{-1};

^{1}H NMR (700 MHz, $CDCl_3$) δ = 7.24 (1H, ddd, *J* = 7.9 Hz, *J* = 7.6 Hz, *J* = 6.1 Hz, 10-H), 6.93 (1H, d, *J* = 7.6 Hz, 11-H), 6.90 (1H, ddd, *J* = 8.5 Hz, *J* = 7.9 Hz, *J* = 2.2 Hz, 9-H), 6.87 (1H, dd, *J* = 9.9 Hz, *J* = 2.2 Hz, 7-H), 3.01 (1H, dd, *J* = 13.8 Hz, *J* = 7.0 Hz, 4-*H*H), 2.83 (1H, ddq, *J* = 7.6 Hz, *J* = 7.0 Hz, 3-H), 2.56 (1H, dd, *J* = 13.8 Hz, *J* = 7.6 Hz, 4-H*H*), 2.11 (3H, s, 1-H), 1.11 (3H, d, *J* = 7.0 Hz, 5-H);

^{13}C NMR (176 MHz, $CDCl_3$) δ = 211.6 (C-2), 162.8 (d, *J* = 246.1 Hz, C-8), 142.3 (d, *J* = 7.3 Hz, C-6), 129.8 (d, *J* = 8.0 Hz, C-10), 124.6 (d, *J* = 2.7 Hz, C-11), 115.7 (d, *J* = 21.0 Hz, C-7), 113.2 (d, *J* = 21.0 Hz, C-9), 48.5 (C-3), 38.4 (C-4) 28.8 (C-1) 16.3 (C-5);

m/z [LRMS, ES+] (relative intensity, M) 142 (100, $[M\text{-}C_2H_2FO+Na]^+$); [HRMS, ESI] Calcd. $(C_{11}H_{13}FO+H)^+$ 181.1023, found 181.1023;

4-(2-Methyl-3-oxobutyl)benzonitrile (84)

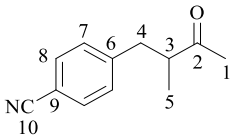

Following ***General Procedure 3***, compound **47** (100 mg, 0.540 mmol, 1 eq.) was chemically reduced.

Flash column chromatography (10 – 30% EtOAc/pet. ether, then 5 – 10% MeOH/CH_2Cl_2) yielded title compound **84** (85 mg, 84%) as a white solid:

R_f 0.54 (20% EtOAc/pet. ether);

m.p. 54 – 56 °C;

υ_{max} (solid) 2965 (CH sp^3), 2226 (CN), 1699 (C=O), 1605 (C=C aromatic) cm^{-1};

^{1}H NMR (700 MHz, $CDCl_3$) δ = 7.57 (2H, d, *J* = 8.3 Hz, 7-H), 7.26 (2H, d, *J* = 8.3 Hz, 8-H), 3.07 (1H, dd, *J* = 13.8 Hz, *J* = 7.2 Hz, 4-*H*H), 2.83 (1H, ddq, *J* = 7.3 Hz, *J* = 7.2 Hz, *J* = 7.1 Hz, 3-H), 2.61 (1H, dd, *J* = 13.8 Hz, J = 7.3 Hz, 4-H*H*), 2.11 (3H, s, 1-H), 1.12 (3H, d, *J* = 7.1 Hz, 5-H);

^{13}C NMR (176 MHz, $CDCl_3$) δ = 210.9 (C-2), 145.5 (C-6), 132.2 (C-7), 129.8 (C-8), 118.9 (C-10), 110.2 (C-9), 48.3 (C-3), 38.6 (C-4), 28.8 (C-1), 16.5 (C-5);

m/z [LRMS, ES+] (relative intensity, M) 145 (100, $[M-C_2H_3O+H]^+$); [HRMS, ESI] Calcd. $(C_{12}H_{13}NO+H)^+$ 188.1070, found 188.1070;

By-product: **4-(4-(Aminomethyl)phenyl)-3-methylbutan-2-one (115)**

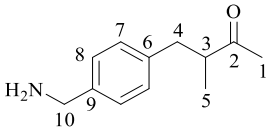

Flash column chromatography (10 – 30% EtOAc/pet. ether, then 5 – 10% MeOH/CH_2Cl_2) yielded by-product title compound **115** (4 mg, 4%) as a white solid:

R_f 0.35 (5% MeOH/CH_2Cl_2);

υ_{max} (solid) 2924 (CH sp^3), 1704 (C=O), 1453 (C=C aromatic) cm^{-1};

^{1}H NMR (700 MHz, $CDCl_3$) δ = 7.27 (2H, d, *J* = 7.9 Hz, 8-H), 7.12 (2H, d, *J* = 7.9 Hz, 7-H), 3.78 (2H, s, 10-H), 2.98 (1H, dd, *J* = 13.7 Hz, *J* = 6.8 Hz, 4-*H*H), 2.82 (1H, dqd, *J* = 7.7 Hz, *J* = 7.0 Hz, *J* = 6.8 Hz, 3-H), 2.55 (1H, dd, *J* = 13.8 Hz, *J* = 7.7 Hz, 4-H*H*), 2.10 (3H, s, 1-H), 1.09 (3H, d, *J* = 7.0 Hz, 5-H);

^{13}C NMR (176 MHz, $CDCl_3$) δ = 212.1 (C-2), 138.6 (C-6), 137.2 (C-9), 129.0 (C-7), 128.5 (C-8), 52.4 (C-10), 48.8 (C-3), 38.5 (C-4), 28.8 (C-1), 16.2 (C-5);
m/z [LRMS, ES+] (relative intensity, M) 142 (88, $[M-C_3H_8NO+Na]^+$); [HRMS, ESI] Calcd. $(C_{12}H_{15}NO+H)^+$ 190.1226, found 190.1227;

1-Hydroxy-3-methyl-4-phenylbutan-2-one (85)

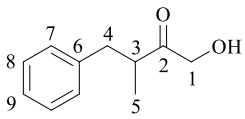

Following ***General Procedure 3***, compound **63** (300 mg, 1 eq.) was chemically reduced.

Flash column chromatography (20 – 100% EtOAc/pet. ether) yielded title compound **85** (221 mg, 73%) as a yellow oil:
R_f 0.44 (50% Et_2O/pet. ether);
υ_{max} (film) 3431 (OH), 2972 (CH sp^3), 1713 (C=O), 1453 (C=C aromatic) cm^{-1};
^{1}H NMR (700 MHz, $CDCl_3$) δ = 7.26 - 7.29 (2H, m, 8-H), 7.19 - 7.22 (1H, m, 9-H), 7.12 (2H, d, *J* = 7.4 Hz, 7-H), 4.24 (1H, dd, *J* = 19.1 Hz, *J* = 4.6 Hz, 1-*H*H), 3.95 (1H, dd, *J* = 19.2 Hz, *J* = 4.6 Hz, 1-H*H*), 3.12 (1H, t, *J* = 4.6 Hz, OH), 2.98 (1H, dd, *J* = 13.6 Hz, *J* = 7.4 Hz, 4-*H*H), 2.83 (1H, ddq, *J* = 7.4 Hz, *J* = 7.4 Hz, *J* = 7.1 Hz, 3-H), 2.67 (1H, dd, *J* = 13.6 Hz, *J* = 7.4 Hz, 4-H*H*), 1.15 (3H, d, *J* = 7.1 Hz, 5-H);
^{13}C NMR (176 MHz, $CDCl_3$) δ = 213.0 (C-2), 138.8 (C-6), 128.7 (C-7), 128.5 (C-8), 126.5 (C-9), 67.6 (C-1), 44.5 (C-3), 39.1 (C-4), 16.4 (C-5);
m/z [LRMS, ES+] (relative intensity, M) 377 (76, $[2M+NH_4+H]^+$), 142 (100, $[M-C_2H_3O_2+Na]^+$, 101.4 (72, $[M-C_6H_5+H]^+$; [HRMS, ESI] Calcd. $(C_{11}H_{14}O_2+Na)^+$ 201.0886, found 201.0887;
Data was in agreement with the literature.[319]

(*S*)-1-Hydroxy-3-methyl-4-phenylbutan-2-one [(*S*)-85]

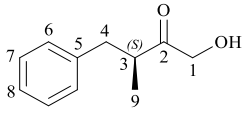

Preparative scale NCR bioreduction of **63** was performed, as described in experimental procedures.

Title compound (*S*)-**85** (107 mg, 96%) was afforded as a yellow oil:

$[\alpha]_D^{24}$ +51.2 (c. 1.0, $CHCl_3$);

υ_{max} (film) 3438 (OH), 2971 (CH sp^3), 1713 (C=O), 1454 (C=C aromatic) cm^{-1};

^{1}H NMR (700 MHz, $CDCl_3$) δ = 7.29 (2H, dd, *J* = 7.5 Hz, *J* = 7.3 Hz, 7-H), 7.23 (1H, d, *J* = 7.3 Hz, 8-H), 7.13 (2H, d, *J* = 7.5 Hz, 6-H), 4.25 (1H, d, *J* = 19.1 Hz, 1-*H*H), 3.95 (1H, d, *J* = 19.2 Hz, 1-H*H*), 3.00 (1H, dd, *J* = 13.6 Hz, *J* = 7.7 Hz, 4-*H*H), 2.84 (1H, ddq, *J* = 7.7 Hz, *J* = 7.0 Hz, *J* = 6.9 Hz, 3-H), 2.69 (1H, dd, *J* = 13.5 Hz, *J* = 7.0 Hz, 4-H*H*), 1.17 (3H, d, *J* = 6.9 Hz, 9-H);

^{13}C NMR (176 MHz, $CDCl_3$) δ = 213.0 (C-2), 138.8 (C-5), 128.8 (C-6), 128.6 (C-7), 126.6 (C-8), 67.7 (C-1), 44.6 (C-3), 39.2 (C-4), 16.5 (C-9);

m/z [HRMS, ESI] Calcd. $(C_{11}H_{14}O_2+H)^+$ 179.1067, found 179.1066;

1-Hydroxy-4-phenylpentan-2-one (86)

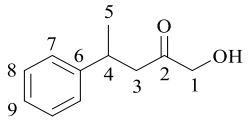

Following ***General Procedure 3***, compound **55** (200 mg, 1.13 mmol) was chemically reduced.

Flash column chromatography (30 – 100% Et_2O/pet. ether) yielded title compound **86** (97 mg, 48%) was afforded as a colourless oil:

υ_{max} (film) 3453 (OH), 2963 (CH sp^3), 1716 (C=O), 1452 (C=C aromatic) cm^{-1};

^{1}H NMR (700 MHz, $CDCl_3$) δ = 7.29 - 7.33 (2H, m, 8-H), 7.22 - 7.24 (1H, m, 9-H), 7.19 - 7.21 (2H, m, 7-H), 4.15 (1H, dd, *J* = 19.0 Hz, *J* = 4.7 Hz, 1-*H*H), 4.02 (1H, dd, *J* = 19.0 Hz, *J* = 4.6 Hz, 1-H*H*), 3.37 (1H, ddq, *J* = 7.4 Hz, *J* = 7.3 Hz, *J* = 7.0 Hz, 4-H), 3.04 (1H, dd, *J* = 4.7 Hz, *J* = 4.6 Hz, OH), 2.73 (1H, dd, *J* = 15.8 Hz, *J* = 7.3 Hz, 3-*H*H), 2.65 (1H, dd, *J* = 15.8 Hz, *J* = 7.4 Hz, 3-H*H*), 1.31 (3H, d, *J* = 7.0 Hz, 5-H);

^{13}C NMR (176 MHz, $CDCl_3$) δ = 208.6 (C-2), 145.2 (C-6), 128.7 (C-8), 126.6 (C-9), 126.6 (C-7), 68.8 (C-1), 46.8 (C-3), 35.6 (C-4), 22.0 (C-5);

m/z [LRMS, GCMS] (relative intensity, M) 179 (13, $[M+H]^+$) 160 (41, $[M-H_2O+H]^+$) 105 (100, $[M-C_3H_5O_2+H]^+$); [HRMS, ESI] Calcd. $(C_{11}H_{14}O_2+Na)^+$ 201.0886, found 201.0888;

Data was in agreement with the literature.[319]

1-Hydroxy-4-(4-methoxyphenyl)-3-methylbutan-2-one (87)

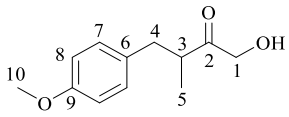

Following ***General Procedure 3***, compound **64** (80 mg, 0.688 mmol, 1 eq.) was chemically reduced.

Flash column chromatography (20 – 60% EtOAc/pet. ether) yielded title compound **87** (59 mg, 73%) as a colourless oil:

υ_{max} (film) 3452 (OH), 2931 (CH sp^3), 1711 (C=O), 1510 (C=C aromatic) cm^{-1};

^{1}H NMR (700 MHz, $CDCl_3$) δ = 7.04 (2H, d, *J* = 8.7 Hz, 7-H), 6.83 (2H, d, *J* = 8.7 Hz, 8-H), 4.23 (1H, d, *J* = 19.2 Hz, 1-*H*H), 3.94 (1H, d, *J* = 19.2 Hz, 1-H*H*), 3.79 (3H, s, 10-H), 2.92 (1H, dd, *J* = 13.6 Hz, *J* = 7.9 Hz, 4-*H*H), 2.80 (1H, ddq, *J* = 7.9 Hz, *J* = 6.9 Hz, *J* = 6.9 Hz, 3-H), 2.64 (1H, dd, *J* = 13.6 Hz, *J* = 6.9 Hz, 4-H*H*), 1.15 (3H, d, *J* = 6.9 Hz, 5-H);

^{13}C NMR (176 MHz, $CDCl_3$) δ = 213.2 (C-2), 158.3 (C-9), 130.8 (C-6), 129.7 (C-7), 114.0 (C-8), 67.8 (C-1), 55.2 (C-10), 44.8 (C-3), 38.5 (C-4), 16.4 (C-5);

m/z [LRMS, ES+] (relative intensity, M) 231 (100, $[M-H+Na]^+$) 439 (53, $[2M+H+NH_4]^+$); [HRMS, ESI] Calcd. $(C_{12}H_{16}O_3+Na)^+$ 231.0992, found 231.0991;

By-product: **4-(4-Methoxyphenyl)-3-methylbutane-1,2-diol (116)**

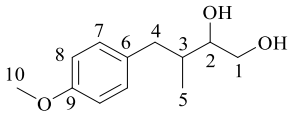

Flash column chromatography (20 – 60% EtOAc/pet. ether) yielded by-product title compound **116** (2 mg, 2%) as a colourless oil:

υ_{max} (film) 3271 (OH), 2927 (CH sp^3), 1508 (C=C aromatic) cm^{-1};

m/z [LRMS, ES+] (relative intensity, M) 233 (100, $[M+Na]^+$) 443 (19, $[2M+Na]^+$); [HRMS, ES+] Calcd. $(C_{12}H_{18}O_3+Na)^+$ 233.1154, found 233.1149;

Diastereomer 1:

^{1}H NMR (700 MHz, $CDCl_3$) δ = 7.11 or 7.09 (2H, d, *J* = 8.4 Hz, 7-H), 6.84 (2H, d, *J* = 8.4 Hz, 8-H), 3.80 (3H, s, 10-H), 3.75 - 3.78 (1H, m, 1-*H*H), 3.56 - 3.59 (1H, m, 1-H*H*), 3.53 - 3.56 (1H, m, 2-H), 2.91 (1H, dd, *J* = 13.6 Hz, *J* = 4.7 Hz, 4-*H*H), 2.39 (1H, dd, *J*

= 13.6 Hz, *J* = 4.3 Hz, 4-H*H*), 1.88 (1H, qdd, *J* = 6.8 Hz, *J* = 4.7 Hz, *J* = 4.3 Hz, 3-H), 1.66 (2H, br. s., OH), 0.84 (3H, d, *J* = 6.8 Hz, 5-H);

^{13}C NMR (176 MHz, $CDCl_3$) δ = 157.9 (C-9), 132.4 (C-6), 130.1 (C-7), 113.8 or 113.7 (C-8), 75.8 (C-2), 64.7 (C-1), 55.2 (C-10), 38.3 (C-4), 38.1 (C-3), 14.0 (C-5);

Diastereomer 2:

^{1}H NMR (700 MHz, $CDCl_3$) δ = 7.11 or 7.09 (2H, d, *J* = 8.4 Hz, 7-H), 6.84 (2H, d, *J* = 8.4 Hz, 8-H), 3.80 (3H, s, 10-H), 3.64 - 3.67 (1H, m, 1-*H*H), 3.63 - 3.64 (1H, m, 2-H), 3.61 - 3.63 (1H, m, 1-H*H*), 2.75 (1H, dd, *J* = 13.6 Hz, *J* = 6.6 Hz, 4-*H*H), 2.42 (1H, dd, *J* = 13.7 Hz, *J* = 5.3 Hz, 4-H*H*), 1.85 (1H, qdd, *J* = 6.8 Hz, *J* = 6.6 Hz, *J* = 5.3 Hz, 3-H), 1.66 (2H, br. s., OH), 0.91 (3H, d, *J* = 6.8 Hz, 5-H);

^{13}C NMR (176 MHz, $CDCl_3$) δ = 157.9 (C-9), 132.5 (C-6), 130.0 (C-7), 113.8 or 113.7 (C-8), 74.5 (C-2), 65.3 (C-1), 55.2 (C-10), 38.8 (C-4), 37.8 (C-3), 15.2 (C-5);

4-(4-Hydroxy-2-methyl-3-oxobutyl)benzonitrile (88)

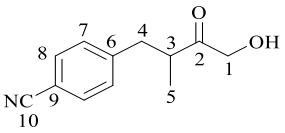

Following ***General Procedure 3***, compound **65** (80 mg, 0.398 mmol, 1 eq.) was chemically reduced.

Title compound **88** (57 mg, 70%) was afforded as a colourless oil:

R_f 0.28 (40% EtOAc/pet. ether);

υ_{max} (film) 3462 (OH), 2970 (CH sp^3), 2225 (CN), 1713 (C=O), 1606 (C=C aromatic) cm^{-1};

^{1}H NMR (700 MHz, $CDCl_3$) δ = 7.59 (2H, d, *J* = 8.2 Hz, 8-H), 7.25 (2H, d, *J* = 8.2 Hz, 7-H), 4.32 (1H, d, *J* = 19.2 Hz, 1-*H*H), 4.00 (1H, d, *J* = 19.2 Hz, 1-H*H*), 3.10 (1H, dd, *J* = 13.6 Hz, *J* = 7.7 Hz, 4-*H*H), 2.85 (1H, ddq, *J* = 7.7 Hz, *J* = 7.0 Hz, *J* = 7.0 Hz, 3-H), 2.74 (1H, dd, *J* = 13.6 Hz, *J* = 7.0 Hz, 4-H*H*), 1.18 (3H, d, *J* = 7.0 Hz, 5-H);

^{13}C NMR (176 MHz, $CDCl_3$) δ = 212.0 (C-2), 144.5 (C-6), 132.4 (C-8), 129.7 (C-7), 118.7 (C-10), 110.7 (C-9), 67.5 (C-1), 44.0 (C-3), 38.7 (C-4), 16.7 (C-5);

m/z [LRMS, ES-] (relative intensity, M) 237.9 (100, $[M+Cl]^-$); [HRMS, ESI] Calcd. $(C_{12}H_{13}NO_2+H)^+$ 204.1019, found 204.1020;

4-(3-Fluorophenyl)-1-hydroxy-3-methylbutan-2-one (89)

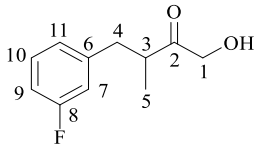

Following ***General Procedure 3***, compound **66** (50 mg, 0.257 mmol, 1 eq.) was chemically reduced.

Flash column chromatography (5 – 30% EtOAc/pet. ether) yielded title compound **89** (37 mg, 73%) as a yellow oil:

υ_{max} (film) 3443 (OH), 2970 (CH sp^3), 1711 (C=O), 1586 (C=C aromatic) cm^{-1};

^{1}H NMR (700 MHz, $CDCl_3$) δ = 7.25 (1H, ddd, *J* = 8.3 Hz, *J* = 7.5 Hz, *J* = 6.1 Hz, 10-H), 6.93 (1H, ddd, *J* = 8.4 Hz, *J* = 8.3 Hz, *J* = 2.2 Hz, 9-H), 6.91 (1H, d, *J* = 7.5 Hz, 11-H), 6.85 (1H, dd, *J* = 9.7 Hz, *J* = 2.2 Hz, 7-H), 4.29 (1H, d, *J* = 19.2 Hz, 1-*H*H), 3.99 (1H, d, *J* = 19.2 Hz, 1-H*H*), 3.01 (1H, dd, J = 13.7 Hz, *J* = 7.7 Hz, 4-*H*H), 2.83 (1H, ddq, *J* = 7.7 Hz, *J* = 7.0 Hz, *J* = 6.9 Hz, 3-H), 2.68 (1H, dd, *J* = 13.6 Hz, *J* = 7.0 Hz, 4-H*H*), 1.17 (3H, d, *J* = 6.9 Hz, 5-H);

^{13}C NMR (176 MHz, $CDCl_3$) δ = 212.6 (C-2), 162.9 (C-8), 141.4 (C-6), 130.1 (C-10), 124.5 (C-11), 115.7 (C-7), 113.6 (C-9), 67.7 (C-1), 44.3 (C-3), 38.7 (C-4), 16.6 (C-5);

^{19}F NMR (659 MHz, $CDCl_3$) δ = -113.0 (1F, ddd, *J* = 9.2 Hz, *J* = 8.3 Hz, *J* = 6.1 Hz, 8-F);

[HRMS, ESI] Calcd. $(C_{11}H_{13}FO_2+Na)^+$ 219.0797, found 219.0797;

(2*R*,3*S*)-2-Amino-3-methyl-4-phenylbutan-1-ol [(2*R*,3*S*)-100]

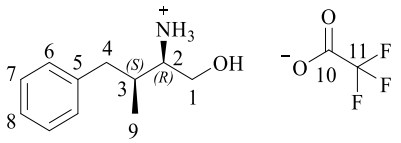

Preparative scale NCR – 13-TAm biotransformations via a two-step, one-pot cascade was performed, as described in experimental procedures.

Preparative HPLC (***Method J***) afforded title compound (2*R*,3*S*)-**100** (11 mg, 30%) as a fine off-white solid:

R_t 19.3 min (***Method J***);

$[\alpha]_D^{20}$ +480 (c. 0.1, H_2O);

υ_{max} (solid) 3310 (NH_2), 3064 (OH), 2973 (CH sp^3), 1678 (C=O), 1454 (C=C aromatic) cm^{-1};

^{1}H NMR (600 MHz, D_2O) δ = 7.30 (2H, dd, *J* = 8.3 Hz, *J* = 7.4 Hz, 7-H), 7.22 (1H, d, *J* = 7.4 Hz, 8-H), 7.20 (2H, d, *J* = 8.3 Hz, 6-H), 3.81 (1H, dd, *J* = 12.3 Hz, *J* = 4.0 Hz, 1-*H*H), 3.67 (1H, dd, *J* = 12.3 Hz, *J* = 8.2 Hz, 1-H*H*), 3.19 (1H, ddd, *J* = 8.2 Hz, *J* = 5.2 Hz, *J* = 4.0 Hz, 2-H), 2.79 (1H, dd, *J* = 13.5 Hz, *J* = 5.2 Hz, 4-*H*H), 2.42 (1H, dd, *J* = 13.6 Hz, *J* = 9.7 Hz, 4-H*H*), 2.08 (1H, dqdd, *J* = 9.7 Hz, *J* = 6.9 Hz, *J* = 5.2 Hz, *J* = 5.2 Hz, 3-H), 0.84 (3H, d, *J* = 6.9 Hz, 9-H);

^{13}C NMR (151 MHz, D_2O) δ = 163.7 (q, *J* = 35.7 Hz, C-10), 140.2 (C-5), 129.9 (C-6), 129.3 (C-7), 127.2 (C-8), 117.0 (q, 291.6 Hz, C-11), 60.6 (C-1), 57.7 (C-2), 38.9 (C-4), 34.8 (C-3), 14.5 (C-9);

m/z [HRMS, ESI] Calcd. $(C_{11}H_{17}NO+H)^+$ 180.1383, found 180.1380;

(2*S*,3*S*)-2-amino-3-methyl-4-phenylbutan-1-ol [(2*S*,3*S*)-100]

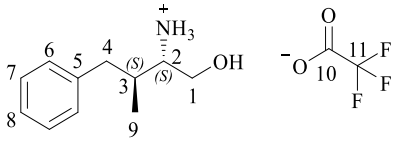

Preparative scale NCR – Mv-TAm biotransformations via a two-step, one-pot cascade was performed, as described in experimental procedures.

Preparative HPLC (***Method J***) afforded title compound (2*S*,3*S*)-**100** (59 mg, 32%) as a fine off-white solid:

R_t 19.4 min (***Method J***);

$[\alpha]_D^{20}$ +4 (c. 0.1, H_2O);

υ_{max} (solid) 3325 (NH_2), 3087 (OH), 2972 (CH sp^3), 1676 (C=O), 1513 (C=C aromatic) cm^{-1};

^{1}H NMR (700 MHz, D_2O) δ = 7.39 (2H, dd, *J* = 8.1 Hz, *J* = 7.4 Hz, 7-H), 7.31 (1H, d, *J* = 7.4 Hz, 8-H), 7.30 (2H, d, *J* = 8.1 Hz, 6-H), 3.96 (1H, dd, *J* = 12.3 Hz, *J* = 3.7 Hz, 1-*H*H), 3.75 (1H, dd, *J* = 12.3 Hz, *J* = 8.7 Hz, 1-H*H*), 3.27 (1H, ddd, *J* = 8.7 Hz, *J* = 5.5 Hz, *J* = 3.7 Hz, 2-H), 2.85 (1H, dd, *J* = 13.6 Hz, *J* = 5.8 Hz, 4-*H*H), 2.53 (1H, dd, *J* =

13.6 Hz, *J* = 9.5 Hz, 4-H*H*), 2.20 (1H, dqdd, *J* = 9.5 Hz, *J* = 6.9 Hz, *J* = 5.8 Hz, *J* = 5.5 Hz, 3-H), 0.91 (3H, d, *J* = 6.9 Hz, 9-H);

^{13}C NMR (176 MHz, D_2O) δ = 163.7 (q, *J* = 30.5 Hz, C-10), 140.2 (C-5), 129.8 (C-6), 129.3 (C-7), 127.2 (C-8), 116.4 (q, *J* = 292.5 Hz, C-11), 59.4 (C-1), 57.4 (C-2), 39.0 (C-4), 35.6 (C-3), 14.1 (C-9);

m/z [HRMS, ESI] Calcd. $(C_{11}H_{17}NO+H)^+$ 180.1383, found 180.1382;

3-Phenylbutan-1-ol (111)

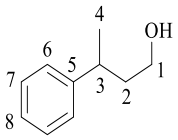

To a flame-dried round bottom flask purged with Ar was added ethyl (*E*)-3-phenylbut-2-enoate (0.750 mL, 3.94 mmol) and dry THF (15 mL). The solution was cooled to 0 °C prior to $LiAlH_4$ (1 M in THF, 4.73 mL, 4.73 mmol) being added dropwise. The solution was stirred for 1 h at room temperature and was then quenched with H_2O (5 mL) and extracted with EtOAc (3 × 40 mL). The combined organic layers were dried ($MgSO_4$) and the solvent removed *in vacuo* to afford the title compound **111** (0.568 g, 96%) as a colourless oil:

R_f 0.36 (20% EtOAc/pet. ether);

υ_{max} (oil) 3290 (OH), 2955 (CH sp^3), 1450 (C=C aromatic) cm^{-1};

^{1}H NMR (700 MHz, $CDCl_3$) δ = 7.30 - 7.33 (2H, m, 7-H), 7.22 (2H, m, 6-H), 7.21 (1H, m, 8-H), 3.57 - 3.61 (1H, m, 1-*H*H), 3.53 - 3.57 (1H, m, 1-H*H*), 2.90 (1H, qdd, *J* = 7.2 Hz, *J* = 7.0 Hz, 3-H), 1.87 - 1.89 (1H, m, 2-*H*H), 1.85 - 1.87 (1H, m, 2-H*H*), 1.30 (3H, d, *J* = 7.2 Hz, 4-H);

^{13}C NMR (176 MHz, $CDCl_3$) δ = 146.8 (C-5), 128.4 (C-7), 126.9 (C-6), 126.1 (C-8), 61.2 (C-1), 40.9 (C-2), 36.4 (C-3), 22.4 (C-4);

m/z [LRMS, CI] (relative intensity, M) 168 (100, $[M+NH_4]^+$); [HRMS, ESI] Calcd. $(C_{10}H_{14}O+NH_4)^+$ 168.1383, found 168.1383;

Data was in agreement with the literature.[315]

4-(2-Fluoro-3-oxoheptyl)benzonitrile (105)

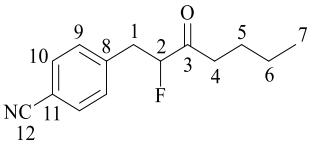

Three cycles of vacuum/Ar provided the suspension of 2 mol% palladium on carbon (10% wt.), compound (*E*)-**104** (30 mg, 0.130 mmol, 1 eq.) and 1 mol% diphenylsulfide in EtOAc (1 mL) with an inert atmosphere. At 0 °C, vacuum was applied followed by hydrogen. The reaction mixture was left to stir at 0 °C under a hydrogen atmosphere for 1 h and was then filtered through celite, had the solvent removed *in vacuo* and subjected to flash column chromatography (3% EtOAc/pet. ether) to yield title compound **105** (3 mg, 10%) was afforded as a colourless oil:

R_f 0.42 (10% EtOAc/pet. ether);
υ_{max} (film) 2927 (CH sp^3), 2226 (CN), 1719 (C=O), 1607 (C=C aromatic) cm^{-1};
^{1}H NMR (700 MHz, $CDCl_3$) δ = 7.62 (2H, d, *J* = 8.1 Hz, 10-H), 7.35 (2H, d, *J* = 8.1 Hz, 9-H), 4.96 (1H, ddd, *J* = 49.5 Hz, *J* = 7.7 Hz, *J* = 3.6 Hz, 2-H), 3.26 (1H, ddd, *J* = 28.6 Hz, *J* = 14.7 Hz, *J* = 3.6 Hz, 1-*H*H), 3.12 (1H, ddd, *J* = 25.7 Hz, *J* = 14.7 Hz, *J* = 7.7 Hz, 1-H*H*), 2.54 - 2.63 (1H, m, 4-*H*H), 2.35 - 2.43 (1H, m, 4-H*H*), 1.47 - 1.55 (2H, m, 5-H), 1.24 - 1.31 (2H, m, 6-H), 0.88 (3H, t, *J* = 7.4 Hz, 7-H);
^{13}C NMR (176 MHz, $CDCl_3$) δ = 209.2 (d, *J* = 24.8 Hz, C-3), 141.1 (C-8), 132.3 (C-10), 130.4 (C-9), 118.7 (C-12), 111.2 (C-11), 95.2 (d, *J* = 188.8 Hz, C-2), 38.3 (C-4), 38.1 (d, *J* = 20.2 Hz, C-1), 24.5 (C-5), 22.1 (C-6), 13.7 (C-7);
m/z [LRMS, ES+] (relative intensity, M) 142 (77, $[M\text{-}C_6H_9NO+Na]^+$); [HRMS, ESI] Calcd. $(C_{14}H_{16}FNO+H)^+$ 234.1289, found 234.1288;

Ethyl (*E*)-3-(4-cyanophenyl)-2-fluoroacrylate [(*E*)-109a]

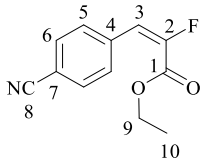

Following ***General Procedure 5***, Horner-Wadsworth-Emmons reaction with 4-formylbenzonitrile (250 mg, 1.91 mmol) and diethoxyphosphoryl-2-fluoroacetate (425 µL, 2.10 mmol) was performed.

Flash column chromatography (5 – 30% EtOAc/pet. ether) yielded title compound (*E*)-**109a** (97 mg, 23%) as a white solid:

R_f 0.44 (20% EtOAc/pet. ether);

m.p. 83 – 83 ºC;

υ_{max} (solid) 2986 (CH sp^3), 2225 (CN), 1720 (C=O), 1401 (C=C aromatic) cm^{-1};

^{1}H NMR (600 MHz, $CDCl_3$) δ = 7.65 (2H, d, *J* = 8.3 Hz, 6-H), 7.55 (2H, d, *J* = 8.2 Hz, 5-H), 6.88 (1H, d, *J* = 20.6 Hz, 3-H), 4.26 (2H, q, *J* = 7.1 Hz, 9-H), 1.26 (3H, t, *J* = 7.1 Hz, 10-H);

^{13}C NMR (151 MHz, $CDCl_3$) δ = 159.9 (d, *J* = 36.1 Hz, C-1), 148.1 (d, *J* = 262.6 Hz, C-2), 135.9 (d, *J* = 9.6 Hz, C-4), 131.8 (s, C-6), 130.2 (d, *J* = 2.4 Hz, C-5), 119.5 (d, *J* = 27.7 Hz, C-3), 118.5 (s, C-8), 112.1 (s, C-7), 62.1 (s, C-9), 13.8 (s, C-10);

^{19}F NMR (376 MHz, $CDCl_3$) δ = -113.2 (1F, d, *J* = 20.4 Hz, 2-F);

m/z [LRMS, ESI] (relative intensity, M) 261 (27, $[M+CH_3CN+H]^+$), 220 (100, $[M+H]^+$);

Data was in agreement with the literature.[320]

Ethyl (*Z*)-3-(4-cyanophenyl)-2-fluoroacrylate [(*Z*)-109a]

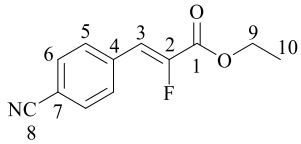

Following ***General Procedure 4***, $TiCl_4$ mediated aldol condensation with 4-cyanobenzaldehyde (500 mg, 3.81 mmol, 1 eq.) and ethyl fluoroacetate (405 µL, 4.19 mmol, 1.1 eq.) was performed.

Flash column chromatography (5 – 30% EtOAc/pet. ether) yielded title compound (*Z*)-**109a** (191 mg, 23%) as a fine white solid:

R_f 0.64 (20% EtOAc/pet. ether);

m.p. 118 ºC;

υ_{max} (solid) 3000 (CH sp^3), 2223 (CN), 1717 (C=O), 1505 (C=C aromatic) cm^{-1};

^{1}H NMR (700 MHz, $CDCl_3$) δ = 7.74 (2H, d, *J* = 8.6 Hz, 5-H), 7.70 (2H, d, *J* = 8.6 Hz, 6-H), 6.95 (1H, d, *J* = 33.8 Hz, 3-H), 4.38 (2H, q, *J* = 7.1 Hz, 9-H), 1.40 (3H, t, *J* = 7.1 Hz, 10-H);

^{13}C NMR (176 MHz, $CDCl_3$) δ = 160.7 (d, *J* = 34.3 Hz, C-1), 148.7 (d, *J* = 274.3 Hz, C-2), 135.5 (d, *J* = 4.6 Hz, C-4), 132.5 (s, C-6), 130.5 (d, *J* = 8.4 Hz, C-5), 118.3 (s, C-8), 115.3 (d, *J* = 4.6 Hz, C-3), 112.8 (d, *J* = 3.4 Hz, C-7), 62.4 (s, C-9), 14.2 (s, C-10);

^{19}F NMR (659 MHz, $CDCl_3$) δ = -120.2 (1 F, d, *J* = 33.8 Hz, F-2);

[HRMS, ESI] Calcd. $(C_{12}H_{10}FNO_2+H)^+$ 220.0768, found 220.0768;

Data was in agreement with the literature.[297]

Ethyl (*E*)-2-fluoro-3-(4-(trifluoromethyl)phenyl)acrylate [(*E*)-109b]

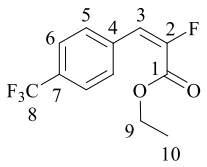

Following ***General Procedure 5***, Horner-Wadsworth-Emmons reaction 4-(trifluoromethyl)benzaldehyde (250 mg, 1.44 mmol) and diethoxyphosphoryl-2-fluoroacetate (291 µL, 1.58 mmol) was performed.

Flash column chromatography (1 – 4% EtOAc/pet. ether) yielded title compound (*E*)-**109b** (78 mg, 21%) as a colourless oil:

υ_{max} (film) 2988 (CH sp^3), 1732 (C=O), 1322 (C=C aromatic) cm^{-1};

^{1}H NMR (600 MHz, $CDCl_3$) δ = 7.62 (2H, d, *J* = 8.2 Hz, 6-H), 7.55 (2H, d, *J* = 8.3 Hz, 5-H), 6.93 (1H, d, *J* = 21.1 Hz, 3-H), 4.26 (2H, q, *J* = 7.1 Hz, 9-H), 1.25 (3H, t, *J* = 7.2 Hz, 10-H);

^{13}C NMR (151 MHz, $CDCl_3$) δ = 160.0 (d, *J* = 36.1 Hz, C-1), 148.0 (d, *J* = 257.8 Hz, C-2), 134.8 (d, *J* = 9.6 Hz, C-4), 130.4 (q, *J* = 32.5 Hz, C-7), 129.8 (d, *J* = 2.4 Hz, C-5), 124.9 (q, *J* = 3.6 Hz, C-6), 123.9 (q, *J* = 273.5 Hz, C-8), 119.9 (d, *J* = 26.5 Hz, C-3), 61.9 (s, C-9), 13.8 (s, C-10);

^{19}F NMR (659 MHz, $CDCl_3$) δ = -62.8 (1F, s, 2-F), -114.6 (3F, d, *J* = 21.2 Hz, 8-F);

m/z [LRMS, EI] (relative intensity, M) 262 (52, $[M+H]^+$), 169 (100, $[M-C_5H_5FO_2+Na]^+$);

Data was in agreement with the literature.[321]

Ethyl (*Z*)-2-fluoro-3-(4-(trifluoromethyl)phenyl)acrylate [(*Z*)-109b]

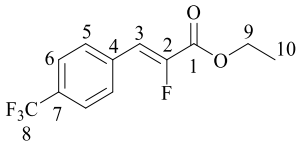

Following ***General Procedure 4***, $TiCl_4$ mediated aldol condensation with 2-(trifluoromethyl)benzaldehyde (392 µL, 2.87 mmol, 1eq.) and ethyl fluoroacetate (305 µL, 3.16 mmol, 1.1 eq.) was performed.

Flash column chromatography (2 – 8% EtOAc/pet. ether) yielded title compound (*Z*)-**109b** (354 mg, 47%) as a fine white solid:

R_f 0.49 (5% EtOAc/pet. ether);

m.p. 50 – 52 ºC;

υ_{max} (solid) 3001 (CH sp^3), 1720 (C=O), 1373 (C=C aromatic) cm^{-1};

^{1}H NMR (700 MHz, $CDCl_3$) δ = 7.75 (2H, d, *J* = 8.4 Hz, 5-H), 7.66 (2H, d, *J* = 8.4 Hz, 6-H), 6.95 (1H, d, *J* = 35.1 Hz, 3-H), 4.38 (2H, q, *J* = 7.2 Hz, 9-H), 1.40 (3H, t, *J* = 7.2 Hz, 10-H);

^{13}C NMR (176 MHz, $CDCl_3$) δ = 160.8 (d, *J* = 38.5 Hz, C-1), 148.4 (d, *J* = 266.3 Hz, C-2), 134.5 (d, *J* = 4.6 Hz, C-7), 131.0 (s, C-4), 130.3 (d, *J* = 8.4 Hz, C-5), 125.7 (q, *J* = 3.8 Hz, C-6), 123.8 (q, *J* = 271.6 Hz, C-8), 115.8 (d, *J* = 4.2 Hz, C-3), 62.2 (s, C-9), 14.2 (s, C-10);

^{19}F NMR (659 MHz, $CDCl_3$) δ = -63.0 (3F, s, 8-F), -122.0 (1F, d, *J* = 34.6 Hz, 2-F);

m/z [LRMS, ES+] (relative intensity, M) 334 (100, $[M+CH_3OH+K]^+$), 295 (19, $[M+CH_3OH+H]^+$);

Data was in agreement with the literature.[322]

Ethyl (*E*)-2-fluoro-3-(2-(trifluoromethyl)phenyl)acrylate [(*E*)-109c]

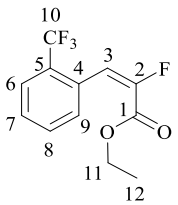

Following ***General Procedure 5***, Horner-Wadsworth-Emmons reaction with 4-(trifluoromethyl)benzaldehyde (250 mg, 1.44 mmol) and diethoxyphosphoryl-2-fluoroacetate (382 mg, 1.58 mmol) was performed.

Flash column chromatography (2 – 4% EtOAc/pet. ether) yielded title compound (*E*)-**109c** (180 mg, 48%) as a colourless oil:

υ_{max} (film) 2989 (CH sp^3), 1735 (C=O), 1315 (C=C aromatic) cm^{-1};

^{1}H NMR (700 MHz, $CDCl_3$) δ = 7.70 (1H, d, *J* = 7.8 Hz, 6-H), 7.53 (1H, dd, *J* = 7.7 Hz, *J* = 7.6 Hz, 8-H), 7.46 (1H, dd, *J* = 7.8 Hz, *J* = 7.7 Hz, 7-H), 7.37 (1H, d, *J* = 7.6 Hz, 9-H), 7.08 (1H, d, *J* = 17.9 Hz, 3-H), 4.11 (2H, q, *J* = 7.2 Hz, 11-H), 1.06 (3H, t, *J* = 7.2 Hz, 12-H);

^{13}C NMR (176 MHz, $CDCl_3$) δ = 159.8 (d, *J* = 37.0 Hz, C-1), 148.3 (d, *J* = 259.4 Hz, C-2), 131.3 (s, C-8), 131.0 (d, *J* = 2.7 Hz, C-9), 130.5 (dq, *J* = 9.9, 1.9 Hz, C-4), 128.3 (s, C-7), 128.2 (dd, *J* = 30.1, 3.1 Hz, C-5), 125.7 (q, *J* = 5.3 Hz, C-6), 123.9 (q, *J* = 273.5 Hz, C-10), 117.6 (d, *J* = 26.7 Hz, C-3), 61.6 (s, C-11), 13.6 (s, C-12);

^{19}F NMR (659 MHz, $CDCl_3$) δ = -61.0 (3F, d, *J* = 0.9 Hz, 10-F), -116.0 (1F, d, *J* = 17.9 Hz, 2-F);

[HRMS, ESI] Calcd. $(C_{12}H_{10}F_4O_2+H)^+$ 263.0690, found 229.0688;

Ethyl (*Z*)-2-fluoro-3-(2-(trifluoromethyl)phenyl)acrylate [(*Z*)-109c]

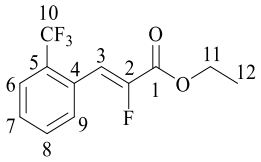

Following ***General Procedure 4***, $TiCl_4$ mediated aldol condensation with 2-(trifluoromethyl)benzaldehyde (379 µL, 2.87 mmol, 1eq.) and ethyl fluoroacetate (305 µL, 3.16 mmol, 1.1 eq.) was performed.

Flash column chromatography (2 – 8% EtOAc/pet. ether) yielded title compound (*Z*)-**109c** (487 mg, 65%) as a yellow oil:

υ_{max} (film) 2987 (CH sp^3), 1732 (C=O), 1373 (C=C aromatic) cm^{-1};

^{1}H NMR (700 MHz, MeOD-d_4) δ = 7.94 (1H, d, *J* = 7.8 Hz, 9-H), 7.79 (1H, d, *J* = 7.8 Hz, 6-H), 7.69 (1H, dd, *J* = 7.8 Hz, *J* = 7.8 Hz, 8-H), 7.57 (1H, t, *J* = 7.8 Hz, *J* = 7.8 Hz, 7-H), 7.25 (1H, dq, *J* = 32.0 Hz, *J* = 1.6 Hz, 3-H), 4.37 (2H, q, *J* = 7.1 Hz, 11-H), 1.37 (3H, t, *J* = 7.1 Hz, 12-H);

^{13}C NMR (176 MHz, MeOD-d_4) δ = 162.1 (d, *J* = 35.1 Hz, C-1), 149.7 (d, *J* = 269.3 Hz, C-2), 133.7 (s, C-8), 132.8 (d, *J* = 11.4 Hz, C-9), 130.8 (d, *J* = 1.1 Hz, C-7), 130.2

(q, *J* = 1.9 Hz, C-4), 129.8 (qd, *J* = 30.1, 1.1 Hz, C-5), 127.4 (q, *J* = 5.5 Hz, C-6), 125.6 (q, *J* = 273.1 Hz, C-10), 113.5 (dq, *J* = 4.6, 2.3 Hz, C-3), 63.6 (s, C-11), 14.5 (s, C-12); ^{19}F NMR (659 MHz, MeOD-d_4) δ = -61.1 (1F, s, 2-F), -125.5 (3F, d, *J* = 32.0 Hz, 10-F); [HRMS, ESI] Calcd. $(C_{12}H_{10}F_4O_2+H)^+$ 263.0690, found 263.0691;

Ethyl (*E*)-2-fluoro-3-(4-nitrophenyl)acrylate [(*E*)-109d]

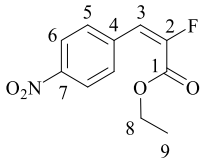

Following ***General Procedure 5***, the Horner-Wadsworth-Emmons reaction with 4-nitrobenzaldehyde (250 mg, 1.65 mmol) and diethoxyphosphoryl-2-fluoroacetate (369 µL, 1.82 mmol) was performed.

Flash column chromatography (3 – 50% EtOAc/pet. ether) yielded title compound (*E*)-**109d** (187 mg, 47%) as a light yellow solid:

m.p. 62 – 63 ºC;

υ_{max} (solid) 2987 (CH sp^3), 1723 (C=O), 1514 (C=C aromatic) cm^{-1};

^{1}H NMR (600 MHz, $CDCl_3$) δ = 8.22 (1H, d, *J* = 8.5 Hz, 6-H), 7.61 (1H, d, *J* = 8.5 Hz, 5-H), 6.93 (1H, d, *J* = 20.7 Hz, 3-H), 4.27 (1H, q, *J* = 7.1 Hz, 8-H), 1.26 (2H, t, *J* = 7.1 Hz, 9-H);

^{13}C NMR (151 MHz, $CDCl_3$) δ = 159.8 (d, *J* = 36.1 Hz, C-1), 148.4 (d, *J* = 263.8 Hz, C-2), 147.5 (s, C-7), 137.9 (d, *J* = 10.8 Hz, C-4), 130.4 (d, *J* = 3.6 Hz, C-5), 123.2 (s, C-6), 119.1 (d, *J* = 26.5 Hz, C-3), 62.1 (s, C-8), 13.8 (s, C-9);

^{19}F NMR (376 MHz, $CDCl_3$) δ = -112.5 (1F, d, *J* = 20.4 Hz, 2-F);

m/z [LRMS, ES+] (relative intensity, M) 294 (100, $[M+Na+CH_3OH]^+$), 262 (33, $[M+Na]^+$);

Data was in agreement with the literature.[323]

Ethyl (*Z*)-2-fluoro-3-(4-nitrophenyl)acrylate [(*Z*)-109d]

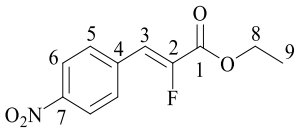

Following ***General Procedure 4***, $TiCl_4$ mediated aldol condensation with 4-nitrobenzaldehyde (500 mg, 3.31 mmol, 1eq.) and ethyl fluoroacetate (352 µL, 3.64 mmol, 1.1 eq.) was performed.

Flash column chromatography (3 – 40% EtOAc/pet. ether) yielded title compound (*Z*)-**109d** (130 mg, 16%) as a fine red solid:

R_f 0.63 (20% EtOAc/pet. ether);

m.p. 124 – 126 ºC (lit. m.p. 131 ºC)[320];

υ_{max} (solid) 2996 (CH sp^3), 1721 (C=O), 1594 (C=C aromatic) cm^{-1};

^{1}H NMR (700 MHz, $CDCl_3$) δ = 8.26 (2H, d, *J* = 8.9 Hz, H-6), 7.80 (2H, d, *J* = 8.9 Hz, H-5), 6.98 (1H, d, *J* = 33.7 Hz, H-3), 4.39 (2H, q, *J* = 7.2 Hz, H-8), 1.41 (3H, t, *J* = 7.2 Hz, H-9);

^{13}C NMR (176 MHz, $CDCl_3$) δ = 160.5 (d, *J* = 36.6 Hz, C-1), 148.9 (d, *J* = 275.8 Hz, C-2), 147.8 (s, C-7), 137.3 (d, *J* = 4.2 Hz, C-4), 130.8 (d, *J* = 8.4 Hz, C-5), 124.0 (s, C-6), 114.9 (d, *J* = 4.2 Hz, C-3), 62.4 (s, C-8), 14.1 (s, C-9);

^{19}F NMR (659 MHz, $CDCl_3$) δ = -119.6 (1F, d, *J* = 33.7 Hz, F-2);

m/z [LRMS, ES+] (relative intensity, M) 272 (16, $[M+CH_3OH+H]^+$), 319 (100, $[M+DMSO+H]^+$);

Data was in agreement with the literature.[322]

Ethyl (*Z*)-3-(4-chlorophenyl)-2-fluoroacrylate [(*E*)-109e]

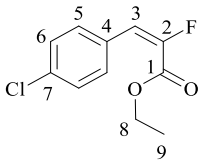

Following ***General Procedure 5***, Horner-Wadsworth-Emmons reaction with 4-chlorobenzaldehyde (250 mg, 1.78 mmol) and diethoxyphosphoryl-2-fluoroacetate (474 mg, 1.96 mmol) was performed.

Flash column chromatography (2 – 10% EtOAc/pet. ether) yielded title compound (*E*)-**109e** (176 mg, 43%) as a colourless oil:

υ_{max} (film) 2984 (CH sp^3), 1728 (C=O), 1490 (C=C aromatic) cm^{-1};

^{1}H NMR (700 MHz, $CDCl_3$) δ = 7.43 (2H, d, *J* = 8.7 Hz, 5-H), 7.33 (2H, d, *J* = 8.7 Hz, 6-H), 6.85 (1H, d, *J* = 22.0 Hz, 3-H), 4.27 (2H, q, *J* = 7.2 Hz, 8-H), 1.28 (3H, t, *J* = 7.2 Hz, 9-H);

^{13}C NMR (176 MHz, $CDCl_3$) δ = 160.3 (d, *J* = 35.5 Hz, C-1), 147.2 (d, *J* = 257.5 Hz, C-2), 134.7 (C-7), 131.1 (d, *J* = 2.7 Hz, C-5), 129.4 (d, *J* = 9.9 Hz, C-4), 128.3 (C-6), 120.4 (d, *J* = 27.1 Hz, C-3), 61.8 (C-8), 13.9 (C-9);

^{19}F NMR (659 MHz, $CDCl_3$) δ = -116.1 (1F, d, *J* = 21.2 Hz, 2-F);

[HRMS, ESI] Calcd. $(C_{11}H_{10}FO_2Cl+H)^+$ 229.0426, found 229.0426;

Data was in agreement with the literature.[324]

Ethyl (*Z*)-3-(4-chlorophenyl)-2-fluoroacrylate [(*Z*)-109e]

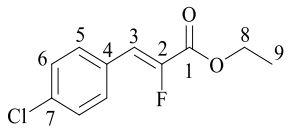

Following ***General Procedure 4***, $TiCl_4$ mediated aldol condensation with 4-chlorobenzaldehyde (500 mg, 3.56 mmol, 1 eq.) and ethyl fluoroacetate (378 µL, 3.91 mmol, 1.1 eq.) was performed.

Flash column chromatography (5 – 40% EtOAc/pet. ether) yielded title compound (*Z*)-**109e** (238 mg, 29%) as a fine white solid:

m.p. 54 – 55 ºC (lit. m.p. 55 – 57 ºC)[325];

υ_{max} (solid) 2991 (CH sp^3), 1718 (C=O), 1490 (C=C aromatic) cm^{-1};

^{1}H NMR (600 MHz, $CDCl_3$) δ = 7.59 (2H, d, *J* = 8.5 Hz, 5-H), 7.39 (2H, d, *J* = 8.5 Hz, 6-H), 6.89 (1H, d, *J* = 34.8 Hz, 3-H), 4.36 (2H, q, *J* = 7.1 Hz, 8-H), 1.39 (3H, t, *J* = 7.1 Hz, 9-H);

^{13}C NMR (151 MHz, $CDCl_3$) δ = 161.2 (d, *J* = 34.9 Hz, C-1), 147.2 (d, *J* = 268.6 Hz, C-2), 135.6 (d, *J* = 4.8 Hz, C-7), 131.4 (d, *J* = 8.4 Hz, C-5), 129.6 (d, *J* = 4.8 Hz, C-4), 129.1 (s, C-6), 116.2 (d, *J* = 4.8 Hz, C-3), 62.0 (s, C-8), 14.2 (s, C-9);

^{19}F NMR (659 MHz, $CDCl_3$) δ = -124.4 (d, *J* = 34.6 Hz, 2-F);

m/z [LRMS, ES+] (relative intensity, M) 229 (100, $[M^{35}Cl+H]^+$), 231 (18, $[M^{37}Cl+H]^+$);

Data was in agreement with the literature.[322]

Ethyl (*E*)-3-(4-bromophenyl)-2-fluoroacrylate [(*E*)-109f]

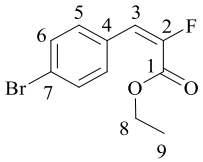

Following ***General Procedure 5***, Horner-Wadsworth-Emmons reaction 4-bromobenzaldehyde (250 mg, 1.35 mmol) and diethoxyphosphoryl-2-fluoroacetate (301 µL, 1.49 mmol) was performed.

Flash column chromatography (2 – 8% EtOAc/pet. ether) to yield title compound (*E*)-**109f** (150 mg, 41%) as a colourless oil:

R_f 0.37 (4% EtOAc/pet. ether);

υ_{max} (film) 2983 (CH sp^3), 1728 (C=O), 1487 (C=C aromatic) cm^{-1};

^{1}H NMR (600 MHz, $CDCl_3$) δ = 7.49 (2H, dd, *J* = 7.5 Hz, *J* = 1.2 Hz, 5-H), 7.35 (2H, dd, *J* = 7.5 Hz, *J* = 0.9 Hz, 6-H), 6.83 (1H, d, *J* = 22.1 Hz, 3-H), 4.27 (2H, qd, *J* = 7.1 Hz, *J* = 1.4 Hz, 8-H), 1.27 (3H, td, *J* = 7.1 Hz, *J* = 1.6 Hz, 9-H);

^{13}C NMR (151 MHz, $CDCl_3$) δ = 160.3 (d, *J* = 34.9 Hz, C-1), 147.1 (d, *J* = 256.6 Hz, C-2), 131.3 (d, *J* = 2.4 Hz, C-5), 131.2 (s, C-6), 129.8 (d, *J* = 9.6 Hz, C-4), 122.9 (s, C-7), 120.5 (d, *J* = 26.5 Hz, C-3), 61.8 (s, C-8), 13.9 (s, C-9);

^{19}F NMR (376 MHz, $CDCl_3$) δ = -115.9 (d, *J* = 21.8 Hz, 2-F);

m/z [LRMS, ESI] (relative intensity, M) 274 (100, $[M^{81}Br+H]^+$), 272 (95, $[M^{79}Br+H]^+$);

Data was in agreement with the literature.[324]

Ethyl (*Z*)-3-(4-bromophenyl)-2-fluoroacrylate [(*Z*)-109f]

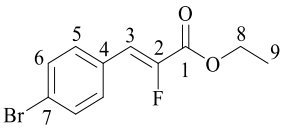

Following ***General Procedure 4***, $TiCl_4$ mediated aldol condensation with 4-bromobenzaldehyde (500 mg, 2.70 mmol, 1 eq.) and ethyl fluoroacetate (287 µL, 2.97 mmol, 1.1 eq.) was performed.

Flash column chromatography (2 – 10% EtOAc/pet. ether) yielded title compound (*Z*)-**109f** (304 mg, 41%) as a fine white solid:

R_f 0.66 (10% EtOAc/pet. ether);

m.p. 58 – 59 ºC (lit. m.p. 57 ºC)[320];

υ_{max} (solid) 2980 (CH sp^3), 1717 (C=O), 1487 (C=C aromatic) cm^{-1};

^{1}H NMR (700 MHz, $CDCl_3$) δ = 7.54 (2H, d, *J* = 8.4 Hz, 6-H), 7.51 (2H, dd, *J* = 8.4 Hz, *J* = 8.4 Hz, 5-H), 6.86 (1H, d, *J* = 34.6 Hz, 3-H), 4.36 (2H, q, *J* = 7.1 Hz, 8-H), 1.39 (3H, t, *J* = 7.2 Hz, 9-H);

^{13}C NMR (176 MHz, $CDCl_3$) δ = 161.1 (d, *J* = 34.3 Hz, C-1), 147.4 (d, *J* = 269.7 Hz, C-2), 132.1 (s, C-6), 131.6 (d, *J* = 8.4 Hz, C-5), 130.0 (d, *J* = 4.6 Hz, C-7), 124.0 (d, *J* = 3.8 Hz, C-4), 116.3 (d, *J* = 4.6 Hz, C-3), 62.0 (s, C-8), 14.2 (s, C-9);

^{19}F NMR (659 MHz, $CDCl_3$) δ = -124.0 (d, *J* = 34.3 Hz, F-2);

m/z [LRMS, ESI] (relative intensity, M) 229 (100, $[M^{79}Br+H]^+$), 275 (95, $[M^{81}Br+H]^+$);

Data was in agreement with the literature.[322]

Methyl (*Z*)-3-(4-cyanophenyl)-2-fluoroacrylate [(*Z*)-110a]

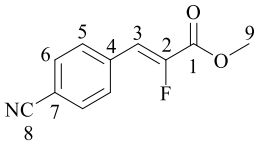

Following ***General Procedure 6***, transesterification of (*Z*)-**109a** (75 mg, 0.342 mmol, 1 eq.) was performed.

Following reaction completion by TLC analysis, the solvent was then removed *in vacuo*, $CHCl_3$ added, and suspension filtered through celite. The filtrate solvent was removed *in vacuo* to yield title compound (*Z*)-**110a** (51 mg, 73%) as a fine white solid: m.p. 146 – 147 ºC (lit. m.p. 152 – 154 ºC)[326];

υ_{max} (solid) 2959 (CH sp^3), 2224 (CN), 1723 (C=O), 1428 (C=C aromatic) cm^{-1};

^{1}H NMR (700 MHz, $CDCl_3$) δ = 7.74 (2H, d, *J* = 8.6 Hz, 5-H), 7.70 (2H, d, *J* = 8.6 Hz, 6-H), 6.92 (1H, d, *J* = 33.9 Hz, 3-H), 3.93 (3H, s, 9-H);

^{13}C NMR (176 MHz, $CDCl_3$) δ = 161.1 (d, *J* = 34.7 Hz, C-1), 148.4 (d, *J* = 274.7 Hz, C-2), 135.4 (d, *J* = 4.6 Hz, C-4), 132.5 (s, C-6), 130.5 (d, *J* = 8.4 Hz, C-5), 118.3 (s, C-8), 115.6 (d, *J* = 4.6 Hz, C-3), 112.9 (d, *J* = 3.4 Hz, C-7), 53.0 (s, C-9);

^{19}F NMR (659 MHz, $CDCl_3$) δ = -120.5 (d, *J* = 33.9 Hz, 2-F);

[HRMS, ESI] Calcd. $(C_{11}H_8FNO_2+CH_3OH+H)^+$ 238.0874, found 238.0874;

Data was in agreement with the literature.[326]

Methyl (*E*)-2-fluoro-3-(4-(trifluoromethyl)phenyl)acrylate [(*E*)-110b]

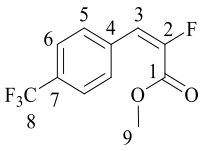

Following ***General Procedure 6***, transesterification of (*E*)-**109b** (45 mg, 0.172 mmol, 1 eq.) was performed.

Flash column chromatography (2 – 3% EtOAc/pet. ether) yielded title compound (*E*)-**110b** (14 mg, 33%) as a colourless oil:

υ_{max} (film) 1738 (C=O), 1323 (C=C aromatic) cm^{-1};

^{1}H NMR (600 MHz, $CDCl_3$) δ = 7.63 (2H, d, *J* = 8.2 Hz, 6-H), 7.57 (2H, d, *J* = 8.2 Hz, 5-H), 6.95 (1H, d, *J* = 21.4 Hz, 3-H), 3.81 (3H, s, 9-H);

^{13}C NMR (151 MHz, $CDCl_3$) δ = 160.5 (d, *J* = 34.9 Hz, C-1), 147.6 (d, *J* = 260.2 Hz, C-2), 134.5 (d, *J* = 9.6 Hz, C-4), 130.5 (q, *J* = 32.5 Hz, C-7), 129.8 (d, *J* = 2.4 Hz, C-5), 125.0 (q, *J* = 3.6 Hz, C-6), 123.9 (q, *J* = 273.5 Hz, C-8), 120.4 (d, *J* = 25.3 Hz, C-3), 52.5 (s, C-9);

^{19}F NMR (659 MHz, $CDCl_3$) δ = -62.8 (3F, d, *J* = 0.6 Hz, 8-F), -114.9 (1F, d, *J* = 21.2 Hz, 2-F);

m/z [LRMS, ESI] (relative intensity, M) 249 (40, $[M+H]^+$), 235 (71, $[M-CH_2+H]^+$), 219 (100, $[M-OCH_2+H]^+$); [HRMS, ESI] Calcd. $(C_{11}H_8F_4O_2+H)^+$ 249.0533, found 249.0532;

Methyl (*Z*)-2-fluoro-3-(4-(trifluoromethyl)phenyl)acrylate [(*Z*)-110b]

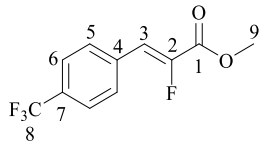

Following ***General Procedure 6***, transesterification of (*Z*)-**109b** (102 mg, 0.389 mmol, 1 eq.) was performed.

Following reaction completion by TLC analysis, the solvent was removed *in vacuo*, $CHCl_3$ added, and suspension filtered through Celite™. The filtrate solvent was removed *in vacuo* to yield title compound (*Z*)-**110b** (31 mg, 32%) as a fine white solid:

R_f 0.51 (5% EtOAc/pet. ether);

m.p. 84 – 86 ºC (lit. m.p. 90 – 92 ºC)[326];

υ_{max} (solid) 2958 (CH sp^3), 1730 (C=O), 1440 (C=C aromatic) cm^{-1};

^{1}H NMR (600 MHz, $CDCl_3$) δ = 7.76 (2H, d, *J* = 8.1 Hz, 5-H), 7.67 (2H, d, *J* = 8.1 Hz, 6-H), 6.97 (1H, d, *J* = 34.5 Hz, 3-H), 3.93 (3H, d, *J* = 0.9 Hz, 9-H);

^{13}C NMR (151 MHz, $CDCl_3$) δ = 161.4 (d, *J* = 34.9 Hz, C-1), 148.0 (d, *J* = 271.0 Hz, C-2), 134.4 (d, *J* = 3.6 Hz, C-4), 131.2 (qd, *J* = 32.5, 2.4 Hz, C-7), 130.4 (d, *J* = 7.2 Hz, C-5), 125.7 (dq, *J* = 7.2 Hz, *J* = 3.6 Hz, C-6), 123.8 (q, *J* = 271.0 Hz, C-8), 116.1 (d, *J* = 3.6 Hz, C-3), 52.9 (s, C-9);

^{19}F NMR (659 MHz, $CDCl_3$) δ = -63.0 (s, 8-F), -122.4 (d, *J* = 33.4 Hz, 2-F);

m/z [LRMS, ESI] (relative intensity, M) 280 (76, $[M+CH_3OH]^+$), 249 (82, $[M+H]^+$);

Data was in agreement with the literature.[327]

Methyl (*Z*)-2-fluoro-3-(2-(trifluoromethyl)phenyl)acrylate [(*Z*)-110c]

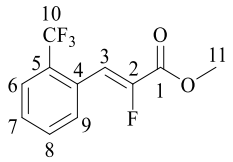

Following ***General Procedure 6***, transesterification of (*Z*)-**109c** (201 mg, 0.767 mmol, 1 eq.) was performed.

Flash column chromatography (2 – 4% EtOAc/pet. ether) yielded title compound (*Z*)-**110c** (107 mg, 56%) as a fine white solid:

m.p. 34 – 36 ºC;

υ_{max} (solid) 2921 (CH sp^3), 1732 (C=O), 1440 (C=C aromatic) cm^{-1};

^{1}H NMR (600 MHz, MeOD-d_4) δ = 7.95 (1H, d, *J* = 7.9 Hz, H-9), 7.80 (1H, d, *J* = 7.9 Hz, H-6), 7.70 (1H, t, *J* = 7.6 Hz, H-8), 7.58 (1H, t, *J* = 7.7 Hz, H-7), 7.27 (1H, dq, *J* = 31.9 Hz, *J* = 1.6 Hz, H-3), 3.91 (3H, s, H-11);

^{13}C NMR (151 MHz, MeOD-d_4) δ = 162.5 (d, *J* = 34.9 Hz, C-1), 149.5 (d, *J* = 269.8 Hz, C-2), 133.7 (s, C-8), 132.8 (d, *J* = 12.0 Hz, C-9), 130.9 (s, C-7), 130.1 (s, C-4), 129.6 (q, *J* = 30.1 Hz, C-5), 127.4 (q, *J* = 6.0 Hz, C-6), 125.6 (q, *J* = 269.8 Hz, C-10), 113.6 (dq, *J* = 4.8, 2.4 Hz, C-3), 53.6 (s, C-11);

^{19}F NMR (282 MHz, MeOD-d_4) δ = -61.1 (d, *J* = 1.8 Hz, F-10), -125.6 (q, *J* = 2.1 Hz, F-2);

m/z [LRMS, ESI] (relative intensity, M) 249.1 (100, $[M+H]^+$), 280.3 (44, $[M+CH_3OH]^+$);

Data was in agreement with the literature.[327]

Methyl (*Z*)-2-fluoro-3-(4-nitrophenyl)acrylate [(*Z*)-110d]

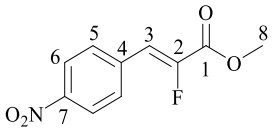

Following ***General Procedure 6***, transesterification of (*Z*)-**109d** (92 mg, 0.385 mmol, 1 eq.) was performed.

Flash column chromatography (5 – 40% EtOAc/pet. ether) yielded title compound (*Z*)-**110d** (65 mg, 75%) as a fine light yellow solid:

m.p. 172 – 173 ºC;

υ_{max} (solid) 2963 (CH sp^3), 1720 (C=O), 1430 (C=C aromatic) cm^{-1};

^{1}H NMR (600 MHz, $CDCl_3$) δ = 8.27 (1H, d, *J* = 8.1 Hz, 6-H), 7.81 (1H, d, *J* = 8.1 Hz, 5-H), 7.00 (1H, d, *J* = 33.5 Hz, 3-H), 3.94 (3H, s, 8-H);

^{13}C NMR (151 MHz, $CDCl_3$) δ = 161.2 (d, *J* = 34.9 Hz, C-1), 148.9 (d, *J* = 266.2 Hz, C-2), 147.9 (s, C-7), 137.3 (d, *J* = 3.6 Hz, C-4), 131.0 (d, *J* = 8.4 Hz, C-5), 124.2 (s, C-6), 115.4 (d, *J* = 4.8 Hz, C-3), 53.2 (s, C-8);

^{19}F NMR (376 MHz, $CDCl_3$) δ = -120.0 (1F, d, *J* = 34.1 Hz, 2-F);

m/z [LRMS, ESI] (relative intensity, M) 195 (68, $[M\text{-}CH_3OH+H]^+$), 226 (9, $[M+H]^+$), 249 (31, $[M+Na]^+$);

Data was in agreement with the literature.[322]

Methyl (*Z*)-3-(4-chlorophenyl)-2-fluoroacrylate [(*Z*)-110e]

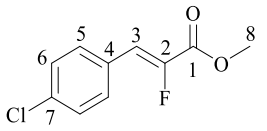

Following ***General Procedure 6***, transesterification of (*Z*)-**109e** (75 mg, 0.328 mmol, 1 eq.) was performed.

Following reaction completion by TLC analysis, the solvent was then removed *in vacuo*, $CHCl_3$ added, and suspension filtered through Celite™. The filtrate solvent was removed *in vacuo* to yield title compound (*Z*)-**110e** (49 mg, 70%) as a fine white solid:

Decomposed at 170 ºC;

υ_{max} (solid) 2948 (CH sp^3), 1724 (C=O), 1490 (C=C aromatic) cm^{-1};

^{1}H NMR (600 MHz, $CDCl_3$) δ = 7.59 (2H, d, *J* = 8.4 Hz, 5-H), 7.39 (2H, d, *J* = 8.5 Hz, 6-H), 6.90 (1H, d, *J* = 35.0 Hz, 3-H), 3.91 (3H, s, 8-H);

^{13}C NMR (151 MHz, $CDCl_3$) δ = 161.6 (d, *J* = 33.7 Hz, C-1), 147.0 (d, *J* = 268.6 Hz, C-2), 135.7 (d, *J* = 3.6 Hz, C-7), 131.5 (d, *J* = 8.4 Hz, C-5), 129.5 (d, *J* = 3.6 Hz, C-4), 129.1 (s, C-6), 116.5 (d, *J* = 4.8 Hz, C-3), 52.8 (s, C-8);

^{19}F NMR (376 MHz, $CDCl_3$) δ = -124.8 (d, *J* = 34.1 Hz, 2-F);

m/z [LRMS, ESI] (relative intensity, M) 215 (100, $[M^{35}Cl+H]^+$), 217 (31, $[M^{37}Cl+H]^+$);

Methyl (*E*)-3-(4-bromophenyl)-2-fluoroacrylate [(*E*)-110f]

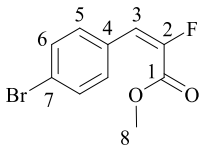

Following ***General Procedure 6***, transesterification of (*E*)-**109b** (50 mg, 0.183 mmol, 1 eq.) was performed.

Flash column chromatography (2% EtOAc/pet. ether) yielded title compound (*E*)-**110b** (30 mg, 63%) as a fine white solid:

m.p. 58 ºC;

υ_{max} (solid) 2967 (CH sp^3), 1735 (C=O), 1438 (C=C aromatic) cm^{-1};

^{1}H NMR (700 MHz, CD_3CN) δ = 7.54 (1H, dd, *J* = 8.7 Hz, *J* = 2.1 Hz, 6-H), 7.41 (1H, dd, *J* = 8.7 Hz, *J* = 0.7 Hz, 5-H), 6.95 (1H, d, *J* = 22.8 Hz, 3-H), 3.74 (1H, s, 8-H);

^{13}C NMR (176 MHz, CD_3CN) δ = 162.0 (d, *J* = 35.1 Hz, C-1), 148.5 (d, *J* = 257.9 Hz, C-2), 132.9 (d, *J* = 2.7 Hz, C-5), 132.5 (s, C-6), 131.7 (d, *J* = 10.3 Hz, C-4), 123.7 (s, C-7), 121.5 (d, *J* = 27.5 Hz, C-3), 53.4 (s, C-8);

^{19}F NMR (659 MHz, CD_3CN) δ ppm -117.7 (1F, dd, *J* = 22.9, 2.7 Hz, 2-F);

m/z [LRMS, EI] (relative intensity, M) 259 (100, $[M^{81}Br+H]^+$), 258 (95, $[M^{79}Br+H]^+$);

Methyl (*Z*)-3-(4-bromophenyl)-2-fluoroacrylate [(*Z*)-110f]

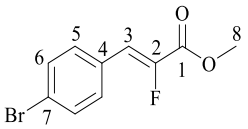

Following ***General Procedure 6***, transesterification of (*Z*)-**109f** (150 mg, 0.549 mmol, 1 eq.) was performed.

Flash column chromatography (2 – 4% EtOAc/pet. ether) yielded title compound (*Z*)-**110f** (118 mg, 83%) as a fine white solid:

m.p. 90 ºC (lit. m.p. 93 – 95 ºC)[326];

υ_{max} (solid) 2946 (CH sp^3), 1721 (C=O), 1487 (C=C aromatic) cm^{-1};

^{1}H NMR (600 MHz, $CDCl_3$) δ = 7.55 (2H, d, *J* = 8.7 Hz, 6-H), 7.51 (2H, d, *J* = 8.7 Hz, 5-H), 6.88 (1H, d, *J* = 34.6 Hz, 3-H), 3.91 (3H, s, 8-H);

^{13}C NMR (151 MHz, $CDCl_3$) δ = 161.7 (d, *J* = 34.9 Hz, C-1), 147.1 (d, *J* = 269.8 Hz, C-2), 132.1 (s, C-6), 131.7 (d, *J* = 8.4 Hz, C-5), 129.9 (d, *J* = 4.8 Hz, C-4), 124.1 (d, *J* = 3.6 Hz, C-7), 116.6 (d, *J* = 3.6 Hz, C-3), 52.8 (s, C-8);

^{19}F NMR (376 MHz, $CDCl_3$) δ = -124.3 (d, *J* = 34.1 Hz, 2-F);

m/z [LRMS, ESI] (relative intensity, M) 259 (100, $[M^{79}Br+H]^+$), 261 (95, $[M^{81}Br+H]^+$);

Data was in agreement with the literature.[326]

10. Appendix

10.1 Taxonomical Assignment

Metagenomic ER and TAm genes were cloned into pET29(a) (**Table 19**). For ERs, putative protein annotation, organism and percentage identity is to the closet homologue in GeneBank.[xlii] For TAms, putative protein annotation, organism and percentage identity is to the closet homologue in NCBI database.[xliii] Protein length and predicted molecular weight were determined using ExPASy Protparam.[xliv] Enzymes were expressed in *E. coli* BL21 (DE3).

Table 19: Metagenomic enzymes protein length (aa), predicted molecular weight (Da), putative protein annotation, organism, and percentage identity to the closest homologue in GeneBank or NCBI database.

pQR	Length (aa)	MW (Da)	Putative protein annotation	Bacteria	% Identity
1440	367	39.3	Alkene reductase	*Sphingopyxis*	95
1445	355	37.9	Alkene reductase	unclassified *Pseudomonas*	77
1446	375	41.3	NADH:flavin oxidoreductase	*Pseudomonas sequence ID: WP_061903666.1*	100
1907	370	40.5	Alkene reductase	*Moraxellaceae bacterium*	85
1909	374	40.1	Oxidoreductase	*Stenotrophomonas acidaminiphila*	98
2189	484	52.3	Aminotransferase	*Sphingopyxis sp*	96
2191	450	49.2	Glutamate-1-semialdehyde 2,1-aminomutase	*Novosphingobium aromaticivorans*	63
2208	1380, 466	50.1	Aspartate aminotransferase family protein	*Sphingomonas sp*	83
1	476	51.7	-- [a]	*Rhodococuss sp.*	-- [a]
13	468	51.5	-- [a]	*Rhodococuss sp.*	-- [a]
16	455	49.4	-- [a]	*Rhodococuss sp.*	-- [a]
23	459	50.2	-- [a]	*Aminobacter sp.*	-- [a]

[a] Not currently available to disclose.

[xlii] Cloning and analysis performed by Dr Dragana Dobrijevic, a former member of the Ward group.
[xliii] Analysis performed by Dr Leona Leipold, a former member of the Hailes group.
[xliv] Analysis performed by Dr Dragana Dobrijevic, a former member of the Ward group and Dr Leona Leipold, a former member of the Hailes group.

10.2 DNA Sequences of Metagenomic Ene-Reductases

Nucleotides corresponding to the vector pET29-a (+) are in bold.

>pQR1440

ATGGCCGTATCACTATTCGATCCGATTAAACTGGGCGCGATCGACGCCCC
GAACCGCATCATCATGGCGCCGCTGACGCGTGGCCGCGCCGGACCGGGCT
TCGTGCCCACCGAACTCGCACGCGACTATTATCGTCAGCGCGCTTCGGCG
GGGCTCATCATCTCCGAAGCCACGGGCATTTCGCAGGAAGGCCTCGGCTG
GCCGAGCGCGCCGGGCCTGTGGACCGATGCGCAGGTTGAAGGCTGGAAG
CCGGTGACCGACGCCGTCCACGCCGCCGGCGGTCGCATCGTCGCACAGCT
TTGGCATATGGGCCGCGTCGTCCATTCGGTGTTCAACGATGGGAAGCCGC
CGGTTTCGGCGTCGGCAACGCAGGCGCCGGGCAAGGCGCACACGCCCGTG
GGCCGGCTCGATTATGAAGTCGCGCGGCCGCTGGAGCTTGGCGAGATCCC
GCGGGTGATAGCCGATTATGCCAAGGCGGCCGAAAATGCGAAAAGGGCC
GGCTTCGACGGCGTGCAGTTGCACGGCGCGAACGGCTATCTGATCGACCA
GTTCCTGCGCGACGGCAGCAATCTGCGCGACGATGATTATGGCGGCCCGA
TCGAGAATCGCATCCGTTTGCTCCGCGAAGTCACAGAGGCGCTGATTTCG
GTTTGGGGCGCCGACCGCGTGGGCGTCCGCCTGTCGCCCAACGGCGACAC
GCAAGGTGTCGACGACAGCGCACCCGAACAGCTGTTCCCGGTCGCCGCCG
CTGCGCTCGACGCGCTTGGCATCGCTTTCCTCGAACTGCGCGAGCCGGGC
CCCGAGGGCACCTTCGGACGCACCGATGTTCCCAAACAGTCGCCCGCGAT
CCGCGCGGCATTCAAAGGGCCGCTGATCCTCAACAGCGACTATGACGTCG
CGAAAGCTGAAGCTGCACTGGCCGACGGGCTCGCCGACGCGATCGCCTTT
GGCCGTCCGTTCATCGGCAACCCCGACCTTGTCGAGCGGATCCGTAACGG
CGCCGAATGGGCCGCCGACAATCCGCAGACCTGGTATTCGCCGGGCCCCG
AGGGCTACACCGACTATCCGGCGCTGCAAACGGCGC**ACCACCACCACCA**
CCACTGA

>pQR1445

ATGTCCAATTTATTCACCCCCCTACAGGTCGGCGCGTGGCAGTTGCCCAAT
CGGATCATCATGGCACCCCTCACCCGTTGCCGTGCCAGCGAAGGCCGCGT
GCCCAATGCGCTGATGGCAGAATACTACGCGCAGCGTGCCAGTGCCGGTT
TGATCATCAGTGAAGCCACCTCAGTTACACCAATGGGCGTGGGATATCCC
AACACACCGGGTATTTGGTCGGATGCGCAAGTGGACGGCTGGAAGCTGAT
CACCGATGCGGTGCATCAAGCCGGTGGGCGGATTGTGCTGCAACTGTGGC

ATGTGGGGCGGATTTCTGATCCGGTGTATTTGGATGGTCAATTGCCGGTTG
CCCCTAGCGCGATTGCCCCACAAGGCCATGTCAGTTTGGTACGCCCGACC
AAAGCGTTTGAAACCCCACGTGCACTCGACACCGCAGAGCTAGTCGACGT
GGTCGCTGCCTATCGTTTGGGTGCAGAGAATGCGAAAAAGGCTGGTTTTG
ATGGCGTTGAGATTCATGGAGCCAATGGCTATTTGCTCGATCAATTCTTGC
AAAGCTCAACCAATCAACGCACCGATCAATATGGCGGCAGCTTAGAGAAC
CGTGCACGCTTGCTGCTTGAAGTGGTCGATGCTTGTATTGAGGTATGGGGT
GCAGATCGGGTGGGGGTGCATCTGGCGCCGCGTGGCGATGCGCATGATAT
GGGTGATGCCAACCCTGCCGAAACCTTTGGCTATGTGGCGGAGCAATTGG
GTGCGCGCCAAGTGGCGTTTATTTGTACCCGTGAATATCTGGCCGACGAC
AGCCTTGCCGGTTTGATCAAAGCCAAATTTGGCGGCGTGTATATCGCCAA
TGAAAAATACGACCAAGCCCAAGCCGATGCAGCCATTGCCAGCGGCGCTG
CCGATGCGGTGGCGTTTGGGGTGAAGTTTATTGCCAACCCCGATTTGCCTG
CGCGTTTTGCTCAAGGTGCAGTGCTGAATGCACCTGATCCGAGCACCTTTT
ATGGGGCAGGCAGTAAAGGCTATACCGACTATCTGACCTTG**CACCACCA**
CCACCACCACTGA

>pQR1446

ATGACCGCACCTGTTCAAGCCCTGTTCGCGCCCTTCCGCCTGGGTAACCTG
GAGCTGCCCACCCGCGTGGTGATGGCGCCGATGACCCGTTCCTTCTCGCC
GGGCGGCGTGCCCAATGCCCAGGTGGTCGAGTACTACCGCCGCCGTGCCG
CCGCCGGCGTCGGCCTGATCGTCACCGAGGGCACCACCGTTGGCCACAAG
GCCGCCAACGGCTATCCGCACGTGCCGCGCTTCTACGGCGAGGATGCCCT
GGCCGGCTGGAAGCAGGTGGTCGATGCCGTGCACGCCGAAGGCGGCAAG
ATCGTCCCGCAGCTGTGGCACGTGGGTAACGTGCGCAAGGCCGGCACCGA
GCCGGATGCCAGCGTGCCGGGTTACGGCCCGTCGGAGAAGGTCAAGGAC
GGCACCGTGGTCGTGCATGGCATGACCAAGGACGACATCCAGGAGGTGAT
CGCCGCCTTCGCCCAGGCCGCCCGCGACGCCAAGGCCATCGGCATGGACG
GCGTGGAGATCCACGGCGCCCACGGCTACCTGATCGACCAGTTCTTCTGG
GAAGGCAGCAACAAGCGCACCGACGAGTACGGCGGCGACCTGGCCCAGC
GCTCGCGCTTCGCCATTGAGCTGATCCAGGCCGTGCGCGCCGCCGTTGGC
CCGGACTTCCCGATCATCTTCCGCTTCTCCCAGTGGAAGCAGCAGGACTAC
ACCGCACGCCTGGTACAGACCCCGGAAGAACTGGGGGCCTTCCTCAAGCC
GCTGTCCGACGCCGGCGTGGATATCTTCCACTGCTCGACCCGCCGCTTCTG

GGAGCCGGAGTTCGAAGGCAGCGACCTCAACCTGGCCGGCTGGACCCGCC
AGCTCACCGGCAAGCCGACCATCACCGTCGGCAGCGTCGGCCTGGACGGC
GAGTTCCTGCAGTTCATGGTCAACACCGACAAGGTGGCCGAGCCGGCCAG
CCTGGAGAACCTGCTGGAGCGCCTGAACAAGCAGGAGTTCGACCTGGTGG
CCGTGGGCCGTGCCCTGCTGGTCGACCCGGACTGGGCGGTGAAGGTGCGC
GATGGCCGCGAGAGCGACATCCTGCCGTTCAGCCGCGAGGCGCTCAAGCA
GCTGGTC**CACCACCACCACCACCACTGA**

>pQR1907

ATGTCCGGCAAGTTGTTCACCCCGTTCAGCTCGGGTTCCTTCACCTTCCCC
AACCGCGTTATCATGGCGCCGCTGACGCGTATGCGCGCTTCGCAGCCGGG
TGACATTCCCAACGAGCTGATGCAGACCTATTACGTGCAGCGCGCCAGCG
CCGGCCTCATCATCGCCGAGGCCACGCAGATCTCCCCGCAGGGCAAGGGC
TATATGGACACTCCGGGGATTTATTCCGCGGAGCAGGTGCAGGGCTGGCG
CAAGATCACCCAGGCCGTGCATGAGGCCGGTGGCCATATCGCCCTGCAGC
TCTGGCATGTGGGTCGTGTTTCGCATCACAGCCTGCAGCCCGACCAGCAA
CTGCCGGTGTCCGCTTCTGCCATTCCCTACCAGAACCGCACCACGGTCCGT
GGTGAAGACGGCAAGCCCACGCGCGTGGATTGCGATACCCCACGTGCGCT
GGAACTGTCCGAAATCCCCGGTGTGATCGAAGACTACCGCCGCGCCACCG
TGAATTCGCGCGAAGCCGGTTTCGACATGGTGGAAGTGCATGCCGCGCAT
GGCTATCTGCTGCACCAGTTCCAGTCCGCCGAAAGCAACAAGCGTGAAGA
CGCCTATGGTGGTTCGCTGGAAAACCGTGCCCGCCTGACGCTGGAAGCCC
TGGATGCCGTGATCGGTGCCTGGGATGCCAAGCATGTAGGTATCCGCATT
TCCCCGCTGGGCACCTTCAACGGCCTGGACGACAAGGACGGCCTGGAAAT
GGCGCTGTATCTCACGCGTGAATTCACCAAGCGCGGTATCGCCTACCTGC
ATCTGTCCGAGCCGGACTGGGCCGGCGGTCCGGCGCATGGCGACGAATTC
CGCCAGGCCCTGCGCGACGCTTTCCCGGGCACCATCATCGGTGCCGGCAA
CTACACGGTGGAAAAATCGGAGATGCTGCTGGCCAAGGGCTTTATCGATG
CCGCCGCGTTTGGTCGTCCCTTTATTGCCAATCCGGACCTGCCGGTGCGTC
TGCAGAAGGGCGCTGAGTTGAACAATGTGGTGGCGGCTACGCTGTATGGC
GGTGGCGCCGAAGGCTATACGGATTATCCGGCGCTGGCC**CACCACCACC**
ACCACCACTGA

>pQR1909

ATGAGTCGCCTGTTCTCGCCCCTCGCGCTGGGGCCGTTGCCGTTGTCCAAC
CGCATCGTCATCGCGCCCATGTGCCAGTACTCCGCCGACGAAGGTCGTGC
GACCGACTGGCACGCCTTCCACTGGCCGAACCTGGCCCAGTCCGGTGCTG
CGCTGGCGATCATCGAAGCCACCGCGGTCGAGCCGCGCGGGCGCATCAGC
TGGGCGGACCTTGGCCTGTGGGACGACACGACGGAAGCCGCCTTCGCCCG
CGCGCTGGCGGCGGCACGCAGGTACTCGACGATGCCGATCGGCGTGCAGC
TGGCGCATGCGGGACGCAAGGCATCCACGCACCGCCCGTGGGAGCATCAC
GGCGCACAGATAGCACCCGACGCGCCGCAGGGATGGCGGACGGTATCGG
CGTCGTCGTTGCCCTATGCCGAGGGGCAGCATCCGCCGGACTCGTTGGAC
CAGGCGGGCATCGACGCGATCATCGCCGCCTTCGCCGACAGCGCGCATCG
CGCTGTGCGACTCGGGCTGGACCTGATCGAGATCCATGCCGCCCACGGCT
ACCTGCTGCACCAGTTCCTGTCGCCGCTGAGCAACCGGCGCGACGACGCC
TACGGCGGCGCGCTGGAAAATCGCATGCGCCTGGTGTTGCAGGTGTTCGA
TGCGATCAAGGCCGTGGTGCCGGCGTCGATGGCGGTCGGGGTACGCATTT
CCGCGACCGACTGGGTCGACGGCGGCTGGGATCTGGCGCAGAGCATCGCG
CTGGCGAAGGCGCTGGATGCGCGTGGCAGCCACTTCATCCATGTGTCGAG
CGGCGGCCTGCATCCGGCGCAGAAGATCGCGCTGGGGCCCGGCTACCAGG
TGCCCTTCGCAGCGGCGATCAAGCGTGAAGTCGCGATGCCGGTGATCGCG
GTCGGCCTGATCACGGCGCCGCAACAGGCGGAGGACATCCTGCTGCAGGC
GCAGGCCGATGCCATCGCCATCGCGCGCGCCGTTCTCTACGATCCTCGTTG
GCCGTGGCACGCGGCGGCATCGCTTGGCGAGACGATCGCCATCGCGCCGC
AGTACCTGCGCAGCGCACCGCGGGAGGTCGCGGCGAGCTTCGTGGAGGC
GACG**CACCACCACCACCACCACTGA**

10.3 DNA Sequences of Metagenomic Transaminases

> pQR2189

ATGCCCCGCAATCACGACATCGCCGAACTGCGCCGCCTCGACGTCGCGCA
CCATCTTCCCGCACAGGCCGACTGGGCCGAAATCGAAAAGCTCGGCGGCA
GCCGCATCATCACGCACGCAGAGGGCTGTTATATTCACGACGGTGACGGC
CACCGCATTCTCGACGGCATGGCGGGCCTCTGGTGCGTCAATGTCGGCTA
TGGCCGCGAGGAACTGGTTGAGGCGGCGGCGGCGCAGATGCGCGAGCTG
CCCTTCTACAACACCTTCTTCAAGACCGCGACGCCGCCAACGGTGACGCT

GGCGGCTAAGATCGCGAGCCTGACCGGCAATCGCCTGCCGCACATCTTCT
TCAACGCTTCGGGCAGCGAGGCGAACGACACCGTGTTCCGGATGGTGCGC
CATTATTGGAAGCTGAAGGGCGAGCCGAAGCGCACCGTCTTTATCAGCCG
CTGGAATGCCTATCACGGCTCGACCGTCGCGGGCGTGTCGCTTGGGGGCA
TGAAGGCGATGCACGCGCAGGGCGATTTGCCCATTCCCGGCATCGAACAT
GTGCGCCAGCCGTACAGCTTCGGCGAAGGGCAGGGAATGACCGAGGAGG
AGTTCTGCGACGCCTGCGTTCATGCGATCGAGGACAAGATCCTCGAAGTT
GGTCCCGAAAATTGCGCCGCATTTATCGGCGAGCCGGTGCAGGGCGCGGG
CGGGGTCGTTATTCCGCCAAAGGGCTATTGGCCTAAAGTCGAAGCGGTGG
CGCGCAAATATGGCCTTTTAGTCGTTTCCGACGAGGTGATCTGCGGGTTCG
GACGCACGGGCAAGATGTGGGGGCATGAGACGATGGGTTTCACCCCCGA
CCTGATGCCGATGGCAAAGGGGCTGTCGTCGGGCTATCTGCCGATTTCGG
CGACCGCGGTCGCGACACATGTCGTTGACGTGCTCAAGACCGGCGGCGAT
TTCGTCCATGGCTTCACTTACTCGGGCCATCCCGTCGCGGCGGCGGTCGCG
CTCAAGAATATCGAAATCATCGAACGCGAAGGGCTCGTCGAGCGCACCGG
CAGCGTCACCGGCCCGCATCTGGCGAAGGCGCTCGCGACGCTGAACGATC
ATCCGCTCGTTGGCGAGACGCGCTCAATCGGATTGCTGGGCGCGGTCGAG
ATCGTGGGGGAAAAGGTGACGCGCGCCCGCTTCGGCGGCGCCGAAGGCA
CGGCGGGACCGATGGCGCGCGACGCGTGCATTGCGAACGGGCTGATGGT
GCGCGGCATCCGCGATAGCCTGGTTATGTGTCCGCCGCTGATCATCTCCAC
CGAACAGATTGACGAGATGGTTGCCATCATCCGCAAATCTCTCGATGAGG
TGATGCCGAAACTCCGCGCTTGA

>pQR2191

ATGTCGGGTCAAAGGGATCAGGAATTGCGCGCGCGCCGCGAAGGTCAT
GCCGAGCTCGGCATTTGGCCACGTGGGCACAGCGCTGTTGCCCGCAAATT
ACCCCCAGTTCTTCGAACGGGCCGAGGGCGCCTATGTCTGGGACGCCGAC
GGCAACCGCTATCTCGACTACATGTGCGCATTCGGGCCGAACCTGCTTGG
TTATCGCGATCCTCGCGTCGAGTCCGCGGCCAGCGCACAGGCGGCACGCG
GCGACGTCATGACCGGCCCCTCGCCTCTTGCAGTGGAACTCGCCGAGAAA
TTCGTGGAGATCGTCAGTCACGCCGACTGGGCGTTCTTCTGCAAGAACGG
CACCGATGCGACCACCATCGCGCGCACCATCGCGCGCGCGCAAACCGGAC
GACGCAAGATATTAATCGCGGAGGGCAGCTATCATGGCGCCGCTCCCTGG
TGCAATCCCTTCCCGGCCGGAACAGTGCCCGAGGATCGGGCGCATATGCT

CACTTTCACCTTCAACGACATCGCCAGTCTCGAAGCGGCAGTGGCCGAGG
CGGGCGACGATCTCGCAGGGATCATCGCGACGCCGTTCAAGCATGAAGCC
TTTGCCAATCAGGAATTTCCGACCCAGGACTATGCTCGCCGCTGCCGTGA
AATCTGCGATGCGTCAGGCGCCGTCCTGGTCGTCGACGATGTCCGCGCCG
GCTTCCGGCTCGCCGTCGACTGCAGCTGGGCAACCGTTGGCGTGAAGCCC
GATCTCAGCTGCTGGGGCAAATGCTTCGCCAACGGATATTCGATTTCAGC
CGTGATGGGGTCGAACCGGGTCAAGCAAGGCGCGGACTCGATCTTCGCAA
CCGGCTCATTCTGGCAATCCGCCATCTCCATGGCCGCGGCGCTCGCGACG
CTCGACATCATTCGGGATGGCAAGGTGATCGAGAAGACGGTTCGCCTCGG
CCAGCGCCTGCGCGATGGCCTTGATGAGGTCTCGCGCCGGCACGGCTTTA
CCCTCAATCAAACCGGTCCGGTGCAGATGCCGCAGATACTCTTCGAAGGC
GATCCGGATTTCCGCGTCGGCTTCGCCTGGACATCGGCAATGATCGATCG
CGGCTTCTACCTCCATCCCTGGCACAACATGTTCCTGTGCGACGCGATGAC
CGAAGAGGACATCGACCAGACAATCGAAGCGGCGGATTCCGCTTTCGCCA
CCGTCCGTGCCGCTCTGCCGACGCTCCAGCCGCACGAGCGCGTTCTAGCG
CTCTTTTCGGC CAGAGCGCACTGA

>pQR2208

ATGACCCTGCGTAATTACGACATGGCCGAGCTCAAGCGGCTCGACCTCGC
CCATCATCTGCCCGCGCAGGCAAGCTACGGCCTGATCCGCGACCTGGGCG
GCAGCCGGATCATCACCCGCGCCGAAGGATCGACGATCTGGGATGCGGA
GGGCAATGCGATCCTCGACGGGATGGCGGGCCTGTGGTGCGTCGACGTCG
GCTATGGCCGCGCCGAGCTGGCCGAGGTCGCACGCGAGCAGATGCTCGAG
CTTCCCTATTACAACACCTTCTTCCGCACCGCGACGCCGCCACCGGTGAAG
CTTGCCGCGAAGATCGCCGGACTGCTCGGCGGATCGCTCCAGCATATCTT
CTTCAACTCGTCGGGCTCCGAATCGAACGATACGGTGTTCCGCCTCGTGCG
CACCTATTGGGCGCTGAAGGGACAGCCCGAACGCACGATCTTCATCTCGC
GCCGCAACGCCTATCATGGCTCGACCGTCGCCGGCGTCAGCCTGGGCGGC
ATGGCGGCGATGCATGCGCAGGGCGGGCTCCCGATCGCCGGCATCGAGCA
TGTGATGCAGCCTTATGCGTTCGGCGAAGGCTTCGGCGAGGATCCCGAGG
CGTTCGCCGCGCGCGCCGCTCAGGAGATCGAGGATCGTATATTGGCTGTC
GGGCCTGAAAAGGTCGCTGCCTTCATCGGCGAGCCGGTGCAGGGCGCCGG
CGGCGTCATCATCCCGCCCCCCGGATACTGGCCGCGGGTCGATGCGATCT
GCCGCAAATATGGCATCCTGCTCGTGTCGGACGAGGTGATTTGCGGCTT

CGGGCGGCTGGGCGAATGGTTCGGCTTCCAGAAATATGGCTATACGCCCG
ATATCGTTTCGATGGCGAAGGGGCTGTCGTCGGGCTATCTGCCGATCTCG
GCCACGGGCGTGAGCAGCGAGATTGTCGAGACGCTGCGCGCGTCGGGCG
ACGATTTCGTCCACGGCTATACCTATTCGGGGCATCCGGTGGCCGCGGCC
GTGGCGCTGCGCAATCTGGAGATTATCAAGCGCGAAGGGCTGGTCGATCG
CGTGCGCGACGATCTGGCACCCTATTTCGCGAAGGCGCTGGCGACGCTCG
ACGATCATCCGCTGGTGGGCGAGGCGCGCTCGGTCGGGCTGCTCGGCGCG
GTGGAGATCGTTTCCGAGAAGGGCACCAACCACCGCTTCGGCGGCAAGGA
AGGCACCGCCGGGCCGGTCGTGCGCGATCACTGCATCGCGGGCGGGCTGA
TGGTGCGCGCGATCCGTGACTCGATCGTCATGTGCCCGCCCTATGTTATCA
CGCATGACGAGATCGACCGGATGGTTGCCATCATCCGCTCGGCGCTCGAC
AAGGCTGCGGTCGATCTGGG TGGAGGCGCCTGA

> 1-TAm

ATGACCATCTCCCCGCTCAACGATCTCAATCCAGGACTGGATGCCGATTC
GTCGGTTGATCTGCAAGAGCTCGCCCAACAGCACCTCATCATGCACTTCA
CCGGCGCTGGCGCCTACAACGAGGCGCCCCCGCGAGTCATGGTGTCAGGT
GATGGATGCTGGTTGACCGATTCCACCGGCAAGCGCTACCTCGATGCACT
CGCCGGCCTGTTCTGCGTAAACGTCGGCTACGGGTACGGAGCGGAGATCG
GTCACGCTGTACAACAGCAGATGGCCACACTGCCCTATTTCTCGAACTGG
GGGTACGCTCAGCCCCCGTCGATCCTCCTTGCCGCGAAGATCGCGGAACT
CGCCCCCGCCGGCCTGGACCGCGTCTTCCTCACTTCCGGTGGCTCCGAATC
GAACGAGGCCGCTGTCAAGCTTATTCGCCAGTACCACCAGGCCCGGGGAG
AGCATTCCCGGATGAAGTTCATCGCCAGGCGTGTGTCGTACCACGGAACC
TCGTACGCGGCGCTCTCCCTCAACGGCATGACAAACTTCAAAAAGGTCTT
CGAGCCGCTCATGCACGGAACCCGACACATCTCCAACACCAAACGCTACA
AGCGTCCCTTCGGCGAAACCGAGGAACAGTTCACTGCTTTGCTGCTGCAA
GAACTGGAAGCACTCATCGTCCAAGAAGGTCCCGATACCGTCGCCGGCAT
CTTCCTCGAACCCCTCCAGAACGCAGGCGGCTCGCTCACCCCTCCGGAAG
GCTATTGCGCTGGCGTACGCGAGATCTGCGACCGCCACGGCATCCTGCTT
GTGGCCGACGAGGTGATCTGCGGATTCGGCCGCCTCGGCGAGTGGTTCGG
GTCCACCCGTTACGGAATGGAACCAGATATCATTACCTTCGCGAAGGGCG
TGTCCTCGGGCCACGTTCCTCTGGGTGGGATGATCACGACGAGCGCAGTG
ATCGATACAGTCCTGTCAGGCCCGCAGGGCATGTATCTCCACGGCTTGAC

CTTCGGAGGCCACCCGGTGGCGTGCGCGGCGGGGCTAGCCAACATCGCCA
TCATGGAGCGCGAAGACATCCTCGGACATGTCCGCCGCACCGAACCGTAC
TTCCGGGCACGTTTGTCCGAGCTGCTCGAACACCCGCTCGTCGGCGACCTT
CGCGGCGACGGATTTCATTACTCGCTGGAATTGGTAACCGACAAGAACGC
AAGGGCCTGGCGCAGCACGATTTCATCGAATGACTTCGTCGCTCAACACC
TCAACCCCGCGCTGGTCGATGCCGGCATCCTCTGCCGAGCAGCAGTCGAC
CACGAAGGAACACCCCTGATCCAGTTCTCGCCGCCGCTGGTCTTCGATAC
CGACGACATCAACTTCCTCGTCGAGCACGTTCGCACCGTACTCGACGCGA
TGAGCAACATCGACGGGCTCACCGCTTGA

> 13-TAm

GTGACCACGACCGAAACCGAGATTCAGCACCTCGACACACCGGCCCTCCG
CGATTCGGCCGGCGCCCATCTGTGGCGGCATTTCTCCGACATGACCACCA
CCGAGAAGCAGCCACTTCGCGTGATGGTGAAGGGTGAGGGGTGCTACCTT
ATCGACTCCGAAGGAAATCGATTCCTCGACGCACTGTCCAACCTGTTCTGC
GTCAACATCGGCTACAGCTACGGCGAAGAACTCGGGCAGGCCGCGCTGGC
GCAGTACCGCGAACTGGGCTACCACTCCAACTGGGGCTCAACCCATCCGA
AGGCCATCGAACTGGCACACACCCTCGCGGACCTCGCCCCCGAGGGCCTC
GATCACGTCTTCTTCACCCCCAGCGGCGGCGAGTCGGTCGAGGCCGCCTG
GAAGATCGCACGCGAGTACCACCATCTGCGCGGCGAAAAGCGCTGGAAG
GCGATCGGCCGGAGCATGGCCTATCACGGAACCACCATGGGCGCCCTGTC
GATCAACGGAATTCCCGAGATCCGGAGCATGTTCGAGCCGCTCCTGCCCG
GAGCCTCCCATGTTCGCAACACCAAGCGCTTCGGCCGACCCGAGAAGGAA
ACAGAGGAAGAATTCACCCAGTTCCTTCTCGACGACCTCGAACAGCGAAT
CCTCGCCGAAGACCCCGCCACGGTCGCCATGATCATCATGGAGCCGGTAC
AGAACCACGGCGGCATGCTGGTACCACCAGCCGGCTACTCCGCCGGGGTG
CGCGCGCTGTGCGACCGGTACGGAATCCTGTTGGTCGCCGACGAGACGAT
CACCGCCTTCGGACGGTGCGGCGCCTGGTTCGCCTCGGAACGATACGAGA
TGAAACCGGACATCATCACGACCGCGAAGGGGCTGTCCTCGGCGCATGCG
GTGATCGGTGCGGTGATCACGACGGACGAGGTGTATTCGACGTTCTACGT
GGCTGGACGGAAATTCACCCACGGCAACACCTTCGGCGGGCACCCCGTGA
TGGCAGCCGTAGCACTGCGCAACATCGAAATCATGCAAGAACTCGACATC
CCGCGTCACGTAGCCGCGAAGGAGGACGAACTCCGGAGCAAACTCGAGT
CTCTTCGAGCGCTCCCCATCGTGGAGGACGTCCGCGGCTCCGGATTCTTCT

ACGCGATCGAACTGACGTCCACCGACGCACGAGGGCAGCGCTTCTCGGAT
ACCGAACTGGCCAGGCTCTACGGGGACGAGCTCCTGTCCGACCGTCTGGT
CGACCGTGGCATCCTTCTTCGCCTCTCCCTCGACGGCGGCGACCCGGTGCT
GTGCATCGCGCCGCCGCTGATCGCAGACAGCCCTGAATTCGACGAGCTCG
TCGACGGTCTCCGCGACGTACTGTCGGCCCTTTCGCTCGACGCGGGCCTCG
TCTGA

> 16-TAm

TTGAGTACGAATCCCGTGCAGACCGTCGATTCCGACCCGAGCAGGCATCT
GTGGATGCATTTCAGCAACATGGGTGCGTATGCGCAGGGGGTCGAAGTCC
CGGTCATCGTCCGCGGAGAGGGTTGCTACGTGTGGGACCAGCACGGGAAC
CGATACCTCGACGGCCTGAGTTCGCTCTACTGCGTGAACGTCGGCCACGG
CCGCACCGAGCTGGCCGAGGCTGCGGCCAAGCAGGCTACCGAGTTGGCCT
TCTTCCCGACGTGGTCCTTCGCTCATCCCCGCGCGATCGAGCTCGCGACCA
AGATCGCCGACCTGGCGCCTGCGGATCTCAACCGCGTGTTCTTCGTCGGC
GGTGGCGGCGAAGCCGTGGACTCCGCCTTCAAGCTCGCCCGGCAGTACCA
CAAGATTCGCGGCAAGGCCGGCAAGTACAAGGTGATCTCCCGCAACACCG
CCTACCACGGCACCACCTTGGGCGCACTGGCGGCGACCGCGTTGTCGCCG
GCAAGGGCCCCTTTCGAGCCGCTGCCCATCGGCGGAAGCCACGTGACAAA
CACCAACGTCTACCGGCTGGACCCGCAGGCGGTCGATACGCTCGCCGAGG
CGATCCGGGAAAGAATCGAGTTCGAGGGACCGGACACCGTCGCGGCGGT
GATCCTCGAACCGGTCCAGAATTCGGGAGGCTGTTTCGTCCCGCCGGAGG
GCTACTTCCAGCGCGTGCGGCAGATCTGCGACCAGTACGACGTCCTGCTG
ATCTCCGACGAGGTCATCTGCGCCTTCGGACGACTGGGCGAGTGGTTCGG
CGCCCAACGGTTCGACTACGTGCCCGACATCATCACCACAGCCAAGGGCC
TCACCTCCGCCTATGCACCGATGGGGGCGGTCATCGCCTCCGACCGCGTC
ATCGAGCCGTTCCTCACCGACAACAACGTGTTCGCCCACGGTGTCACCTTC
GGTGGGCACCCGGTCGCCTCGGCGGTCGCGCTGGCGAACATCGAGCTGAT
GGAGAGCGAGAAGATGCTCGAAAACGTGCGCGCCAACGAACCAGTGTTG
CGCGGAATGCTCGAGTCGCTGCGCGACATTCCCCTGGTCGGTGACGTGCG
CGGGGCGGGCTACTTCTGGGCGATCGAACTGGTCAAAGACCCCGCGACGA
GGCAACGCTTCTCGCCGGCCGAGGGCAAAGCGCTGCTGGCGTTCCTGGCC
CCCGAACTCTATCGGCGGGGACTGATCTGCCGCGCGGACATGCGCGGAGA
CCTCGTGGTCCAACTGGCGCCGCCGCTCATCGCCGGCCCCCCACACTTCGC

CGAGATCGAAACCATCCTGCGATCGACACTCGTCGACGCCGCGGCGCTCT
CGTTGCCGACCGACTGA

> 23-TAm

ATGACCTATCAGAACTATTCGCTGAAGCAGCTTCAGCAGATCGATGCCGC
GCACCATCTTCATCCCTTCACCGACCACAAGGAACTGCGCGACATCGGCT
CGCGCATGATCACCCGTGCCGAAGGGCCGTTCATCTACGATTCGGAAGGG
ACGGAACTGCTCGACGGCATGGCCGGCCTGTGGTGCGTCAATGTCGGCTA
CGGCCGCACCGAACTGGCCGAGGCAGCCTATGAGCAGATGAAGGAGCTG
CCCTACTACAACTCCTTCTTCAAGTGCTCGACGCCGACGCCGGTGCTGCTG
TCCAAGAAGCTTGCGGAATTGGCGCCAAAGAACATCAACCAGGTGTTCTA
TGGCTCGTCGGGCTCCGAATCCAACGACACCGCGCTGCGGCTCGTGCGCC
ACTACTGGGCGATCGAGGGCAAGCCCGAGAAGAACCGCATCATCTCGCGC
AAGATGGCCTATCACGGCTCGACGGTTGCCGGCACCTCGCTCGGCGGCAT
GGACGGCATGCACCAGCAGCTCGGCGGCGCTGTGCCGAACATCGTCCATG
TGATGATGCCCTATGCCTACGAGTTGGCCCTGCCGGGCGAAAGCGACCAC
GATTTCGGCCTGCGTGCCGCCAAGTCGGTAGAGGATGCAATCCTGGAGGC
TGGCGCCGAAAACGTCGCGGCCTTCATCGGCGAGCCGATCATGGGCGCCG
GCGGCGTCAAGATCCCGCCGGCCAGCTACTGGCCGGAGATCCAGCGCATC
TGCCGTAAGTACGACGTGCTGTTGATGCTCGACGAGGTCATCACCGGCTA
TGGCCGCACCGGCGAGTGGTTCGCCGCCCAGACTTTCGGCATCGAAGCGG
ACACCATCACCACCGCCAAGGCGCTGACTTCGGGCTACCAGCCGCTTTCG
GCGCTGCTGGTCGGCGACCGGATCGCCGCGACGCTGGTCGACAAGGGCGG
CGAGTTCTACCACGGTTACACCTATTCCGGTCACCCGGTGGCCTGTGCCGT
GGCGCTCAAGAACCTCGAGATCATCGAACGTGAAGGACTGGTCGAACGC
GTTAAGACCGACACGGGTCCGTATTTCGCCCAGATGCTCAAGGAGCGCAT
TTCCGGTCACGGCCTGGTTGGCGAGGTTCGTTCGGTCGGCCTGATGGGTGC
CATCGAGATCGTCAAGGACAAGGCGACCAAGGAGCGCTTTTCGCCGGTCG
GCAGTGCCGCGGTCGCCGTCCGCGATCATGCCATCGCCAACGGCATGATG
ATGCGCGCGACTGGCGACTCGATGATCCTGTCGCCACCGCTGATCTGGAC
CCGCGCCACCATCGACATGGCCTGCGATCGTATTCTCAAGGCGCTCGATCT
CGCCGAGCGCGACCTGAGAAAGGCCTGA

10.4 Amino Acid Sequences of Metagenomic Ene-Reductases

>pQR1440

MAVSLFDPIKLGAIDAPNRIIMAPLTRGRAGPGFVPTELARDYYRQRASAGLII
SEATGISQEGLGWPSAPGLWTDAQVEGWKPVTDAVHAAGGRIVAQLWHMG
RVVHSVFNDGKPPVSASATQAPGKAHTPVGRLDYEVARPLELGEIPRVIADY
AKAAENAKRAGFDGVQLHGANGYLIDQFLRDGSNLRDDDYGGPIENRIRLLR
EVTEALISVWGADRVGVRLSPNGDTQGVDDSAPEQLFPVAAAALDALGIAFL
ELREPGPEGTFGRTDVPKQSPAIRAAFKGPLILNSDYDVAKAEAALADGLAD
AIAFGRPFIGNPDLVERIRNGAEWAADNPQTWYSPGPEGYTDYPALQTA

>pQR1445

MSNLFTPLQVGAWQLPNRIIMAPLTRCRASEGRVPNALMAEYYAQRASAGLI
ISEATSVTPMGVGYPNTPGIWSDAQVDGWKLITDAVHQAGGRIVLQLWHVG
RISDPVYLDGQLPVAPSAIAPQGHVSLVRPTKAFETPRALDTAELVDVVAAYR
LGAENAKKAGFDGVEIHGANGYLLDQFLQSSTNQRTDQYGGSLENRARLLL
EVVDACIEVWGADRVGVHLAPRGDAHDMGDANPAETFGYVAEQLGARQV
AFICTREYLADDSLAGLIKAKFGGVYIANEKYDQAQADAAIASGAADAVAFG
VKFIANPDLPARFAQGAVLNAPDPSTFYGAGSKGYTDYLTL

>pQR1446

MTAPVQALFAPFRLGNLELPTRVVMAPMTRSFSPGGVPNAQVVEYYRRRAA
AGVGLIVTEGTTVGHKAANGYPHVPRFYGEDALAGWKQVVDAVHAEGGKI
VPQLWHVGNVRKAGTEPDASVPGYGPSEKVKDGTVVVHGMTKDDIQEVIA
AFAQAARDAKAIGMDGVEIHGAHGYLIDQFFWEGSNKRTDEYGGDLAQRSR
FAIELIQAVRAAVGPDFPIIFRFSQWKQQDYTARLVQTPEELGAFLKPLSDAGV
DIFHCSTRRFWEPEFEGSDLNLAGWTRQLTGKPTITVGSVGLDGEFLQFMVNT
DKVAEPASLENLLERLNKQEFDLVAVGRALLVDPDWAVKVRDGRESDILPFS
REALKQLV

>pQR1907

MSGKLFTPFSSGSFTFPNRVIMAPLTRMRASQPGDIPNELMQTYYVQRASAGL
IIAEATQISPQGKGYMDTPGIYSAEQVQGWRKITQAVHEAGGHIALQLWHVG
RVSHHSLQPDQQLPVSASAIPYQNRTTVRGEDGKPTRVDCDTPRALELSEIPG
VIEDYRRATVNSREAGFDMVEVHAAHGYLLHQFQSAESNKREDAYGGSLEN
RARLTLEALDAVIGAWDAKHVGIRISPLGTFNGLDDKDGLEMALYLTREFTK

RGIAYLHLSEPDWAGGPAHGDEFRQALRDAFPGTIIGAGNYTVEKSEMLLAK
GFIDAAAFGRPFIANPDLPVRLQKGAELNNVVAATLYGGGAEGYTDYPALA

>pQR1909

MSRLFSPLALGPLPLSNRIVIAPMCQYSADEGRATDWHAFHWPNLAQSGAAL
AIIEATAVEPRGRISWADLGLWDDTTEAAFARALAAARRYSTMPIGVQLAHA
GRKASTHRPWEHHGAQIAPDAPQGWRTVSASSLPYAEGQHPPDSLDQAGIDA
IIAAFADSAHRAVRLGLDLIEIHAAHGYLLHQFLSPLSNRRDDAYGGALENRM
RLVLQVFDAIKAVVPASMAVGVRISATDWVDGGWDLAQSIALAKALDARGS
HFIHVSSGGLHPAQKIALGPGYQVPFAAAIKREVAMPVIAVGLITAPQQAEDIL
LQAQADAIAIARAVLYDPRWPWHAAASLGETIAIAPQYLRSAPREVAASFVE
AT

10.5 Amino Acid Sequences of Metagenomic Transaminases

Amino acids corresponding to the vector sequence are in bold.

>pQR2189

MGSSHHHHHHSSGLVPRGSHMPRNHDIAELRRLDVAHHLPAQADWAEIEK
LGGSRIITHAEGCYIHDGDGHRILDGMAGLWCVNVGYGREELVEAAAAQMR
ELPFYNTFFKTATPPTVTLAAKIASLTGNRLPHIFFNASGSEANDTVFRMVRH
YWKLKGEPKRTVFISRWNAYHGSTVAGVSLGGMKAMHAQGDLPIPGIEHVR
QPYSFGEGQGMTEEEFCDACVHAIEDKILEVGPENCAAFIGEPVQGAGGVVIP
PKGYWPKVEAVARKYGLLVVSDEVICGFGRTGKMWGHETMGFTPDLMSMA
KGLSSGYLPISATAVATHVVDVLKTGGDFVHGFTYSGHPVAAAVALKNIEIIE
REGLVERTGSVTGPHLAKALATLNDHPLVGETRSIGLLGAVEIVGEKVTRARF
GGAEGTAGPMARDACIANGLMVRGIRDSLVMCPPLIISTEQIDEMVAIIRKSL
DEVMPKLRAL**EHHHHHH**

>pQR2191

MGSSHHHHHHSSGLVPRGSHMSGQRDQELRARAAKVMPSSAFGHVGTAL
LPANYPQFFERAEGAYVWDADGNRYLDYMCAFGPNLLGYRDPRVESAASA
QAARGDVMTGPSPLAVELAEKFVEIVSHADWAFFCKNGTDATTIARTIARAQ
TGRRKILIAEGSYHGAAPWCNPFPAGTVPEDRAHMLTFTFNDIASLEAAVAEA
GDDLAGIIATPFKHEAFANQEFPTQDYARRCREICDASGAVLVVDDVRAGFR
LAVDCSWATVGVKPDLSCWGKCFANGYSISAVMGSNRVKQGADSIFATGSF

WQSAISMAAALATLDIIRDGKVIEKTVRLGQRLRDGLDEVSRRHGFTLNQTG
PVQMPQILFEGDPDFRVGFAWTSAMIDRGFYLHPWHNMFLCDAMTEEDIDQ
TIEAADSAFATVR AALPTLQPHERVLALFSARA**EHHHHHH**

>pQR2208

MTLRNYDMAELKRLDLAHHLPAQASYGLIRDLGGSRIITRAEGSTIWDAEGN
AILDGMAGLWCVDVGYGRAELAEVAREQMLELPYYNTFFRTATPPPVKLAA
KIAGLLGGSLQHIFFNSSGSESNDTVFRLVRTYWALKGQPERTIFISRRNAYHG
STVAGVSLGGMAAMHAQGGLPIAGIEHVMQPYAFGEGFGEDPEAFAARAAQ
EIEDRILAVGPEKVAAFIGEPVQGAGGVIIPPPGYWPRVDAICRKYGILLVSDE
VICGFGRLGEWFGFQKYGYTPDIVSMAKGLSSGYLPISATGVSSEIVETLRASG
DDFVHGYTYSGHPVAAAVALRNLEIIKREGLVDRVRDDLAPYFAKALATLD
DHPLVGEARSVGLLGAVEIVSEKGTNHRFGGKEGTAGPVVRDHCIAGGLMV
RAIRDSIVMCPPYV ITHDEIDRMVAIIRSALDKAAVDLGGGA**HHHHHH**

>1-TAm

MTISPLNDLNPGLDADSSVDLQELAQQHLIMHFTGAGAYNEAPPRVMVSGD
GCWLTDSTGKRYLDALAGLFCVNVGYGYGAEIGHAVQQQMATLPYFSNWG
YAQPPSILLAAKIAELAPAGLDRVFLTSGGSESNEAAVKLIRQYHQARGEHSR
MKFIARRVSYHGTSYAALSLNGMTNFKKVFEPLMHGTRHISNTKRYKRPFGE
TEEQFTALLLQELEALIVQEGPDTVAGIFLEPLQNAGGSLTPPEGYCAGVREIC
DRHGILLVADEVICGFGRLGEWFGSTRYGMEPDIITFAKGVSSGHVPLGGMIT
TSAVIDTVLSGPQGMYLHGLTFGGHPVACAAGLANIAIMEREDILGHVRRTEP
YFRARLSELLEHPLVGDLRGDGFHYSLELVTDKNARAWRSTISSNDFVAQHL
NPALVDAGILCRAAVDHEGTPLIQFSPPLVFDTDDINFLVEHVRTVLDAMSNI
DGLTA

>13-TAm

MTTTETEIQHLDTPALRDSAGAHLWRHFSDMTTTEKQPLRVMVKGEGCYLID
SEGNRFLDALSNLFCVNIGYSYGEELGQAALAQYRELGYHSNWGSTHPKAIE
LAHTLADLAPEGLDHVFFTPSGGESVEAAWKIAREYHHLRGEKRWKAIGRS
MAYHGTTMGALSINGIPEIRSMFEPLLPGASHVRNTKRFGRPEKETEEEFTQFL
LDDLEQRILAEDPATVAMIIMEPVQNHGGMLVPPAGYSAGVRALCDRYGILL
VADETITAFGRCGAWFASERYEMKPDIITTAKGLSSAHAVIGAVITTDEVYST
FYVAGRKFTHGNTFGGHPVMAAVALRNIEIMQELDIPRHVAAKEDELRSKLE

SLRALPIVEDVRGSGFFYAIELTSTDARGQRFSDTELARLYGDELLSDRLVDR
GILLRLSLDGGDPVLCIAPPLIADSPEFDELVDGLRDVLSALSLDAGLV

>16-TAm

MSTNPVQTVDSDPSRHLWMHFSNMGAYAQGVEVPVIVRGEGCYVWDQHG
NRYLDGLSSLYCVNVGHGRTELAEAAAKQATELAFFPTWSFAHPRAIELATK
IADLAPADLNRVFFVGGGGEAVDSAFKLARQYHKIRGKAGKYKVISRNTAY
HGTTLGALAATALSPARAPFEPLPIGGSHVTNTNVYRLDPQAVDTLAEAIRER
IEFEGPDTVAAVILEPVQNSGGCFVPPEGYFQRVRQICDQYDVLLISDEVICAF
GRLGEWFGAQRFDYVPDIITTAKGLTSAYAPMGAVIASDRVIEPFLTDNNVFA
HGVTFGGHPVASAVALANIELMESEKMLENVRANEPVLRGMLESLRDIPLVG
DVRGAGYFWAIELVKDPATRQRFSPAEGKALLAFLAPELYRRGLICRADMRG
DLVVQLAPPLIAGPPHFAEIETILRSTLVDAAALSLPTD

>23-TAm

MTYQNYSLKQLQQIDAAHHLHPFTDHKELRDIGSRMITRAEGPFIYDSEGTEL
LDGMAGLWCVNVGYGRTELAEAAYEQMKELPYYNSFFKCSTPTPVLLSKKL
AELAPKNINQVFYGSSGSESNDTALRLVRHYWAIEGKPEKNRIISRKMAYHGS
TVAGTSLGGMDGMHQQLGGAVPNIVHVMMPYAYELALPGESDHDFGLRAA
KSVEDAILEAGAENVAAFIGEPIMGAGGVKIPPASYWPEIQRICRKYDVLLML
DEVITGYGRTGEWFAAQTFGIEADTITTAKALTSGYQPLSALLVGDRIAATLV
DKGGEFYHGYTYSGHPVACAVALKNLEIIEREGLVERVKTDTGPYFAQMLKE
RISGHGLVGEVRSVGLMGAIEIVKDKATKERFSPVGSAAVAVRDHAIANGM
MMRATGDSMILSPPLIWTRATIDMACDRILKALDLAERDLRKA

10.6 Sodium Dodecyl Sulfate Polyacrylamide Gel Electrophoresis

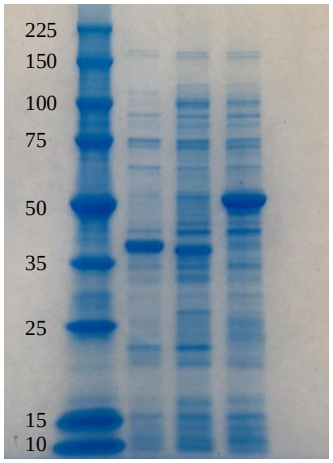

Figure 80: SDS-Page gel of clarified lysates used in preparative scale biotransformations. Lanes from left to right: Protein ladder (Promega), NCR+pQR1811, Mv-TAm, 13-TAm.

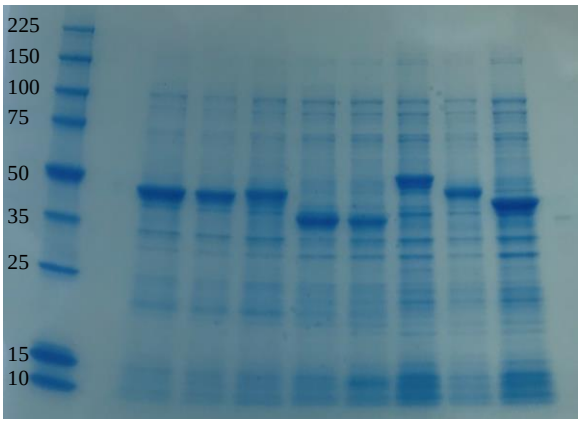

Figure 81: SDS-Page gel of literature and metagenomic TAms. Lanes from left to right: Protein ladder (Promega), Cv-TAm, Cv-TAm, Rh-TAm, Mv-TAm, As-TAm, pQR2189, pQR2191, pQR2208.

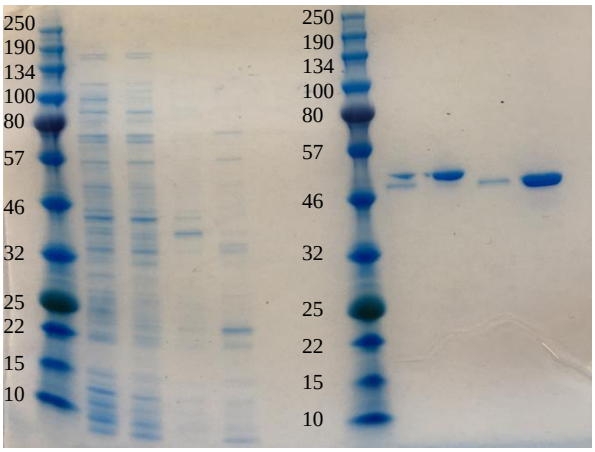

Figure 82: SDS-Page gel of metagenomic ERs and TAms. Lanes from left to right: Protein ladder, pQR1440+1811, pQR1445+1811, pQR1446+1811, pQR1907+1811, protein ladder, 1-TAm, 13-TAm, 16-TAm, 23-TAm.

10.7 Calibration Curves

Calibration curves were attained by the chromatographic analysis of chemical compounds in solutions of known concentration. Serial dilutions were performed to attain solutions of known concentration, starting with the most concentrated solution and diluting by half each time (ie. 10 mM solution diluted by half to give 5 mM solution, which was then diluted by half to give 2.5 mM solution, etc).

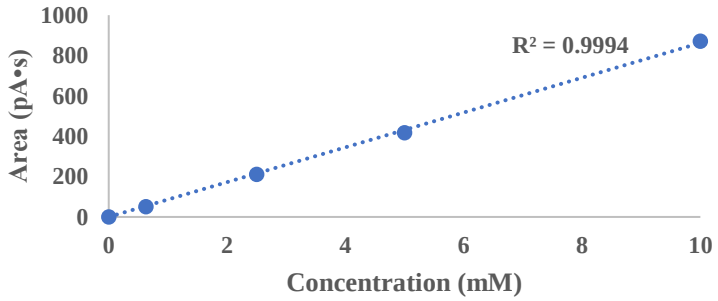

Figure 83: Calibration curve for cyclohexenone **90** using ***Method D***.

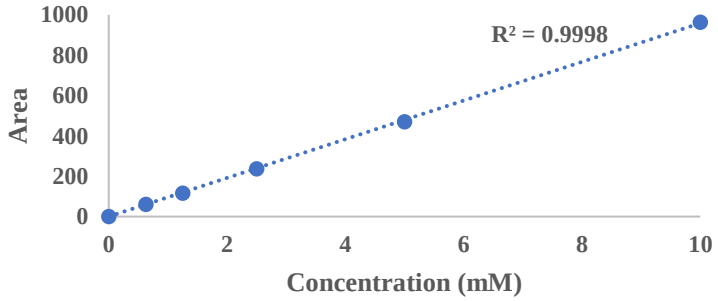

Figure 84: Calibration curve for cyclohexanone **91** using ***Method D***.

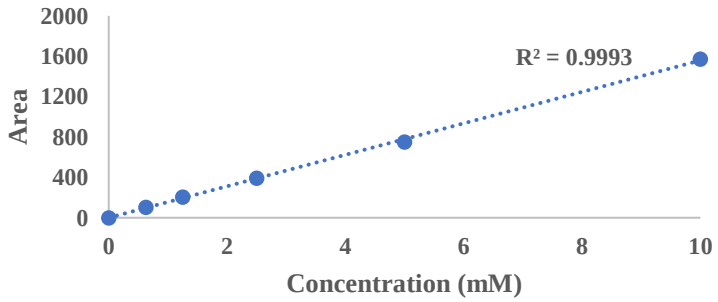

Figure 85: Calibration curve of cinnamaldehyde **70** using ***Method D***.

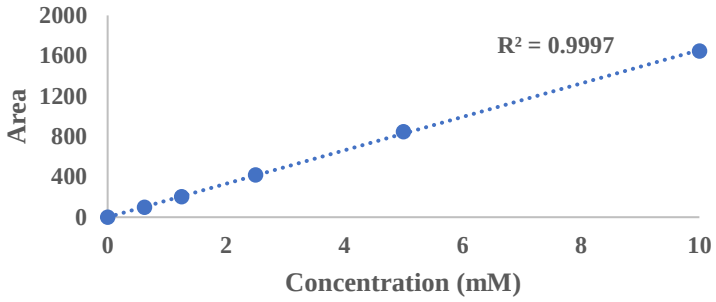

Figure 86: Calibration curve of hydrocinnamaldehyde **74** using ***Method D***.

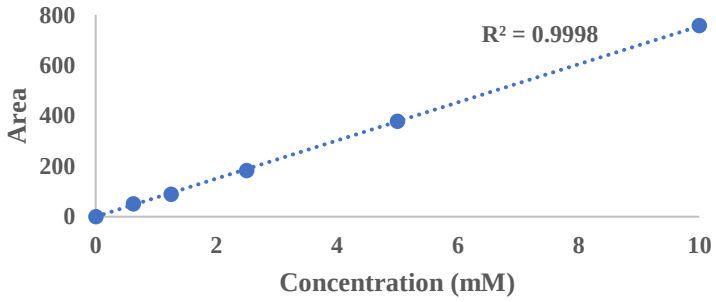

Figure 87: Calibration curve for saturated ADH by-product **92** using ***Method D***.

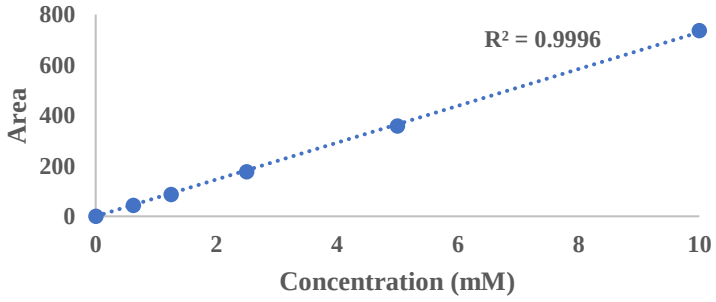

Figure 88: Calibration curve for unsaturated ADH by-product **93** using ***Method D***.

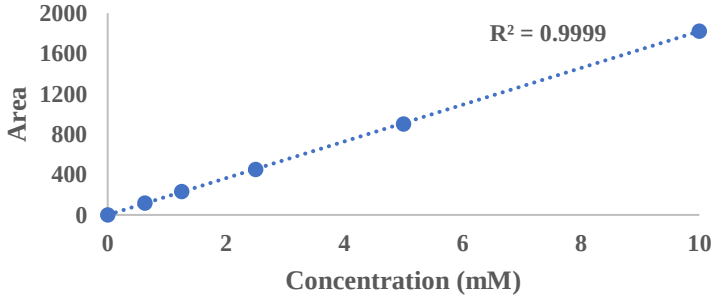

Figure 89: Calibration curve of α-methyl cinnamaldehyde **67** using ***Method D***.

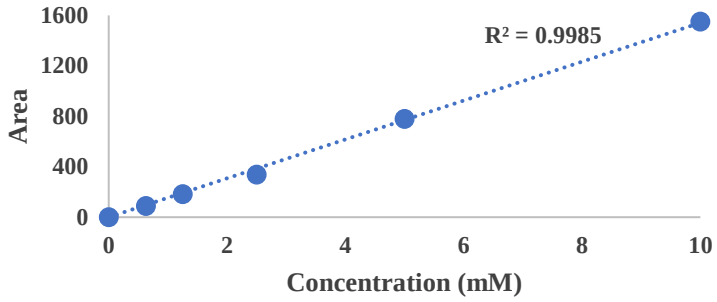

Figure 90: Calibration curve of α-methyl hydrocinnamaldehyde **68** using ***Method D***.

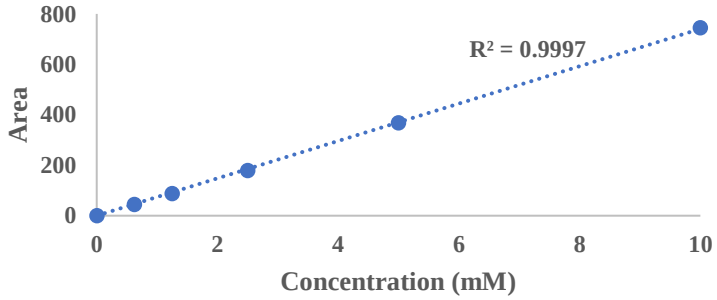

Figure 91: Calibration curve for β-methyl cinnamaldehyde **40** using ***Method D***.

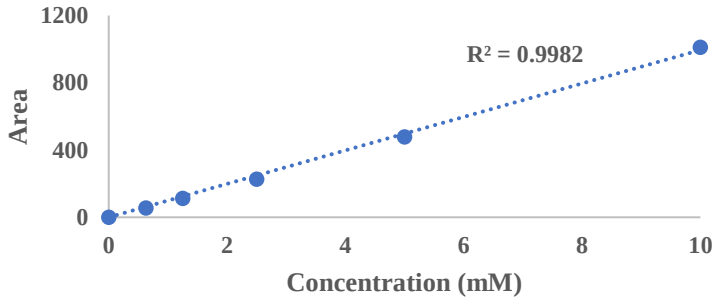

Figure 92: Calibration curve for β-methyl hydrocinnamaldehyde **75** using ***Method D***.

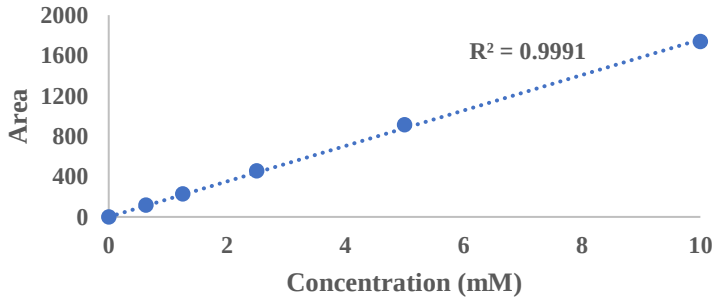

Figure 93: Calibration curve of β-phenyl cinnamaldehyde **71** using ***Method D***.

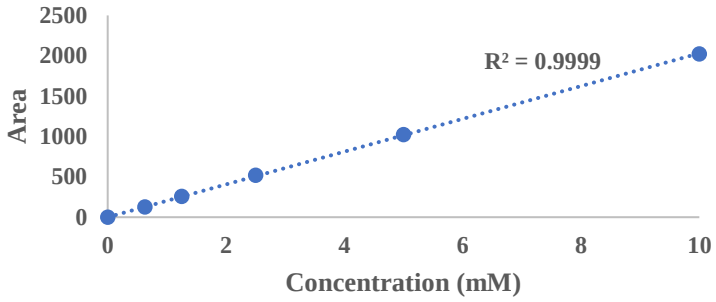

Figure 94: Calibration curve of β-phenyl hydrocinnamaldehyde **76** using ***Method D***.

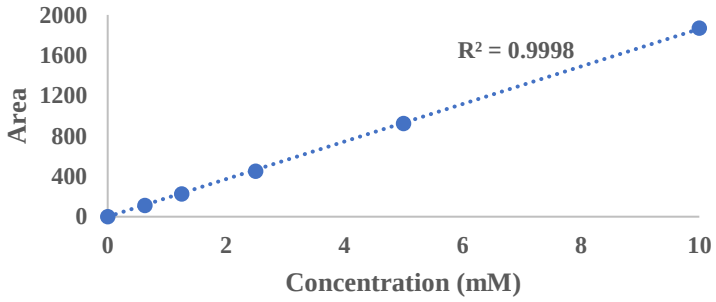

Figure 95: Calibration curve for 4-methoxy cinnamaldehyde **72** using ***Method D***.

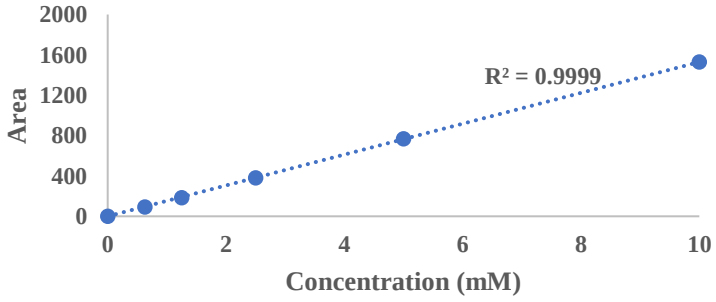

Figure 96: Calibration curve for 4-methoxy hydrocinnamaldehyde **77** using ***Method D***.

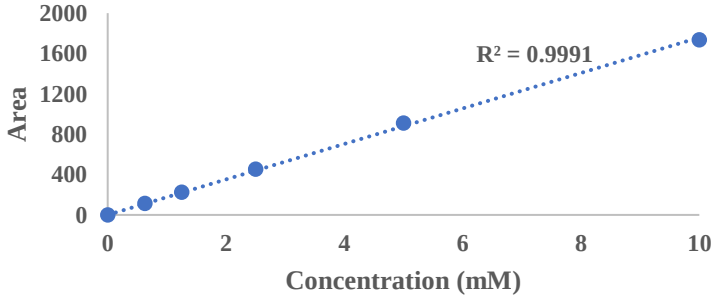

Figure 97: Calibration curve of 4-NMe_2 cinnamaldehyde **73** using ***Method D***.

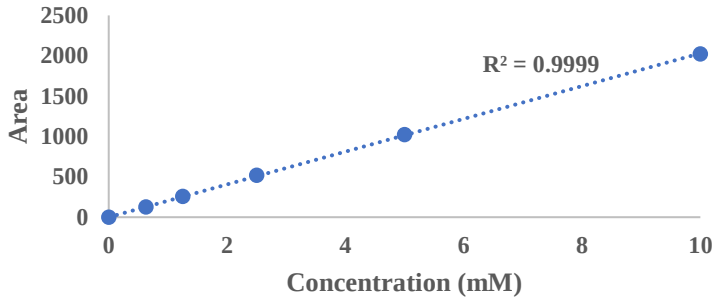

Figure 98: Calibration curve of 4-NMe_2 hydrocinnamaldehyde **78** using ***Method D***.

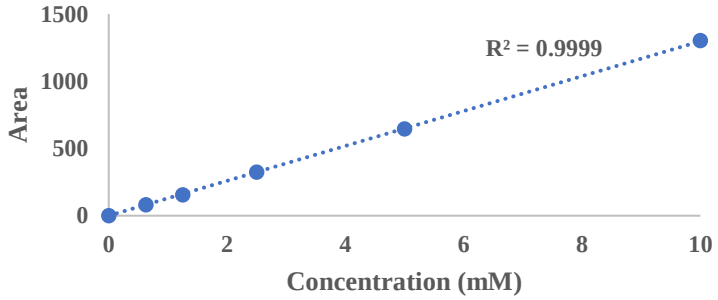

Figure 99: Calibration curve for aliphatic starting material **98** using ***Method E***.

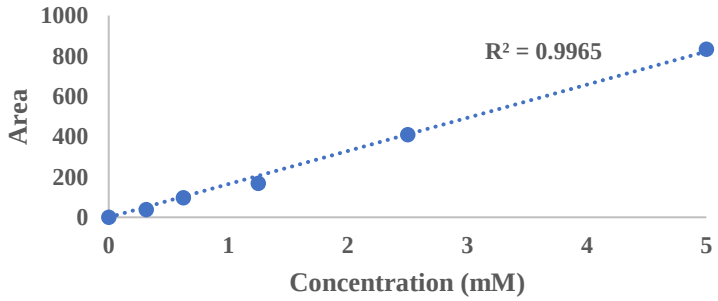

Figure 100: Calibration curve for the saturated product from bioreduction of aliphatic **98** using ***Method E***.

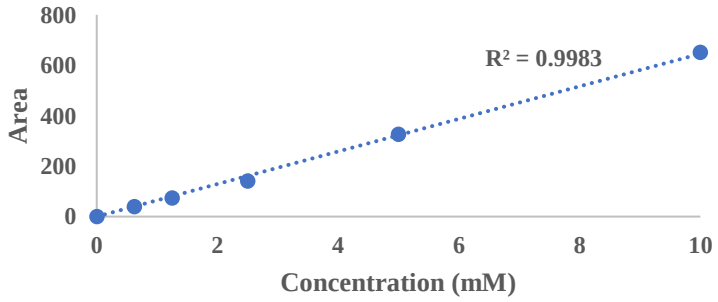

Figure 101: Calibration curve of aliphatic starting material **99** using ***Method E***.

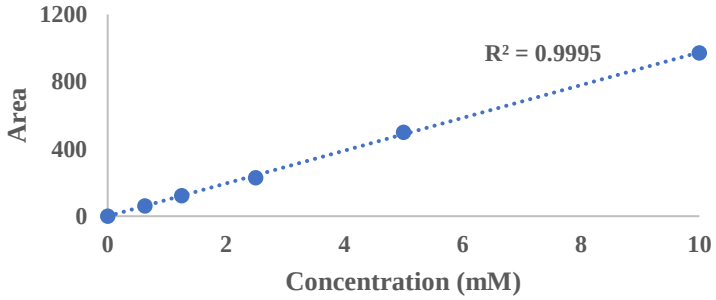

Figure 102: Calibration curve of the saturated product from bioreduction of aliphatic **99** using ***Method E***.

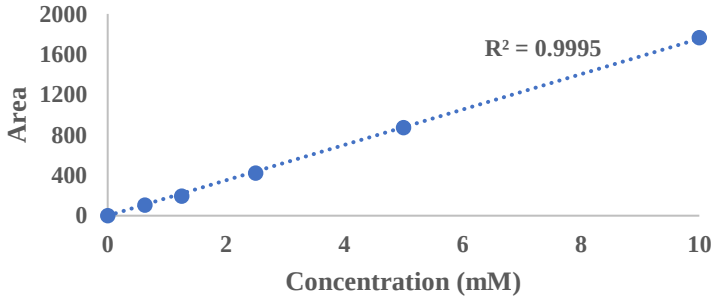

Figure 103: Calibration curve for (*E*/*Z*)-citral starting material (*E*/*Z*)-**18** using ***Method E***.

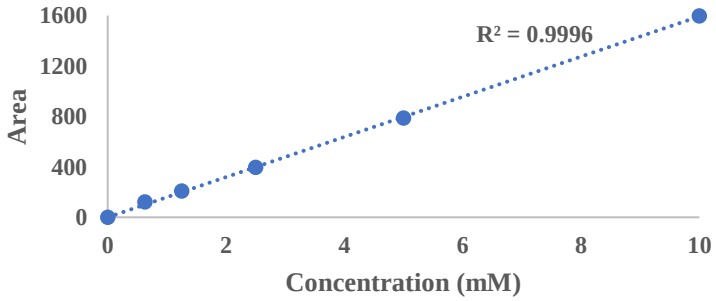

Figure 104: Calibration curve for *rac*-citronellal product using ***Method E***.

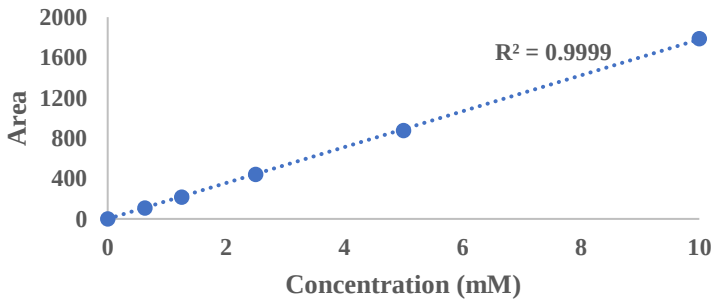

Figure 105: Calibration curve of unsubstituted ketone starting material **41** using ***Method D***.

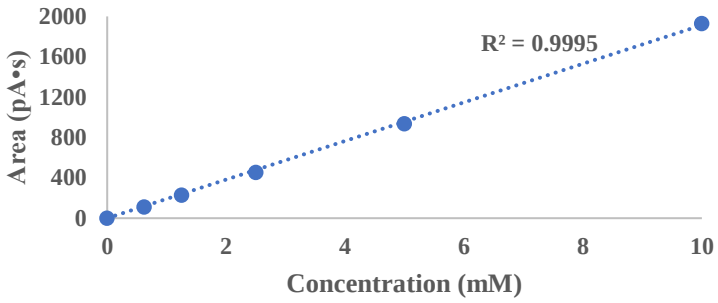

Figure 106: Calibration curve of unsubstituted ketone product **79** using ***Method D***.

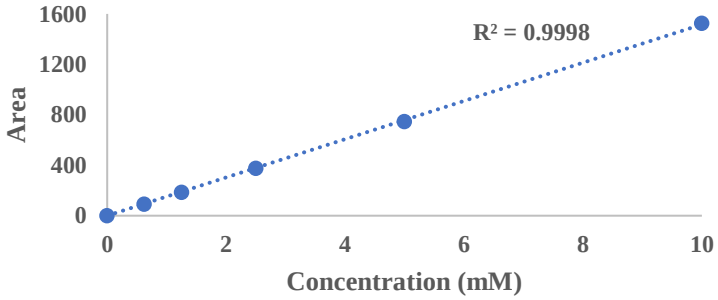

Figure 107: Calibration curve for unsaturated α-methyl ketone starting material **7a** using ***Method D***.

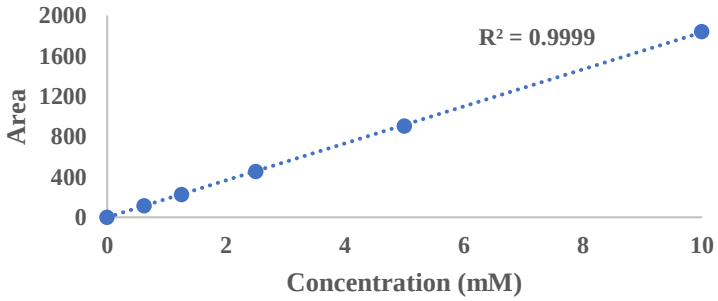

Figure 108: Calibration curve for saturated α-methyl ketone product **8a** using ***Method D***.

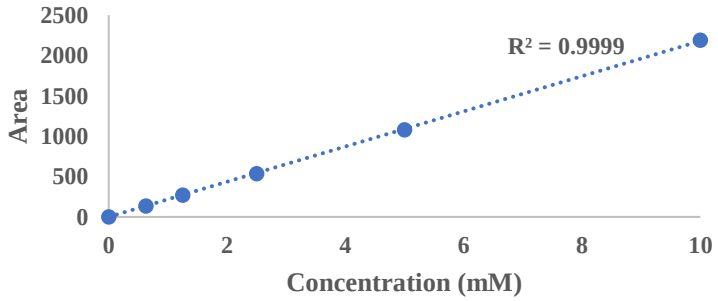

Figure 109: Calibration curve of unsaturated β-methyl ketone starting material **42** using ***Method D***.

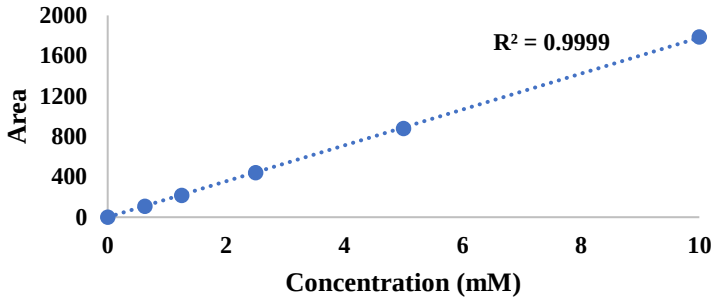

Figure 110: Calibration curve of unsubstituted α-hydroxyketone starting material **52** using ***Method D***.

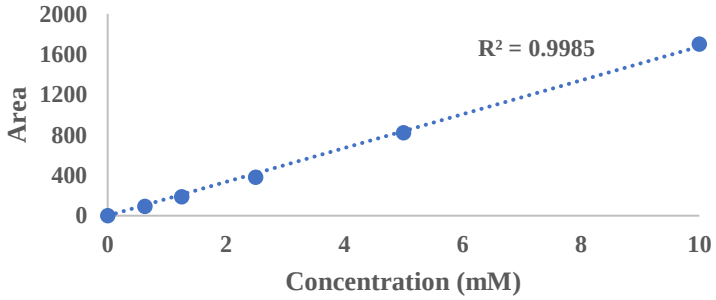

Figure 111: Calibration curve for saturated unsubstituted α-hydroxyketone product **84** using ***Method D***.

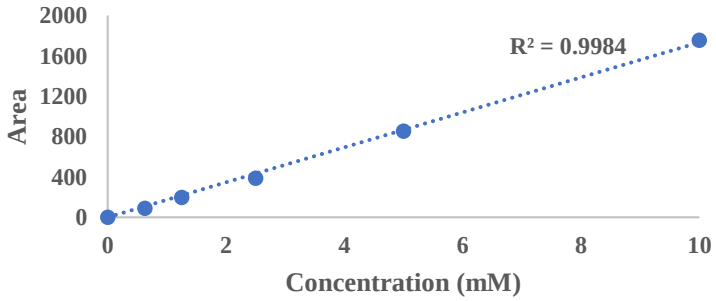

Figure 112: Calibration curve for unsaturated α-methyl hydroxyketone starting material **63** using ***Method D***.

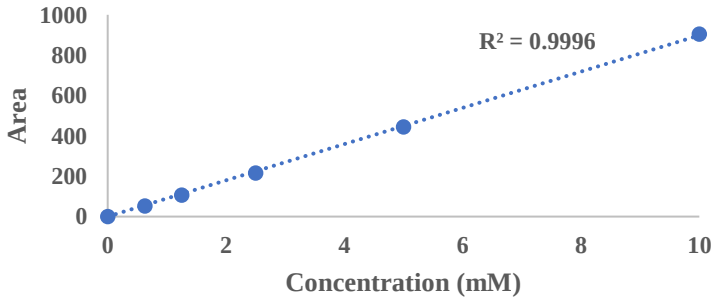

Figure 113: Calibration curve of (*S*)-α-methyl hydroxyketone product (*S*)-**85** using ***Method D***.

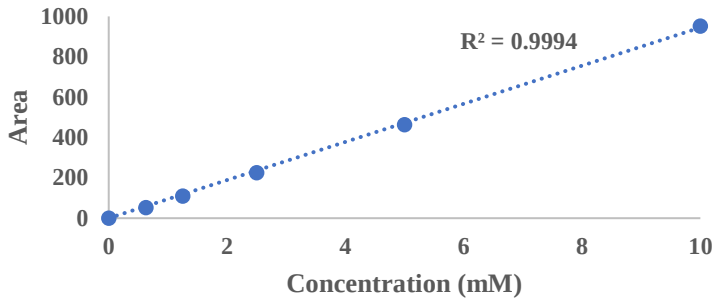

Figure 114: Calibration curve of (*R*)-α-methyl hydroxyketone product (*R*)-**85** using ***Method D***.

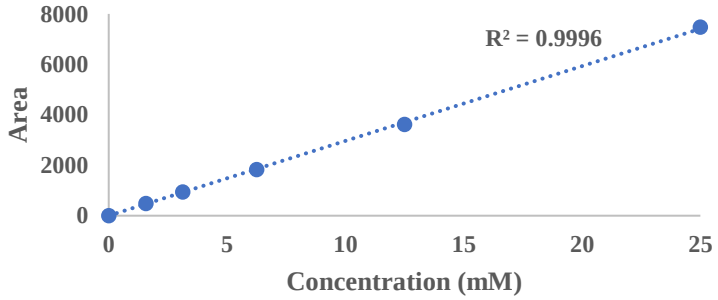

Figure 115: Calibration curve for 4-methoxy ketone starting material **46** using ***Method D***.

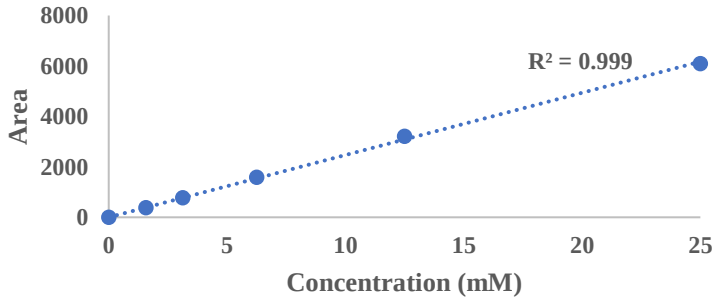

Figure 116: Calibration curve for 4-methoxy ketone product **81** using ***Method D***.

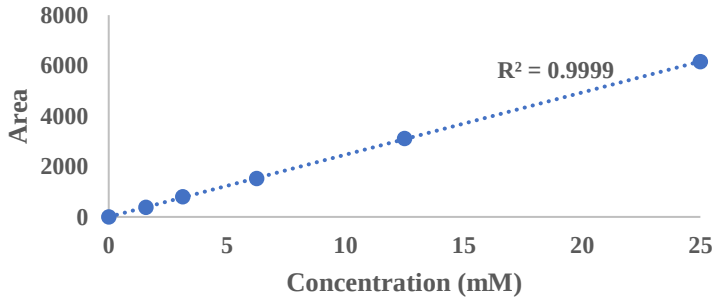

Figure 117: Calibration curve of 4-cyano ketone starting material **47** using ***Method D***.

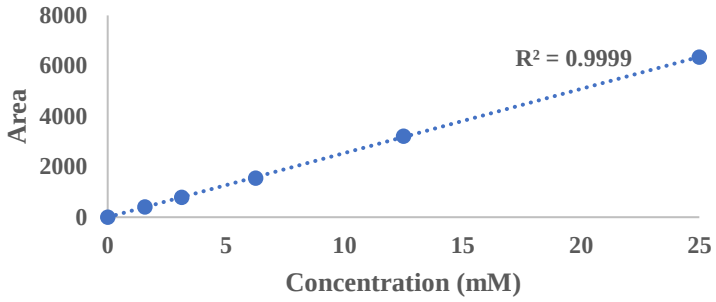

Figure 118: Calibration curve of 4-cyano ketone product **82** with ***Method D***.

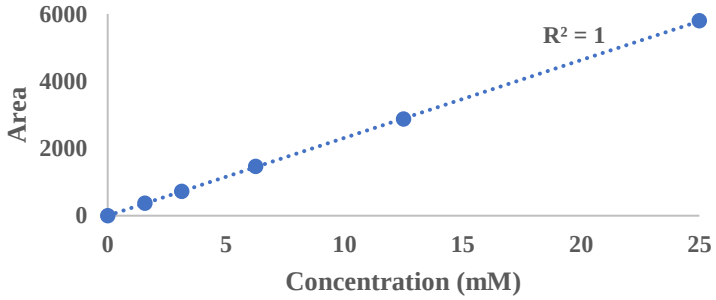

Figure 119: Calibration curve for 3-fluoro ketone starting material **48** using ***Method D***.

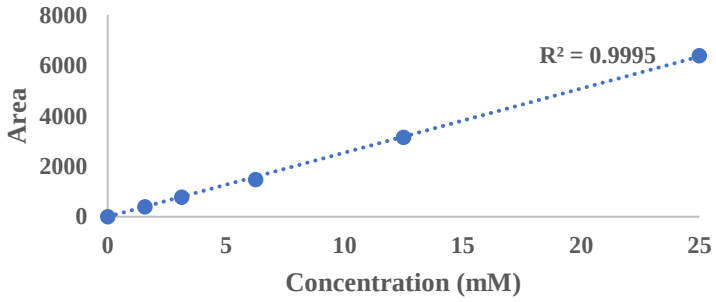

Figure 120: Calibration curve for 3-fluoro ketone product **83** using ***Method D***.

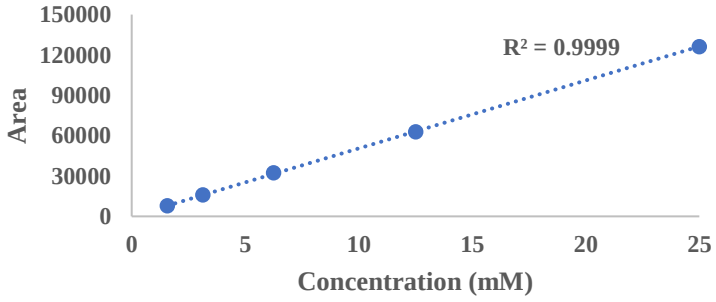

Figure 121: Calibration curve of 4-methoxy hydroxyketone product **87** using ***Method H***.

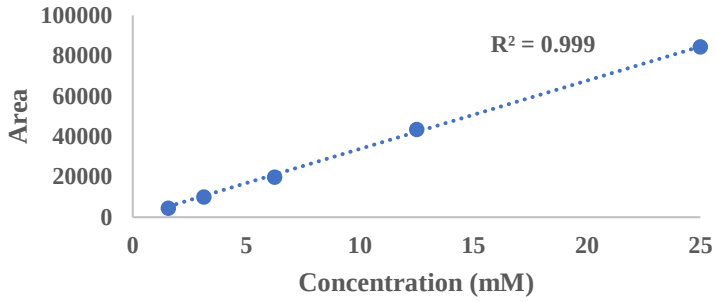

Figure 122: Calibration curve of 4-cyano hydroxyketone product **88** using ***Method I***.

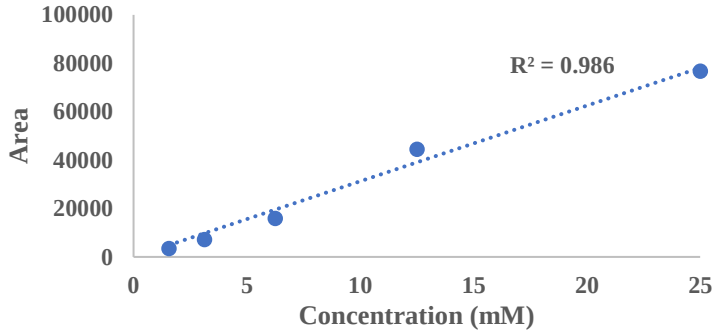

Figure 123: Calibration curve for 3-fluoro hydroxyketone starting material **89** using ***Method H***.

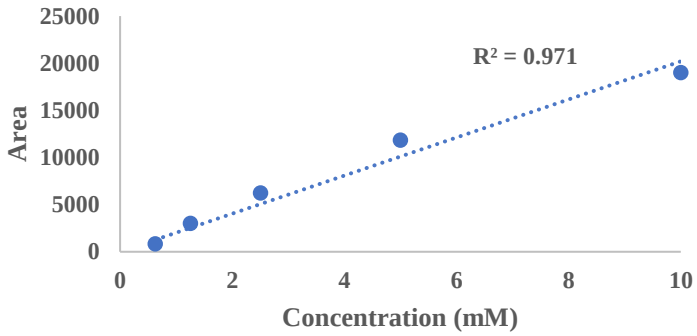

Figure 124: Calibration curve for 4-methoxy hydroxyketone starting material **87** using ***Method B***.

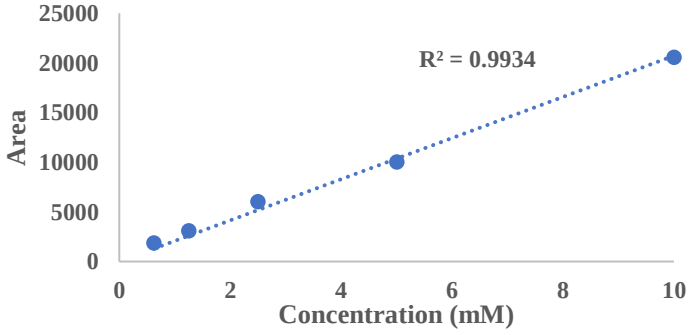

Figure 125: Calibration curve of 4-cyano hydroxyketone product **88** using ***Method B***.

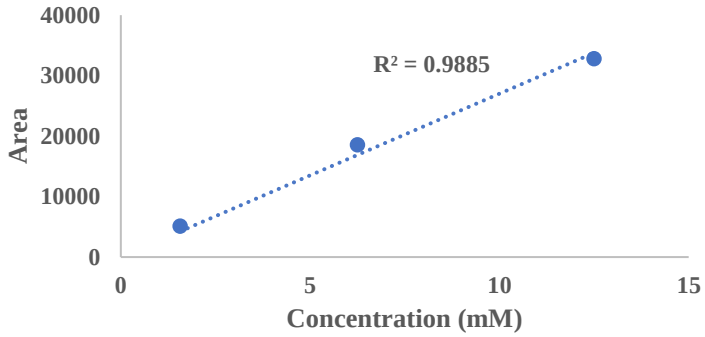

Figure 126: Calibration curve of 3-fluoro hydroxyketone product **89** using ***Method B***.

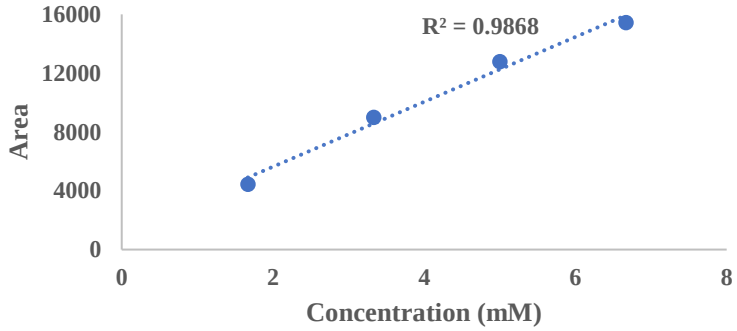

Figure 127: Calibration curve for α-methyl hydroxyketone starting material **85** using ***Method B***.

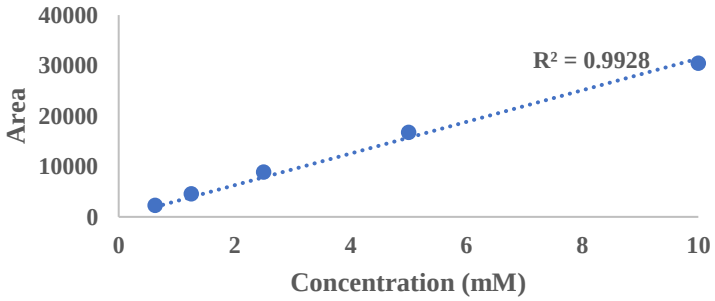

Figure 128: Calibration curve for acetophenone using ***Method B***.

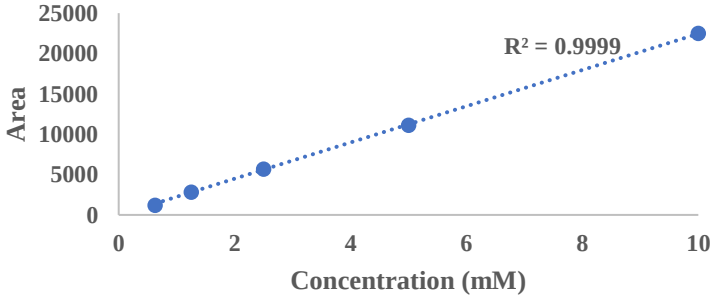

Figure 129: Calibration curve for amino alcohol product **100** using ***Method C***.

10.8 Chromatograms

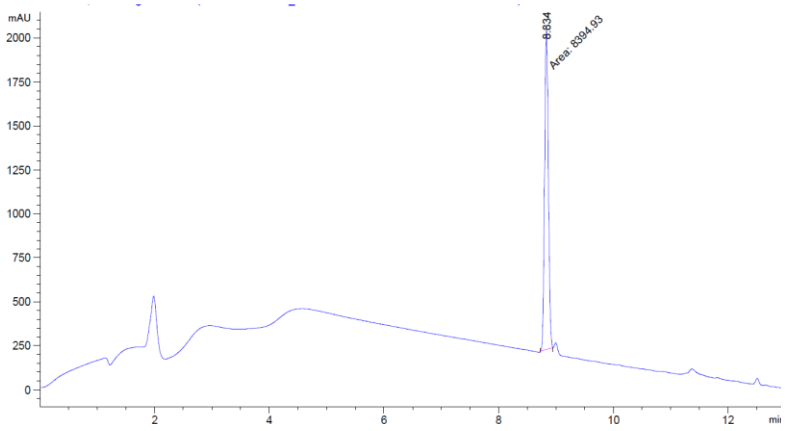

Figure 130: Chromatogram (analytical HPLC, ***Method B***) of compound **85**. Retention time of compound **85**, 8.8 min.

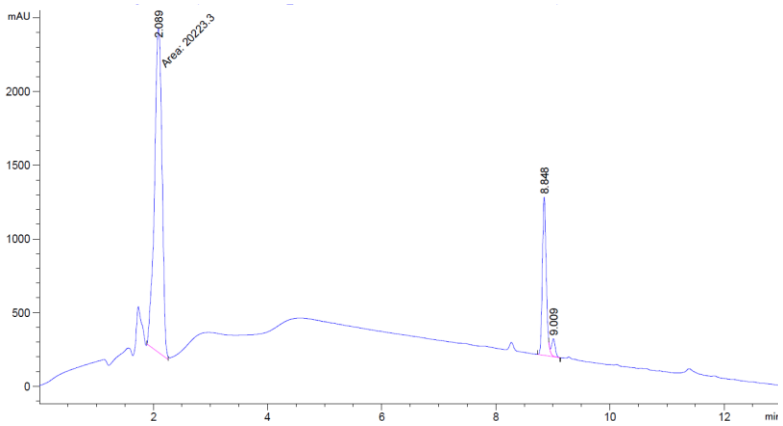

Figure 131: Chromatogram (analytical HPLC, ***Method B***) of the optimised small scale Mv-TAm transamination of (*S*)-**85**, with a conversion of 83%. Retention time of (*S*)-**85**, 8.8 min.

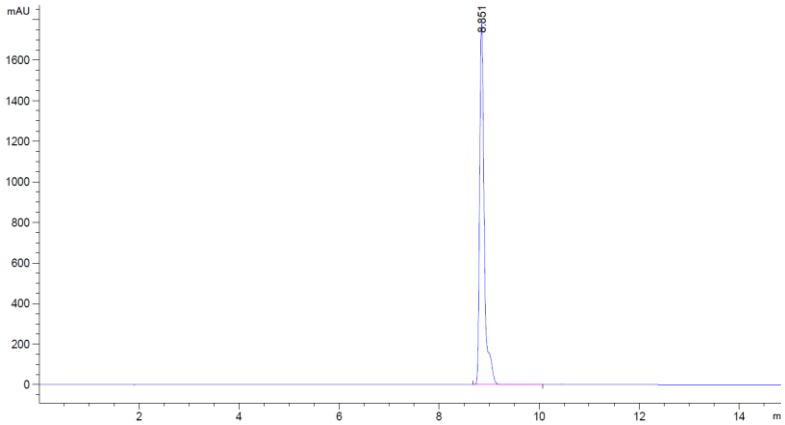

Figure 132: Chromatogram (analytical HPLC, ***Method A***) of acetophenone. Retention time of acetophenone, 8.8 min.

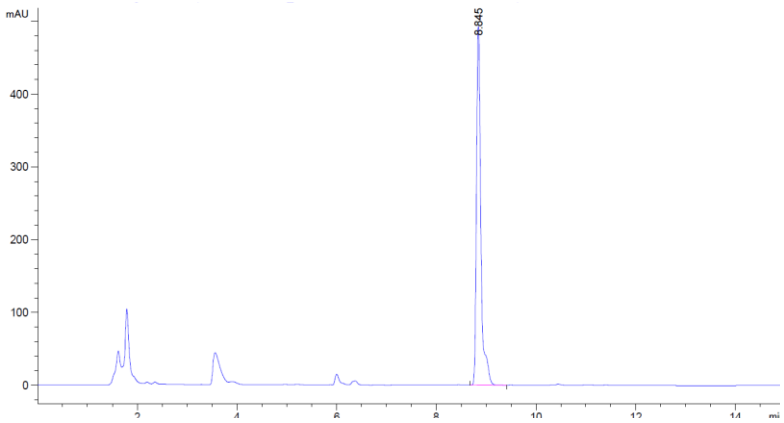

Figure 133: Chromatogram (analytical HPLC, ***Method A***) of the optimised small scale 13-TAm transamination of (*S*)-**85**, with a 72% conversion yield (of acetophenone produced). Retention time of acetophenone, 8.8 min.

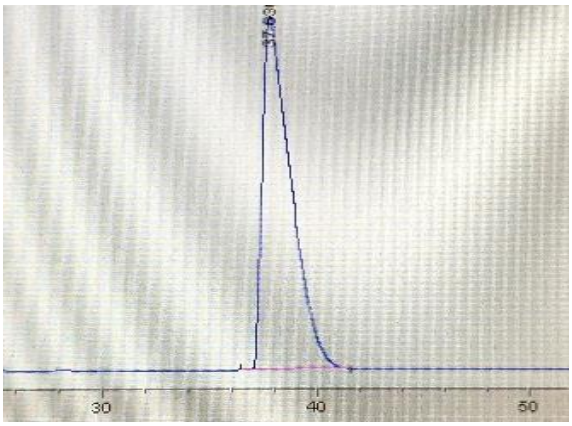

Figure 134: Chromatogram (Chiral HPLC, ***Method G***) of the optimised preparative scale NCR biotransformation of **63** (25 mM substrate loading, 25 mL volume) in 50 mM HEPES (pH 7.4), producing (*S*)-**85** in 99.5% *ee*, as pictured. Retention time of (*S*)-**85**, 37.6 min. Product formation was confirmed by co-injection with the racemic product standard.

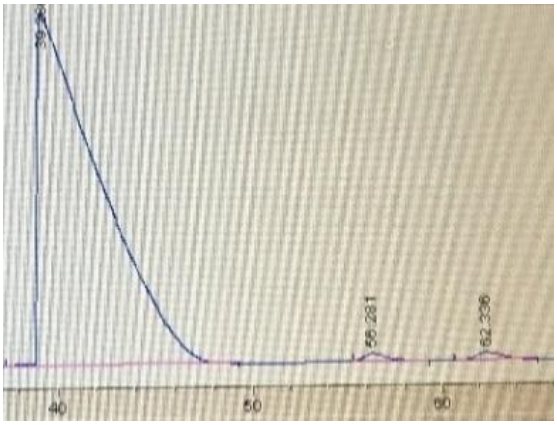

Figure 135: Chromatogram (Chiral HPLC, ***Method G***) of the optimised semi-preparative scale NCR biotransformation of **63** (5 mM substrate loading, 25 mL volume) in 50 mM HEPES (pH 7.4), producing (*S*)-**85** in 98% *ee*. Product (*S*)-**85** at retention time 37.6 min, (*R*)-**85** at retention time 62.3 min, starting material **63** at retention time 56.3 min. Product formation was confirmed by co-injection with the racemic product standard. Starting material **63** was confirmed by co-injection.

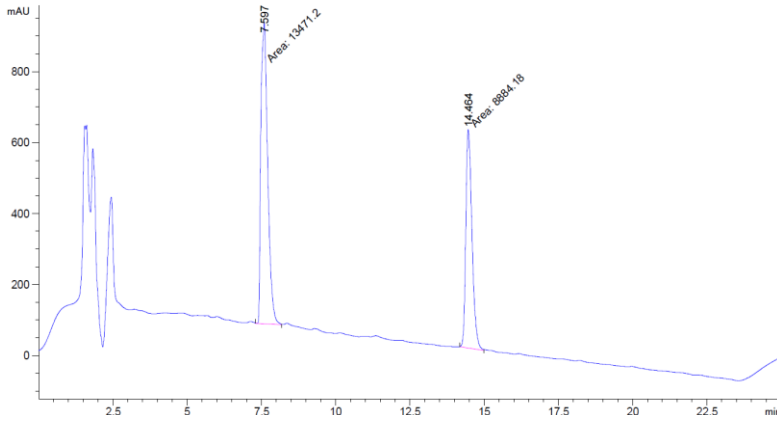

Figure 136: Chromatogram (analytical HPLC, ***Method C***) of the amino alcohol product (2*S*,3*S*)-**100** and intermediate (*S*)-**85** from the preparative scale NCR – Mv-TAm cascade (25 mM substrate loading, 2 mL volume, two step, one-pot cascade, in 50 mM HEPES pH 7.4 then 9). Retention times 7.6 min and 14.5 min respectively. Product yield by HPLC, 52%.

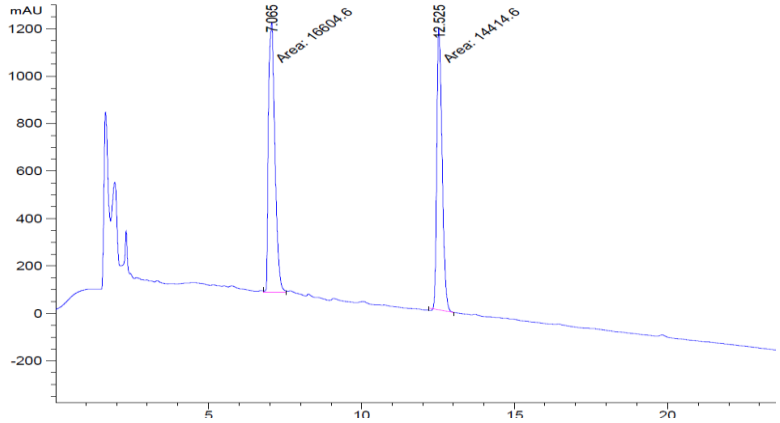

Figure 137: Chromatogram (analytical HPLC) of the amino alcohol product (2*S*,3*S*)-**100** and intermediate (*S*)-**85** from preparative scale NCR – Mv-TAm cascade (25 mM substrate loading, 25 mL volume, two step, one-pot cascade, in 50 mM HEPES pH 7.4 then 9). Product yield by HPLC, 63%.

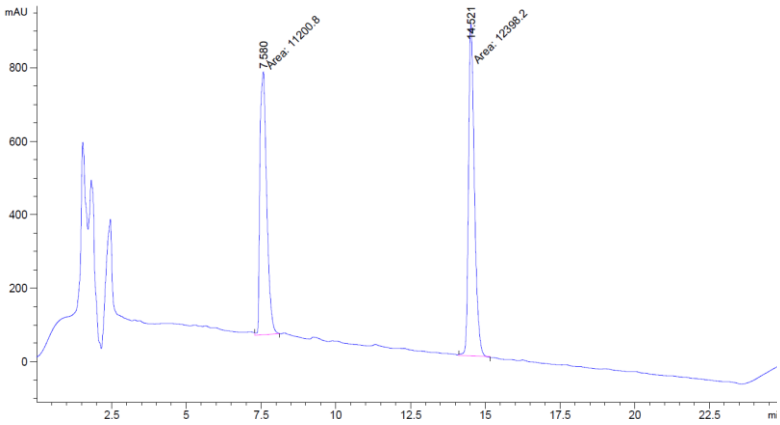

Figure 138: Chromatogram (analytical HPLC, ***Method C***) of the amino alcohol product (2*S*,3*S*)-**100** and intermediate (*S*)-**85** from the optimised preparative scale NCR – Mv-TAm cascade (25 mM substrate loading, 25 mL volume, two-step, one-pot cascade, in water pH 7.4 then 9). Retention times 7.6 min and 14.5 min respectively. Product yield by HPLC, 58%.

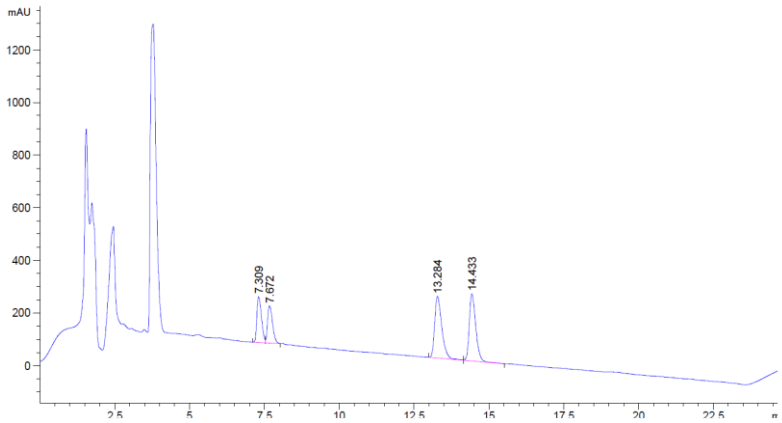

Figure 139: Chromatogram (analytical HPLC, ***Method C***) of the amino alcohol product (2*R*,3*S*)-**100** and intermediate (*S*)-**85** from the preparative scale NCR – 13-TAm cascade (5 mM substrate loading, 25 mL volume, one step, one-pot cascade, in water pH 7.4). Retention times 7.7 min and 14.5 min respectively. Product yield by HPLC, 29%. Also shown, (*S*)-α-MBA at retention time 3.8 min, by-product (*R*)-**103** at retention time 7.3 min, and acetophenone at retention time 13.3 min.

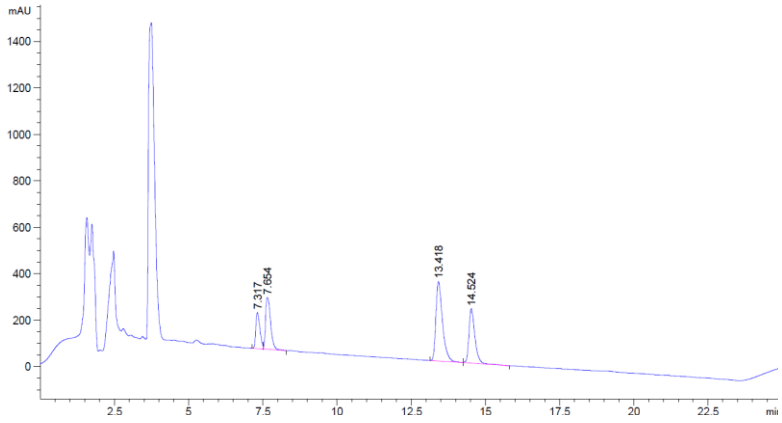

Figure 140: Chromatogram (analytical HPLC, ***Method C***) of the amino alcohol product (2*R*,3*S*)-**100** and intermediate (*S*)-**85** from the preparative scale NCR – 13-TAm cascade (5 mM substrate loading, 25 mL volume, one step, one-pot cascade, in 50 mM HEPES pH 7.4). Retention times times 7.7 min and 14.5 min respectively. Product yield by HPLC, 70%. Also shown, (*S*)-α-MBA at retention time 3.8 min, by-product (*R*)-**103** at retention time 7.3 min, and acetophenone at retention time 13.3 min.

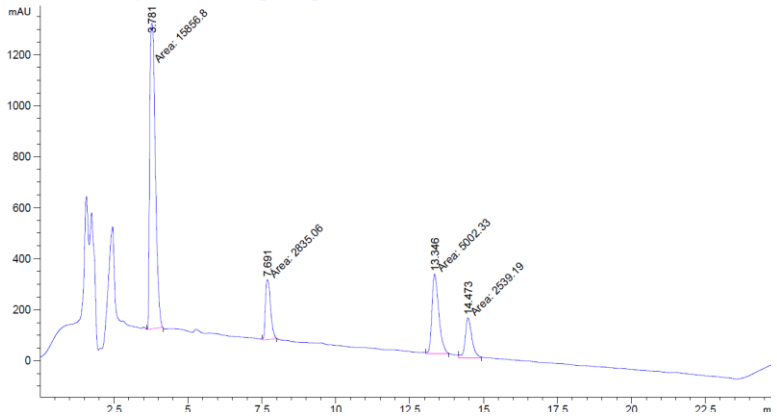

Figure 141: Chromatogram (analytical HPLC, ***Method C***) of the amino alcohol product (2*R*,3*S*)-**100** and intermediate (*S*)-**85** from the optimised preparative scale NCR – 13-TAm cascade (5 mM substrate loading, 25 mL volume, two-step, one-pot cascade, in 50 mM HEPES pH 7.4). Retention times 7.7 min and 14.5 min respectively. Product yield by HPLC, 68%. Also shown, (*S*)-α-MBA at retention time 3.8 min and acetophenone at retention time 13.3 min.

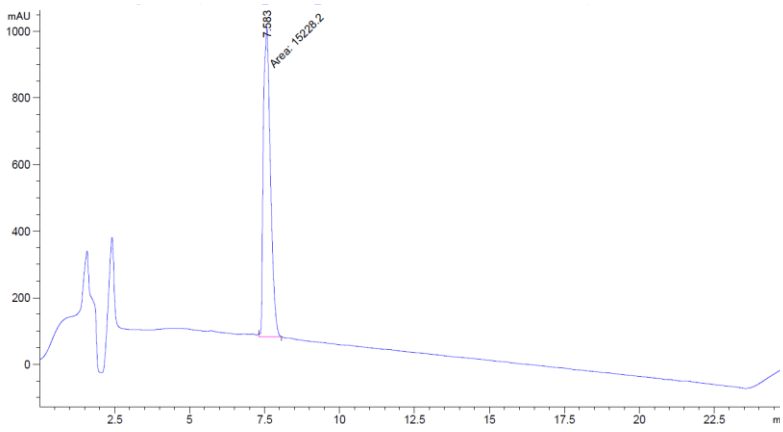

Figure 142: Chromatogram (analytical HPLC, ***Method C***) of the amino alcohol (2*S*,3*S*)-**100**. Retention time of (2*S*,3*S*)-**100**, 7.7 min.

10.9 2D Nuclear Magnetic Resonance Spectra

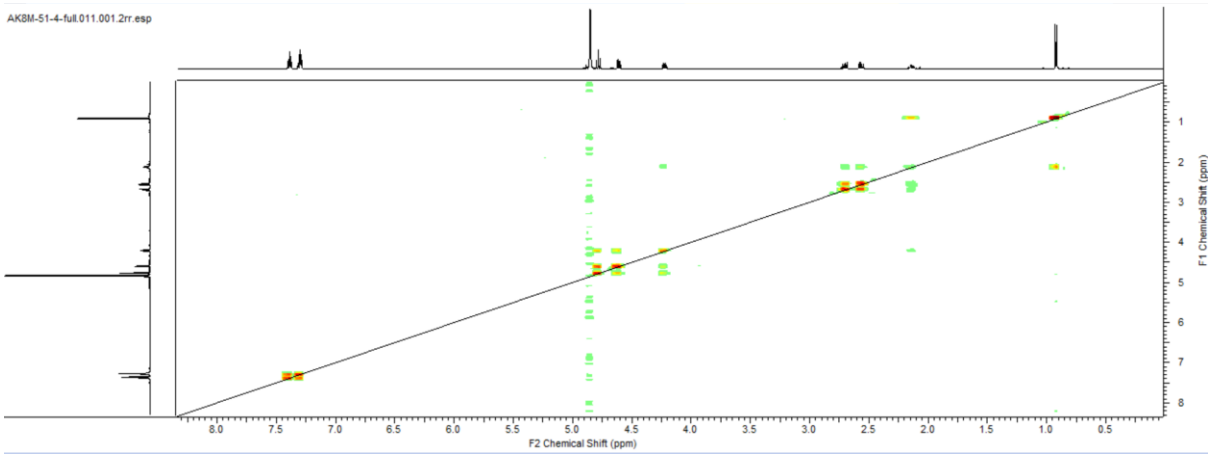

Figure 143: COESY spectra for (2*R*,4*S*)-**37**.

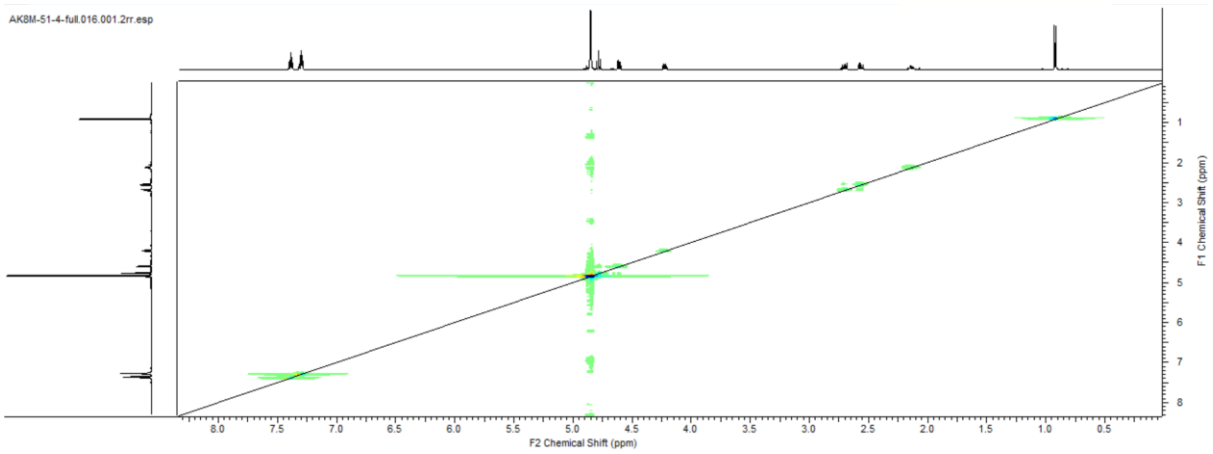

Figure 144: NOESY spectra for (2*R*,4*S*)-**37**.

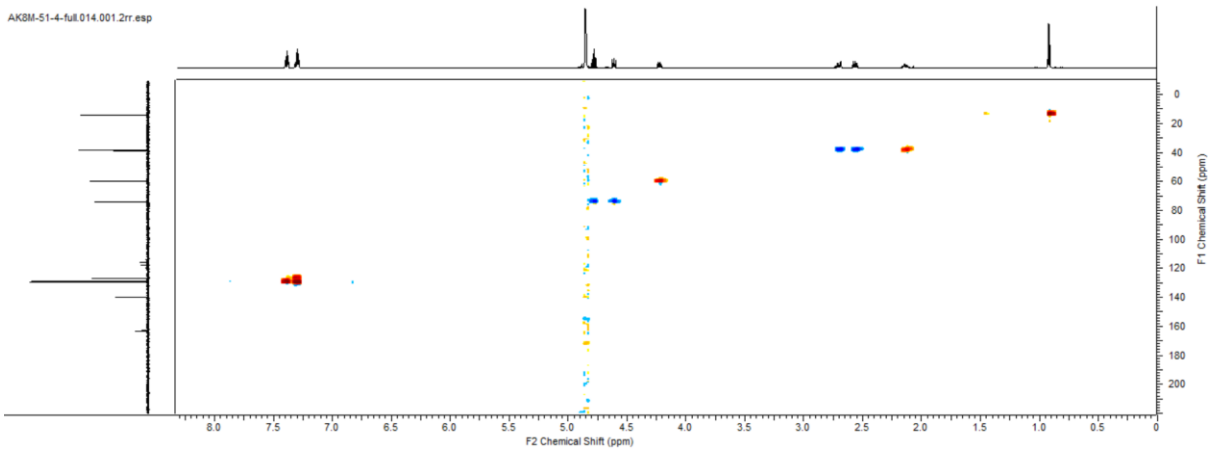

Figure 145: HSQC spectra for (2*R*,4*S*)-**37**.

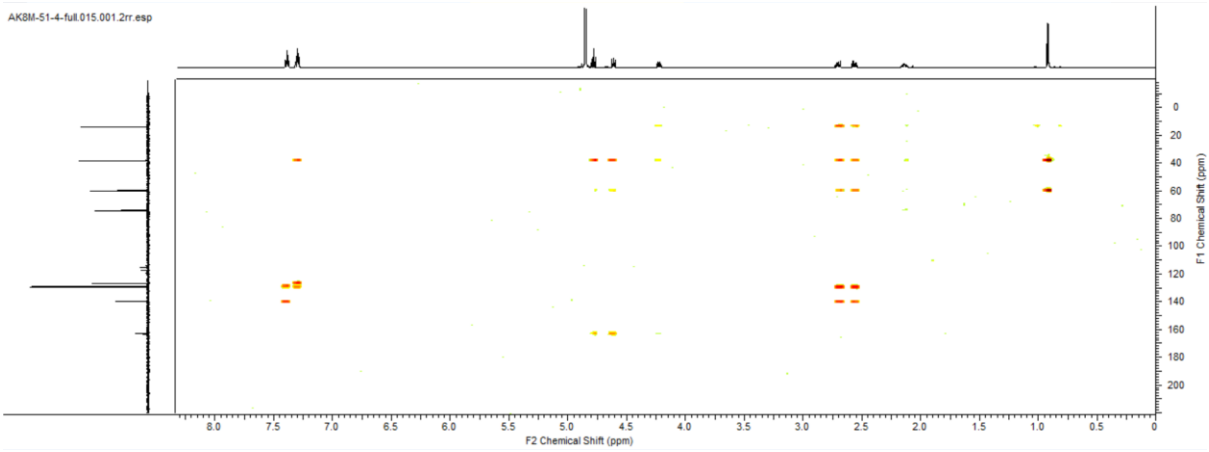

Figure 146: HMBC spectra for (2*R*,4*S*)-**37**.

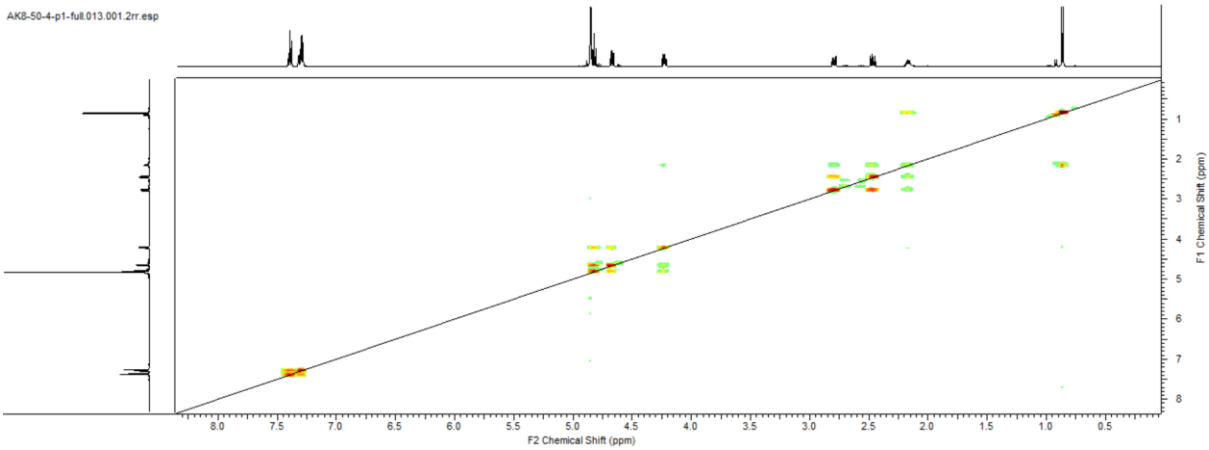

Figure 147: COESY spectra for (2*S*,4*S*)-**37**.

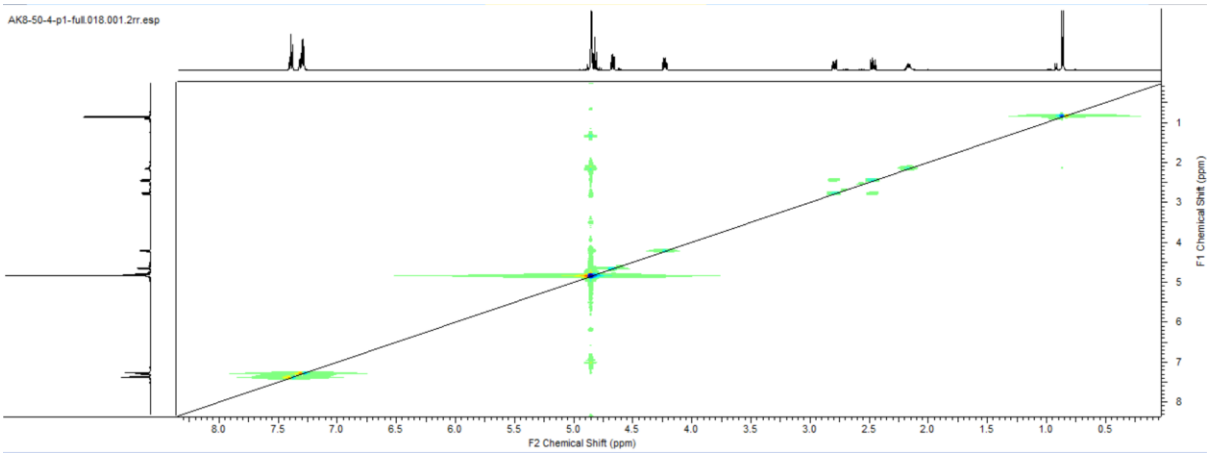

Figure 148: NOESY spectra for (2*S*,4*S*)-**37**.

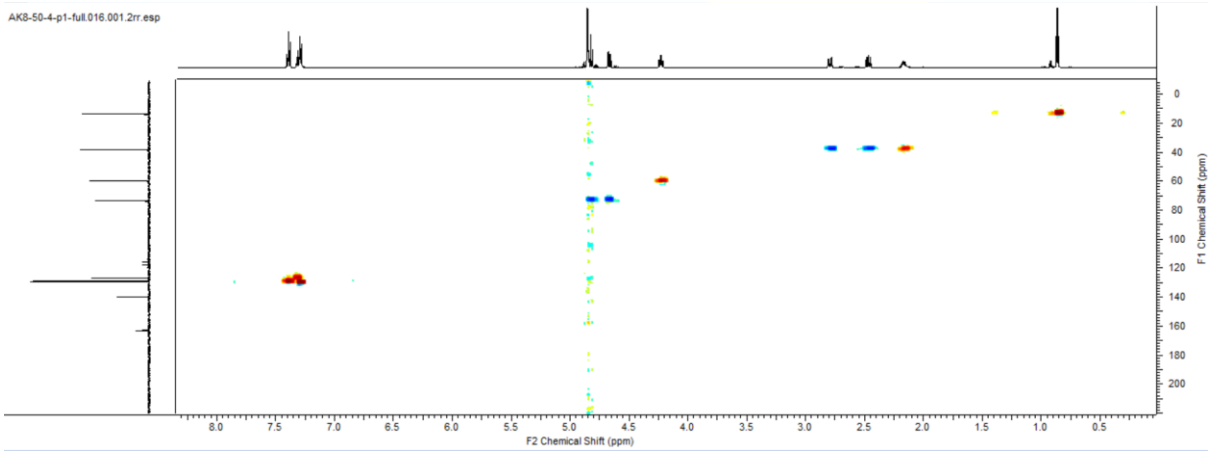

Figure 149: HSQC spectra for (2*S*,4*S*)-**37**.

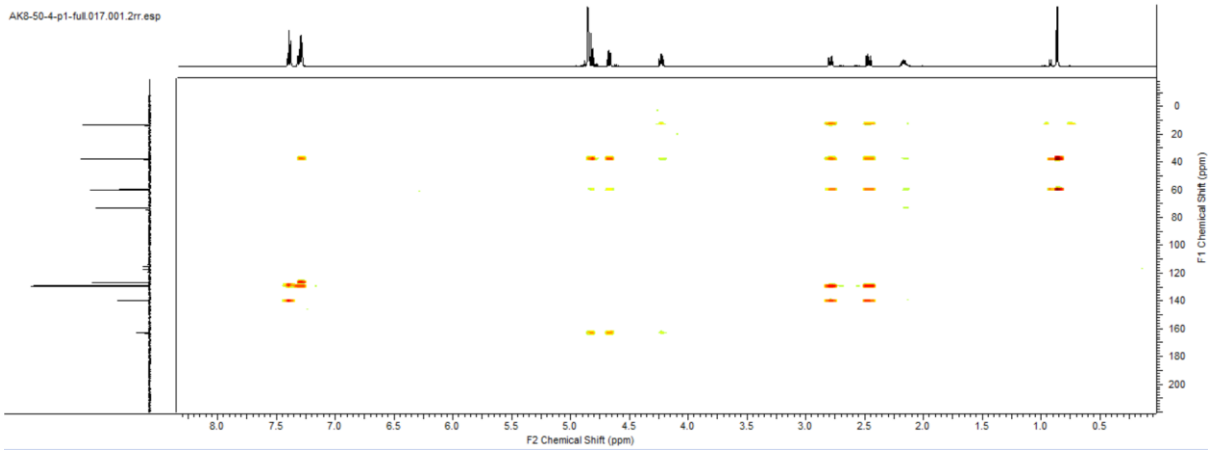

Figure 150: HMBC spectra for (2*S*,4*S*)-**37**.

11. References

1. Anastas, P. T. & Warner, J. C. *Green Chemistry: Theory and Practice*. (Oxford University Press, 1998).

2. Report of the World Commission on Environment and Development: Our Common Future. (Oxford University Press, 1987).

3. Bernhardt, A. & Gysi, N. *World's worst pollution problems - The new top six toxic threats: A priority list for remediation*. *Pure Earth Blacksmith Institute & Green Cross* (2015).

4. Matus, K. J. M., Clark, W. C., Anastas, P. T. & Zimmerman, J. B. Barriers to the implementation of green chemistry in the United States. *Environ. Sci. Technol.* **46**, 10892–10899 (2012).

5. Matus, K. J. M., Xiao, X. & Zimmerman, J. B. Green chemistry and green engineering in China: Drivers, policies and barriers to innovation. *J. Clean. Prod.* **32**, 193–203 (2012).

6. Leahy, D. K. *et al.* Seven important elements for an effective green chemistry program: An IQ consortium perspective. *Org. Process Res. Dev.* **17**, 1099–1109 (2013).

7. Roschangar, F., Sheldon, R. A. & Senanayake, C. H. Overcoming Barriers to Green Chemistry in the Pharmaceutical Industry - THe Green Aspiration Level^{TM} Concept. *Green Chem.* **17**, 752–768 (2015).

8. Food and Drug Administration. *Guidance for Industry: Changes to an Approved NDA or ANDA. Center for Drug Evaluation and Research* (2004).

9. Vernon, J. A., Golec, J. H. & Dimasi, J. A. Drug Development Costs When Financial Risk is Measured Using the Fama-French Three-Factor Model. *Heal. Econ. Lett.* **19**, 1002–1005 (2010).

10. Green Chemistry Institute, A. Green Chemistry Research & Innovation. *ACS Green Chemistry Institute* Available at: https://www.acs.org/content/acs/en/greenchemistry/research-innovation/catalysis.html.

11. Woodmansee, D. H. & Pfaltz, A. Asymmetric hydrogenation of alkenes lacking coordinating groups. *Chem. Commun.* **47**, 7912–7916 (2011).

12. Ma, Y. N., Li, S. X. & Yang, S. D. New Approaches for Biaryl-Based Phosphine Ligand Synthesis via P-O Directed C-H Functionalizations. *Acc. Chem. Res.* **50**, 1480–1492 (2017).

13. van Leeuwen, P. W. N. M. *Homogeneous Catalysis: Understanding the Art*. (Kluwer Academic Publishers, 2004).

14. Friedfeld, M. R. *et al.* Cobalt precursors for high-throughput discovery of base metal asymmetric alkene hydrogenation catalysts. *Science* **342**, 1076–1080 (2013).

15. Pereira, M. M., Calvete, M. J. F., Carrilho, R. M. B. & Abreu, A. R. Synthesis of binaphthyl based phosphine and phosphite ligands. *Chem. Soc. Rev.* **42**, 6990–7027 (2013).

16. Tungler, A., Tarnai, T., Hegedus, L., Fodor, K. & Mathe, T. Palladium-mediated heterogeneous catalytic hydrogenations. *Platin. Met. Rev.* **42**, 108–115 (1998).

17. Chinchilla, R. & Nájera, C. The Sonogashira reaction: A booming methodology in synthetic organic chemistry. *Chem. Rev.* **107**, 874–922 (2007).

18. Blakemore, D. *Suzuki – Miyaura Coupling*. **1**, (The Royal Society of Chemistry, 2016).

19. Constable, D. *et al.* Key green chemistry research areas - A perspective from pharmaceutical manufacturers. *Green Chem.* **9**, 411–420 (2007).

20. Clayden, J., Greeves, N. & Warren, S. *Organic Chemistry*. (Oxford University Press, 2012).

21. Nugent, T. C. Asymmetric Reductive Amination. *Chiral Amin. Synth. Methods, Dev. Appl.* 225–245 (2010).

22. Sheldon, R. A., Brady, D. & Bode, M. L. The Hitchhiker's guide to biocatalysis: Recent advances in the use of enzymes in organic synthesis. *Chem. Sci.* **11**, 2587–2605 (2020).

23. D. Patil, M., Grogan, G., Bommarius, A. & Yun, H. Recent Advances in ω-Transaminase-Mediated Biocatalysis for the Enantioselective Synthesis of Chiral Amines. *Catalysts* **8**, 254 (2018).

24. Gomm, A. & O'Reilly, E. Transaminases for chiral amine synthesis. *Curr. Opin. Chem. Biol.* **43**, 106–112 (2018).

25. Schoemaker, H. E., Mink, D. & Wubbolts, M. G. Dispelling the Myths--Biocatalysis in Industrial Synthesis. *Science* **299**, 1694–1697 (2003).

26. Berg, P. & Mertz, J. E. Personal reflections on the origins and emergence of recombinant DNA technology. *Genetics* **184**, 9–17 (2010).

27. Adrio, J. L. & Demain, A. L. Recombinant organisms for production of industrial products. *Bioeng. Bugs* **1**, 116–131 (2010).

28. Sheldon, R. A. & Pereira, P. C. Biocatalysis engineering: the big picture. *Chem. Soc. Rev.* **46**, 2678–2691 (2017).

29. Schmid, A. *et al.* Industrial Biocatalysis and Tomorrow. *Nature* **409**, 258–268 (2001).

30. Duetz, W. A., Van Beilen, J. B. & Witholt, B. Using proteins in their natural environment: Potential and limitations of microbial whole-cell hydroxylations in applied biocatalysis. *Curr. Opin. Biotechnol.* **12**, 419–425 (2001).

31. Goretti, M., Turchetti, B., Cramarossa, M. R., Forti, L. & Buzzini, P. Production of flavours and fragrances via bioreduction of (4*R*)-(-)-carvone and (1*R*)-(-)-myrtenal by non-conventional yeast whole-cells. *Molecules* **18**, 5736–5748 (2013).

32. Kell, D. B., Swainston, N., Pir, P. & Oliver, S. G. Membrane transporter engineering in industrial biotechnology and whole cell biocatalysis. *Trends Biotechnol.* **33**, 237–246 (2015).

33. Sheldon, R. A. & Woodley, J. M. Role of Biocatalysis in Sustainable Chemistry. *Chem. Rev.* **118**, 801–838 (2018).

34. Bommarius, A. S. & Payne, M. F. Stabilizing biocatalyts. *Chem. Soc. Rev.* **42**, 6534–6565 (2013).

35. Savile, C. K. *et al.* Biocatalytic Asymmetric Synthesis of Sitagliptin Manufacture. *Science* **329**, 305–310 (2010).

36. Stepankova, V. *et al.* Strategies for stabilization of enzymes in organic solvents. *ACS Catal.* **3**, 2823–2836 (2013).

37. Villeneuve, P., Muderhwa, J. M., Graille, J. & Haas, M. J. Customizing lipases for biocatalysis: A survey of chemical, physical and molecular biological approaches. *J. Mol. Catal. B Enzym.* **9**, 113–148 (2000).

38. Azevedo, A. M., Prazeres, D. M. F., Cabral, J. M. S. & Fonseca, L. P. Stability of free and immobilised peroxidase in aqueous-organic solvents mixtures. *J. Mol. Catal. B Enzym.* **15**, 147–153 (2001).

39. Rodriguez-Mertinez, J. A. *et al.* with Reduced Structural Dynamics. *Biotechnol. Bioeng.* **101**, 1142–1149 (2008).

40. Castillo, B.; Mendez, J.; Al-Azzam, W.; Barletta, G.; Griebenow, K. On the Relationship Between the Activity and Structure of PEG-α-Chymotrypsin Cnojugates in Organic Solvents. *Biotechnol. Bioeng.* **94**, 566–574 (2006).

41. Eppler, R. K. *et al.* Water dynamics and salt-activation of enzymes in organic media: Mechanistic implications revealed by NMR spectroscopy. *Proc. Natl. Acad. Sci. U.S.A.* **103**, 5706–5710 (2006).

42. Van Unen, D. J., Engbersen, J. F. J. & Reinhoudt, D. N. Why do crown ethers activate enzymes in organic solvents? *Biotechnol. Bioeng.* **77**, 248–255 (2001).

43. Pavlidis, I. V., Gournis, D., Papadopoulos, G. K. & Stamatis, H. Lipases in water-in-ionic liquid microemulsions: Structural and activity studies. *J. Mol. Catal. B Enzym.* **60**, 50–56 (2009).

44. Moniruzzaman, M., Kamiya, N., Nakashima, K. & Goto, M. Water-in-ionic liquid microemulsions as a new medium for enzymatic reactions. *Green Chem.* **10**, 497–500 (2008).

45. Turnbaugh, P. J. & Gordon, J. I. An Invitation to the marriage of metagenomics and metabolomics. *Cell* **134**, 708–713 (2008).

46. Sleator, R. D., Shortall, C. & Hill, C. Metagenomics. *Lett. Appl. Microbiol.* **47**, 361–366 (2008).

47. Handelsman, J., Rondon, M. R., Brady, S. F., Clardy, J. & Goodman, R. M. Molecular biological access to the chemistry of unknown soil microbes: A new frontier for natural products. *Chem. Biol.* **5**, 245–249 (1998).

48. Colin, P. Y. *et al.* Ultrahigh-throughput discovery of promiscuous enzymes by

picodroplet functional metagenomics. *Nat. Commun.* **6**, 1–12 (2015).

49. Handelsman, J. Metagenomics: Application of Genomics to Uncultured Microorganisms. *Microbiol. Mol. Biol. Rev.* **68**, 669–685 (2005).

50. Dinsdale, E. A. *et al.* Functional metagenomic profiling of nine biomes. *Nature* **452**, 629–632 (2008).

51. Simon, C. & Daniel, R. Metagenomic Analyses: Past and Future Trends. *Appl. Environ. Microbiol.* **77**, 1153–1161 (2011).

52. Harrington, E. D. *et al.* Quantitative assessment of protein function prediction from metagenomics shotgun sequences. *Proc. Natl. Acad. Sci. U.S.A.* **104**, 13913–13918 (2007).

53. Fernández-Arrojo, L., Guazzaroni, M. E., López-Cortés, N., Beloqui, A. & Ferrer, M. Metagenomic era for biocatalyst identification. *Curr. Opin. Biotechnol.* **21**, 725–733 (2010).

54. Hjort, K. *et al.* Chitinase genes revealed and compared in bacterial isolates, DNA extracts and a metagenomic library from a phytopathogen-suppressive soil. *FEMS Microbiol. Ecol.* **71**, 197–207 (2010).

55. Bartossek, R., Nicol, G. W., Lanzen, A., Klenk, H. P. & Schleper, C. Homologues of nitrite reductases in ammonia-oxidizing archaea: Diversity and genomic context. *Environ. Microbiol.* **12**, 1075–1088 (2010).

56. Schmidt, O., Drake, H. L. & Horn, M. A. Hitherto unknown [Fe-Fe]-hydrogenase gene diversity in anaerobes and anoxic enrichments from a moderately acidic fen. *Appl. Environ. Microbiol.* **76**, 2027–2031 (2010).

57. Sul, W. J. *et al.* DNA-stable isotope probing integrated with metagenomics for retrieval of biphenyl dioxygenase genes from polychlorinated biphenyl-contaminated river sediment. *Appl. Environ. Microbiol.* **75**, 5501–5506 (2009).

58. Baud, D., Jeffries, J. W. E., Moody, T. S., Ward, J. M. & Hailes, H. C. A metagenomics approach for new biocatalyst discovery: application to transaminases and the synthesis of allylic amines. *Green Chem.* **19**, 1134–1143 (2017).

59. Dobrijevic, D. *et al.* Metagenomic ene-reductases for the bioreduction of sterically challenging enones. *RSC Adv.* **9**, 36608–36614 (2019).

60. Leipold, L. *et al.* The identification and use of robust transaminases from a domestic drain metagenome. *Green Chem.* **21**, 75–86 (2019).

61. Pathak, G. P., Ehrenreich, A., Losi, A., Streit, W. R. & Gärtner, W. Novel blue light-sensitive proteins from a metagenomic approach. *Environ. Microbiol.* **11**, 2388–2399 (2009).

62. Waschkowitz, T., Rockstroh, S. & Daniel, R. Isolation and characterization of metalloproteases with a novel domain structure by construction and screening of metagenomic libraries. *Appl. Environ. Microbiol.* **75**, 2506–2516 (2009).

63. Uchiyama, T., Abe, T., Ikemura, T. & Watanabe, K. Substrate-induced gene-expression screening of environmental metagenome libraries for isolation of

catabolic genes. *Nat. Biotechnol.* **23**, 88–93 (2005).

64. Stein, J. L., Marsh, T. L., Wu, K. Y., Shizuya, H. & Delong, E. F. Characterization of uncultivated prokaryotes: Isolation and analysis of a 40-kilobase-pair genome fragment from a planktonic marine archaeon. *J. Bacteriol.* **178**, 591–599 (1996).

65. Simon, C., Herath, J., Rockstroh, S. & Daniel, R. Rapid identification of genes encoding DNA polymerases by function-based screening of metagenomic libraries derived from glacial ice. *Appl. Environ. Microbiol.* **75**, 2964–2968 (2009).

66. Rhee, J. K., Ahn, D. G., Kim, Y. G. & Oh, J. W. New thermophilic and thermostable esterase with sequence similarity to the hormone-sensitive lipase family, cloned from a metagenomic library. *Appl. Environ. Microbiol.* **71**, 817–825 (2005).

67. Leipold, L. *et al.* The identification and use of robust transaminases from a domestic drain metagenome. *Green Chem.* **21**, 75–86 (2018).

68. Torsvik, V., Øvreås, L. & Thingstad, T. F. Prokaryotic diversity - Magnitude, Dynamics, and Controlling Factors. *Science* **296**, 1064–1066 (2002).

69. Hutchison, C. A. *et al.* Mutagenesis at a specific position in a DNA sequence. *J. Biol. Chem.* **253**, 6551–6560 (1978).

70. Svedendahl, M., Branneby, C., Lindberg, L. & Berglund, P. Reversed Enantiopreference of an ω-Transaminase by a Single-Point Mutation. *ChemCatChem* **2**, 976–980 (2010).

71. Hernandez, K. & Fernandez-Lafuente, R. Control of protein immobilization: Coupling immobilization and site-directed mutagenesis to improve biocatalyst or biosensor performance. *Enzyme Microb. Technol.* **48**, 107–122 (2011).

72. Packer, M. S. & Liu, D. R. Methods for the directed evolution of proteins. *Nat. Rev. Genet.* **16**, 379–394 (2015).

73. Leung D.W., Chen E. & Goeddel D.V. A method for random mutagenesis of a defined DNA segment using a modified polymerase chain reaction. *Technique* **1**, 11–15 (1989).

74. Sheldon, R. A. & Brady, D. The limits to biocatalysis: Pushing the envelope. *Chem. Commun.* **54**, 6088–6104 (2018).

75. Chen, K. & Arnold, F. H. Tuning the activity of an enzyme for unusual environments: Sequential random mutagenesis of subtilisin E for catalysis in dimethylformamide. *Proc. Natl. Acad. Sci. U. S. A.* **90**, 5618–5622 (1993).

76. Wang, X. X., Lin, C. P., Zhang, X. J., Liu, Z. Q. & Zheng, Y. G. Improvement of a newly cloned carbonyl reductase and its application to biosynthesize chiral intermediate of duloxetine. *Process Biochem.* **70**, 124–128 (2018).

77. Stemmer, W. P. Rapid evolution of a protein in vitro by DNA shuffling. *Nature* **370**, 389–391 (1994).

78. Bommarius, A. S., Blum, J. K. & Abrahamson, M. J. Status of protein

engineering for biocatalysts: How to design an industrially useful biocatalyst. *Curr. Opin. Chem. Biol.* **15**, 194–200 (2011).

79. Carey, J. S., Laffan, D., Thomson, C. & Williams, M. T. Analysis of the reactions used for the preparation of drug candidate molecules. *Org. Biomol. Chem.* **4**, 2337 (2006).

80. Breuer, M. *et al.* Industrial methods for the production of optically active intermediates. *Angew. Chemie Int. Ed.* **43**, 788–824 (2004).

81. Hageluken, C. Markets for the Catalyst Metals Platinum, Palladium and Rhodium. *Metall* **1**–**2**, 31–32 (2006).

82. Sperl, J. M. & Sieber, V. Multi-enzyme cascade reactions – status and recent advances. *ACS Catal.* **8**, 2385–2396 (2018).

83. Ricca, E., Brucher, B. & Schrittwieser, J. H. Multi-enzymatic cascade reactions: Overview and perspectives. *Adv. Synth. Catal.* **353**, 2239–2262 (2011).

84. Ran, N., Zhao, L., Chen, Z. & Tao, J. Recent applications of biocatalysis in developing green chemistry for chemical synthesis at the industrial scale. *Green Chem.* **10**, 361–372 (2008).

85. Martinez, C. A. *et al.* Development of a chemoenzymatic manufacturing process for Pregabalin. *Org. Process Res. Dev.* **12**, 392–398 (2008).

86. Tao, J. & Xu, J. H. Biocatalysis in development of green pharmaceutical processes. *Curr. Opin. Chem. Biol.* **13**, 43–50 (2009).

87. Panke, S., Held, M. & Wubbolts, M. Trends and innovations in industrial biocatalysis for the production of fine chemicals. *Curr. Opin. Biotechnol.* **15**, 272–279 (2004).

88. Patel, R. N. Chemo-enzymatic synthesis of pharmaceutical intermediates. *Expert Opin. Drug Discov.* **3**, 187–245 (2008).

89. Noyori, R. Asymmetrische Katalyse: Kenntnisstand und Perspektiven (Nobel-Vortrag). *Angew. Chem.* **114**, 2108–2123 (2002).

90. Knowles, W. S. Asymmetric hydrogenations (Nobel lecture). *Angew. Chem. Int. ed.* **41**, 1998–2007 (2002).

91. Knowles, W. S. & Noyori, R. Pioneering Perspectives on. *Acc. Chem. Res.* **40**, 1238–1239 (2007).

92. Hall, M. & Bommarius, A. S. Enantioenriched compounds via enzyme-catalyzed redox reactions. *Chem. Rev.* **111**, 4088–4110 (2011).

93. Toogood, H. S., Gardiner, J. M. & Scrutton, N. S. Biocatalytic Reductions and Chemical Versatility of the Old Yellow Enzyme Family of Flavoprotein Oxidoreductases. *ChemCatChem* **2**, 892–914 (2010).

94. Christian, W. & Warburg, O. Ein zweites sauerstofffibertragendes Ferment und sein Absorpfionsspektrum. *Naturwissenschaften* **20**, 688 (1932).

95. Haas, E. *Biochem. Z.* **298**, 369–390 (1938).

96. Chaparro-Riggers, J. F., Rogers, T. A., Vazquez-Figueroa, E., Polizzi, K. M. &

Bommarius, A. S. Comparison of three enoate reductases and their potential use for biotransformations. *Adv. Synth. Catal.* **349**, 1521–1531 (2007).

97. Toogood, H. S. *et al.* Structure-based insight into the asymmetric bioreduction of the C=C double bond of α,β-unsaturated nitroalkenes by pentaerythritol tetranitrate reductase. *Adv. Synth. Catal.* **350**, 2789–2803 (2008).

98. Hall, M. *et al.* Asymmetric bioreduction of C=C bonds using enoate reductases OPR1, OPR3 and YqjM: Enzyme-based stereocontrol. *Adv. Synth. Catal.* **350**, 411–418 (2008).

99. Knaus, T., Toogood, H. S. & Scrutton, N. S. Ene-reductases and their Applications. in *Green Biocatalysis* (ed. Patel, R. N.) 473–488 (John Wiley and Sons Inc., 2016).

100. Toogood, H. S. & Scrutton, N. S. Discovery, Characterization, Engineering, and Applications of Ene-Reductases for Industrial Biocatalysis. *ACS Catal.* **8**, 3532–3549 (2018).

101. Aregger, D., Peters, C. & Buller, R. M. Characterization of the novel ene reductase ppo-er1 from paenibacillus polymyxa. *Catalysts* **10**, 254–268 (2020).

102. Rohdich, F., Wiese, A., Feicht, R., Simon, H. & Bacher, A. Enoate reductases of Clostridia. Cloning, sequencing, and expression. *J. Biol. Chem.* **276**, 5779–5787 (2001).

103. Moummou, H., Kallberg, Y., Tonfack, L. B., Persson, B. & van der Rest, B. The Plant Short-Chain Dehydrogenase (SDR) superfamily: Genome-wide inventory and diversification patterns. *BMC Plant Biol.* **12**, 219–236 (2012).

104. Lygidakis, A. *et al.* Pinpointing a Mechanistic Switch Between Ketoreduction and "Ene" Reduction in Short-Chain Dehydrogenases/Reductases. *Angew. Chemie Int. Ed.* **55**, 9596–9600 (2016).

105. Mansell, D. J. *et al.* Biocatalytic asymmetric alkene reduction: Crystal structure and characterization of a double bond reductase from Nicotiana tabacum. *ACS Catal.* **3**, 370–379 (2013).

106. Nordling, E., Jörnvall, H. & Persson, B. Medium-chain dehydrogenases/reductases (MDR): Family characterizations including genome comparisons and active site modelling. *Eur. J. Biochem.* **269**, 4267–4276 (2002).

107. Steinkellner, G. *et al.* Identification of promiscuous ene-reductase activity by mining structural databases using active site constellations. *Nat. Commun.* **5**, 1–9 (2014).

108. Adalbjörnsson, B. V. *et al.* Biocatalysis with thermostable enzymes: Structure and properties of a thermophilic 'ene'-reductase related to old yellow enzyme. *ChemBioChem* **11**, 197–207 (2010).

109. Peters, C., Frasson, D., Sievers, M. & Buller, R. Novel Old Yellow Enzyme Subclasses. *ChemBioChem* **20**, 1569–1577 (2019).

110. Nizam, S., Verma, S., Borah, N. N., Gazara, R. K. & Verma, P. K. Comprehensive genome-wide analysis reveals different classes of enigmatic old yellow enzyme in fungi. *Sci. Rep.* **4**, (2014).

111. Breithaupt, C. *et al.* X-ray structure of 12-Oxophytodienoate reductase 1 provides structural insight into substrate binding and specificity within the family of OYE. *Structure* **9**, 419–429 (2001).

112. Karplus, P. A. & Fox, K. M. Structure-function relations for old yellow enzyme relations for old yellow enzyme. *Faseb J.* **9**, 1518–1526 (2015).

113. Brown, B. J., Deng, Z., Karplus, P. A. & Massey, V. On the Active Site of Old Yellow Enzyme turnover . Solution of the crystal structure of OYE1 from. *Biochemistry* **273**, 32753–32762 (1998).

114. Kohli, R. M. & Massey, V. The oxidative half-reaction of old yellow enzyme: The role of tyrosine 196. *J. Biol. Chem.* **273**, 32763–32770 (1998).

115. Nakamura, T., Yoshimura, J. & Ogura, Y. Action mechanism of the old yellow enzyme. *J. Biochem.* **57**, 554–564 (1965).

116. Hall, M. *et al.* Asymmetric bioreduction of activated C=C bonds using Zymomonas mobilis NCR enoate reductase and old yellow enzymes OYE 1-3 from yeasts. *European J. Org. Chem.* **9**, 1511–1516 (2008).

117. Stueckler, C. *et al.* Stereocomplementary bioreduction of α,β-unsaturated dicarboxylic acids and dimethyl esters using enoate reductases: Enzyme- And substrate-based stereocontrol. *Org. Lett.* **9**, 5409–5411 (2007).

118. Stueckler, C. *et al.* Stereo-controlled asymmetric bioreduction of α,β-dehydroamino acid derivatives. *Adv. Synth. Catal.* **353**, 1169–1173 (2011).

119. Walsh, C. Chemical Approaches to the Study of Enzymes Catalyzing Redox Transformations. *Ann. Rev. Biochem.* **47**, 881–931 (1978).

120. Brenna, E. *et al.* Substrate scope and synthetic applications of the enantioselective reduction of α-alkyl-β-arylenones mediated by Old Yellow Enzymes. *Org. Biomol. Chem.* **11**, 2988 (2013).

121. Brenna, E., Gatti, F. G., Monti, D., Parmeggiani, F. & Sacchetti, A. Cascade Coupling of Ene Reductases with Alcohol Dehydrogenases: Enantioselective Reduction of Prochiral Unsaturated Aldehydes. *ChemCatChem* **4**, 653–659 (2012).

122. Muller, A., Hauer, B. & Rosche, B. Asymmetric Alkene Reduction by Yeast Old Yellow Enzymes and by a Novel Zymomonas mobilis Reductase. *Biotechnol. Bioeng.* **98**, 22–29 (2007).

123. Fu, Y., Castiglione, K. & Weuster-Botz, D. Comparative characterization of novel ene-reductases from cyanobacteria. *Biotechnol. Bioeng.* **110**, 1293–1301 (2013).

124. Reich, S., Hoeffken, H. W., Rosche, B., Nestl, B. M. & Hauer, B. Crystal Structure Determination and Mutagenesis Analysis of the Ene Reductase NCR. *ChemBioChem* **13**, 2400–2407 (2012).

125. Ciriminna, R. & Pagliaro, M. Green Chemistry in the Fine Chemicals and Pharmaceutical Industries. *Org. Process Res. Dev.* **17**, 1479–1484 (2013).

126. Wang, X. *et al.* Cofactor NAD(P)H Regeneration Inspired by Heterogeneous

Pathways. *Cell* **2**, 621–654 (2017).

127. Brown, G., Moody, T. S., Smyth, M. & Taylor, S. J. C. Almac: An Industrial Perspective of Ene Reductase (ERED) Biocatalysis. in *Biocatalysis: An Industrial Perspective* (eds. de Gonzalo, G. & Dominguez de Maria, P.) **29**, 229–256 (The Royal Society of Chemistry, 2018).

128. Faber, K. Biocatalytic Applications. in *Biotransformations in Organic Chemistry* 31–313 (Springer, 2011).

129. Calvin, S. J., Mangan, D., Miskelly, I., Moody, T. S. & Stevenson, P. J. Overcoming equilibrium issues with carbonyl reductase enzymes. *Org. Process Res. Dev.* **16**, 82–86 (2012).

130. Jones, J. B., Sneddon, D. W., Higgins, W. & Lewis, A. J. Preparative-scale reductions of cyclic ketones and aldehyde substrates of horse liver alcohol dehydrogenase with in situ sodium dithionite recycling of catalytic amounts of NAD. *J. Chem. Soc. Chem. Commun.* 856–857 (1972).

131. Taylor, K. E. & Jones, J. B. Nicotinamide Coenzyme Regeneration by Dihydropyridine and Pyridinium Compounds. *J. Am. Chem. Soc.* **98**, 5689–5694 (1976).

132. Maenaka, Y., Suenobu, T. & Fukuzumi, S. Efficient catalytic interconversion between NADH and NAD^+ accompanied by generation and consumption of hydrogen with a water-soluble iridium complex at ambient pressure and temperature. *J. Am. Chem. Soc.* **134**, 367–374 (2012).

133. Abril, O. & Whitesides, G. M. Hybrid Organometallic/Enzymatic Catalyst Systems: Regeneration of NADH Using Dihydrogen. *J. Am. Chem. Soc.* **104**, 1552–1554 (1982).

134. Wang, X. & Yiu, H. H. P. Heterogeneous Catalysis Mediated Cofactor NADH Regeneration for Enzymatic Reduction. *ACS Catal.* **6**, 1880–1886 (2016).

135. Weckbecker, A., Groger, H. & Hummel, W. Regeneration of Nicotinamide Coenzymes: Principles and Applications for the Synthesis of Chiral Compounds. in *Adv Biochem Engin/Biotechnol* 195–242 (Springer-Verlag, 2010).

136. Brown, K. A. *et al.* Photocatalytic Regeneration of Nicotinamide Cofactors by Quantum Dot-Enzyme Biohybrid Complexes. *ACS Catal.* **6**, 2201–2204 (2016).

137. Liu, J. & Antonietti, M. Bio-inspired NADH regeneration by carbon nitride photocatalysis using diatom templates. *Energy Environ. Sci.* **6**, 1486–1493 (2013).

138. Wu, H. *et al.* Methods for the regeneration of nicotinamide coenzymes. *Green Chem.* **15**, 1773–1789 (2013).

139. Chenault, H. K. & Whitesides, G. M. Regeneration of Nicotinamide Cofactors. *Appl. Biochem. Biotechnol.* **14**, 147–197 (1987).

140. Pietrusiewicz, K. M. & Zabłocka, M. Preparation of Scalemic P-Chiral Phosphines and Their Derivatives. *Chem. Rev.* **94**, 1375–1411 (1994).

141. Knowles, W. S., Sabacky, M. J. & Vineyard, B. D. *Adv. Chem. Ser.* **132**, 274

(1974).

142. Winkler, C. K., Tasnadi, G., Clay, D., Hall, M. & Faber, K. Asymmetric bioreduction of activated alkenes to industrially relevant optically active compounds. *J. Biotechnol.* **162**, 381–389 (2012).

143. Brenna, E., Fuganti, C. & Serra, S. Enantioselective perception of chiral odorants. *Tetrahedron Asymmetry* **14**, 1–42 (2003).

144. Enders, D. & Dyker, H. Synthesis and Properties of the Enantiomers of the Two Artificial Frangrances Lilial and Methylundecanal. *Liebigs Ann. Chem.* 1107–1110 (1990).

145. Enders, D. & Backes, M. First asymmetric synthesis of both enantiomers of Tropional®and their olfactory evaluation. *Tetrahedron Asymmetry* **15**, 1813–1817 (2004).

146. Stueckler, C. *et al.* Bioreduction of α-methylcinnamaldehyde derivatives: chemo-enzymatic asymmetric synthesis of Lilial™ and Helional™. *Dalt. Trans.* **39**, 8472–8476 (2010).

147. Ernst, H. Recent advances in industrial carotenoid synthesis. *Pure Appl. Chem.* **74**, 2213–2226 (2002).

148. Vílchez, C. *et al.* Marine carotenoids: Biological functions and commercial applications. *Mar. Drugs* **9**, 319–333 (2011).

149. Wada, M. *et al.* Production of a Doubly Chiral Compound , by Two-Step Enzymatic Asymmetric Reduction Production of a Doubly Chiral Compound , Enzymatic Asymmetric Reduction. *Appl. Environ. Microbiol.* **69**, 933–937 (2003).

150. Cohen, N., Eichel, W. F., Lopresti, R. J., Neukom, C. & Saucy, G. Synthetic Studies on (2*R*,4′*R*,8′*R*)-α-Tocopherol. An Approach Utilizing Side Chain Synthons of Microbiological Origin. *J. Org. Chem.* **41**, 3505–3511 (1976).

151. Ley, S. V. *et al.* Total Synthesis of rapamycin. *Chem. A Eur. J.* **15**, 2874–2914 (2009).

152. Kirkham, J. E. D., Lee, V. & Baldwin, J. E. Biomimetic synthesis of marine sponge metabolite spiculoic acid A and establishment of the absolute configuration of the natural product. *Chem. Commun.* 2863–2865 (2006).

153. Stueckler, C., Winkler, C. K., Bonnekessel, M. & Faber, K. Asymmetric synthesis of (*R*)-3-hydroxy-2-methylpropanoate ('Roche Ester') and derivatives via biocatalytic C=C-bond reduction. *Adv. Synth. Catal.* **352**, 2663–2666 (2010).

154. Aubin, Y., Audran, G. & Monti, H. Improved enantioselective synthesis of natural striatenic acid and its methyl ester. *Tetrahedron Lett.* **47**, 3669–3671 (2006).

155. Dong, Y., McCullough, K. J., Wittlin, S., Chollet, J. & Vennerstrom, J. L. The structure and antimalarial activity of dispiro-1,2,4,5-tetraoxanes derived from (+)-dihydrocarvone. *Bioorganic Med. Chem. Lett.* **20**, 6359–6361 (2010).

156. Lowe, J. R., Tolman, W. B. & Hillmyer, M. A. Oxidized dihydrocarvone as a

renewable resource monomer. *Biomacromolecules* **10**, 2003–2008 (2009).

157. Fryszkowska, A. *et al.* Asymmetrie reduction of activated alkenes by pentaerythritol tetranitrate reductase: Specificity and control of stereochemical outcome by reaction optimisation. *Adv. Synth. Catal.* **351**, 2976–2990 (2009).

158. Mueller, N. J. *et al.* The substrate spectra of pentaerythritol tetranitrate reductase, morphinone reductase, N-ethylmaleimide reductase and estrogen-binding protein in the asymmetric bioreduction of activated alkenes. *Adv. Synth. Catal.* **352**, 387–394 (2010).

159. Mangan, D., Miskelly, I. & Moody, T. S. A three-enzyme system involving an ene-reductase for generating valuable chiral building blocks. *Adv. Synth. Catal.* **354**, 31–32 (2012).

160. Crotti, M. *et al.* Stereoselectivity switch in the reduction of α-alkyl-β-arylenones by structure-guided designed variants of the ene reductase OYE1. *Front. Bioeng. Biotechnol.* **7**, 1–15 (2019).

161. Powell, R. W. *et al.* Investigating: Saccharomyces cerevisiae alkene reductase OYE 3 by substrate profiling, X-ray crystallography and computational methods. *Catal. Sci. Technol.* **8**, 5003–5016 (2018).

162. Crotti, M. *et al.* Stereoselectivity switch in the reduction of α-Alkyl-β-arylenones by structure-guided designed variants of the ene reductase OYE1. *Front. Bioeng. Biotechnol.* **7**, 1–7 (2019).

163. Walton, A. Z., Conerly, W. C., Pompeu, Y., Sullivan, B. & Stewart, J. D. Biocatalytic reductions of Baylis-Hillman adducts. *ACS Catal.* **1**, 989–993 (2011).

164. Pompeu, Y. A., Sullivan, B. & Stewart, J. D. X-ray crystallography reveals how subtle changes control the orientation of substrate binding in an alkene reductase. *ACS Catal.* **3**, 2376–2390 (2013).

165. Rudat, J., Brucher, B. R. & Syldatk, C. Transaminases for the synthesis of enantiopure beta-amino acids. *AMB Express* **2**, 1–10 (2012).

166. Ward, J. & Wohlgemuth, R. High-Yield Biocatalytic Amination Reactions in Organic Synthesis. *Curr. Org. Chem.* **14**, 1914–1927 (2010).

167. Burnett, G., Walsh, C., Yonaha, K., Toyama, S. & Soda, K. Stereospecificity of enzymatic transamination of γ-aminobutyrate. *J. Chem. Soc. Chem. Commun.* **19**, 826–828 (1979).

168. K, Y., K, S., H, M. & S, T. Distribution of omega-amino acid: pyruvate transaminase and aminobutyrate: alpha-ketoglutarate transaminase in microorganisms. *Agric. Biol. Chem.* **47**, 2257–2265 (1983).

169. Yonaha, K., Toyama, S., Yasuda, M. & Soda, K. Properties of crystalline (v-amino acid: Pyruvate aminotransferase of pseudomonas sp. f-126. *Agric. Biol. Chem.* **41**, 1701–1706 (1977).

170. Mehta, P. K., Hale, T. I. & Christen, P. Aminotransferases: Demonstration of Homology and Division Into Evolutionary Subgroups. *Eur. J. Biochem.* **214**, 549–561 (1993).

171. Cassimjee, K. E., Manta, B. & Himo, F. A quantum chemical study of the ω-transaminase reaction mechanism. *Org. Biomol. Chem.* **13**, 8453–8464 (2015).

172. Malik, M. S., Park, E. S. & Shin, J. S. Features and technical applications of ω-transaminases. *Appl. Microbiol. Biotechnol.* **94**, 1163–1171 (2012).

173. Sugio, S., Petsko, G. A., Manning, J. M., Soda, K. & Ringe, D. Crystal Structure of a D-Amino Acid Aminotransferase: How the Protein Controls Stereoselectivity. *Biochemistry* **34**, 9661–9669 (1995).

174. Yoshimura, T., Jhee, K.-H. & Soda, K. Stereospecificity for the Hydrogen Transfer and Molecular Evolution of Pyridoxal Enzymes. *Biosci. Biotechnol. Biochem.* **60**, 181–187 (1996).

175. Lim, Y. H., Yoshimura, T., Kurokawa, Y., Esaki, N. & Soda, K. Nonstereospecific transamination catalyzed by pyridoxal phosphate- dependent amino acid racemases of broad substrate specificity. *J. Biol. Chem.* **273**, 4001–4005 (1998).

176. Humble, M. S., Cassimjee, K. E., Abedi, V., Federsel, H. J. & Berglund, P. Key Amino Acid Residues for Reversed or Improved Enantiospecificity of an ω-Transaminase. *ChemCatChem* **4**, 1167–1172 (2012).

177. Guo, F. & Berglund, P. Transaminase biocatalysis: optimization and application. *Green Chem.* **19**, 333–360 (2017).

178. Shin, J. & Kim, B. Asymmetric Synthesis of Chiral Amines With □ -Transaminase. *Biotechnol. Bioeng.* **65**, 206–211 (1999).

179. Genz, M., Melse, O., Schmidt, S., Vickers, C. & Dçrr, M. Engineering the Amine Transaminase from Vibrio fluvialis towards Branched-Chain Substrates. *ChemCatChem* **8**, 3199–3202 (2016).

180. Chen, S., Campillo-brocal, J. C., Berglund, P. & Humble, M. S. Characterization of the stability of Vibrio fluvialis JS17 amine transaminase. *J. Biotechnol.* **282**, 10–17 (2018).

181. Semproli, R. *et al.* Use of Immobilized Amine Transaminase from Vibrio fluvialis under Flow Conditions for the Synthesis of (S)-1-(5-Fluoropyrmidin-2-yl)-ethanamine. *ChemCatChem* **12**, 1359–1367 (2020).

182. Kaulmann, U., Smithies, K., Smith, M. E. B., Hailes, H. C. & Ward, J. M. Substrate spectrum of ω-transaminase from Chromobacterium violaceum DSM30191 and its potential for biocatalysis. *Enzyme Microb. Technol.* **41**, 628–637 (2007).

183. Iwasaki, A., Yamada, Y., Ikenaka, Y. & Hasegawa, J. Microbial synthesis of (R)- and (S)-3,4dimethoxyamphetamines through stereoselective transamination. *Biotechnol. Lett.* **25**, 1843–1846 (2003).

184. Iwasaki, A., Yamada, Y., Kizaki, N., Ikenaka, Y. & Hasegawa, J. Microbial synthesis of chiral amines by (R)-specific transamination with Arthrobacter sp. KNK168. *Appl. Microbiol. Biotechnol.* **69**, 499–505 (2006).

185. Höhne, M., Schätzle, S., Jochens, H., Robins, K. & Bornscheuer, U. T. Rational assignment of key motifs for function guides in silico enzyme identification. *Nat.*

Chem. Biol. **6**, 807–813 (2010).

186. Coscolín, C. *et al.* crossm Bioprospecting Reveals Class III □-Transaminases Converting Bulky Ketones and Environmentally Relevant Polyamines. *Appl. Environ. Microbiol.* **85**, 1–20 (2019).

187. Pavlidis, I. V *et al.* the asymmetric synthesis of bulky chiral amines. *Nat. Chem.* **8**, 1076–1082 (2016).

188. Weiß, M. S. *et al.* Amine Transaminase Engineering for Spatially Bulky Substrate Acceptance. *ChemBioChem* **18**, 1022–1026 (2017).

189. Voss, M. *et al.* In Silico Based Engineering Approach to Improve Transaminases for the Conversion of Bulky Substrates. *ACS Catal.* **8**, 11524–11533 (2018).

190. Koszelewski, D., Tauber, K., Faber, K. & Kroutil, W. ω-Transaminases for the synthesis of non-racemic α-chiral primary amines. *Trends Biotechnol.* **28**, 324–332 (2010).

191. Richter, N., Simon, R. C., Kroutil, W., Ward, J. M. & Hailes, H. C. Synthesis of pharmaceutically relevant 17-α-amino steroids using an ω-transaminase. *Chem. Commun.* **50**, 6098–6100 (2014).

192. Richter, N. *et al.* ω-Transaminases for the amination of functionalised cyclic ketones. *Org. Biomol. Chem.* **13**, 8843–8851 (2015).

193. Dunbabin, A., Subrizi, F., Ward, J. M., Sheppard, T. D. & Hailes, H. C. Furfurylamines from biomass: transaminase catalysed upgrading of furfurals. *Green Chem.* **19**, 397–404 (2017).

194. Tufvesson, P. *et al.* Economic Considerations for Selecting an Amine Donor in Biocatalytic Transamination. *Org. Process Res. Dev.* **19**, 652–660 (2015).

195. Mallin, H., Höhne, M. & Bornscheuer, U. T. Immobilization of (R)- and (S)-amine transaminases on chitosan support and their application for amine synthesis using isopropylamine as donor. *J. Biotechnol.* **191**, 32–37 (2014).

196. Börner, T. *et al.* Three in One: Temperature, Solvent and Catalytic Stability by Engineering the Cofactor-Binding Element of Amine Transaminase. *ChemBioChem* **18**, 1482–1486 (2017).

197. Gomm, A., Lewis, W., Green, A. P. & O'Reilly, E. A New Generation of Smart Amine Donors for Transaminase-Mediated Biotransformations. *Chem. - A Eur. J.* **22**, 12692–12695 (2016).

198. Slabu, I., Galman, J. L., Weise, N. J., Lloyd, R. C. & Turner, N. J. Putrescine Transaminases for the Synthesis of Saturated Nitrogen Heterocycles from Polyamines. *ChemCatChem* **8**, 1038–1042 (2016).

199. Payer, S. E., Schrittwieser, J. H. & Kroutil, W. Vicinal Diamines as Smart Cosubstrates in the Transaminase-Catalyzed Asymmetric Amination of Ketones. *European J. Org. Chem.* **2017**, 2553–2559 (2017).

200. Wang, B., Land, H. & Berglund, P. Wang_ChemComm_2013.pdf. *Chem. Commun.* **49**, 161–163 (2013).

201. Green, A. P., Turner, N. J. & O'Reilly, E. Chiral Amine Synthesis Using ω-

Transaminases: An Amine Donor that Displaces Equilibria and Enables High-Throughput Screening. *Angew. Chemie* **126**, 10890–10893 (2014).

202. Baud, D., Ladkau, N., Moody, T. S., Ward, J. M. & Hailes, H. C. A rapid, sensitive colorimetric assay for the high-throughput screening of transaminases in liquid or solid-phase. *Chem. Commun.* **51**, 17225–17228 (2015).

203. Patil, M. D., Grogan, G., Bommarius, A. & Yun, H. Oxidoreductase-Catalyzed Synthesis of Chiral Amines. *ACS Catal.* **8**, 10985–11015 (2018).

204. Ghislieri, D. & Turner, N. J. Biocatalytic approaches to the synthesis of enantiomerically pure chiral amines. *Top. Catal.* **57**, 284–300 (2014).

205. Blaser, H. U., Buser, H. P., Jalett, H. P., Pugin, B. & Spindler, F. Iridium ferrocenyl diphosphine catalyzed enantioselective reductive alkylation of a hindered aniline. *Synlett* **S1**, 867–868 (1999).

206. Itoh, N., Yachi, C. & Kudome, T. Determining a novel NAD^+-dependent amine dehydrogenase with a broad substrate range from Streptomyces virginiae IFO 12827: Purification and characterization. *J. Mol. Catal. B Enzym.* **10**, 281–290 (2000).

207. Mayol, O. *et al.* Asymmetric Reductive Amination by a Wild-Type Amine Dehydrogenase from the Thermophilic Bacteria Petrotoga mobilis. *Catal. Sci. Technol.* **6**, 7421–7428 (2016).

208. Huang, H., Liu, X., Zhou, L., Chang, M. & Zhang, X. Direct Asymmetric Reductive Amination for the Synthesis of Chiral β-Arylamines. *Angew. Chemie Int. Ed.* **55**, 5309–5312 (2016).

209. Borlinghaus, N. & Nestl, B. M. Switching the Cofactor Specificity of an Imine Reductase. *ChemCatChem* **10**, 183–187 (2018).

210. Carr, R. *et al.* Directed Evolution of an Amine Oxidase Possessing both Broad Substrate Specificity and High Enantioselectivity. *Angew. Chemie Int. Ed.* **42**, 4807–4810 (2003).

211. Dunsmore, C. J., Carr, R., Fleming, T. & Turner, N. J. A chemo-enzymatic route to enantiomerically pure cyclic tertiary amines. *J. Am. Chem. Soc.* **128**, 2224–2225 (2006).

212. Heberling, M. M., Wu, B., Bartsch, S. & Janssen, D. B. Priming ammonia lyases and aminomutases for industrial and therapeutic applications. *Curr. Opin. Chem. Biol.* **17**, 250–260 (2013).

213. Turner, N. J. Ammonia lyases and aminomutases as biocatalysts for the synthesis of α-amino and β-amino acids. *Curr. Opin. Chem. Biol.* **15**, 234–240 (2011).

214. Buller, R., Hecht, K., Mirata, A. M. & Meyer, H.-P. Context and Challenges for Industrial Biocatalysis. in *Biocatalysis: An Industrial Perspective* (eds. Gonzalo, G. & Dominguez de Maria, P.) 1–43 (The Royal Society of Chemistry, 2017).

215. Koszelewski, D., Pressnitz, D., Clay, D. & Kroutil, W. Deracemization of mexiletine biocatalyzed by ω-transaminases. *Org. Lett.* **11**, 4810–4812 (2009).

216. Peng, Z., Wong, J. W., Hansen, E. C., Puchlopek-Dermenci, A. L. A. & Clarke,

H. J. Development of a concise, asymmetric synthesis of a smoothened receptor (smo) inhibitor: Enzymatic transamination of a 4-piperidinone with dynamic kinetic resolution. *Org. Lett.* **16**, 860–863 (2014).

217. Bravo, F. *et al.* Development of a dynamic kinetic resolution for the isolation of an intermediate in the synthesis of casopitant mesylate: Application of QbD principles in the definition of the parameter ranges, issues in the scale-up and mitigation strategies. *Org. Process Res. Dev.* **14**, 1162–1168 (2010).

218. Mamman, A. S. *et al.* Perspective: Jatropha cultivation in southern India: Assessing farmers' experiences. *Biofuels, Bioprod. Biorefining* **6**, 246–256 (2012).

219. Mariscal, R., Maireles-Torres, P., Ojeda, M., Sádaba, I. & López Granados, M. Furfural: A renewable and versatile platform molecule for the synthesis of chemicals and fuels. *Energy Environ. Sci.* **9**, 1144–1189 (2016).

220. Weintraub, P. *et al.* WO 2005/097750. 1–283 (2005).

221. Zhang, Y., Broekhuis, A. A. & Picchioni, F. Thermally Self-Healing Polymeric Materials : The Next Step to Recycling Thermoset Polymers? *Macromolecules* **42**, 1906–1912 (2009).

222. Dunn, P. J. The importance of Green Chemistry in Process Research and Development. *Chem. Soc. Rev.* **41**, 1452–1461 (2012).

223. Monti, D. *et al.* Cascade Coupling of Ene-Reductases and ω-Transaminases for the Stereoselective Synthesis of Diastereomerically Enriched Amines. *ChemCatChem* **7**, 3106–3109 (2015).

224. Gupta, P. & Mahajan, N. Biocatalytic approaches towards the stereoselective synthesis of vicinal amino alcohols. *New J. Chem.* **42**, 12296–12327 (2018).

225. Galley, G., Groebke Zbinden, K., Norcross, R. & Stalder, H. Novel 2-Aminooxazolines as TAAR1 Ligands. 1–216 (2008).

226. Romagnolo, A. *et al.* Old Yellow Enzyme homologues in Mucor circinelloides: Expression profile and biotransformation. *Sci. Rep.* **7**, 1–10 (2017).

227. Toogood, H. S., Gardiner, J. M. & Scrutton, N. S. Biocatalytic Reductions and Chemical Versatility of the Old Yellow Enzyme Family of Flavoprotein Oxidoreductases. *ChemCatChem* **2**, 892–914 (2010).

228. Murphy, C. D. & Sandford, G. Recent advances in fluorination techniques and their anticipated impact on drug metabolism and toxicity. *Expert Opin. Drug Metab. Toxicol.* **11**, 589–599 (2015).

229. Shaughnessy, M. J. *et al.* Targeted fluorination of a nonsteroidal anti-inflammatory drug to prolong metabolic half-life. *ChemMedChem* **9**, 733–736 (2014).

230. Purser, S., Moore, P. R., Swallow, S. & Gouverneur, V. Fluorine in medicinal chemistry. *Chem. Soc. Rev.* **37**, 320–330 (2008).

231. Meanwell, N. A. Fluorine and Fluorinated Motifs in the Design and Application of Bioisosteres for Drug Design. *J. Med. Chem.* **61**, 5822–5880 (2018).

232. Ardanaz, S. M., Velez Rueda, A. J., Parisi, G., Iribarren, A. M. & Iglesias, L. E. A Mild Procedure for Enone Preparation Catalysed by Bovine Serum Albumin in a Green and Easily Available Medium. *Catal. Letters* (2018).

233. Brenna, E. *et al.* Multi-enzyme cascade synthesis of the most odorous stereoisomers of the commercial odorant Muguesia®. *J. Mol. Catal. B Enzym.* **114**, 37–41 (2015).

234. Kanazawa, Y. *et al.* Asymmetric conjugate reduction of alpha,beta-unsaturated ketones and esters with chiral rhodium(2,6-bisoxazolinylphenyl) catalysts. *Chem. A Eur. J.* **12**, 63–71 (2005).

235. Sang, I. L., Ji, Y. B., So, H. S. & Young, K. C. Gold(I)-catalyzed rearrangement of propargylic alcohols to α,β-unsaturated ketones. *Synthesis (Stuttg).* **14**, 2107–2114 (2007).

236. Urosa, A. *et al.* Synthesis and bioactivity of Luffarin I. *Mar. Drugs* **13**, 2407–2423 (2015).

237. Lee, S. *et al.* Enantioselective conjugate radical addition to α′-hydroxy enones. *Org. Lett.* **8**, 4311–4313 (2006).

238. Carlson, R. G. & Behn, N. S. Stereochemistry of Epoxidation of Rigid Methylenecyclohexane Systems. Determination of Stereochemistry of Exocyclic Epoxides in Rigid Cyclohexanes by Nuclear Magnetic Resonance Half Band Widths. *J. Org. Chem.* **32**, 1363–1367 (1967).

239. Pathak, J., Rawat, K. & Bohidar, H. B. Thermo-reversibility, ergodicity and surface charge–temperature dependent phase diagram of anionic, cationic and neutral co-gels of gelatin–BSA complexes. *RSC Adv.* **6**, 40123–40136 (2016).

240. Murata, M., Tani, F., Higasa, T., Kitabatake, N. & Doi, E. Heat-induced Transparent Gel Formation of Bovine Serum Albumin. *Biosci. Biotechnol. Biochem.* **57**, 43–46 (1993).

241. Wang, C. H. & Damodaran, S. Thermal Gelation of Globular Proteins: Influence of Protein Conformation on Gel Strength. *J. Agric. Food Chem.* **39**, 433–438 (1991).

242. Hazra, C. K., Irran, E. & Oestreich, M. Regio- and diastereoselective copper(I)-catalyzed allylic substitution of δ-hydroxy allylic chlorides by a silicon nucleophile. *European J. Org. Chem.* **2013**, 4903–4908 (2013).

243. Ishikawa, T. *et al.* Catalytic alkynylation of ketones and aldehydes using quaternary ammonium hydroxide base. *J. Org. Chem.* **68**, 3702–3705 (2003).

244. Rubottom, G. M., Gruber, J. M., Boeckman, R. K., Ramaiah, M. & Medwid, J. B. Clarification of the mechanism of rearrangement of enol silyl ether epoxides. *Tetrahedron Lett.* **19**, 4603–4606 (1978).

245. Somasekar Rao, A. & Rama Mohan, H. m-Chloroperbenzoic Acid. *Encyclopedia of Reagents for Organic Synthesis* 1–6 (2005).

246. Mori, A. *et al.* Pd/C-catalyzed chemoselective hydrogenation in the presence of diphenylsulfide. *Org. Lett.* **8**, 3279–3281 (2006).

247. Yang, J. W., Hechavarria Fonseca, M. T. & List, B. A metal-free transfer hydrogenation: Organocatalytic conjugate reduction of ??,??-unsaturated aldehydes. *Angew. Chemie Int. Ed.* **43**, 6660–6662 (2004).

248. Nadine. ERed info **1**, 1–51 (2010).

249. Dobrjevic, D. *et al.* Lupins as crop plants : biology, production and utilization.

250. Scholtissek, A., Tischler, D., Westphal, A. H., van Berkel, W. J. H. & Paul, C. E. Old yellow enzyme-catalysed asymmetric hydrogenation: Linking family roots with improved catalysis. *Catalysts* **7**, 1–24 (2017).

251. Hall, M., Hauer, B., Stuermer, R., Kroutil, W. & Faber, K. Asymmetric whole-cell bioreduction of an α,β-unsaturated aldehyde (citral): competing prim-alcohol dehydrogenase and C-C lyase activities. *Tetrahedron Asymmetry* **17**, 3058–3062 (2006).

252. Müller, A., Hauer, B. & Rosche, B. Enzymatic reduction of the α, β-unsaturated carbon bond in citral. *J. Mol. Catal. B Enzym.* **38**, 126–130 (2006).

253. ACS Green Chemistry Institute Pharmaceutical Roundtable. *Solvent Selection Guide: Version 2.0*. (2011).

254. Graber, M. *et al.* Solvent as a competitive inhibitor for Candida antarctica lipase B. *Biochim. Biophys. Acta - Proteins Proteomics* **1774**, 1052–1057 (2007).

255. Mozhaev, V. V. *et al.* Catalytic activity and denaturation of enzymes in water/organic cosolvent mixtures. *Eur. J. Biochem.* **184**, 597–602 (1989).

256. Stepankova, V., Damborsky, J. & Chaloupkova, R. Organic co-solvents affect activity, stability and enantioselectivity of haloalkane dehalogenases. *Biotechnol. J.* **8**, 719–729 (2013).

257. Serdakowski, A. L. & Dordick, J. S. Enzyme Activation for Organic Solvents Made Easy. *Trends Biotechnol.* **26**, 48–54 (2008).

258. Yoon, J. H. . & Mckenzie, D. . A comparison of the activities of three β-galactosidases in aqueous-organic solvent mixtures. *Enzym. Microb. Technol.* **36**, 439–446 (2005).

259. Sayer, C. *et al.* The substrate specificity, enantioselectivity and structure of the (R)-selective amine: Pyruvate transaminase from Nectria haematococca. *FEBS J.* **281**, 2240–2253 (2014).

260. Yun, H., Lim, S., Cho, B. & Kim, B. B-Amino Acid:Pyruvate Transaminase from Alcaligenes denitrificans Y2k-2: a New Catalyst for Kinetic Resolution of □-Amino Acids and Amines. *Appl. Environ. Microbiol.* **70**, 2529–2534 (2004).

261. Villegas-Torres, M. F. *et al.* Multi-step biocatalytic strategies for chiral amino alcohol synthesis. *Enzyme Microb. Technol.* **81**, 23–30 (2015).

262. Subrizi, F., Benhamou, L., Ward, J. M., Sheppard, T. D. & Hailes, H. C. Aminopolyols from Carbohydrates: Amination of Sugars and Sugar-Derived Tetrahydrofurans with Transaminases. *Angew. Chemie* **131**, 3894–3898 (2019).

263. Zhang, J. D. *et al.* Enantioselective synthesis of enantiopure β-amino alcohols via kinetic resolution and asymmetric reductive amination by a robust

transaminase from Mycobacterium vanbaalenii. *J. Biotechnol.* **290**, 24–32 (2019).

264. Lane, J. F., Willenz, J., Weissberger, A. & Wallis, E. S. Molecular Rearrangements Involving Optically Active Radicals. VIII. The Wolff Rearrangements of Optically Active Diazoketones. *J. Org. Chem.* **5**, 276–285 (1940).

265. Mei, H. *et al.* Fluorine-Containing Drugs Approved by the FDA in 2018. *Chem. A Eur. J.* **25**, 11797–11819 (2019).

266. Inoue, M., Sumii, Y. & Shibata, N. Contribution of Organofluorine Compounds to Pharmaceuticals. *ACS Omega* **5**, 10633–10640 (2020).

267. Fujiwara, T. & O'Hagan, D. Successful fluorine-containing herbicide agrochemicals. *J. Fluor. Chem.* **167**, 16–29 (2014).

268. Müller, K., Faeh, C. & Diederich, F. Fluorine in pharmaceuticals: Looking beyond intuition. *Science* **317**, 1881–1886 (2007).

269. Blanksby, S. J. & Ellison, G. B. Bond dissociation energies of organic molecules. *Acc. Chem. Res.* **36**, 255–263 (2003).

270. Morgenthaler, M. *et al.* Predicting and tuning physicochemical properties in lead optimization: Amine basicities. *ChemMedChem* **2**, 1100–1115 (2007).

271. Chambers, R. D. *Fluorine in Organic Chemistry*. (Blackwell Publishing, 2000).

272. Smith, D. A., van de Waterbeemd, H. & Walker, D. K. Pharmacokinetics and Metabolism in Drug Design. in *Methods and Principles in Medicinal Chemistry* **31**, 19–37 (2006).

273. Furuya, T. & Ritter, T. Carbon-fluorine reductive elimination from a high-valent palladium fluoride. *J. Am. Chem. Soc.* **130**, 10060–10061 (2008).

274. Ball, N. D. & Sanford, M. S. Synthesis and reactivity of a mono-σ-aryl palladium(IV) fluoride complex. *J. Am. Chem. Soc.* **131**, 3796–3797 (2009).

275. Wang, X., Mei, T.-S. & Yu, J.-Q. Versatile Pd(OTf)2·2H2O-Catalyzed ortho-Fluorination Using NMP as a Promoter. *J. Am. Chem. Soc.* **40**, 7520–7521 (2009).

276. Zhang, D. *et al.* Palladium-catalyzed direct ortho C-O bond construction of azoxybenzenes with carboxylic acids and alcohols. *Org. Chem. Front.* **2**, 951–955 (2015).

277. Racowski, J. M., Gary, J. B. & Sanford, M. S. Carbon(sp3)-fluorine bond-forming reductive elimination from palladium(IV) complexes. *Angew. Chemie Int. Ed.* **51**, 3414–3417 (2012).

278. Pitts, C. R. *et al.* Direct, catalytic monofluorination of sp3 c-h bonds: A radical-based mechanism with ionic selectivity. *J. Am. Chem. Soc.* **136**, 9780–9791 (2014).

279. Pitts, C. R., Bume, D. D., Harry, S. A., Siegler, M. A. & Lectka, T. Multiple Enone-Directed Reactivity Modes Lead to the Selective Photochemical Fluorination of Polycyclic Terpenoid Derivatives. *J. Am. Chem. Soc.* **139**, 2208–

2211 (2017).

280. Rueda-Becerril, M. *et al.* Fluorine transfer to alkyl radicals. *J. Am. Chem. Soc.* **134**, 4026–4029 (2012).

281. Bume, D. D. *et al.* Ketones as directing groups in photocatalytic sp3 C-H fluorination. *Chem. Sci.* **8**, 6918–6923 (2017).

282. Szpera, R., Moseley, D. F. J., Smith, L. B., Sterling, A. J. & Gouverneur, V. The Fluorination of C−H Bonds: Developments and Perspectives. *Angew. Chemie Int. Ed.* **58**, 14824–14848 (2019).

283. O'Hagan David, Schaffrath Christoph, Cobb Steven L., Hamilton John T. G. & Murphy Carmac D. Biosynthesis of an organofluorine molecule. *Nature* **416**, 279–279 (2002).

284. Dong, C. *et al.* Crystal structure and mechanism of a bacterial fluorinating enzyme. *Nature* **427**, 561–565 (2004).

285. O'Hagan, D. & Deng, H. Enzymatic fluorination and biotechnological developments of the fluorinase. *Chem. Rev.* **115**, 634–649 (2015).

286. Deng, H. *et al.* Identification of fluorinases from streptomyces sp MA37, norcardia brasiliensis, and actinoplanes sp N902-109 by genome mining. *ChemBioChem* **15**, 364–368 (2014).

287. Qu, X., Wang, Y. & Deng, Z. Characterization of a SAM-dependent fluorinase from a latent biosynthetic pathway for fluoroacetate and 4-fluorothreonine formation in Nocardia brasiliensis. *F1000Research* **3**, 1–14 (2014).

288. Huang, S. *et al.* Fluoroacetate biosynthesis from the marine-derived bacterium Streptomyces xinghaiensis NRRL B-24674. *Org. Biomol. Chem.* **12**, 4828–4831 (2014).

289. Rentmeister, A., Arnold, F. H. & Fasan, R. Chemo-enzymatic fluorination of unactivated organic compounds. *Nat. Chem. Biol.* **5**, 26–28 (2009).

290. Brenna, E., Gatti, F. G., Manfredi, A., Monti, D. & Parmeggiani, F. Biocatalyzed enantioselective reduction of activated C=C bonds: Synthesis of enantiomerically enriched α-halo-β-arylpropionic acids. *European J. Org. Chem.* 4015–4022 (2011).

291. Tasnádi, G. *et al.* A substrate-driven approach to determine reactivities of α,β-unsaturated carboxylic esters towards asymmetric bioreduction. *Chem. - A Eur. J.* **18**, 10362–10367 (2012).

292. Debarge, S. *et al.* Evaluation of several routes to advanced pregabalin intermediates: Synthesis and enantioselective enzymatic reduction using ene-reductases. *Org. Process Res. Dev.* **18**, 109–121 (2014).

293. Winkler, C. K. *et al.* Chemoenzymatic asymmetric synthesis of pregabalin precursors via asymmetric bioreduction of β-cyanoacrylate esters using ene-reductases. *J. Org. Chem.* **78**, 1525–1533 (2013).

294. Brenna, E., Gatti, F. G., Manfredi, A., Monti, D. & Parmeggiani, F. Enoate reductase-mediated preparation of methyl (S)-2-bromobutanoate, a useful key

intermediate for the synthesis of chiral active pharmaceutical ingredients. *Org. Process Res. Dev.* **16**, 262–268 (2012).

295. Utaka, M., Konishi, S., Okubo, T., Tsuboi, S. & Takeda, A. A Facile Synthesis of Optically Pure L-Armentomycin and its D-Isomer. Highly Enantioselective Reduction of the C-C Double Bond of Methyl (*E*)- and (*Z*)-2,4,4-Trichloro-2-Butenoate by Using Baker's Yeast. *Tetrahedron Lett.* **28**, 1447–1450 (1987).

296. Utaka, M. *et al.* Asymmetric Reduction of the Prochiral Carbon-carbon Double Bond of Methyl 2-chloro-2-alkenoates by Use of Fermenting Bakers' Yeast. *J. Org. Chem.* **54**, 4989–4992 (1989).

297. Augustine, J. K., Bombrun, A., Venkatachaliah, S. & Jothi, A. Titanium mediated olefination of aldehydes with α-haloacetates: An exceptionally stereoselective and general approach to (Z)-α-haloacrylates. *Org. Biomol. Chem.* **11**, 8065–8072 (2013).

298. Liao, Y. *et al.* Structure-based design and structure-activity relationships of 1,2,3,4-tetrahydroisoquinoline derivatives as potential PDE4 inhibitors. *Bioorganic Med. Chem. Lett.* **28**, 1188–1193 (2018).

299. Ponra, S. *et al.* Diastereo- and Enantioselective Synthesis of Fluorine Motifs with Two Contiguous Stereogenic Centers. *J. Am. Chem. Soc.* **140**, 13878–13883 (2018).

300. Martinet, P., Sauvetre, R. & Normant, J.-F. Hydrogenation Caralytique D'Aldehydes, Cetones et Esters a,b-Ethyleniques a-Fluores et de Cetones a,b-Ethyleniques a,b-Difluorees. *J. Fluor. Chem.* **52**, 419–432 (1991).

301. Peschiulli, A., Oehlrich, D., Rombouts, F., Vos, A. & Gijsen, H. J. 3,3-Difluoro-3,4,5,6-tetrahydropyridin-2-amines: Potent and permeable BACE-1 inhibitors. *Bioorganic Med. Chem. Lett.* **30**, 126999 (2020).

302. Anandan, S.-K., Gless, Richard, D., J., Aavula, Bhasker, R. & Patel, D. V. Soluble Epoxide Hydrolase Inhibitors. 1–103 (2009).

303. Kaku, H. *et al.* A method to prepare optically active acyclic α-benzyl ketones by thermodynamically controlled deracemization. *European J. Org. Chem.* **36**, 8208–8213 (2013).

304. Morales-Serna, J. A. *et al.* Reduction of carboxylic acids using esters of benzotriazole as high-reactivity intermediates. *Synthesis (Stuttg).* **9**, 1375–1382 (2011).

305. Ren, K. *et al.* Ruthenium-catalyzed oxidation of allyl alcohols with intermolecular hydrogen transfer: Synthesis of α,β-unsaturated carbonyl compounds. *J. Org. Chem.* **79**, 2170–2177 (2014).

306. Albarrán-Velo, J., Lavandera, I. & Gotor-Fernández, V. Sequential Two-Step Stereoselective Amination of Allylic Alcohols through Combination of Laccases and Amine Transaminases. *ChemBioChem* **20**, 1–13 (2019).

307. Garrabou, X., Macdonald, D. S., Wicky, B. I. M. & Hilvert, D. Stereodivergent Evolution of Artificial Enzymes for the Michael Reaction. *Angew. Chem. Int. Ed.* **57**, 5288–5291 (2018).

308. Lippincott, D. J., Linstadt, R. T. H., Maser, M. R. & Lipshutz, B. H. Synthesis of Functionalized [3], [4], [5] and [6]Dendralenes through Palladium-Catalyzed Cross-Couplings of Substituted Allenoates. *Angew. Chemie Int. Ed.* **56**, 847–850 (2017).

309. Erbing, E. *et al.* General, Simple, and Chemoselective Catalysts for the Isomerization of Allylic Alcohols: The Importance of the Halide Ligand. *Chem. A Eur. J.* **22**, 15659–15663 (2016).

310. Zhang, B., Li, H., Ding, Y., Yan, Y. & An, J. Reduction and Reductive Deuteration of Tertiary Amides Mediated by Sodium Dispersions with Distinct Proton Donor-Dependent Chemoselectivity. *J. Org. Chem.* **83**, 6006–6014 (2018).

311. Ye, L., Cui, L., Zhang, G. & Zhang, L. Alkynes as equivalents of α-diazo ketones in generating α-oxo metal carbenes: A gold-catalyzed expedient synthesis of dihydrofuran-3-ones. *J. Am. Chem. Soc.* **132**, 3258–3259 (2010).

312. Ren, W. *et al.* An Effective Pd-Catalyzed Regioselective Hydroformylation of Olefins with Formic Acid. *J. Am. Chem. Soc.* **138**, 14864–14867 (2016).

313. Botteghi, C., Cazzolato, L., Marchetti, M. & Paganelli, S. New Synthetic Route to Pharmacologically Active 1 - (N,N-dialkylamino)-3,3-diarylpropanes via Rhodium-Catalyzed Hydroformylation of 1,1-Diarylethenes. *J. Org. Chem.* **60**, 6612–6615 (1995).

314. Huang, H. *et al.* Chemo- and Regioselective Organo-Photoredox Catalyzed Hydroformylation of Styrenes via a Radical Pathway. *J. Am. Chem. Soc.* **139**, 9799–9802 (2017).

315. Gandamana, D. A. *et al.* Alkyl Ethers as Traceless Hydride Donors in Brønsted Acid Catalyzed Intramolecular Hydrogen Atom Transfer. *Angew. Chemie Int. Ed.* **57**, 6181–6185 (2018).

316. Fujihara, T., Cong, C., Terao, J. & Tsuji, Y. Palladium-catalyzed reduction of carboxylic acids to aldehydes with hydrosilanes in the presence of pivalic anhydride. *Adv. Synth. Catal.* **355**, 3420–3424 (2013).

317. Wendling, T., Risto, E., Krause, T. & Gooßen, L. J. Salt-Free Strategy for the Insertion of CO2into C−H Bonds: Catalytic Hydroxymethylation of Alkynes. *Chem. A Eur. J.* **24**, 6019–6024 (2018).

318. Liu, Z. & Vidović, D. Michael Additions Catalyzed by a β-Diketiminate-Supported Aluminum Complex. *J. Org. Chem.* **83**, 5295–5300 (2018).

319. Huang, A. *et al.* Discovery of 2-[1-(4-Chlorophenyl)cyclopropyl]-3-hydroxy-8-(trifluoromethyl)quinoline-4-carboxylic acid (PSI-421), a P-selectin inhibitor with improved pharmacokinetic properties and oral efficacy in models of vascular injury. *J. Med. Chem.* **53**, 6003–6017 (2010).

320. Elkik, E. Preparation and H, F and C-13 NMR-spectra of para-substituted and meta-substituted alpha-fluoro-cinnamic esters. *Bullentin la Soc. Chim. Fr.* **3**, 423–428 (1986).

321. Zoute, L., Dutheuil, G., Quirion, J. C., Jubault, P. & Pannecoucke, X. Efficient synthesis of fluoroalkenes via diethylzinc-promoted wittig reaction. *Synthesis*

(Stuttg). 3409–3418 (2006). doi:10.1055/s-2006-950208

322. Qian, J., Yi, W., Lv, M. & Cai, C. A facile and mild approach for stereoselective synthesis of α-fluoro-α,β-unsaturated esters from α-fluoro-β-keto esters via deacylation. *Synlett* **26**, 127–132 (2015).

323. Prakash, G. K. S. *et al.* Stereoselective synthesis of fluoroalkenoates and fluorinated isoxazolidinones: N-substituents governing the dual reactivity of nitrones. *Chem. A Eur. J.* **20**, 831–838 (2014).

324. Chintareddy, V. R., Ellern, A. & Verkade, J. G. P[N(*i*-Bu)CH2CH2]3N: Nonionic Lewis base for promoting the room-temperature synthesis of α,β-unsaturated esters, fluorides, ketones, and nitriles using Wadsworth - Emmons phosphonates. *J. Org. Chem.* **75**, 7166–7174 (2010).

325. Michida, M. & Mukaiyama, T. A convenient method for the synthesis of (Z)-α-fluoroacrylates: Lewis base-catalyzed carbonyl fluoroolefination using fluoro(trimethylsilyl)ketene ethyl trimethylsilyl acetal. *Chem. Lett.* **37**, 890–891 (2008).

326. Rousée, K., Bouillon, J. P., Couve-Bonnaire, S. & Pannecoucke, X. Stereospecific synthesis of tri- and tetrasubstituted α-fluoroacrylates by mizoroki-heck reaction. *Org. Lett.* **18**, 540–543 (2016).

327. Xie, S. L., Gao, X. T., Wu, H. H., Zhou, F. & Zhou, J. Direct Electrochemical Defluorinative Carboxylation of gem-Difluoroalkenes with Carbon Dioxide. *Org. Lett.* **22**, 8424–8429 (2020).